energies

MDPI

Review

A Comprehensive Review on Energy Storage Systems: Types, Comparison, Current Scenario, Applications, Barriers, and Potential Solutions, Policies, and Future Prospects

Eklas Hossain [1,*], Hossain Mansur Resalat Faruque [2], Md. Samiul Haque Sunny [3], Naeem Mohammad [3] and Nafiu Nawar [3]

1 Department of Electrical Engineering and Renewable Energy, Oregon Tech, Klamath Falls, OR 97601, USA
2 School of Electrical, Computer and Energy Engineering, Arizona State University, Tempe, AZ 85281, USA; hfaruque@asu.edu
3 Department of Electrical and Electronic Engineering, Khulna University of Engineering & Technology, Khulna 9203, Bangladesh; mdshs31@gmail.com (M.S.H.S.); nmsami36@gmail.com (N.M.); nafiu.nawar@gmail.com (N.N.)
* Correspondence: eklas.hossain@oit.edu

Received: 20 June 2020; Accepted: 13 July 2020; Published: 15 July 2020

Abstract: Driven by global concerns about the climate and the environment, the world is opting for renewable energy sources (RESs), such as wind and solar. However, RESs suffer from the discredit of intermittency, for which energy storage systems (ESSs) are gaining popularity worldwide. Surplus energy obtained from RESs can be stored in several ways, and later utilized during periods of intermittencies or shortages. The idea of storing excess energy is not new, and numerous researches have been conducted to adorn this idea with innovations and improvements. This review is a humble attempt to assemble all the available knowledge on ESSs to benefit novice researchers in this field. This paper covers all core concepts of ESSs, including its evolution, elaborate classification, their comparison, the current scenario, applications, business models, environmental impacts, policies, barriers and probable solutions, and future prospects. This elaborate discussion on energy storage systems will act as a reliable reference and a framework for future developments in this field. Any future progress regarding ESSs will find this paper a helpful document wherein all necessary information has been assembled.

Keywords: energy storage; renewable energy; intermittency mitigation; classification; applications; policies; barriers

1. Introduction

There has been a profuse increase in the global electricity consumption, which is propelled by the technological advancements and stable global economic growth. According to the latest assessment on global energy demand by the International Energy Agency (IEA), the global energy demand increased by 4% or 900 TWh to reach more than 26,700 TWh in 2018 [1]. As the average temperature of winter and summer exceeded previous records, the demand for heating and cooling increased significantly, which accounts for one-fifth of the increase of the global energy demand. Approximately 64% of the annual global energy consumption was met by fossil fuels in 2018, which escalated the energy related CO2 emission by 1.7 % to 33 Gigatonnes [2]. Even though fossil fuel still accounts for majority of this energy demand, the world is gradually moving towards clean energy for the betterment of the environment. In order to achieve the major goals of Paris Agreement—reaching carbon neutrality in energy sector by

2060, and limiting the global temperature increase to 1.750 C by the year 2100—the usage of renewable energy sources (RES) such as solar, wind, and hydropower for electricity generation is gaining prolific attention [3,4]. The total energy generated by RESs in 2018 increased by 7% or 450 TWh, which met almost 45% of this aforementioned global electricity growth and now shares 25% of the total global energy demand [1,2]. The average annual change in electrical energy generation and the electricity generation mix in 2018 are represented in Figure 1a,b, respectively.

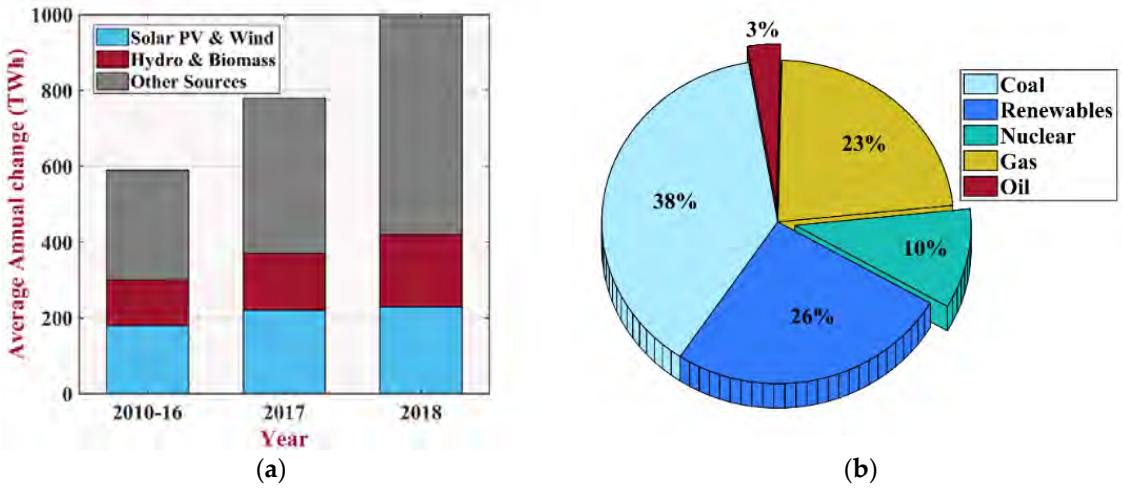

Figure 1. (**a**) The average annual change in electrical energy generation and (**b**) the electricity generation mix in 2018 [1].

The integration of RESs with the grid is not only beneficial for the environment, but also possesses ample economic advantages [5]. Nevertheless, these RESs are intermittent in nature and causes power fluctuations, which seriously affects the reliability, resiliency, and stability of the power. Many researches have been conducted for finding out potential solutions to mitigate these intermittencies which includes shifting the load through demand management, interconnecting external grid, electrical energy storage (EES), etc. Chen et al. posited that out of all the aforementioned solutions, integrating EESs has been considered as the most viable and promising approach [6].

EES is a process of converting the electrical energy to another storable form and then converting the stored energy to electricity during the time of need. According to Nadeem et al., by mapping the renewable intermittent production profile and by charging and discharging real power accordingly, energy storage systems can effectively mitigate the intermittencies introduced by the RESs, thus improving the power quality and reliability [3]. Furthermore, they can also store the excess energy generated by the RESs, therefore, reducing energy spillage. In recent times, electric vehicles (EVs) are becoming very promising source of transportation, whose main source power is EES, i.e., batteries. Moreover, according to Poullikkas et al., EES also has many utility scale applications such as peak shaving, load levelling, providing back-up power, uninterrupted power supply (UPS), etc. [7]. In recent times, many countries have started utilizing the multiple applications and facilities that EES has to offer by building large scale storage systems. Therefore, it is an ideal time to review and summarize the recently conducted research works on this field, which will aid further research and proliferate the implementation and deployment of EES in practical applications.

Throughout this paper, a system or a device which can store electrical energy and has the ability to use this stored energy later when needed is termed as "energy storage system (ESS)". For further delving into the area of energy storage, it is very important to categorize different types of ESSs based on their formation and composition materials. It also necessary to discuss these different types energy storage system, their basic operating principles, mathematical modelling, and their relative advantages and disadvantages based on their technical and economical specifications. Furthermore, it is also vital to discuss the different types of applications these ESSs can serve and specify which particular

ESS is well suited for which applications. Different environmental impacts due to the deployment of ESSs must be discussed in detail. For widespread implementations of the ESSs and making it sustainable, much emphasis should be given on business model analysis, markets and cost analysis, and profitability study of ESS. In addition, it also paramount to discuss different barriers for ESS deployment and their potential solutions, major federal and state policies regarding ESS, and which policy addresses which specific barriers. Moreover, the evolution of ESS, its current scenario, and its future prospects requires further elucidation. The major contribution of this paper is to carry out and accomplish all the tasks mentioned above in order to draw a comprehensive and updated picture of the current condition of ESS and propose necessary actions that needs to be taken in various sectors to ensure widespread sustainable proliferation. The evolution, current scenario, applications, business models, policies and standards, barriers and potential solutions, environmental impacts, and future prospects of energy storage systems have been included in the paper, which are not so frequent among the existing literature. Existing researches focus light on the different storage systems, with little to no inclusion of the other topics, which need to be talked about as well. This paper makes a humble effort to bridge this very gap. The information flow in this paper is represented in Figure 2.

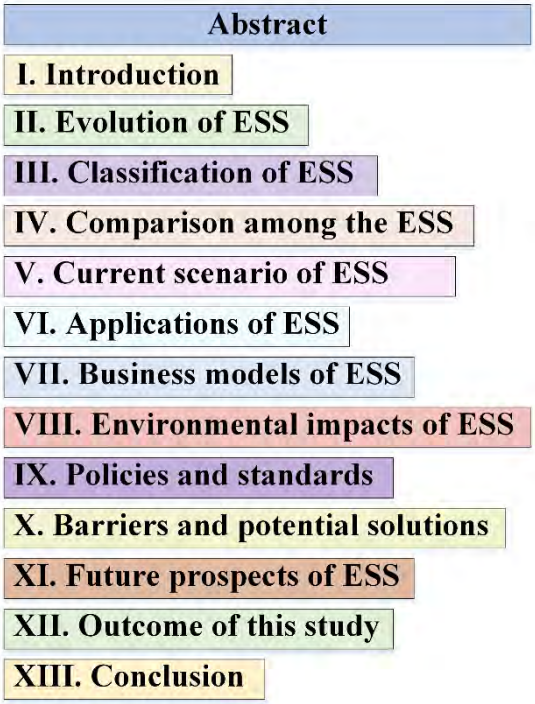

Figure 2. Information flow of this paper.

The rest of the paper is organized as follows: The chronological evolution of ESSs throughout history has been addressed in Section 2. Section 3 represents different types of ESSs, their operating principle, corresponding mathematical modelling, and comparison of their advantages and disadvantages. Comparison of different of types of ESSs are discussed in Section 4. The current scenario of ESSs is represented in Section 5. Different applications of ESSs are discussed in Section 6. Business models and profitability study for widespread deployment of ESSs are represented in Section 7. The environmental impacts of ESS are represented in Section 8. The policies and standards corresponding to ESSs are presented in Section 9. Different barriers of implementing ESSs, their impact levels, potential solution, and mapping of policies addressing these impacts are discussed in Section 10. The future prospects of ESSs are represented in Section 11. The major outcome of this study is summarized in Section 12. Finally, the conclusions are drawn in Section 13.

2. Evolution of Energy Storage Systems

ESSs have traversed a long way to reach the shape they are at today. The deployment of ESSs began roughly in the 19th century. Prior to that, ESS was not a common concept. Previously, biofuels (such as, wood) were in use since ancient times, but humans were not consciously storing energy by their usage. Batteries are the first types of energy storage that man used consciously. The term battery was coined by Benjamin Franklin in the year 1749. The first battery was invented by Alessandro Volta in 1800. He stacked discs of Cu and Zn separated by brine electrolyte [8,9]. Since then, there have been countless developments to the battery, which ushered the numerous types of available batteries, that have been described in this paper already. In fact, a vast amount of time in the 20th century was dedicated in developing different types of batteries only. The evolution of ESSs is seldom discussed in literature. In order to bridge this gap, the evolution of ESSs in a chronological order is depicted in Table 1. This will help to picture the gradual progress in the ES technology, and what a growing role ESSs are playing in the current world.

Table 1. The evolution of energy storage systems (ESSs) in chronological order.

Year	ESS	Introduction	Reference
Oldest	Bio fuels	Biofuels are in use since ancient times, in the form of wood and other types of solid biomass.	[10]
1839	Fuel cells	William Grove, a chemist, physicist, and lawyer invented the fuel cell in 1839.	[11]
1859	Lead acid battery	Invented in 1859 by French physicist Gaston Planté, lead acid battery is the earliest type of rechargeable battery.	[12]
1882	PHS	In 1882, the world's first hydroelectric power plant began operating in the United States along the Fox River in Appleton, Wisconsin.	[13]
1883	FES	The first FES used purely for ES was made of steel. It was developed by John A. Howell in 1883 for military applications.	[14]
1884	Flow batteries	French engineer Charles Renard invented flow batteries in 1884 to power an airship with an electric propeller.	[15]
1899	Nickel Cadmium battery	Nickel cadmium battery was invented by Waldemar Jungner in 1899. Further improvements occurred in 1947 which led to the modern sealed NiCd battery.	[16]
1899	Nickel Zinc battery	Nickel zinc battery was first invented in 1899. Its commercial production started in 1920.	[17]
1901	Nickel iron battery	The nickel iron battery was developed by Thomas Edison in 1901, and used for electric vehicles, such as the Detroit Electric and Baker Electric	[18]
1960	Sodium sulphur battery	Sodium Sulphur battery was first discovered by Ford Motor Company in 1960 to power early-model electric cars.	[19]
1967	Nickel metal hydride battery	Research on nickel-metal-hydride battery started in 1967.	[16]
1968	Sodium metal halide battery	Also known as ZEBRA batteries, sodium metal halide batteries were first introduced in South Africa in 1968.	[20]

Table 1. *Cont.*

Year	ESS	Introduction	Reference
1969	Super magnetic	SMES was first proposed as a method of diurnal storage in the year 1969.	[21]
1970	Nickel hydrogen battery	The Nickel-hydrogen battery was developed Comsat laboratories and Tyco laboratories, sponsored by Intelsat.	[22]
1978	Supercapacitor	Research on supercapacitors began in the 1957 by General Electric Company. Followed by many episodes of development, the supercapacitor was marketed in 1978.	[23]
1978	CAES	The first utility-scale CAES project was the 290 MW Huntorf plant in Germany using a salt dome, which started in 1978.	[24]
1980	Li-ion battery	In 1980, American physicist Professor John Goodenough invented Li-ion battery.	[9]
1980	Li-polymer battery	The discovery of the lithium polymer battery came in the 1980s. The first commercial Li-ion cell was of Sony in 1991.	[25]
Newest	Solar fuels	Driven by environmental concerns, solar fuels are recently gaining attention, and are still under research and development.	-

3. Classification of Energy Storage Systems

The increasing necessity of storing energy drove humans into the never-ending endeavor to discover new methods of energy storage that are more efficient and caters to particular needs. Energy storage systems can be classified based upon their specific function, speed of response, duration of storage, form of energy stored, etc. [26]. The classification of ESS based on the form of stored energy is mainly explored here. Energy can be stored in the form of mechanical, electrochemical, chemical, or thermal energy, as well as in the form of electric or magnetic fields. It is also possible to store energy as a hybrid of two different forms. Figure 3 maps out the different ESSs included in this paper, followed by the elaborate discussions on each type.

3.1. Mechanical Energy Storage

Mechanical energy is one of the oldest forms of energy that humankind has been using for diverse uses. An advantage of mechanical energy is that it can be stored easily and for long periods of time. It is very flexible in the sense that it can be easily converted into and from other energy forms [3]. Mechanical energy can appear as potential energy or kinetic energy. Pressurized gas and forced spring are two variations of potential energy, whereas kinetic energy can be stored within motion of a body. Three forms of mechanical storage systems are elaborated here. Among them, the pumped hydro storage and compressed air energy storage systems store potential energy, whereas flywheel energy storage system stores kinetic energy.

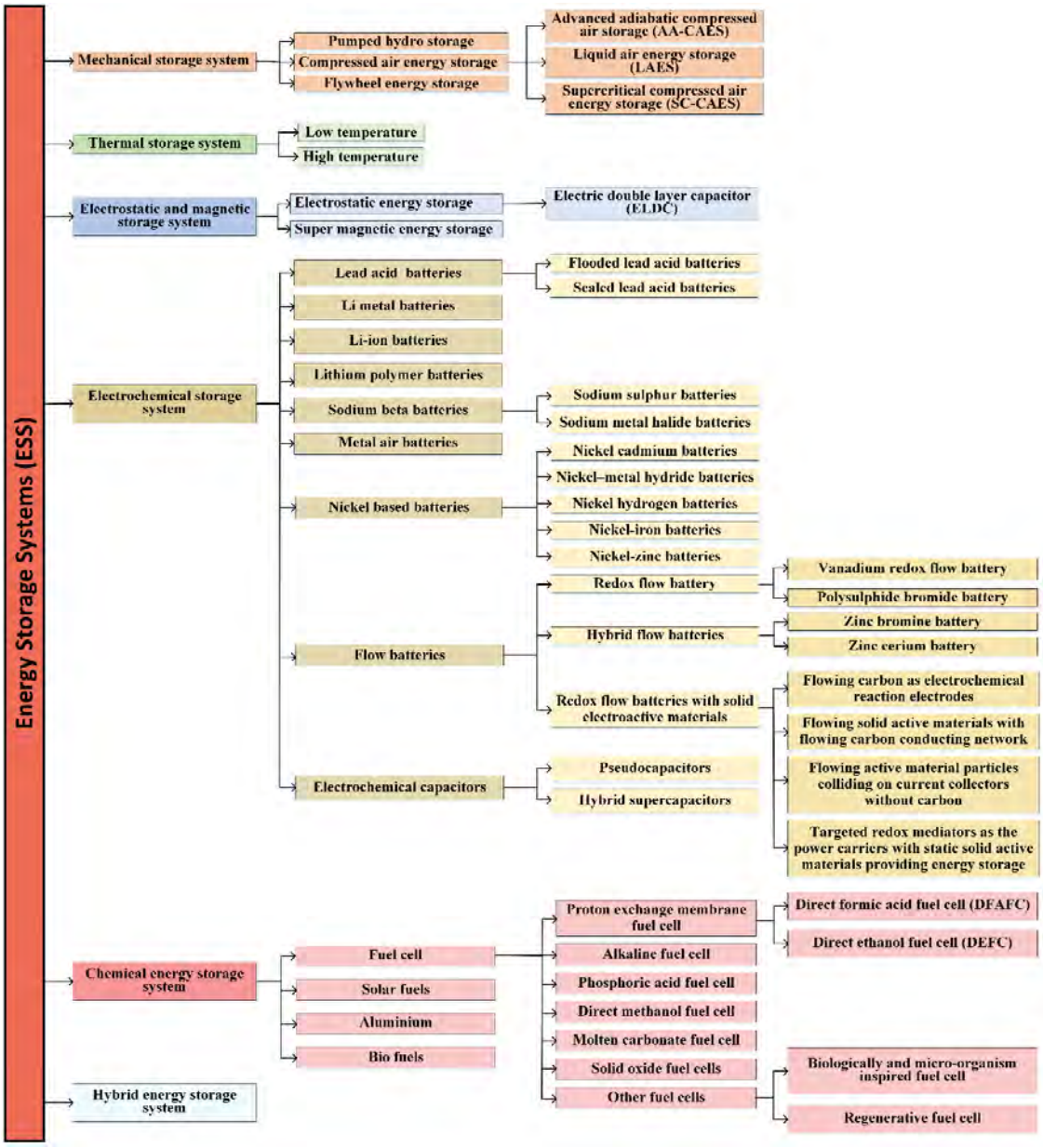

Figure 3. Classification of ESSs as described in this paper.

3.1.1. Pumped Hydro Storage (PHS)

First deployed in 1944 in Switzerland, pumped hydro storage (PHS) is one of the most popular storage techniques due to its simplicity and large storage capacity in the range of 1 to 3000 MW [27]. It is the largest electric storage with a capacity of 125 GW, which is 96% of the world's electric storage capacity and 3% of the world's generation capacity [28]. The globally installed electric storage capacity is represented in Figure 4. PHS is a mature and robust technology with high efficiency of 76–85%, low capital cost per unit energy, long storage period, practically unlimited life cycle, and a very long life of 50 years or more [6,29]. They are particularly used in stationary applications such as load levelling and peak shaving [27]. The PHS is an adaptation of the conventional hydroelectric power plant but working in reverse. In the conventional hydroelectric power plant, water is stored in a reservoir and is released to a turbine to convert the gravitational potential energy of the water into electrical energy. Here, the stored water can be used only once. However, in PHS, there are two reservoirs, one above the other, available along with a turbine/pumping hall [27]. The schematic of PHS is represented in

Figure 5. Similar to the conventional hydroelectric power plant, water from the upper reservoir is used to generate electricity by releasing it to the turbine of the generator. This water is stored in the lower reservoir and pumped to the upper reservoir using the turbine/pumping hall during the low peak time. This water is again released in the high peak time when demand is high to produce electricity. So, the water can be used multiple times, making it a more efficient system. The major PHS projects in the USA are represented in Table 2.

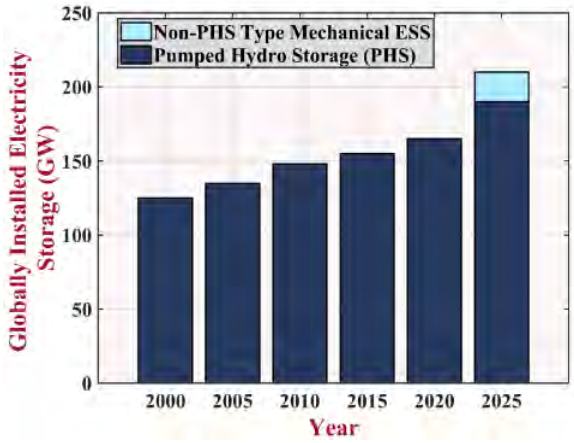

Figure 4. Global increase of pumped hydro storage over the years: it is expected to rise by almost 55 GW in a span of 25 years [3].

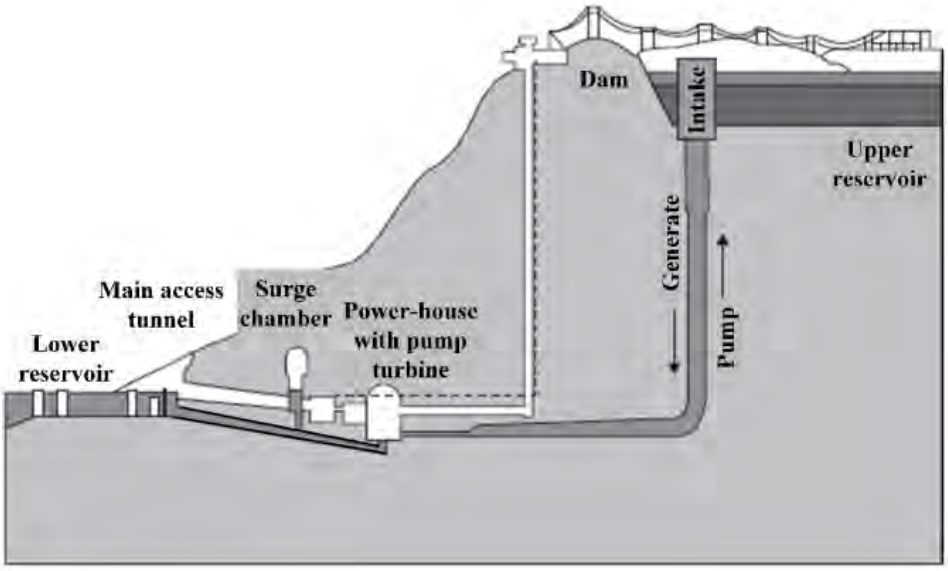

Figure 5. Schematic diagram of a pumped hydro storage system. The potential energy stored by water is converted into electricity at convenient time [27].

Table 2. Existing pumped hydro storage projects in the United States [30].

Project	Initial Operation	Installed Capacity (MW)	Hours of Storage	Energy Storage (MWh)	Average Gross Head (feet)	Water Conduit Length (feet)	Length to Head Ratio; L/H	Number of Existing Reservoirs/Lakes
Taum Sauk	1963	350	7.7	2700	809	7003	8.7	0
Yards Creek	1965	330	8.7	2894	723	3700	5.1	0
Muddy Run	1967	855	14.3	12,200	386	1290	3.3	1
Cabin Creek	1967	280	5.8	1635	1159	4340	3.7	0
Seneca	1969	380	11.2	3920	736	2520	3.4	1
Northfield	1972	1000	10.1	10,100	772	6790	8.8	1
Blenheim Gilboa	1973	1030	11.6	12,000	1099	4355	4.0	0
Ludington	1973	1888	9.0	15,000	337	1252	3.7	1
Jocassee	1973	628	93.5	58,757	310	1700	5.5	1
Bear Swamp	1974	540	5.6	3019	725	2000	2.8	0
Raccoon Mountain	1978	1370	24.0	33,000	968	3650	3.8	1
Fairfield	1978	512	8.1	4096	163	2120	13.0	0
Helms	1984	1200	118.0	14,200	1645	20,519	12.5	2
Bath Country	1985	2100	11.3	23,700	1180	9446	8.0	0

The energy produced from a given quantity of water depends on the head, which is the distance between the turbines and the upper reservoir. The larger the head, the greater the energy generated for a given volume of water will be. Now, the energy required to pump the water from the lower reservoir to the upper reservoir is given by [30]:

$$P = \gamma Q \Delta H \quad (1)$$

where,

γ = Specific weight of the fluid [lb/ft^3; N/m^3]
Q = Flow rate [ft^3/s; m^3/s]
ΔH = Change in head [ft; m]

Now if the efficiency is η, the power generated from the turbine will be [30]:

$$P_{generating} = \eta \gamma Q \Delta H \quad (2)$$

3.1.2. Compressed Air Energy Storage (CAES)

The compressed air energy storage (CAES) is a technology where compressed and pressured air is utilized to store energy. From the late 19th century, systems using CAES technology as an energy distributing medium have been installed in countries such as the United Kingdom, Germany, France, etc., for supplying power to industrial motors, especially in the textile and printing industries [27]. In 1979, Huntorf power plant was built in Germany, where CAES technology was used as an adjunct to the power grid [27]. The CAES technology along with PHS are the only large-scale energy storage systems available. In comparison with PHS, CAES is much smaller in size, however its construction sites are much more widespread, which means that CAES is capable of offering is a more widely distributed large scale storage network [27]. The capacity of CAES systems range from 35 MW to

300 MW, which makes them suitable in stationary applications such as area and frequency regulation, energy arbitrage, and load levelling [3].

The CAES plant consists of two major components—a storage vessel, and a compressor/expander. The storage vessel is used to store air at high pressure without any pressure loss. The air is compressed using the compressor and, when needed, expanded by the expander. The CAES power plant is very similar to PHS when considering its operation. Surplus electricity during the off-peak time, i.e., when demand and energy rate is low, is used to compress the air at high pressure and store it in the storage chamber. During the peak time, this stored energy is retrieved by expanding the compressed air through the expander. In this type of system, rotary gas turbine compensators are used. In some complex CAES systems, two compressors are used where output of one compressor is fed to the other to improve the efficiency. When energy is required, the compressed air is extracted from the storage vessel and is fed into a combustion chamber. It is then mixed with fuel and burnt in the combustion chamber between the first and second chambers. In this case, the generation of electricity and compression of air is separate, hence the CAES plant turbine operates well in both partial and full load conditions [27]. The schematic of the CAES plant according to [30] is represented in Figure 6.

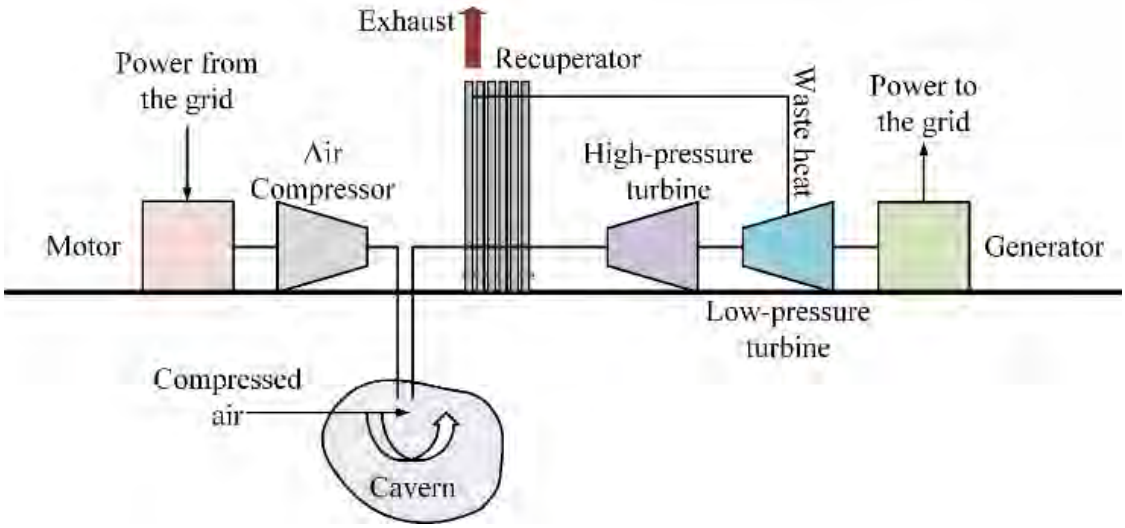

Figure 6. Schematic diagram of a compressed air energy storage (CAES) Plant. Air is compressed inside a cavern to store the energy, then expanded to release the energy at a convenient time.

For modelling the CAES system, Hossein et al. considered the air as ideal gas, having a specific heat independent of temperature [31]. One full charge and one full discharge cycle were considered at full load of the compressor and expander, while ignoring the no-load and partial load conditions. The general ideal gas formulas are represented in Equations (3)–(7), which respectively denote the mass of air inside the cavern, specific enthalpy of air, specific internal energy of air, specific entropy of air, and specific steam energy of air. The temperature was set at 250 °C, whereas the pressure was considered to be 101 kPa.

$$m = \frac{PV}{RT} \tag{3}$$

$$h = (T - T_0)C_p \tag{4}$$

$$u = (C_v T) - \left(C_p T_0\right) \tag{5}$$

$$s = C_p \ln\left(\frac{T}{T_0}\right) - R \ln\left(\frac{P}{P_0}\right) \tag{6}$$

$$\psi = (h - h_0) - (s - s_0)T_0 \tag{7}$$

The air storage has a definite volume, whose pressure ranges from a minimum (P_{em}) and a maximum (P_{fl}) during the processes of charging and discharging. In practice, the cavern is not fully discharged to maintain its mechanical integrity and to ensure high-enough flow rates for the discharging air. When all the working air has been withdrawn, i.e., at the end of the discharge phase, the air mass remaining at the storage is called "cushion air". The cavern has been modeled as adiabatic. The rate of heat transfer depends on several factors. The ambient environment (subscript 0) is set at the standard ambient temperature and pressure of T_o =25 °C and P_o =101 kPa. In the equations to follow, the subscripts denote the following: CN indicates the cavern, CL indicates the cooler, CM indicates the compressor, NG indicates natural gas, TB indicates turbine. Q and W indicate the heat and work exchanges between the surrounding and the system.

After each compression stage, the heat exchangers are assigned a fixed approach temperature Tac, which is the difference between temperature of the cooling fluid entering the cooler ($T^{CL}_{in,coolant}$) and the temperature of the cooled compression air leaving the cooler $T^{CL}_{out,air}$ [31]. The inlet temperature of the cavern and output of all compressor coolers (T^{CN}_{in}) will have a constant value.

$$T^{CN}_{in} = T^{CL}_{out,air} = T_{ac} + T_0 \tag{8}$$

The expander has two operation stages—high pressure (*HP*) and low pressure (*LP*). The aforementioned stages have equal yet variable expansion ratios (*XR*), which are expressed as XR_{HP} and XR_{LP}, respectively.

$$XR_{HP} = XR_{LP} = \sqrt{\frac{P_0}{P_{CN}}} = \sqrt{XR} \tag{9}$$

Let Q be the heat flow. Applying the first and second law of thermodynamics work, heat and energy fluxes are determined for each component of the system. Using the Equations (10)–(14), the roundtrip energy efficiency ($\eta_{storage}$), work ratio (*WR*), heat rate (*HR*), emissions intensity (GI_{plant}), and energy density can be determined.

$$\eta_{storage} = \frac{W_{TB}}{-W_{CM} + X_{NG} - W_{electrolysis}} \tag{10}$$

$$WR = \frac{-W_{CM} - W_{electrolysis}}{W_{TB}} \tag{11}$$

$$HR = \left(\frac{m_{NG} LHV_{NG}}{W_{TB}}\right)\left(\frac{3.6GJ}{MWh}\right) \tag{12}$$

$$GI_{plant} = (HR)(GI_{NG}) \tag{13}$$

$$\rho = \frac{W_{TB}}{V} \tag{14}$$

Finding a suitable geographical location for the storage tank or underground cavern is another major obstacle of the CAES technology [3]. The recently proposed over-ground carbon fiber tank, which is capable of handling high pressures for small- and medium-scale adiabatic CAES systems can be a potential solution the aforementioned limitation [32,33]. The decentralized small-scale CAES system can also be a viable and low-cost solution to this problem. It can also be used to supply electricity to remote places that are not easily accessible [34]. According to [35], the hybrid CAES plants with integrated wind shore plants showed improved efficiency with reduced output power fluctuations when compared to conventional CAES systems. Some advanced CAES technologies and their comparisons are represented in the following sections.

Advanced Adiabatic Compressed Air Energy Storage (AA-CAES)

A major disadvantage of the conventional CAES system is that it is not very environmentally friendly. During the compression process, a prolific amount of heat is generated, which is discharged through the radiator directly to the atmosphere [36]. In addition, during the expansion process, the required heat is generated by means of fossil fuel combustion, due to which a large amount of CO_2 is emitted [3,36]. To overcome this, adiabatic CAES system has been developed, which does not require any combustion, since a thermal storage system is integrated with the existing CAES [3]. According to [3], this system has achieved an efficiency of nearly 70% and has high potential in small- and medium-scale applications. The schematic diagram of an advanced adiabatic CAES system is represented in Figure 7. Here, the heat released during the compression stage is stored in an adiabatic container and is reused during the expansion stage. An adiabatic process occurs without exchanging heat or mass with the surroundings. Contrary to an isothermal process, an adiabatic process liberates energy to the environment only in the form of work. Before the air enters the air reservoir it goes through the thermal storage and gets heated.

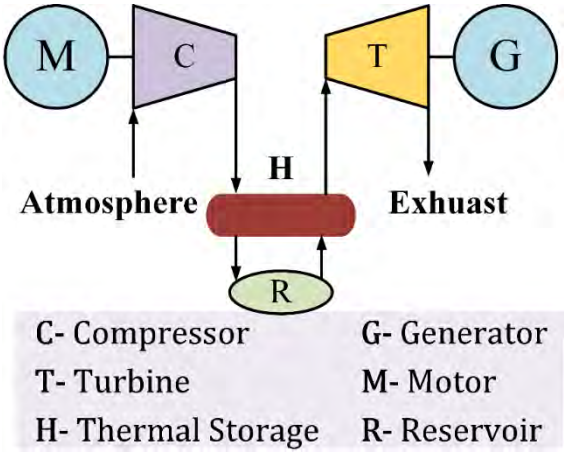

Figure 7. Schematic diagram of advanced adiabatic compressed air energy storage (AA-CAES) system, which is greener than CAES system since it does not release heat into the environment and stores air adiabatically [36].

Liquid Air Energy Storage (LAES)

In recent times, liquid air energy storage (LAES), which is similar to the CAES technology, has gained much attention [27]. In this type of storage, a liquid instead of air is compressed; this is more advantageous than the CAES system in terms of space demands. Using liquid instead of air increases the energy storage density of the system [36]. However, it requires cryogenic liquefaction technology, which makes this system more complex than the CAES [27]. The schematic of LAES is represented in Figure 8, where there are two stages of cycle operation. During the charging stage, the air is liquefied by means of pressure from the compressors and is stored in a low-temperature storage tank. In the discharging stage, the liquefied air is turned into high-pressure air and is allowed to expand through the high temperature expander to drive motors. The design of LAES integrated with wind turbines solves the intermittency problems of wind energy as well as other renewable energy sources. A modified LAES, based on the gas turbine plant, was proposed by Chino et al. and it attained an energy storage efficiency of 73% [36].

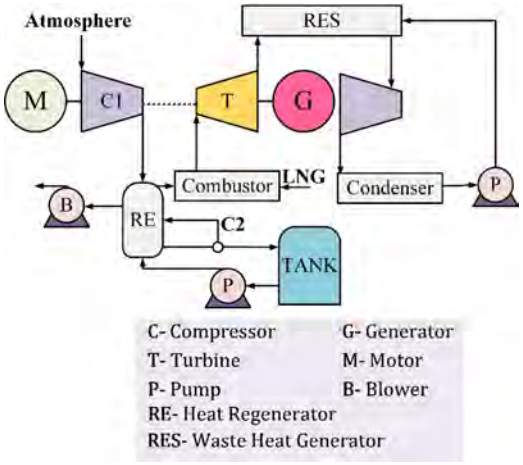

Figure 8. Schematic diagram of liquid air energy storage (LAES) system, where air is liquefied under pressure and stored at low temperature, and then expanded into gaseous form again at high temperature [37].

Supercritical Compressed Air Energy Storage (SC-CAES).

The supercritical compressed air energy storage (SC-CAES) system has high energy density, high thermal efficiency, and is less harmful to the environment when compared to the other CAES systems described previously [36]. It possesses the combined advantages of both the AA-CAES and LAES systems. In this type of system, the air is compressed to a supercritical state having a pressure greater than 37.9 bar and temperature greater than 132 K. This supercritical air after passing through a heat exchanger is stored in a tank as liquid air. The heat exchanger collects the heat from the supercritical air, which is utilized to generate power [37]. There are two methods of liquefying the air—using a throttle liquefaction valve or using a liquefied expander. The throttle liquefaction valve uses the cooled effect of air to obtain the liquid air by the throttling process. The temperature is reduced due to the throttling, which is an irreversible process. Therefore, this process consumes a large amount of energy as well as causes cavitation [36]. On the other hand, by replacing the throttle valve with the liquid expander, throttling depressurization effect can be achieved [37]. According to [38], the SC-CAES system can have energy densities 18 times higher than the conventional CAES with a round trip efficiency of 67.41%. The schematic diagram of the SC-CAES system is represented in Figure 9. A comparison of different types of CAES systems is represented in Table 3.

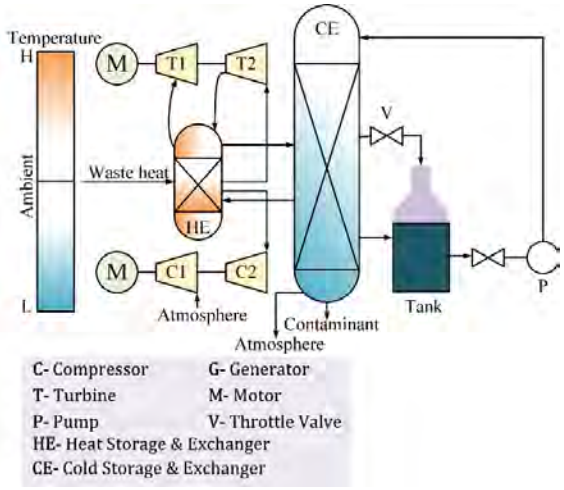

Figure 9. Schematic diagram of SC-CAES system, where air is pressurized into a supercritical state at high temperature and pressure, and then expanded when required [36].

Table 3. Comparison among different CAES technologies [36].

Technology	Energy Density (Wh/L)	Power Rating (MW)	Storage Duration	Lifetime (Years)	Discharge Time	Cycling Times (Cycles)
Large CAES	2–6	110 & 290	Hours–months	20–40	1–24+ hour	8000–12,000
AA-CAES	2–6	110 & 290	Hours–months	20–40	1–24+ hour	-
LAES	8–24	0.3 & 2.5	-	20–40	1–12+ hour	-
SC-CAES	8–24	110 & 290	Hours–months	20–40	1–24+ hour	-
Small CAES	2–6	0.003 & 3	Hours–months	23+	Up to - hour	Test 30,000

3.1.3. Flywheel Energy Storage (FES)

The flywheel energy storage (FES) comprised of steel was first developed by John A. Howell in 1983 for military applications [14]. FES possesses high energy and power density, high energy efficiency, and its power ranges from KW to GW range [39–42]. Furthermore, it has energy storage capabilities up to 500 MJ. These attributes make the FES useful for wide range of energy storage applications in the field of power system, military system, satellites, transportation, etc. [41]. When compared to batteries, FES have longer cycle and the instantaneous response time is also higher. In addition, the depth of discharge (DoD) of the FES systems are also low; therefore, they are much more suitable for uninterruptable power supply (UPS) applications and managing the electrical disturbance occurring on the power systems [43–45]. The FES also has high potentiality in load levelling and peak shaving applications, where energy is stored during the off-peak time and this stored energy is used during the off-peak time [42].

The flywheel uses the kinetic energy, i.e., rotational energy of a massive rotating cylinder to store the energy in the form of mechanical energy. Through magnetically levitated bearings, this large cylinder is supported over a stator and electric motor/generator is coupled with the flywheel. The fundamental parts of the flywheel system are represented in Figure 10. To mitigate the frictional losses and shear disturbance, the whole flywheel is placed in low pressure or a vacuum state. The flywheel system stores and releases kinetic energy according to the energy demand. During the charging stage, by means of electric motor, the flywheel system rotates at a very high speed and stores the kinetic energy. Whereas, in the discharging state, this stored kinetic energy is used to rotate the motor, which functions as a generator and produces electric energy [42]. In the load levelling and peak shaving applications, by means of appropriate control systems and converters, the FES stores the kinetic energy during the off-peak time, when the demand is low and this stored energy is used during the peak time, when the demand is high. They also can be used to reduce the intermittencies of renewable energy system by supplying real power to the system when necessary.

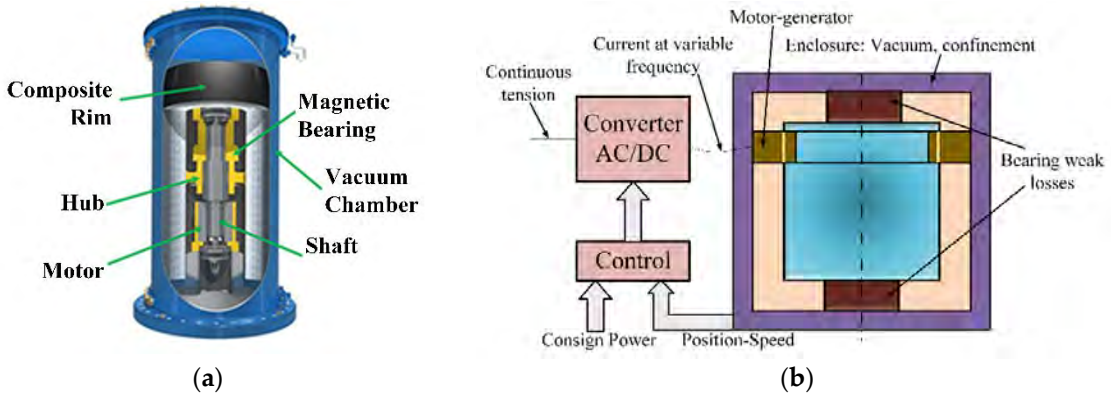

Figure 10. (**a**) Flywheel energy storage system where energy is stored as rotational kinetic energy of a cylinder in vacuum; (**b**) schematic diagram of flywheel energy storage (FES), also called accumulator [37].

Based on the rotational speed ω, the FES can be categorized into two types—low-speed FES and high-speed FES [37]. The low-speed FESs have a rotational speed of less than 6000 rpm, whereas high-speed FESs have a rotational speed of about 10^4 – 10^5 rpm [42]. The low-speed conventional FES is highly suitable for uninterrupted power supply and power reliability applications and its cost is also low. On the other hand, the high-speed FESs are particularly suitable for traction and aerospace applications and can be partially or fully integrated with electrical machines. However, the cost of high-speed FES is almost five times higher than the cost of conventional low-speed FES [43]. The characteristics of low- and high-speed FES are summarized in Table 4.

Table 4. Comparison among the characteristics of low-speed and high-speed flywheel energy storage system (FESS) [42].

Characteristic	Low-Speed FESS	High-Speed FESS
Flywheel material	Steel	Composite materials: glass and C fibers
Electrical machine	Asynchronous, permanent magnet synchronous and reluctance machines	Permanent magnet synchronous and reluctance machines
Integration of electrical machine and flywheel	No or partial integration	Full or partial integration
Confinement atmosphere	Partial vacuum or light gas	Absolute vacuum
Enclosure weight	2× flywheel weight	$\frac{1}{2}$× flywheel weight
Bearings	Mechanical or mixed (mechanical and magnetic)	Magnetic
Main applications	Power quality	Traction and aerospace industry
Cost	1	5

The amount of stored energy in a flywheel depends on the rotor shape and material. If E is the stored energy, I is the moment of inertia, and ω is angular velocity of the rotor, then according to [41],

$$E = \frac{1}{2} I\omega^2 \tag{15}$$

For limiting the voltage variations and maximum mg torque, the flywheel is operated within a certain speed limit. If maximum and minimum speed is ω_{max} and ω_{min}, respectively, the useful energy of the flywheel will be:

$$E = \frac{1}{2} I\left({\omega_{max}}^2 - {\omega_{min}}^2\right) = \frac{1}{2} I{\omega_{max}}^2\left(1 - \frac{{\omega_{min}}^2}{{\omega_{max}}^2}\right) \tag{16}$$

The moment of inertial I, depends on the mass and shape of the rotor. Generally, flywheels are built as solid or hollow cylinders, and it ranges from short disc type to long drum type [46,47]. For solid cylinder type or disc type flywheel, moment inertia will be [41]:

$$I = \frac{1}{2} mr^2 \tag{17}$$

Here, r is the outer radius and m is mass of the rotor. Now, if the flywheel has a length of h and mass density of ρ, and the it is a hollow cylinder with an inner radius of a and outer radius of b.

$$I = \frac{1}{2}\pi\rho h\left(b^4 - a^4\right) \tag{18}$$

Thus,

$$E = \frac{1}{4}\pi\rho h\omega^2\left(b^4 - a^4\right) \tag{19}$$

The strength of the rotor material, i.e., the stress experienced by the rotor is denoted by σ. The maximum energy density and maximum specific density both are proportional to maximum tensile strength of the rotor material (σ_{max})

$$\sigma_{max} = \rho r^2\omega^2 \tag{20}$$

Rotor geometries also has an effect on the specific energy and energy density and is accommodated by introducing a shape factor K [41]. It is a measurement of how much the rotor materials are utilized in storing the energy [48]. The values of K for different types of flywheel geometries are represented in Figure 11.

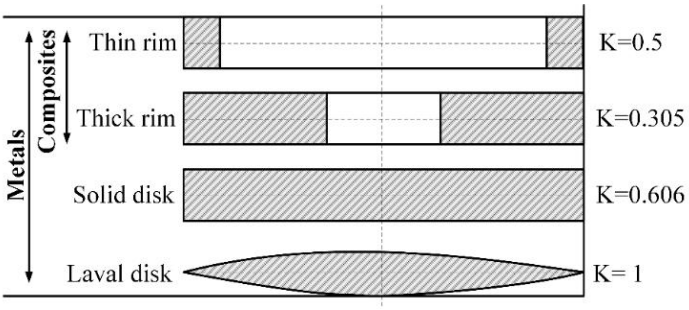

Figure 11. Different flywheel cross sections with differing values of the shape factor K [42].

The maximum specific energy will be

$$\frac{E}{m} = K\frac{\sigma_{max}}{\rho}[\mathrm{J/kg}] \tag{21}$$

and the maximum energy density will be

$$\frac{E}{V} = K\sigma_{max}\left[\mathrm{J/m^3}\right] \tag{22}$$

3.2. Thermal Energy Storage

Thermal energy can be stored in the form of latent heat, sensible heat, and reversible thermochemical reactions. Thermal energy storage (TES) has been in use for a long time for energy redistribution and energy efficiency on short- or long-term basis [37]. In TES, energy is hoarded by cooling or heating a medium, which can be used to cool or heat other objects, or even for generating power [49]. TES finds applications in industries or buildings, and can increase the overall efficiency, reliability, and economics. This system is entirely eco-friendly. TESs are often used in conjunction with solar photovoltaic (PV) systems, wherein the heat energy of the sun is efficiently stored. This way, apart from producing photo-electricity, the solar PV systems can ensure the harvesting of a greater amount of energy from the sun, which can be used during the night or at times of climatic vagaries. Solar concentrators also utilize TESs for the purpose of storing the heat energy concentrated from the sunlight. TES systems can effectively pave the way towards a future with 24-h solar power. Furthermore, they find wide applications in load shifting and electricity production for heat engines. TES has low self-discharge losses (0.05–1%), good energy density (80–500 Wh/L), high specific energy (80–250 Wh/kg), and low capital cost (3–60%), although also has low cycle efficiency of 30–60% [26]. According to the range of operating temperatures, TES can be classified into two types: Low-temperature TES and high-temperature TES, which are described as follows.

3.2.1. Low-Temperature Thermal Energy Storage

In low-temperature TES, the operating temperature of the heat storing material is similar to the spatial temperature of the heating or cooling application. Heat energy can be stored within and extracted from the heat storing material. To exemplify, for cooling purposes, chilled water, phase change materials, or ice can be used during peak hours; thus, load shaving can be accomplished, i.e., the peak load can be shifted to off-peak periods. Cryogenic energy storage (CES) is a special type of low-temperature TES where the substance used for cooling, called cryogen, such as liquid air or liquid nitrogen, is produced during off-peak hours and used during peak hours. The cryogen is produced using renewable power sources or from mechanical energy of turbines. During peak hours, the cryogen is heated, boiled, and used for electricity generation using a cryogenic heat engine arrangement, whose schematic is depicted in Figure 12. CES systems have a high energy density of about 100–200 Wh/kg, making the per unit capital cost quite low. CES systems also have long storage durations and are eco-friendly, which makes them promising candidates for commercial use. However, compared to energy consumption, CES systems are not very energy efficient (only 40–50%) [37]. Low-temperature TES are good for applications with high power density, such as load shaving, industrial cooling, and grid power management [3].

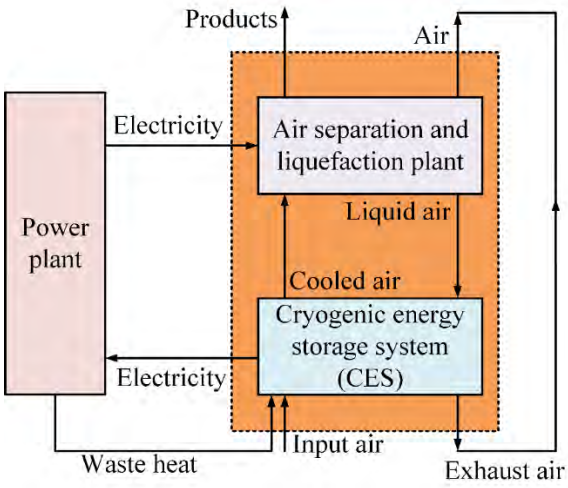

Figure 12. Schematic diagram of cryogenic energy storage (CES), which is a special type of low-temperature thermal energy storage (TES) where a cryogen, such as liquid air or liquid nitrogen, is produced during off-peak hours and used during peak hours [37].

3.2.2. High Temperature Thermal Energy Storage

In high-temperature TES system, energy is stored as sensible heat and latent heat. The heat absorbed or released by a body that changes its temperature without changing its state, pressure, or volume is known as sensible heat. On the other hand, the heat absorbed or released by a body that only changes its state without changing its temperature is called latent heat. The amount of heat energy that can be stored by a body depends on its specific heat and heat capacity. The body, otherwise called the heat storage medium, can be in any form, such as liquid or solid. A major disadvantage of TES is its huge space occupation [3].

Sensible heat storage (SHS) is the simplest method of TES. The temperature of a body rises linearly with increase of heat energy, as demonstrated in Figure 13a. The specific heat of water being one of the highest (4200 J/kg-K) and its abundance tied with low cost makes water an ideal choice for SHS. Water is used as the heat storage medium in many residential and industrial applications. For relatively large-scale applications, solid and liquid heat storage media are used to store heat underground to cope with the space requirements. SHS offers two primary benefits of being inexpensive and non-toxic.

The amount of heat stored depends on the mass of storage material, its specific heat, and the change of temperature [49], and is given by,

$$Q_s = \int_{t_i}^{t_f} mc_p dt = mc_p\left(t_f - t_i\right) \tag{23}$$

where Q_s is the quantity of heat stored, in Joules; m is the mass of heat storage medium, in kg; c_p is the specific heat, in J/(kg.K); t_i is the initial temperature, in °C; t_f is the final temperature, in °C.

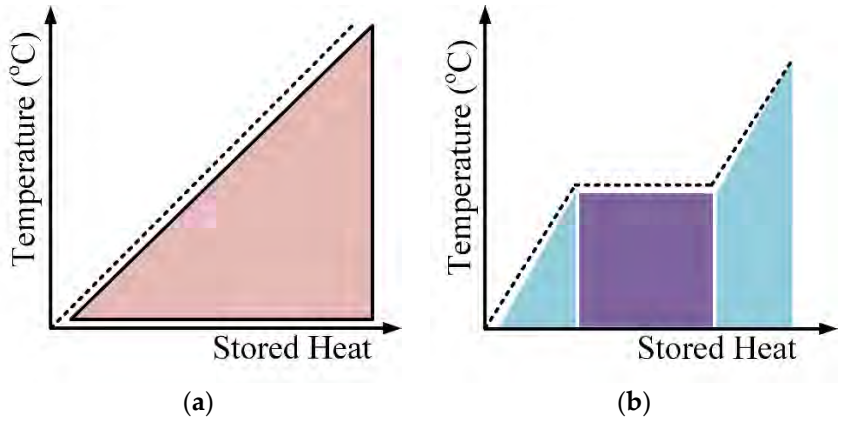

Figure 13. Two methods of storing thermal energy (**a**) sensible heat, which linearly rises the temperature of the body (**b**) latent heat, which changes the state of the body without rising its temperature [37].

The materials used in latent heat storage (LHS) are frequently referred to as phase change materials (PCM) because they can change their physical state upon application or withdrawal of heat. LHS systems are characterized by high energy density. The latent heat is stored in the state change process, which occurs isothermally, i.e., at a constant temperature. The heat energy during this process is utilized to change the physical change by altering the intermolecular forces of attraction, rather than to increase the temperature. The isothermal property of the LHS is a clear advantage over the SHS. Figure 13b shows that the temperature rises steadily up to a certain point, remains steady until the process of state change is complete, and then rises again linearly [49].

In LHS, the exchange of energy takes place during the state change through metallic fillers or metal matrix structures. Based on the combinations, PCMs are of three types, such as solid–solid, solid–liquid, and liquid–gas PCMs. Among these, the solid–liquid PCMs are the most appropriate for TES systems. The solid–liquid PCMs can be either organic (paraffin or organic acids), inorganic (salt hydrates or metallics), or eutectic (i.e., with a very low melting point) [3]. For a solid–liquid PCM, the heat energy stored in a mass m is given by,

$$Q = m\left[c_{ps}(T_m - T_s) + h + c_{pl}(T_l - T_m)\right] \tag{24}$$

where c_{ps} and c_{pl} are the specific heats of the solid and liquid states, respectively, h is the state change enthalpy, and T_m, T_s, T_l are the melting temperature, solid temperature, and liquid temperature, respectively.

The energy storage capacity of the system is defined by the melting point and the enthalpy of state change of the PCM. LHS systems can also be called "hidden heat storage systems" because the latent heat appears to be hidden since it is not expressed in terms of temperature change. LHS constitutes a high storage density irrespective of the size of the storage reservoir. LHS is better than SHS in terms of efficiency and economy. So, LHS systems can be readily deployed for use in buildings. In advanced concentrated solar power (CSP) plants, there are two reservoirs with molten salt as the storage material, one for SHS and the other for LHS. In these reservoirs, heat from solar energy can be

stored at temperatures of 5000°C and 2850°C, respectively. In future smart grids, quartz glass, room temperature ionic liquids, highly pure graphite, PCM, rock bed storage, and saturated steam/water storage methods can be used for TES at temperatures of 400–1000°C. These materials have low melting points, high temperature, and low cost [3]. Furthermore, concrete or other castable materials are used for heat energy storage, and are aided by synthetic oil as the heat transfer fluid [26].

3.3. Electrostatic and Magnetic Energy Storage

Energy can be stored in the form of electric and magnetic fields by means of supercapacitors and superconducting magnets, respectively. They are storage devices with high power and medium energy density and are useful in meeting peak power demands, output power smoothing, and recovery of energy in mass transit devices [3]. This section can be described in two main subsections—electrostatic and magnetic energy storage. Electrostatic energy storage is mainly in the form of capacitors and supercapacitors. Supercapacitors are also popularly known as electric double layer capacitor (EDLC).

3.3.1. Electrostatic Energy Storage

Capacitors are devices that have the capability to store electrical energy between two conductive metal plates separated by an insulating medium, i.e., in the form of electrostatic energy. When voltage is applied across the conductive plates, electric charges are stored between them [37]. The capacitance of a capacitor depends on the distance between the plates, the dielectric constant of the insulating medium, and size of the conductive plates. The energy storage capacity is directly proportional to the capacitance of the capacitor. The capacitors possess long life cycle and instantaneous recharging capabilities; however, the energy density is very low. Therefore, they are particularly useful for small-scale power control applications but cannot be used for large-scale storage applications, which require large dielectric medium area, making it very expensive and unrealistic [37]. The supercapacitors, also known as ultracapacitors and electrochemical capacitors-patented by the Japanese company Nippon Electric Company (NEC) in 1975, overcome the aforementioned disadvantages of the conventional capacitors [50]. Supercapacitors have very high charge density, and their energy storage capacity can be increased from 1 kWh to larger storage units [37]. Furthermore, they have a life expectancy of 12 years with a cycle life 500,000 times that of conventional capacitors, and a very high-power output, which can reach a range of 50–100 KW. However, when compared to lead acid batteries, they have very low energy density (5 Wh/kg), low voltage characteristics, and high self-discharge rate [37]. Nevertheless, by interconnecting them in series configuration and ensuring proper controls, they can have an extremely high-power output. Therefore, supercapacitors are particularly useful for applications where instantaneous high-power output is required, such as engine cranking applications of hybrid vehicles, permanent magnet synchronous generator, etc.

The supercapacitor and conventional capacitor have very similar operating principles. However, in supercapacitors, the traditional dielectric materials such as ceramic, polymer films, etc., are not used to separate the conductive plates [51]. Rather, electrolytic physical barrier comprising of activated carbon, which allows ionic conduction, is used to separate the plates. The ion conduction enables the supercapacitor to have very large specific area, which results in having a higher energy density [37]. Another major difference between the conventional capacitors and supercapacitors is in the electrode materials. Supercapacitors use carbon nano tube (CNT)-based electrodes, which offer a very large surface area with an extremely small separation distance, which allows an absorption of a large amount of charge; therefore, the energy density is further increased [51,52]. Under an electric field, the electrolyte acts as a dielectric and an ion absorption layer is formed on the activated carbon fibers [51,53]. The charging and discharging occur on this ion absorption layer. The schematics of conventional capacitor and supercapacitor are represented in Figures 14 and 15, respectively.

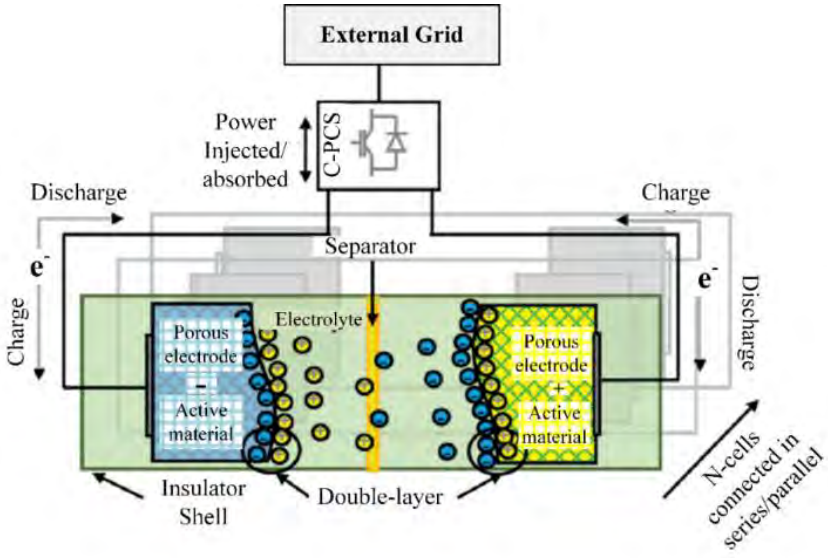

Figure 14. Schematic diagram of a conventional capacitor storage system connected to the external grid trough a converter [37,54].

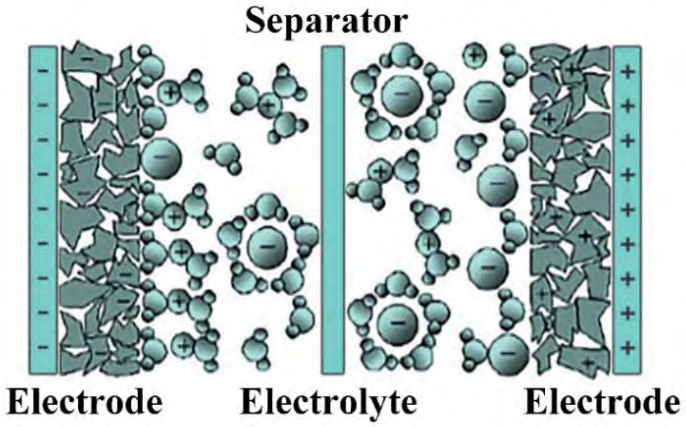

Figure 15. Schematic view of an individual cell of a supercapacitor; under an electric field, the electrolyte acts as the dielectric and the electrodes are made of carbon nanotubes (CNT) [37,55,56].

If C is capacitance and V is the voltage across the capacitor, then the energy stored in an electric field of a supercapacitor is given by [51]:

$$W_{SC} = \frac{CV^2}{2} \tag{25}$$

Equation (25) represents the total energy accumulated in a capacitor. However, in practical applications, a 50% voltage drop from the nominal value is acceptable during discharging. Therefore, capacitor stored energy will be [51]:

$$W_{SC} = \frac{C}{2}\left[V^2 - \left(\frac{V}{2}\right)^2\right] = \frac{3}{8}CV^2 \tag{26}$$

The simplified equivalent circuit of the supercapacitor is represented in Figure 16. Here, R_{esr} is the equivalent series resistance that contributes to the energy loss at the time of charging and discharging, R_p is the equivalent parallel resistance, which represents the energy loss of the supercapacitor due to self-discharge, L is an inductance, which is very small and is a result of the physical construction of the supercapacitor. The total capacitance of the supercapacitor cell can be expressed as the sum

of a constant capacitance C_o and a variable capacitance whose value is dependent on the cell voltage V_{cell} [57].

$$C_{cell} = C_o + kV_c \tag{27}$$

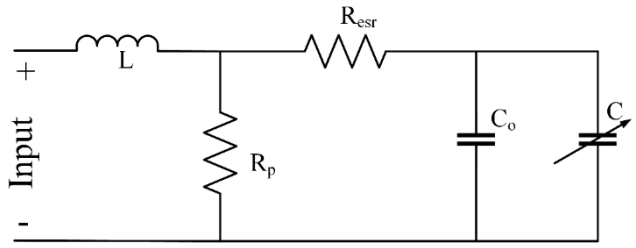

Figure 16. Simplified equivalent circuit of the supercapacitor comprising of two resistors, one inductor, and two capacitors [57].

Now, if the discharging time is t_{dch}, then the energy efficiency will be [57]:

$$\eta_{eff} = e^{-\frac{2R_{ESR}C_{cell}}{t_{dch}}} \tag{28}$$

Electric Double Layer Capacitor (EDLC)

The electric double layer capacitor (EDLC) has a very similar capacitance mechanism to the conventional capacitors [58]. However, its large interfacial surface area of electrodes offers a much higher charge density than the conventional capacitors [59]. The schematic diagram of EDLC is represented in Figure 17.

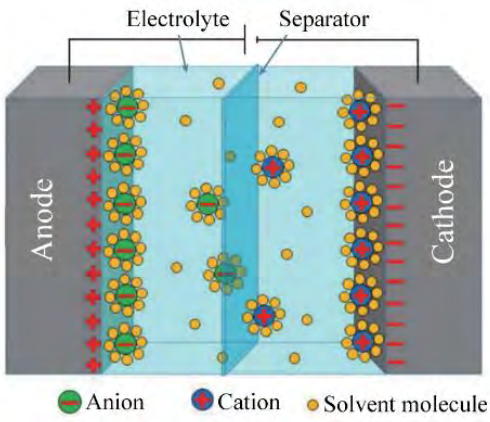

Figure 17. Schematic representation of an electric double layer capacitor (EDLC), where two electrodes are submerged in an aqueous electrolytic solution and are separated by an ion permeable separator [59].

Here, two electrodes are submerged in an aqueous electrolytic solution and are separated by a separator, which is ion permeable. The function of the separator is to avoid short circuit between the electrodes and each electrode is attached with a metallic current collector. The reversible absorption of ions by the electrode from the electrolyte causes the energy to be stored electrostatically inside the EDLC [60]. In this charge storage process, no charge is transferred across the interface of the electrolyte and the double layer of electrode material, rather ion is absorbed. There will be an excess or deficit of charge at the electrode surface, which results in creating oppositely charged ions in the electrolyte and capacitance arises due to the true capacitance effect. This capacitance depends on the width of the binary layer at the electrolyte-electrode boundary and its thickness is much smaller when compared

to the width of the separator [59]. The capacitance can be measured using the general capacitance equation [61]:

$$C = \frac{A\epsilon_0}{d} \tag{29}$$

where C is the capacitance, A is the surface area, ϵ_0 is the permittivity of free space, and d is the effectual length of the electric double layer also called the Debye length. The storing of charge due to the double layer mechanism is a surface process. Therefore, the surface characteristics of the electrode materials has a notable impact on the capacitance. In recent times, carbon-based materials are used as the electrode owing to having a large surface area, less cost, and availability. The different materials and their corresponding capacitances are tabulated in Table 5.

Table 5. Various ELDC electrode materials, electrolytes, and their specific capacitance [59].

Electrode Material	Electrolyte	Specific Capacitance (Fg-1)
AC	Aqueous (NaOH/KOH)	200–400
Templated carbon	Aqueous (NaOH/KOH)	120–350
CNT	Aqueous (NaOH/KOH)	20–180
Carbide-driven carbon	Ionic liquids (KCl/NaCl)	100–150
Carbon black	Aqueous (NaOH/KOH)	<300
Carbon Aerogels/xerogels	Aqueous (NaOH/KOH)	40–200
Graphite and reduced Graphene oxide (rGO)	Tetraethylammonium tetrafluoroborate (Et4NBF4)	10–150
Mesoporous carbon	KOH	180
AC fibers	KOH	180–210

3.3.2. Supermagnetic Energy Storage

The super magnetic energy storage (SMES) system along with the capacitor are the only existing storage systems, which have the capability of storing electrical energy without the need of conversion to another form of energy. In comparison with the other storage systems, the SMES system has large power density and its response time is very short—in the range of few milliseconds. In addition, it has longer cycling time and life expectancy with the feature of controlling the reactive and real power separately by means of distributed SMES (DSMES) [62]. However, the SMES system is not without its inherent disadvantages. Low volumetric and gravimetric energy density, material fatigue due to introduction of mechanical stress, and high cost factors are the main limitations of the SMES system. Nevertheless, due to the high efficiency and very low response time, the SMES system has high potentiality in its load levelling, intermittency reduction, and peak shaving applications.

The SMES system stores electrical energy in a magnetic field without requiring to convert it into chemical or mechanical form [37]. In this system, direct current (DC) is induced into superconducting coils, which exhibit zero resistance to the current flow [62]. These superconducting coils are comprised of niobium-titane (NbTi) filaments and must be maintained below the critical temperature of −2700 °C [37, 62], which is done by integrating a cryogenic system with the SMES. A refrigeration system maintains the temperature of the cryogen below the critical temperature, which requires consuming a prolific amount of energy, therefore, reducing the overall efficiency of the system. However, as the superconducting coil has no resistance, it does not have any ohmic loss, which results in SMES having an overall efficiency of over 95% [62]. The schematic diagram of the SMES system is represented in Figure 18. It is comprised of four main components [62,63], which are as follows:

I. The superconducting magnet, which is kept in a vacuum and is thermally insulated using a Dewar.
II. The cryogenic refrigeration system to maintain the temperature of the superconducting coil below the critical temperature.

III. The power conditioning system, which consists of different power electronic devices such as transistors, capacitors, inductors, etc., and its function is to regulate the electrical energy exchange between the grid and the SMES system.

IV. The control system, whose function is to monitor the different parameters of the system, such as current, pressure, temperature, strain, etc., and tuning the operation of the cryogenic system.

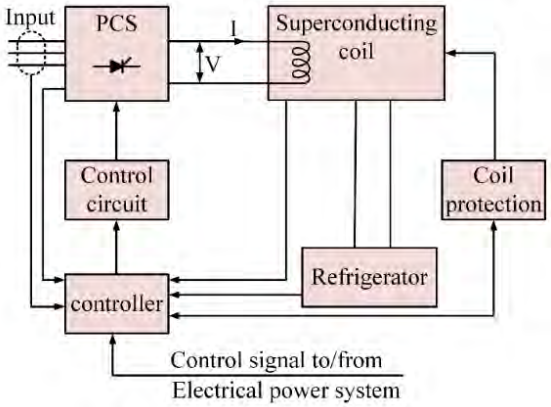

Figure 18. Schematic diagram of an super magnetic energy storage (SMES) system, which consists of four main subsystems and a protection system [63].

In addition to aforementioned subsystems, the SMES also has a protection system, whose function is to protect the superconductor from arc damage, which may arise due to sudden quench [64]. Now, if I is the current flowing through the coil and L is inductance of the coil, then the maximum energy stored in the SMES will be [65]:

$$E_m = \frac{1}{2}LI^2 \approx \frac{1}{2}B_S INS \tag{30}$$

Here, B_S is the saturation magnetic induction, N is the number of turns of the coil, S is the cross-sectional area. Now, the magnetic field strength and the efficiency of the superconductor coil is dependent on the quality factor (Q_{SC}). Now, r and a are defined as the major and minor radius of the coil, respectively, and B_m is the maximum field. Now, the Q_{SC} is described by [65]:

$$Q_{SC} = 5 \times 10^3 \left(\frac{{E_m}^2}{B_m}\right)^{\frac{1}{3}} \times \frac{1}{\left\{\left(\frac{r}{a}-1\right)\left[\frac{r}{a}-\left(\frac{r^2}{a^2}-1\right)^{1/2}\right]^2\right\}^{1/3}} \tag{31}$$

The electrical equivalent circuit of the SMES system is represented in Figure 19. It consists of an inverter, two DC link capacitor, a converter, and a varistor. The DC power is supplied to the SMES system for charging purpose by the converter. The charging and discharging of the SMES is controlled by the switches. During the charging phase of the SMES, the switches Sw1 and Sw4 are closed, whereas switches Sw2 and Sw3 are open. On the other hand, when switches Sw2 and Sw3 are closed and switches Sw1 and Sw4 are open, the SMES is discharged. The varistor function as an overvoltage protection scheme of the SMES and the two DC link capacitors are used for rectification purpose in the input and output side.

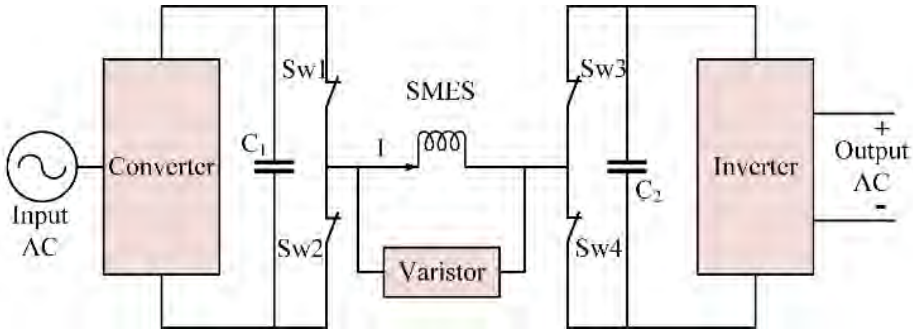

Figure 19. Electrical circuit of the SMES, comprising of an inverter, two DC link capacitors, a converter, and a varistor [65].

3.4. Electrochemical Energy Storage

Electrochemical storage system (ECSS) consists of all rechargeable battery energy storage (BES) and flow batteries (FB), which stores the electrical energy in the form of chemical energy. It is one of the oldest and most mature technologies available [3]. Here, the chemical energy contained in the active materials are converted into electrical energy by means of electrochemical oxidation–reduction reaction [66]. The ECSS, having a wide range of energy density ranging from 10 Wh/kg up to 13 kW/kg, is the largest electrical energy storage system available [67,68]. Furthermore, they have high efficiency of 70–80% and a negligible amount of harmful substance emission [3]. In addition, they require very little maintenance, which makes them a primary contender in energy storage applications. Batteries can be implemented in different utility storage applications such as load shaving, peak leveling, etc. [26].

A schematic diagram of the operation of the Battery Energy Storage System (BESS) is represented in Figure 20. A battery cell consists of two oppositely charged electrodes—anode and cathode. These electrodes are submerged in an electrolyte, which can be in liquid, solid, or viscous state [26]. During the discharge phase, electrochemical reaction takes and the metal in anode dissolves into the electrolyte as anions, leaving behind electrons in the anode. These electrons travel from the anode to cathode through the external circuit; therefore, current is produced due to the flow of electrons. During the charging phase, the electrons travel in the opposite direction, i.e., from cathode to anode. The voltage produced by a single battery cell is not enough to meet the requirements. Therefore, multiple battery cells are connected in series to produce the desired output voltage [3,26].

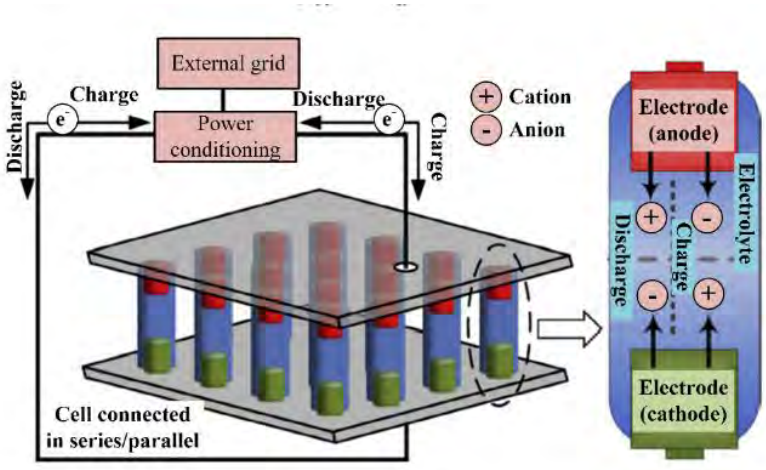

Figure 20. Schematic diagram of a battery energy storage system (BESS) operation, where energy is stored as chemical energy in the active materials, whose redox reactions produce electricity when required [26].

Depending on the chemistry and construction, batteries can be categorized into different types such as lead-acid, lithium ion (li-ion), metal air, nickel-based, flow, lithium polyphosphate (li-po), etc. In this section, a detailed description of various types of BESs is presented. Furthermore, the equivalent electrical circuit modelling of the major BESs are also represented in this section, which is done by experimentally determining the battery parameters such as internal resistance, external resistance, capacitance, electromotive force (EMF), transient response, open circuit voltage, short circuit current, and degradation pattern of the batteries. These parameters are non-linearly dependent on the current state, temperature, and state of charge (SOC) [69]. The reduction chemical reactions which occur in the different battery types and their corresponding reduction potentials are tabulated in Table 6.

Table 6. List of standard reduction potential of chemicals in battery energy storage (BES) [3].

Reduction Half Reaction	Standard Electrode Potential (V)
$\mathbf{F_2(g) + 2e^- \rightarrow 2F^-(aq)}$	+2.87
$\mathbf{S_2O_8{}^{2-}(aq) + 2e^- \rightarrow 2SO_4{}^{2-}(aq)}$	+2.01
$\mathbf{O_2(g) + 4H^+(aq) + 4e^- \rightarrow 2H_2O(l)}$	+1.23
$\mathbf{Br_2(l) + 2e^- \rightarrow 2Br^-(aq)}$	+1.09
$\mathbf{Ag^+(aq) + e^- \rightarrow Ag(s)}$	+0.80
$\mathbf{Fe^{3+}(aq) + e^- \rightarrow Fe^{2+}(aq)}$	+0.77
$\mathbf{I_2(l) + 2e^- \rightarrow 2I^+(aq)}$	+0.54
$\mathbf{Cu^{2+}(aq) + 2e^- \rightarrow Cu(s)}$	+0.34
$\mathbf{Sn^{4+}(aq) + 2e^- \rightarrow Sn^{2+}(aq)}$	+0.15
$\mathbf{S(s) + 2H^+(aq) + 2e^- \rightarrow H_2S(g)}$	+0.14
$\mathbf{2H^+(aq) + 2e^- \rightarrow H_2(g)}$	0.00
$\mathbf{Sn^{2+}(aq) + 2e^- \rightarrow Sn(g)}$	−0.14
$\mathbf{V^{3+}(aq) + e^- \rightarrow V^{2+}(aq)}$	−0.26
$\mathbf{Fe^{2+}(aq) + 2e^- \rightarrow Fe(s)}$	−0.44
$\mathbf{Cr^{3+}(aq) + 3e^- \rightarrow Cr(s)}$	−0.74
$\mathbf{Zn^{2+}(aq) + 2e^- \rightarrow Zn(s)}$	−0.76
$\mathbf{Mn^{2+}(aq) + 2e^- \rightarrow Mn(s)}$	−1.18
$\mathbf{Na^+(aq) + e^- \rightarrow Na(s)}$	−2.71
$\mathbf{Li^+(aq) + e^- \rightarrow Li(s)}$	−3.04

3.4.1. Lead Acid Batteries

Invented in 1859, the lead acid battery was the first battery that could be charged by passing reverse current through it [70]. It has been used for more than 150 years, and thus lead acid batteries are a highly reliable, matured, and globally accepted technology [71]. Their self-discharge rate is very low, which results in less charge fading. On the other hand, they can deliver profuse amount of energy owing to their high discharge rate. Furthermore, it requires negligible maintenance and no memory, therefore, repeated charging of partially charged lead acid battery does not affect the maximum capacity. In addition, according to Battery Council International (BCI), the recycling rate of lead acid batteries is 99.4%, which makes them the top recycled product of the USA [72]. In terms of these advantages of the lead acid battery, they are widely used by many different industries, such as telecommunication, power systems, radio, and television systems, solar, UPS, electric vehicles, automobile, forklifts, emergency lights, etc. [73].

Lead acid batteries consist of two plates—a positively charged cathode and negatively charged anode. The cathode is made up of sponge lead, whilst the anode consists of lead dioxide. Both the

electrodes are immersed in a electrolyte of 37.7% sulfuric acid [6]. Furthermore, in addition to the active materials such as anode, cathode, and electrolyte, the lead acid battery contains other materials such as wood, cardboard, cables and connectors, paper, steel, and polyethylene [74]. The percentages of different material content in lead acid batteries are represented in Figure 21.

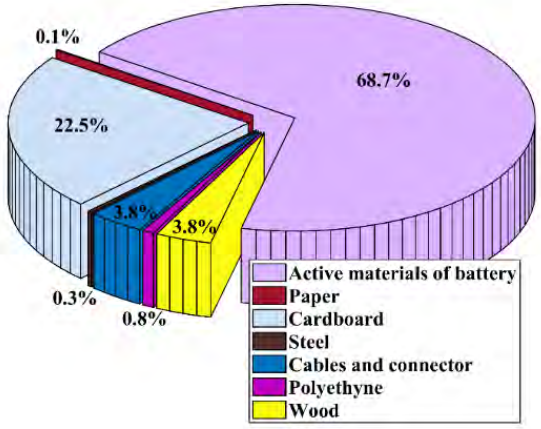

Figure 21. Percentage of different material content in lead acid batteries, with the active material comprising the major portion [74].

During the discharge phase, lead in the negative plate dissolves into the electrolyte to and forms lead sulphate leaving two electrons behind. These two electrons flow through the external circuit to the positive plate. Hereafter, the lead in the positive also dissolves into the electrolyte as lead sulphate. Consequently, the electrolyte loses much of its dissolved sulfuric acid and primarily becomes water. The lead plates become more chemically alike when a battery discharges, causing the acid to weaken and the voltage to drop. The battery will eventually become so discharged that it loses its ability to deliver useful voltage. A battery, however, can be recharged by feeding it electrical current, restoring the chemical difference between the plates and returning the battery to full operational power. The working principle of lead acid batteries is shown in Figure 22. The chemical reactions that take place in the lead acid batteries are given below [71]:

Negative plate reaction: $Pb(s) + HSO_4^-(aq) \rightarrow PbSO4(s) + H_+(aq) + 2e^-$

Positive plate reaction: $PbO_2(s) + HSO_4^-(aq) + 3H^+(aq) + 2e^- \rightarrow PbSO_4(s) + 2H_2O(l)$

Overall chemical reaction: $Pb(s) + PbO_2(s) + 2H_2SO_4(aq) \rightarrow 2PbSO_4(s) + 2H_2O(l)$

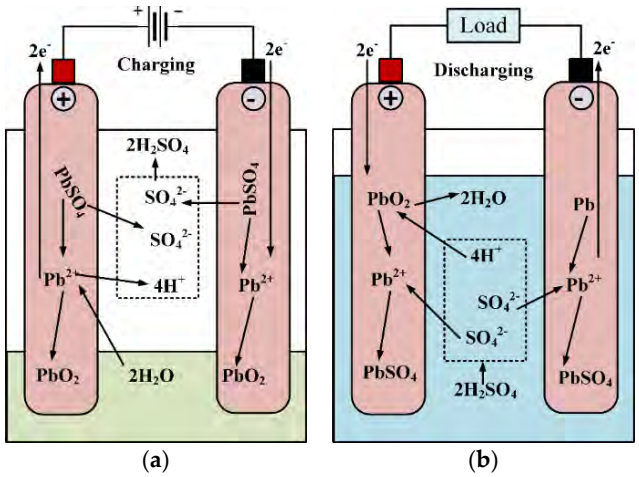

Figure 22. Working principle of rechargeable lead acid battery during (**a**) charging and (**b**) discharging [75].

However, over charging the lead acid battery i.e., exceeding the cell voltage value to ~2.39 V [3], leads to loss of water in the electrolyte. Therefore, water needs to be added as maintenance for proper operation of the battery. On the contrary, during over discharging case, a sulphate layer is formed on the positive plate. This deposition of sulphate layer is a permanent consequence and cannot be reversed by charging the battery. This results in degradation of the life the cycle of the lead acid battery. The chemical reactions during the over-charging phase are as follows [71]:

$$H_2O \rightarrow 2H^+ + \frac{1}{2}O_2 + 2e^-$$

$$Pb + \frac{1}{2}O_2 + H_2SO_4 \rightarrow PbSO_4 + H_2O$$

An arrangement of electrochemical cells that convert chemical energy into electrical energy by means of redox reactions is what is known as an electrical battery. If the open circuit voltage of fully discharged battery can be measured, then lead acid batteries are fully charged [76]. A battery is termed discharged when there are no free charges inside the battery and the cell voltage V_O is the only source of voltage. For mathematical modelling purposes, a simplified equivalent circuit of a lead acid battery is adopted based on the nonlinear Thevenin model, which is illustrated in Figure 23. This model considers the dynamic behavior of the battery caused by the capacitive effects of the plates of the battery, C, the voltage across which is V_c, and by the charge transfer resistance of the battery, R_B. Here, R_c and R_d are the resistances encountered by the battery current i_B during charging and discharging, respectively. V_B is the terminal voltage of the battery.

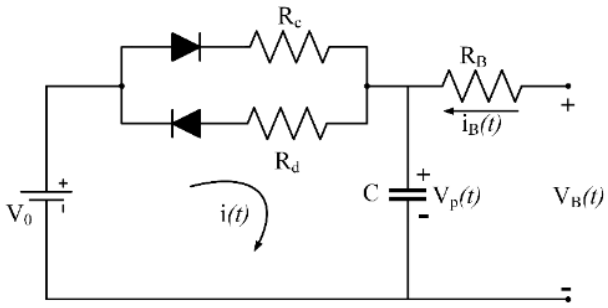

Figure 23. Equivalent circuit of a rechargeable lead-acid battery based on the nonlinear Thevenin model [76].

For designing control strategies for the battery during charging and discharging, the state space equations are needed. For the discharge process, the Equations (32)–(36) are found [76]:

$$V_o = R_d i(t) + \frac{1}{C}\left[i(t) + i_B(t)\right]dt \tag{32}$$

$$V_p(t) = \frac{1}{C}\int \left[i(t) + i_B(t)\right]dt \tag{33}$$

$$V_o = R_d C\frac{dV_p(t)}{dt} + \frac{1}{C}i_B(t) + \frac{1}{R_d C}V_o \tag{34}$$

$$\frac{dV_p(t)}{dt} = -\frac{1}{R_d C}V_p(t) - \frac{1}{C}i_B(t) + \frac{1}{R_d C}V_o \tag{35}$$

$$V_B(t) = V_p(t) - R_B i_B(t) \tag{36}$$

To determine the state-of-charge (SOC) of the battery, Equation (37) can be used,

$$SOC = \frac{v_{OC} - b}{a} \tag{37}$$

where v_{OC} is the open circuit voltage of the battery, b is the terminal voltage of the battery when it is discharged, i.e., SOC = 0%, and a is found by knowing the value of v_{OC} and b at SOC = 100%.

Based on construction, there are two types of lead acid batteries: Flooded and sealed.

Flooded Lead Acid Batteries

Flooded lead acid batteries come in a variety of shapes due to their expansive applications and usage in the industry and is more economical than most of the existing batteries, and therefore are the most widely used batteries on the market [77]. However, to reach its potential life span, extensive maintenance is required in the form of watering, equalizing charges, and keeping the terminals clean [78,79]. It can deliver a peak current of approximately 450 A [73]. Just like previously discussed, the flooded or wet lead acid batteries consists of lead plates, sulfuric acid as electrolyte, and a separator plate. However, in this case, the electrolyte is free to move around the battery casement as the batteries are not sealed [77,78]. Therefore, these batteries must be mounted upright so that the electrolyte does not leak out. Here, the gases do not recombine to liquids internally, rather these gases are externally vented. The hazardous internal gases such as hydrogen gas are released direct to direct to the environment at the time of charging. These vents can also flow liquid such as the electrolyte used in the batteries. Therefore, maintenance in the form of water is a requisite for proper operation flooded lead acid batteries to restore the loss electrolyte through the vents. Even though the flooded lead acid batteries are very economical in terms of good rates of charge for the cost, they have the weakest internal construction and high internal resistance [77]. The internal construction of flooded lead acid battery is represented in Figure 24.

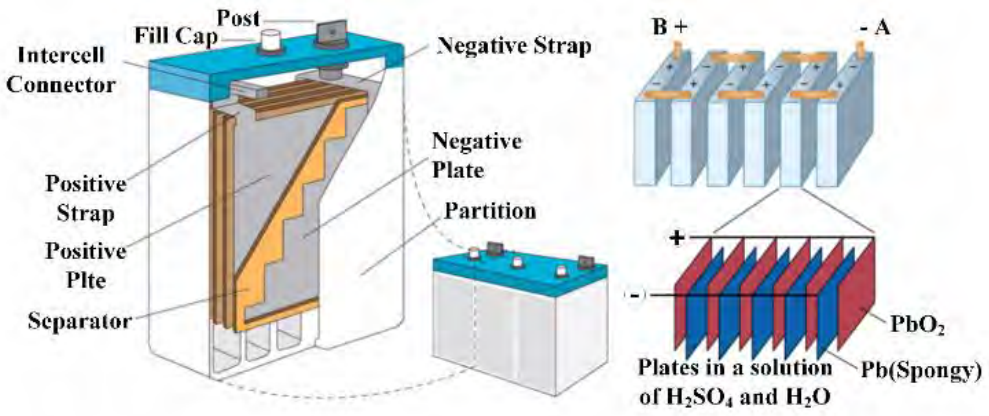

Figure 24. Anatomy of a flooded or wet lead acid cell; the sulfuric acid electrolyte is free to move inside the battery, lead plates act as the electrolyte [80].

Sealed Lead Acid Batteries

Sealed lead acid batteries consist of coagulated sulfuric acid as electrolyte; therefore, it cannot leak out. The inside compartment is inaccessible, and thus distilled water cannot be added in sealed lead acid batteries. Even though they are called sealed lead acid batteries, they are actually partially sealed because they contain vents. During the charging phase, gases can escape through the valves, therefore they are also called valve regulated lead acid (VRLA) batteries. These batteries are safer to use but at the same time more expensive. There two types of lead sealed lead acid batteries—absorbed glass matte (AGM) and gel cell batteries.

Absorbed Glass Matte (AGM) Batteries

AGM battery is the most modern lead acid battery, which was developed in 1985 [73,77]. It consists of a separator made of very fine fiber glass mat between the plates and the electrolyte, i.e., acid is absorbed in the glass mat. Due to the capillary reaction, the electrolyte is immobilized by the glass mate, and thus becomes spill proof. However, the acid is still available to the plates to continue the chemical reactions. The electrolyte, plates, and the fiber glass mat are confined in a tight packaging due to which the AGM batteries have very low internal resistance [77]. It is also the most impact resistant battery available in the market. The low internal resistance combined with fast migration of the electrolyte results in higher ampere rates, higher output voltage, and decreased charging time compared to other sealed lead acid batteries. Furthermore, the AGM batteries do not require any maintenance with zero acid spill and no corrosion on the surrounding parts.

Gel Cell Batteries

Just like the AGM batteries, the gel batteries are also sealed lead acid batteries. However, in this case, silica gel is used, which turns the electrolyte, i.e., the acid, into solid mass jelly type substance, and thus the acid cannot be spilled even if the battery is broken [77]. Gel batteries are not suitable for fast or high ampere charging/discharging. If the battery is used in the aforementioned situation, a scar may be created in the jelly of the battery, which leads to creating a pocket. The plates begin to corrode due to these pockets, which results in early failure of the battery. Gel batteries are best applicable in deep cycle application [73]. Their internal construction is stronger than the flooded battery but weaker than the AGM batteries. The comparison of flooded, AGM, and gel batteries is tabulated in Table 7.

Table 7. A comparative picture of deep-cycle flooded, absorbed glass matte (AGM), and gel batteries [80].

Property	Deep Cycle Flooded	Deep Cycle AGM	Deep Cycle Gel
Maintenance	Needed	Not needed	Not needed
Cost	Lowest	Low	Highest
Cycle Life	Excellent	Good	Good
Shipping	Hazardous	Non-hazardous	Non-hazardous
Temperature Range	Wide	Wide	Wide
Set Points	Generic	Special	Special
Self-Discharge Rate	High	Low	Low
Vibration/Shock Resistance	Excellent	Good	Good
Recyclability/Infrastructure	Good	Good	Good
Discharge Currents	Wide range	Wide range	Small
Charge Currents	Wide range	Wide range	Small
Applications	Wide range of power applications	High power/fast charge	Low power applications only
Float Characteristics	Not good for float or standby applications	Excellent float characteristics	Good for float applications

3.4.2. Lithium Metal Batteries

Lithium metal batteries are a type of primary or disposable batteries, which use metallic lithium as the anode. M. Stanley Whittingham, a chemist at Exxon in the 1970s, pioneered the lithium metal batteries. Li was great as an anode material because it is a highly reactive metal, which readily releases an electron to form a Li^+ ion. In the initial design, Titanium disulfide was used as the cathode. At that time, it was a concept hard to implement, since this design resulted in explosions. The researchers then went for the intercalation design—inserting layers of a different material between layers of the host material, which is lithium in this case. By intercalating graphite into lithium, its reactivity could be

reduced. Followed by research from several researchers, the developments to the lithium metal battery gradually gave birth to the Nobel-prize-winning discovery of the lithium ion batteries [81], which is described in the next section. Whittingham patented the initially developed Li anode - TiS_2 cathode 2.5 V battery [82,83], but it took the attempts of John B. Goodenough, Whittingham, and Akira Yoshino together to the development of the lithium-ion battery as we know it today.

Lithium is one of the lightest metals, which makes Li metal batteries very light in weight. They also have a high charge density. Their output voltage can range 1.5–3.7 V. Li metal batteries could have a vast range of applications from consumer electronics to electric vehicles. They could be strong contenders for many prominent battery types of today. Lithium metal batteries were overshadowed by the success of the Li ion batteries. However, almost half a century later, they are set for a comeback, as researchers are hinting that Li metal batteries could hold possibilities to overtake Li ion batteries [84,85]. There were two main problems associated with Li metal batteries—being prone to explosion and the formation of dendrites. Dendrites are small spike-like protrusions that are formed at the anode of Li metal batteries. These can rupture the separator between the anode and the cathode, creating a short circuit within the battery. Researchers are working to mitigate these issues by developing novel cathode materials and structures, intercalation designs, and surface coatings for the anode. Some notable progress on the rejuvenated research on Li metal batteries can be found in references [86–91]. Soon enough, Li metal batteries might go into large-scale production and surpass other battery technologies available today.

3.4.3. Lithium Ion Batteries

At present times, Li-ion batteries have gained profound popularity owing to their long life cycle, high operating voltage, and lower self-discharge rate, etc. [92]. The commercial Li-ion batteries were first introduced in 1990 [93]. This battery possesses higher charge density than the other rechargeable batteries and in terms of battery capacity, it also has a lighter weight. Therefore, the Li-ion battery has a higher power capacity without being too bulky. Furthermore, this battery has a low self-discharge rate, which is about 1.5% per month. In addition, repeatedly charging the Li-ion batteries after being partially discharged does not have a negative impact on the maximum capacity of the batteries, therefore the aforementioned battery has a negligible memory effect. Li-ion battery has a chemistry that results in higher open-circuit voltage than other aqueous batteries such as lead acid, nickel-metal hydride, and nickel-cadmium. Li-ion battery can typically handle hundreds of charge–discharge cycles. Some lithium ion batteries lose 30% of their capacity after 1000 cycles while more advanced lithium ion batteries still have better capacity only after 5000 cycles [94].

The Li-ion battery consists of a positive electrode-anode, a negative electrode-cathode, separator, electrolyte, and two current collectors [95]. The anode consists of lithiated metal oxide ($LiCoO_2$, $LiMO_2$, $LiNiO_2$ etc.), whereas, the cathode consists of graphitic carbon with a layering structure. The electrolyte is made up of lithium salt ($LiPF_6$), which is dissolved in organic carbonates [6]. During the discharging phase, lithium atoms in the anode become ionized and diffuse due to the small change in the electrolyte concentration. These ions are carried out by the electrolyte to the cathode where they combine with the external electron and get deposited as lithium atoms. The movement of the lithium ions creates free electrons in the anode, which flows through the external circuit and then to the cathode where it recombines with the lithium ions. The separator stops the direct flow of electron from anode to cathode. The reverse reaction takes place during the charging phase. The working principle of Li-ion batteries is shown in Figure 25. The chemical reactions that take place in the Li-ion batteries are as follows [71]:

At anode: $Li_{1-x}CoO_2 + xLi^+ + xe^- \leftrightarrow LiCoO_2$
At cathode: $Li_xC_6 \leftrightarrow xLi^+ + xe^- + C_6$
Overall chemical reaction: $LiC_6 + CoO_2 \leftrightarrow C_6 + LiCoO_2$

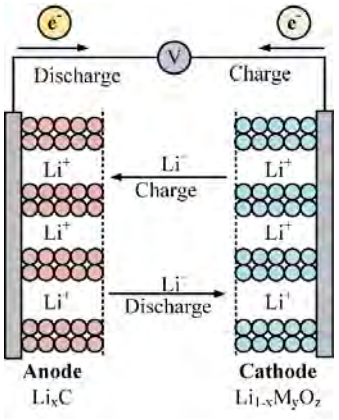

Figure 25. Charge and discharge cycles of a typical Li-ion battery; the anode consists of lithiated metal oxide and the cathode consists of graphitic carbon with a layering structure [96].

The equivalent circuit model of Li-ion batteries according to [92] is represented in Figure 26. Parameters R_s, R_P, and C_P are temperature and SOC dependent. Due to the fact that the change in SOC and temperature with respect to time is very small, these parameters are considered time invariant over a short period time, i.e., quasi-stationary. The voltage equations of Li-ion battery can be expressed by Equations (38) and (39) [92]. Here, $v_b(t)$ and $i_b(t)$ are the terminal voltage and current, respectively, whereas, $v_c(t)$ is the voltage across the Resistor Capacitor (RC) network.

$$v_b(t) = v_{oc}(h(t)) - R_s i_b(t) - v_c(t) \tag{38}$$

$$\frac{dv_c(t)}{dt} = -\frac{1}{C_p R_p} v_c(t) + \frac{1}{C_p} i_b(t) \tag{39}$$

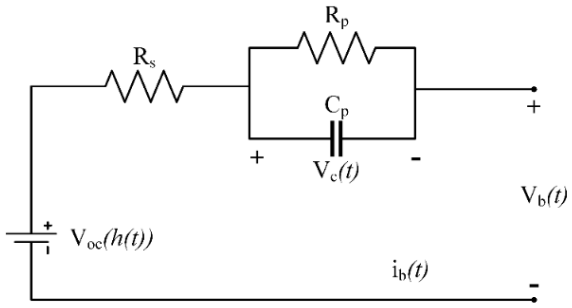

Figure 26. Equivalent circuit model of the Li-ion battery, consisting of a resistor in series with an RC parallel branch and a voltage source [92].

Based on the cathode materials, Li-ion batteries can be classified into six different types—lithium cobalt oxide (LCO), lithium manganese oxide (LMO), lithium nickel manganese cobalt oxide (NMC), lithium iron phosphate (LFP), lithium nickel cobalt aluminum oxide (NCA), and lithium titanate (LTO). Comparison of different Li-ion batteries based on their characteristics is tabulated in Table 8. All the important characteristics have been assimilated in this table.

Table 8. Different Li-ion batteries and their characteristics [97].

Type of Lithium Ion (Li-Ion) Battery	Lithium Cobalt Oxide	Lithium Manganese Oxide	Lithium Nickel Manganese Cobalt Oxide	Lithium Iron Phosphate	Lithium Nickel Cobalt Aluminum Oxide	Lithium Titanate
Available since	1991	1996	2008	1996	1999	2008
Short Form	LCO or Li-cobalt	LMO or Li-manganese (spinel structure)	NMC	LFP or Li-phosphate	NCA or Li-aluminum	LTO or Li-titanate
Cathode	$LiCoO_2$ (60% Co)	$LiMn_2O_4$	$LiNiMnCoO_2$	$LiFePO_4$	$LiNiCoAlO_2$	$LiMnO_2$ or $LiNiMnCoO_2$
Anode	Graphite	Graphite	Graphite	Graphite	Graphite	$Li_4Ti_5O_{12}$ (titanate)
Voltages	3.6 V nominal; typical operating range: 3–4.2 V/cell	3.7 (3.8) V nominal; typical operating range: 3–4.2 V/cell	3.6 V, 3.7 V nominal; typical operating range: 3–4.2 V/cell or higher	3.2 V, 3.3 V nominal; typical operating range: 2.5–3.65 V/cell	3.6 V nominal; typical operating range: 3–4.2 V/cell	2.4 V nominal; typical operating range: 1.8–2.85 V/cell
Specific Energy (Capacity)	150–200 Wh/kg; Specialty cells provide upto 240 Wh/kg	100–150 Wh/kg	150–220 Wh/kg	90–120 Wh/kg	200–260 Wh/kg; 300 Wh/kg predictable	50–80 Wh/kg
Charge (C-rate)	0.7–1 C, charges to 4.2 V (most cells); 3 h charge typical. Charge current above 1 C shortens battery life.	0.7–1 C typical; 3 C maximum; charges to 4.2 V (most cells)	0.7–1 C, charges to 4.2 V, some go to 4.3 V, 3 h charge typical. Charge current above 1 C shortens battery life.	1 C typical; charges to 3.65 V; 3 h charge time typical	0.7 C; charges to 4.2 V (most cells); 3 h charge typical; fast charge possible with some cells	1 C typical; 5 C maximum; charges to 2.85 V
Discharge (C-rate)	1 C; 2.5 V cut-off. Discharge current above 1 C shortens battery life.	1 C; 10 C possible with some cells; 30 C pulse (5 s), 2.5 V cut-off	1 C; 2 C possible on some cells; 2.5 V cut-off	1 C; 25 C possible on some cells; 40 A pulse (2 s), 2.5 V cut-off (lower than 2 V causes damage)	1 C typical; 3 V cut-off; high discharge rate shortens battery life	100 C possible, 30 C 5 s pulse; 1.8 V cut-off on LCO/LTO
Cycle life	500–1000, related to depth of discharge, load, temperature.	300–700 (related to depth of discharge, temperature)	1000–2000 (related to depth of discharge, temperature)	1000–2000 (related to depth of discharge, temperature)	500 (related to depth of discharge, temperature)	3000–7000
Thermal runaway	150 °C (302 °F). Full charge promotes thermal runaway.	250 °C (482 °F). High charge promotes thermal runaway.	210 °C (410 °F). High charge promotes thermal runaway.	270 °C (518 °F). Very safe battery even if fully charged.	150 C or 302^{0}F typical; high charge promotes thermal runaway	One of the safest Li-ion batteries
Cost	~450$/kWh [98]	~650$/kWh (as per 2014 data) [99]	~420$/kWh (Source: RWTH Aachen)	~580$/kWh (Source: RWTH Aachen)	~350$/kWh (Source: RWTH Aachen)	~1005$/kWh (Source: RWTH Aachen)
Applications	Mobile phones, tablets, laptops, cameras	Power tools, medical devices, electric powertrains	e-bikes, medical devices, EVs, industrial	Portable and stationary needing high load currents and endurances	Medical devices, industrial, electric powertrains (Tesla)	UPS, electric powertrain (Mitsubishi i-MiEV, Honda Fit EV), solar powered street lighting

Table 8. *Cont.*

Type of Lithium Ion (Li-Ion) Battery	Lithium Cobalt Oxide	Lithium Manganese Oxide	Lithium Nickel Manganese Cobalt Oxide	Lithium Iron Phosphate	Lithium Nickel Cobalt Aluminum Oxide	Lithium Titanate
Comments	Very high specific energy, limited specific power; Cobalt is expensive; Used as energy cells; Market share has stabilized.	High power but less capacity; Safer than Li-Cobalt; Commonly mixed with NMC to improve performance.	Provides high capacity and high power; Serves as hybrid cell; Favorite chemistry for many uses; Market share is increasing.	Very flat voltage discharge curve but low capacity; one of the safest Li-ions; Used for special markets; Elevated self-discharge.	Shares similarities with Li-cobalt. Serves as energy cell.	Long-life, fast-charge, wide temperature range; but low specific energy and expensive; among safest Li-ion batteries
2019 Update	Early version; no longer relevant	Less relevant now; limited growth potential	Leading system; dominant cathode chemistry	Used primarily for energy storage; moderate growth	Mainly used by Panasonic and Tesla; growth potential	Ultra-fast charging ability; high cost limits special applications

3.4.4. Lithium Polymer Batteries

The lithium polymer (Li-Po) batteries are very similar and thus, belong to the family of Li-ion batteries. However, the type of electrolyte used in these batteries is what that differentiates them from the conventional batteries. Invented back in 1978, the Li-Po batteries used a dry solid polymer electrolyte. The dry polymer electrolyte makes the fabrication of Li-Po much simpler; however, due to high internal resistance, it suffers from poor conductivity and thus is not suitable for high current applications [100]. In the modern Li-Po batteries, gelled electrolyte is added with the dry polymer electrolyte, which solves the aforementioned poor conductivity problems and makes the Li-Po batteries useful for high current applications having a very high discharge rate. The Li-Po batteries have low self-discharge rate and a long life cycle compared to other batteries. In addition, the Li-Po batteries are thinner and lighter in weight when compared to Li-ion batteries of similar capacity [101].

A typical Li-Po battery consists of a positive electrode, negative electrode, electrolyte, and a separator. A sandwich-like Li-Po cell is represented in Figure 27.

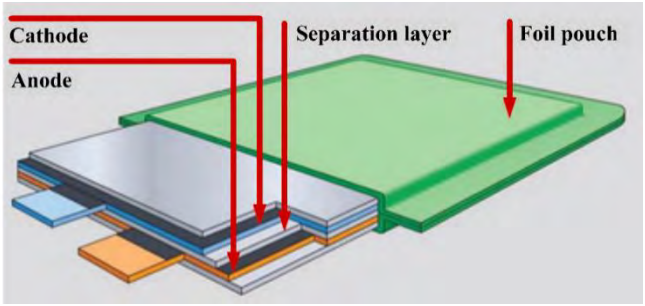

Figure 27. Basic construction of sandwich like Li-polymer cells. A typical Li-Po battery consists of a positive electrode, negative electrode, electrolyte, and a separator [102].

The positive electrode, i.e., the anode has three parts—transition metal oxide such as $LiCoO_2$ or $LiMn_2O_4$; conductive additive such as graphite or acetylene black; and polymer binder of polyvinylidene fluoride (PVDF) [103]. Similarly, the cathode has the same two parts, however the only exception is that the lithium metal oxide is replaced by carbon [103]. Conductive lithium salts such as lithium hexafluorophosphate ($LiPF_6$) are used as the electrolyte, whereas polypropylene film, which is electrically insulating but ironically conductive, is used as the separator layer [102]. This means that even if the electrolyte is liquid it still contains components of polymer. Li-Po batteries also have a thin,

pouch-like housing, which consists of deep-drawn aluminum foil with polymer coating, and thus they are also known as soft or pouch cells [102,103]. The operation of these batteries is identical to Li-ion batteries. During the charging phase, lithium ion intercalates from the cathode to anode, passing through the electrolyte and increases the gap between the layers, which leads to the increase in cell thickness. During the discharge phase, the cell reverses the aforementioned process and the cell thickness is again decreased [102]. The chemical mechanism within the Li-Po battery cell is represented in Figure 28.

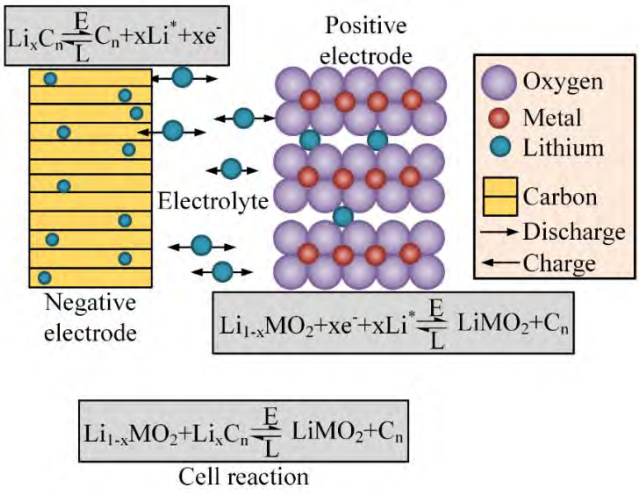

Figure 28. Chemical processes in Li-polymer cells. While charging, Li+ intercalates from the cathode to anode, passing through the electrolyte and increases the gap between the layers, increasing the cell thickness. While discharging, the reverse occurs and the cell thickness decreases [102].

The temperature-dependent, I-V characteristics of Li-Po batteries are represented in Figure 29. The I-V characteristics are a function of SOC, current, and temperature. For avoiding complexity, the subordinate parameter, which has very little effect, has been ignored. According to [101], the equivalent circuit modelling of Li-Po battery is represented in Figure 30. The parameters estimation of the different circuit components is done by utilizing the I-V characteristics. The equivalent circuit consists of a resistor R_1, in series with two parallel RC networks. For step response, the series resistor R_1 is used to represent the immediate voltage drop. The two parallel RC networks (R_2C_2 and R_3C_3) are responsible for short and long time constants of the step response.

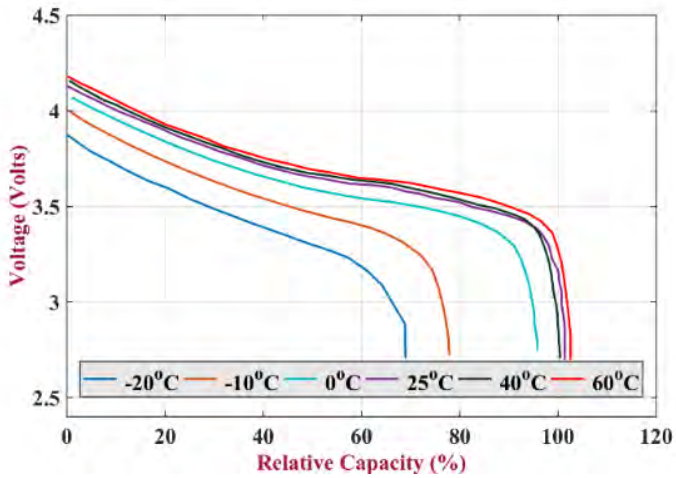

Figure 29. Graphical demonstration of voltage versus relative capacity of a typical Li-Po cell at different temperatures [101].

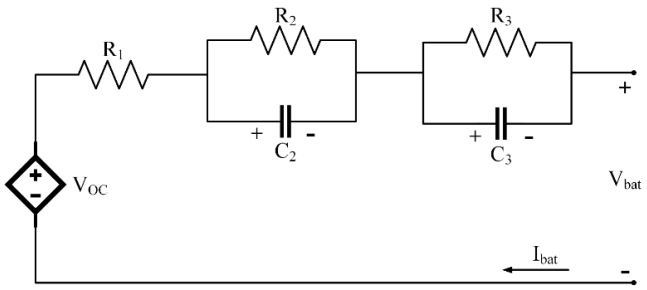

Figure 30. Equivalent circuit used for the simulation of the Li-polymer battery consisting of a resistor in series with two RC parallel branches [101].

3.4.5. Sodium Beta Batteries

Two types of sodium beta (Na-beta) batteries or NBBs are available—Sodium sulfur and Sodium metal halide—depending on the type of cathode used. They use an electrolytic membrane made of solid beta alumina $\left(\beta^{''}Al_2O_3\right)$ that transports ions selectively between the sodium anode and the cathode.

Sodium Sulphur Batteries

Sodium sulfur batteries are one of the most matured battery technologies existing in the current market [3]. It was first discovered by Ford Motor Company back in 1960 [19]. It possess high energy density of in the range of 150–240 W, high power of 150–230 W/kg, and high coulombic efficiency [6,104]. Furthermore, sodium sulfur batteries can operate at high temperature range (300–350 °C) [19], long life cycles of 2500 cycles [6], and the material used in fabrication of NaS batteries are comparatively low. In addition, the high DC conversion efficiency of 85% [105] makes the NaS batteries and ideal prospect for future distribution system, which are based on DC power [106]. These attributes of NaS batteries makes them suitable in wide range of applications such as load levelling, peak shaving, renewable energy integration, emergency power, and power reliability [107].

In NaS batteries, molten sulfur is used in the positive electrode, whereas molten sodium is used in the negative electrode. Solid beta alumina ceramic functions as the electrolyte and also separates the aforementioned active materials [6,108]. Only the sodium ions from the positive electrodes are allowed to go through the electrolyte to the negative electrode, where recombination with sulfur takes place to sodium polysulfides. During the discharge phase, when the sodium releases electrons and becomes Na+ ions, these electrons flow from the negative electrode through the external circuit of battery to the positive electrode, and thus produces 2.0 V [6]. These electrochemical reaction are reversible, therefore the sodium polysulfides releases the Na+ ions through the electrolyte, which recombines back as elemental sodium [6]. The schematic representation of sodium sulfur battery is represented in Figure 31.

The internal resistance of NaS batteries is dependent on depth of discharge (DoD), i.e., it varies throughout charging and discharging of the battery. The change in the internal resistance with respect to DoD is represented in Figure 32. The ideal operating range for NaS battery according to [19], is 300–360 °C. It is evident that the battery temperature increases during charging and decreases during discharging. The variation of internal resistance with respect to number of charge and discharge cycles are presented in Figure 33. The electromotive force also varies due to the charge and discharge cycles. An equivalent circuit model based on the effect of DoD and temperature on the EMF and internal resistance is proposed in Figure 34. Here, the internal resistance of the battery, which varies with temperature and DoD, are represented by Rc and Rd. E represents the battery voltage source. The deterioration of the battery is represented by Rlc.

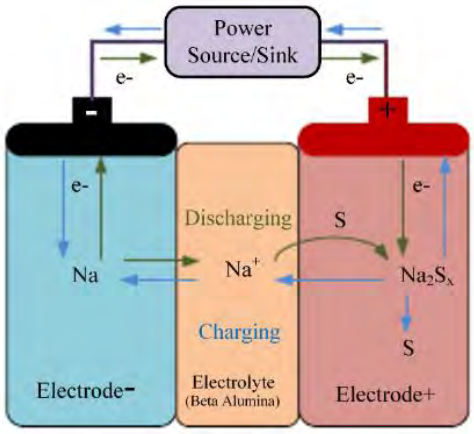

Figure 31. Schematic diagram of NaS battery: Molten S is used in the positive electrode and molten Na is used in the negative electrode; solid beta alumina ceramic is the electrolyte and separator [75].

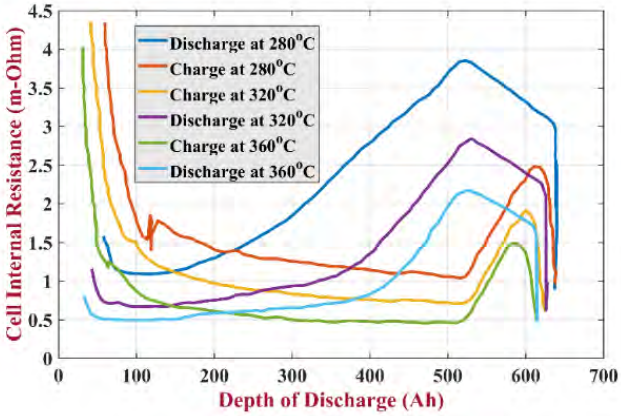

Figure 32. Graph of the internal resistance versus depth of discharge of NaS at various temperatures [19].

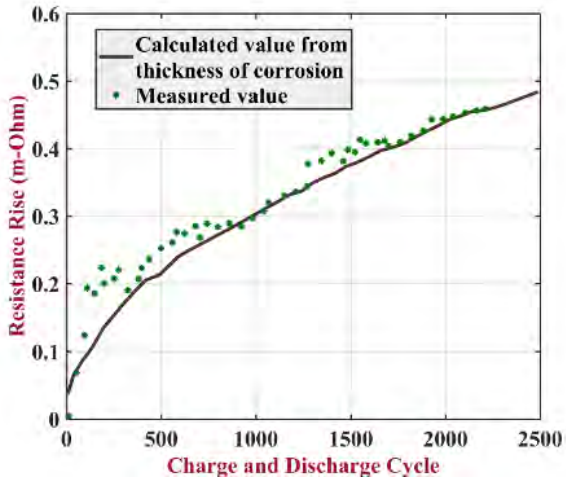

Figure 33. Graph of the internal resistance of NaS cell with respect to charge discharge cycle [109].

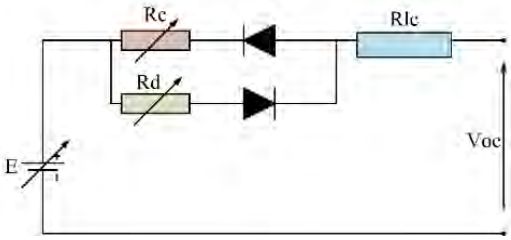

Figure 34. The equivalent circuit model of NaS cell based on the effect of depth of discharge (DoD) and temperature on the electromotive force (EMF) and internal resistance [19].

Sodium Metal Halide Batteries

Sodium metal halide (Na-MX) batteries are quite similar to Na-S batteries in regards to using inorganic molten salt as the electrolyte [26]. These batteries are also known as ZEBRA batteries and were first introduced in South Africa back in 1968 [20]. ZEBRA batteries have a high tolerance to overcharge and discharge, high energy density, and long life time cycling [110,111]. Furthermore, they have a very high operating temperature range (523–623 K), very low self-discharge, and good pulse power capability [26,112]. In addition, these batteries are maintenance free and have very high mechanical strength [113]. These attributes make the Na-Mx batteries a popular choice for stationary power quality and heavy-duty transportation applications [110]. Continuous research for developing this highly potential storage technology is ongoing. GE has refined this technology a significant amount and launched Durathon sodium-metal halide batteries. These batteries are a part of the continuous improvement of ZEBRA batteries and are mainly implemented in the utility-scale energy storage applications [26]. The Durathon batteries are superior to the lead acid batteries and have the lowest life cycle cost when compared to the existing battery technologies [110].

In Ni-MH batteries, the liquid sodium functions as the negative electrode, whereas a solid metal halide works as the positive electrode [20]. The electrodes are separated from each other by a ceramic beta alumina separator [110]. The electrolytes are immersed in a secondary electrolyte sodium chloroaluminate ($NaAlCl_4$) [69]. The battery operates at 300°C temperature, which makes the electrolyte molten and increases its ionic conductivity [110]. This beta alumina separator only allows the migration of sodium ions and it also provides insulation between the oppositely charged electrodes [69]. During the discharging phase, the sodium ions flow from the anode to cathode through the ceramic beta alumina separator leaving behind electrons. These electrons migrate to the positive electrode through the external power circuit. The positive sodium ions react with the metal halide, in this case NiCl, which is converted to metallic nickel and sodium chloride precipitates. The electrochemical reactions, which takes place in the Na-MX batteries, are given below [69]. The schematic of Na-MX is represented in Figure 35.

Cell reactions:

Positive Electrode: $NiCl_2 + 2Na^+ + 2e^- \leftrightarrow Ni + 2NaCl$

Negative Electrode: $2Na \leftrightarrow 2Na^+ + 2e^-$

Net Cell Reaction: $NiCl_2 + 2Na \leftrightarrow Ni + 2NaCl; E_{eq} = 2.58V@300\,\mathrm{C}$

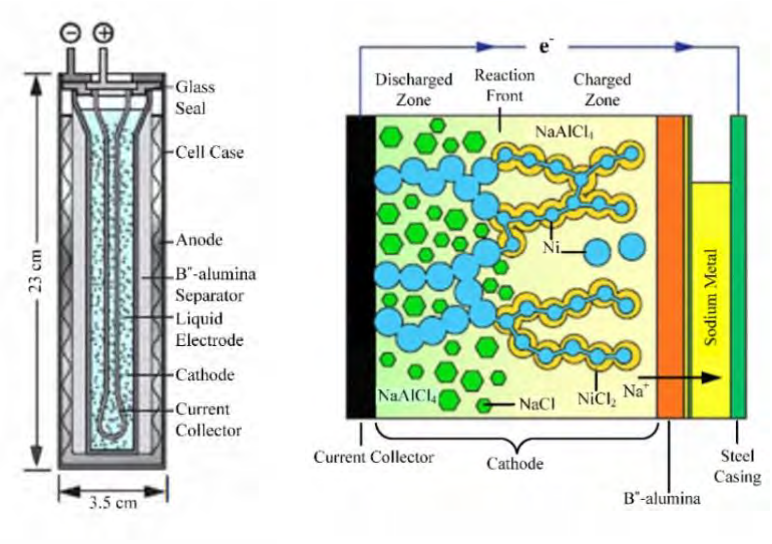

(**a**) (**b**)

Figure 35. (**a**) Cell schematic highlighting main components of the Sodium metal halide (Na-MX) cell. (**b**) Pictorial representation of the charging reaction, which consumes NaCl to form $NiCl_2$ from the β″-alumina ceramic separator inward [26].

The electrical equivalent circuit of the Na-MX is presented in Figure 36. Here, V_{OC} is the voltage of the battery at equilibrium condition, R_O is the internal resistance of solid beta alumina electrolyte and interconnecting metals [69]. Two RC branches are connected in series for reproducing the transient response. The parameters are non-linearly dependent on the SOC, current state, and temperature [114]. R_2 and C_2 correspond to slower dynamics of the diffusion process, whereas R_1 and C_1 represent the fast battery dynamics, which are related to surface effects and reaction kinetics [69]. The surface effects on the electrodes occur due to the double layer formation of the battery. Based on the physical and electrochemical phenomena taking place inside the battery, the configuration of the electrical circuit has been designed. Referring to Figure 36, V_{OC} is the equilibrium potential of the battery, R_o is the internal resistance of the solid ceramic electrolyte and the interconnection metal; the two RC branches reproduce the transient response of the battery. All the parameters in the equivalent circuit are dependent on the state of charge (SOC) of the battery, which at any time t, can be simply estimated by,

$$SOC(t) = SOC(0) + \frac{1}{C_B}\int_0^t i_L(t)dt \tag{40}$$

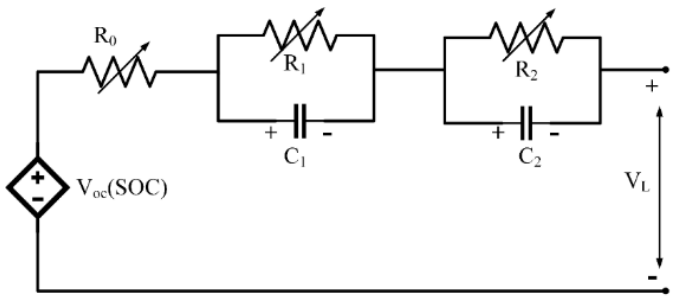

Figure 36. The Thevenin equivalent circuit for modelling batteries. All the parameters in the equivalent circuit are dependent on the state of charge (SOC) of the battery [69].

Here, C_B is the nominal battery capacity and i_L is the current in the battery. In the circuit of Figure 36, applying Kirchhoff's voltage law, the terminal battery voltage of the battery can be expressed as,

$$v_L(t) = v_{OC}(t) - v_0(t) - v_1(t) - v_2(t) \tag{41}$$

The Laplace transformation of Equation (41) can be applied to find the solution of the terminal voltage when step currents are applied.

$$V_L(t) = V_{OC}(t) - V_0(t) - V_1(t) - V_2(t) \tag{42}$$

If a step current from magnitude i_L to zero is applied at any time t_r, each element of Equation (42) can be evaluated as under:

$$V_0(s) = R_0 I_L \left(\frac{1 - e^{-t_r s}}{s} \right) \tag{43}$$

$$V_1(s) = \left(\frac{\tau_1}{1 + \tau_1 s} \right) v_1(t_r) + R_1 I_L \left[\frac{1 - e^{-t_r s}}{s(1 + \tau_1 s)} \right] \tag{44}$$

$$V_2(s) = \left(\frac{\tau_2}{1 + \tau_2 s} \right) v_2(t_r) + R_2 I_L \left[\frac{1 - e^{-t_r s}}{s(1 + \tau_2 s)} \right] \tag{45}$$

where $\tau_1 = R_1 C_1$ and $\tau_2 = R_2 C_2$ are the time constants.

3.4.6. Metal Air Batteries

Metal air batteries, which consist of metal electrode (anode) such as Li, Zn, Mg, Al, etc., are considered to be one of the most inexpensive and compact batteries available in the market [93,115]. The electrolyte may be aqueous or non-aqueous, with a bi-functional air electrode (cathode) [93]. The cathode consists of metal mesh or porous carbon structure, which are covered with proper catalysts. Good OH- ion conductors such as KOH are used as the electrolyte in this type of battery. These batteries are very similar to the fuel batteries where the metal is used as the fuel, whereas air functions as the oxidant [6]. The metal are batteries are very environmentally friendly and, as such, have less weight and volume compared to the li-ion batteries. Even though high charge density, low-cost metal is used in the metal air batteries, it has major a disadvantage, which is that it is very difficult and inefficient to electrically recharge the metal air batteries [6]. However, the batteries can be refueled—the consumed metal can be mechanically replaced and processed separately. According to [116], the electrochemistry differs for aqueous and non-aqueous system, therefore the metal air batteries can be categorized into aqueous and non-aqueous metal air batteries. The schematic diagrams of aqueous and non-aqueous metal air batteries are represented in Figure 37.

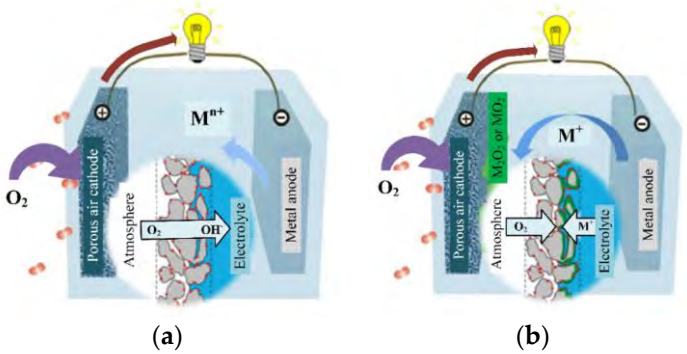

Figure 37. Schematic configuration and operation principle for (**a**) aqueous and (**b**) non-aqueous metal–air batteries. Inserts illustrate the oxygen reduction reaction taking place at the porous air cathode [116].

The chemical reactions for aqueous and non-aqueous reaction are as follows [116].

Aqueous reaction:

$$\text{Anode: } M \leftrightarrow M^{n+} + ne^-$$
$$\text{Cathode: } O_2 + ne^- + 2H_2O \leftrightarrow 4OH^-$$

Here, M represents the metal and n represents the oxidation number of the metallic ion. These electrochemical reactions might be reversed upon recharge with metals plated at the anode and O_2 evolving at the cathode.

Non-aqueous reaction:

$$\text{Anode: } M \leftrightarrow M^+ + e^-$$
$$\text{Cathode: } xM^+ + O_2 + xe^- \leftrightarrow M_xO_2(x = 1or2)$$

Zn, Mg, Al, and Fe metals are thermodynamically unstable in the aqueous medium. However, by passivating their surface by corresponding oxides or hydroxide, they can be made compatible with aqueous electrolytes used in the metal air batteries. On the other hand, Li, Na, and K metals are not suitable in aqueous solution due to their high reactivity. Using an ionic conductive film, which only permits ion transportation, they can be protected. However, this type of protected battery fabrication will be much too expensive for practical implementation [116]. The Zn air batteries are the first metal batteries invented with very high energy densities and low-cost fabrication. These batteries are matured enough to be already being implemented in practical applications. The Mg air batteries are very much appealing due to the homogenous deposition of Mg [117–119]. However, the Mg electrode suffers severe corrosion in an aqueous solution. Even in an ionic electrolyte, Mg electrode raises a major concern of electrochemical instability, which is more prominent in the charging phase, hence limiting the reversibility of the cell [120]. The Al air batteries possesses high specific energy and theoretical energy density, however their susceptibility to corrosion and inadequate cycling stability are the major impediment in their widespread implementation [121–123]. On the other hand, due to the abundance of sodium and similar properties with lithium, the Na air batteries are drawing profuse attention [124,125]. However, they are still in not mature enough and require more research to be implemented in practical applications. The Si air batteries have high theoretical energy density and are highly stable in aqueous solution. Experimentally, the Si air batteries have been tested for both ionic and alkaline electrolytes [126,127]. The comparison of different types of metal air batteries are tabulated in Table 9.

Table 9. A comparison among different types of metal –air batteries [128].

Battery	Theoretical Specific Energy (kWh/kg)	Practical Specific Energy (kWh/kg)	Demonstrated Rechargeability	Calculated Open Circuit Voltage (V)	Advantages	Challenges
Fe-air	1.2	0.7	Yes	1.3	Approaching peak efficiency	Corrosion, easily changeable oxidation states, potentially cost prohibitive
Zn-air	1.3	0.7–0.9	Yes	1.65	Cost efficiency, approaching peak efficiency, long life-times probable, mutuality	Dendrite formation at Zn anode, air cathode materials need improvement, zincate supersaturation
Na-air	2	N/A *	No	2.3	Cost effective, mutuality	Cell maintenance requires high temperature, room temperature operation needs alternative solvents (ionic liquids, etc.), more effective air catalysts needed

Table 9. *Cont.*

Battery	Theoretical Specific Energy (kWh/kg)	Practical Specific Energy (kWh/kg)	Demonstrated Rechargeability	Calculated Open Circuit Voltage (V)	Advantages	Challenges
Mg-air	6.8	N/A *	No	2.93	High theoretical specific energy, high working voltage	Any aqueous exposure results in corrosion, potentially expensive solvents, more effective air catalysts needed
Al-air	8	0.4–1.8	No	1.2	High theoretical specific energy, high working voltage, mutuality	Reactive in alkaline electrolyte causing electrode degradation, more effective air catalysts needed
Li-air	12	0.9–5	No	2.91	High theoretical specific energy, high working voltage	Multiple catalysts needed to control reactions on peroxide side, dendrite formation at Li electrode, pure Li presently required, high cost, more effective air catalysts needed

* The practical specific energy for the Na-air battery is not reported since most systems run above ambient temperature, and for the Mg-air battery since it has low cell lifetime.

The equivalent circuit of a typical metal air battery, i.e., Zn air batteries are represented in Figure 38. In this model, R_e is the external resistance—sum of the electronic resistance of the cell components, contact resistance, and electrolyte resistance [128]. Z_M is mass transport impedance, which is the parallel combination of mass transport resistance R_m and capacitance C_m [129]. R_k and R_i are the kinetic and internal ohmic resistance, respectively. C_{d1} and C_{d2} are the double layer capacitance.

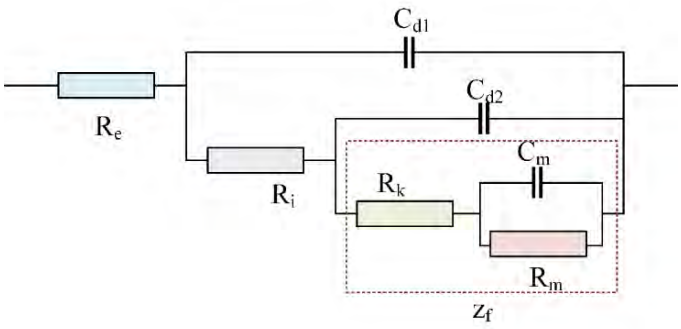

Figure 38. Schematic representation of the equivalent circuit of a typical metal air battery, i.e., Zn air battery [130].

3.5. Nickel-Based Batteries

Nickel-based batteries are called so since they employ nickel oxide hydroxide (NiOOH) as the positive electrode [131]. They were invented over 100 years ago, when the only existing battery technology was lead acid battery [132]. Nickel batteries have evolved themselves as a tough and robust battery. Although some of the existing batteries are offering more efficient operation, nickel-based batteries are still extant due to their high stability, longer operating life, and extreme temperature handling capability [132]. There are different types of nickel-based batteries, such as nickel-hydrogen ($Ni - H_2$), nickel-cadmium (Ni-Cd), nickel metal hydride (Ni-MH), nickel-iron (Ni-Fe), and nickel-zinc (Ni-Zn) [131]. Among the aforementioned nickel-based batteries, Ni-MH and NI-cd batteries are more popular in their application in power backup and vehicle propulsion applications [131].

Nickel Cadmium Batteries

Nickel cadmium batteries along with lead acid batteries are considered to be the most matured and popular battery technologies, having been invented more than 100 years ago [6]. Ni-Cd batteries possess exceptional tolerance to high discharge rates, high energy density of 50–75 Wh/kg, versatility

in size, and very low maintenance requirement [6,131]. The aforementioned qualities make the Ni-Cd suitable for generator starting, UPS, portable device, emergency lighting, etc. [3,6]. However, this battery is not free of its disadvantages. The relative cost is very high, which is the major disadvantage of this battery. Furthermore, the Ni-Cd batteries suffers from the issue of requiring a proper disposal system due to containing Cadmium—a heavily toxic metal. The European Union has banned Ni-Cd batteries from being used in vehicles due to the environmental issues [17,133]. In addition, this battery also has memory effect, i.e., the full charging the battery will be available only after a series of full discharges. However, due to the robustness and high tolerance, the nickel cadmium batteries is preferable in utility-scale application [17].

The Ni-Cd battery consists of a positive plate made of nickel oxyhydroxide, a negative plate made of metallic cadmium as negative electrode, and alkaline as electrolyte. The positive and negative electrode are separated by a nylon divider [6], which blocks the direct charge transfer between the electrodes. The operation of the battery is based on the redox reaction between nickel oxide hydroxide and cadmium [131]. During the discharge phase, at the positive plate, nickel oxyhydroxide reacts with water to form nickel hydroxide, whereas at the negative plate, cadmium reacts and produces cadmium hydroxide [7]. The whole process is reversed during the charging phase. However, there is a possibility of producing oxygen at the positive plate and hydrogen at the negative plate, which effectively reduces the water [6]. Therefore, some water needs to be added for proper operation of the battery. Based on the construction, there are two types of nickel cadmium battery-sealed nickel cadmium battery and vented nickel cadmium battery. The sealed Ni-Cd batteries as the name suggests are sealed using a metal case, and thus; does not leak any gas unless any fault occurs [6,134]. The construction of sealed and vented Ni-Cd batteries is represented in Figures 39 and 40, respectively. The vented Ni-Cd batteries have the same operating principle of the sealed Ni-Cd batteries, however they are susceptible to gas leakage during the time of overcharging or rapid discharging [6]. The vented Ni-Cd batteries possesses a low-pressure valve through which oxygen and hydrogen are released. Therefore, this type of battery is lightweight, robust, and more economical [135].

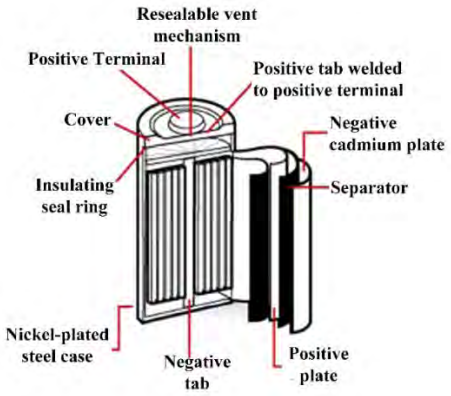

Figure 39. Structure of sealed Nickel-cadmium battery; it is sealed using a metal case, and thus does not leak any gas unless any fault occurs [136].

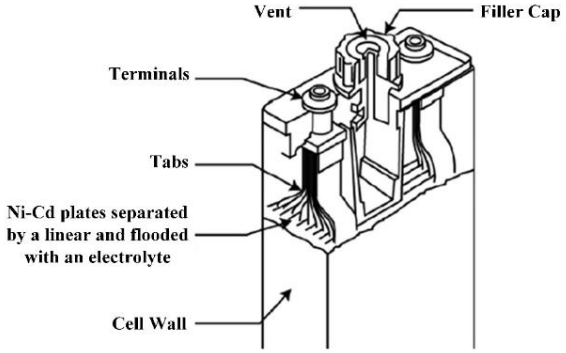

Figure 40. Structure of vented Nickel-cadmium battery; it is susceptible to gas leakage; there is a low-pressure valve through which oxygen and hydrogen are released [136].

The equivalent circuit of Ni-Cd battery for discharging and charging phase are represented in Figures 41 and 42, respectively. The battery voltage and charging voltage is denoted by v(t) and v(g), respectively. R_{ex} is the external resistance, and, C_2 is the capacitance value for both charging and discharging phases. R_1 and R_2 are the resistance values parallel to the capacitor during the discharging and charging phase, respectively. The corresponding equations are as follows [137].

$$\left(\frac{dv}{dt}\right)_d = -\frac{R_{ex}V_{oc}}{(R+R_{ex})^2 C_1} \tag{46}$$

$$\left(\frac{dv}{dt}\right)_c = -\frac{R_{ex}(V_g - V_{oc})}{(R+R_{ex})^2 C_2} \tag{47}$$

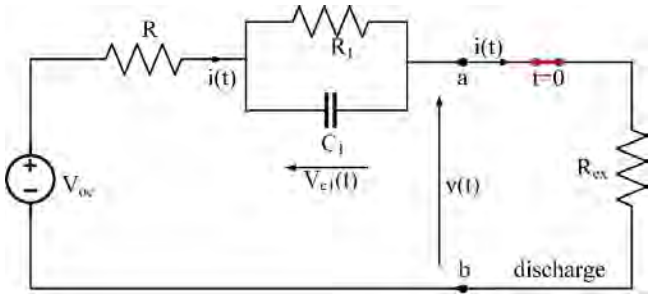

Figure 41. Equivalent circuit of Ni-Cd battery for discharging phase. Charges flow from V_{OC} towards the external resistance R_{ex} [137].

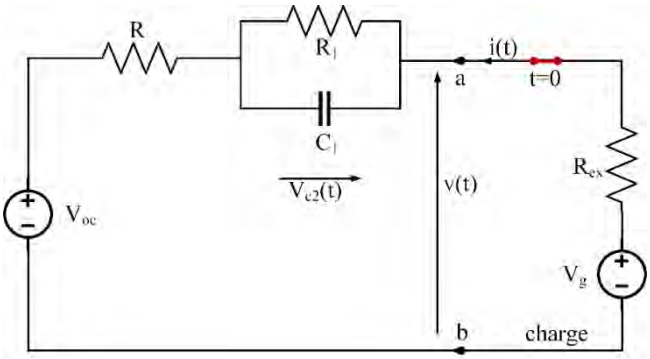

Figure 42. Equivalent circuit of Ni-Cd battery for charging phase. Charges flow from V_g and R_{ex} towards V_{OC} [137].

Nickel Metal Hydride Batteries

Nickel metal hydride (Ni-MH) have essentially the same construction as the Ni-Cd batteries in the sense that they have same positive electrode and electrolyte [131]. However, the major difference is that in this type of battery the cadmium-based negative electrode is replaced by hydrogen absorbing electrode [138]. This eliminates the use of toxic material cadmium, therefore Ni-MH batteries have less detrimental effects on the environment, when compared to Ni-Cd batteries. Furthermore, the substitution of the cadmium-based electrode with hydrogen absorbing electrode also increases the battery capacity for a given weight [138]. The Ni-MH batteries can be used and recharged hundreds of times during their lifetime making them equivalent to hundreds of alkaline batteries [138]. However, they are more susceptible to self-discharge. Furthermore, they generate heat during fast charging and high load discharging and have a low coulombic efficiency of 65% [16].

Figure 43 shows a cylindrical Ni-MH battery. As discussed previously, just like the Ni-Cd battery, the positive electrode of the Ni-MH consists of nickel oxi-hydroxide. On the other hand, the negative electrode consists of hydrogen absorbing alloys and are separated from the positive electrode by a separator. The separator averts the short circuiting between the electrodes, while at the same time, allowing ion diffusion through the electrolyte. Alkaline potassium hydroxide (KOH) is used as the electrolyte along with other constituents to ensure the concentration of aqueous remains constant throughout the operation of the battery, therefore improving performance of the battery. During shorting, overcharging, or reverse charging situations, excessive gasses can be produced, which harms the efficacy of the system, therefore a self-sealing vent is available to release the gasses. The current is collected through the current collector—a metal path with a low-resistance metal sheet or grid, which leads to improving battery performance. Furthermore, all the materials and constituents are sealed within a confined space, which ensures good mechanical strength and low mechanical price [139].

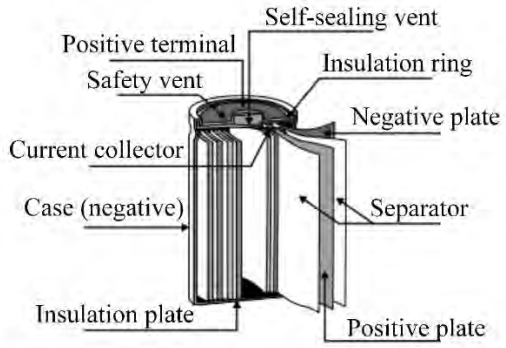

Figure 43. Structural components of a cylindrical Ni-MH battery; the positive electrode consists of nickel oxi-hydroxide and the negative electrode consists of hydrogen absorbing alloys [139].

Based on experimentally determining the different components, the equivalent circuit of the Ni-MH battery is proposed, which is represented in Figure 44. Here, E_{eq} is the equilibrium voltage of the cell, and Z_w is the Warburg impedance, which represents the diffusion phenomena at low frequencies [139]. $\tau = R_{tc}\ C_{dl}$ is the time constant-relative to the charge transfer phenomena, which is less the time constant of the diffusion phenomena [140]. In the frequency domain, the total equivalent impedance Z_T is given by [140]:

$$Z_T(s) = R_\Omega + \frac{R_{tc}}{1 + sR_{tc}C_{dl}} + Z_w(s) \quad (48)$$

is the equilibrium voltage of the cell, and Z_w is the Warburg impedance representing the diffusion phenomena at low frequencies, $\tau = R_{tc}\ C_{dl}$ is the time constant-relative to the charge transfer phenomena [139,140].

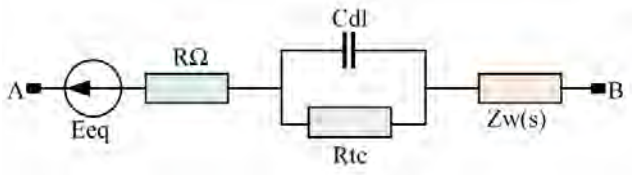

Figure 44. Equivalent circuit of the Ni-MH battery. E_{eq} is the equilibrium voltage of the cell, and Z_w is the Warburg impedance representing the diffusion phenomena at low frequencies, $\tau = R_{tc}$ is the time constant-relative to the charge transfer phenomena [139,140].

For finding the Warburg impedance, spectroscopy measurements are carried out at various SOCs upon NiMH. In this process, a low sinusoidal voltage of amplitude 10 mV is applied to the equilibrium voltage of the cell at a particular SOC. A current will flow with the same frequency as the voltage but shifted in phase. The ratio of the voltage and the current can give the value of the total impedance Z_T of the cell.

$$Z_T(s) = \frac{V_{max}}{I_{max}} e^{j\varphi} \tag{49}$$

At a specific SOC, the impedance spectrum of the cell can be found by changing the frequency level. At low frequencies, the gain of Z_T(s) can be obtained by two asymptotes drawn on the Bode plot. One asymptote is a non-integer integrator H_1, and the other is a high pass function H_2. The Warburg impedance can be obtained from the product of H_1 and H_2.

$$H_1(s) = \frac{1}{(\tau_1 s)^{n_1}} \tag{50}$$

$$H_2(s) = (1 + \tau_2 s)^{n_2} \tag{51}$$

$$Z_W(s) = H_1(s)H_2(s) = \frac{(1 + \tau_2 s)^{n_2}}{(\tau_1 s)^{n_1}} \tag{52}$$

Having determined Z_W(s), the voltage V(t) can be found in terms of the echelon current I(t).

$$V(t) = E_o + R_\Omega I(t) + R_{tc}\left(1 - e^{-\frac{t}{R_{tc}C_{dl}}}\right)I(t) + L^{-1}\left[\frac{(1 + \tau_2 s)^{n_2}}{(\tau_1 s)^{n_1}} I(s)\right] \tag{53}$$

Nickel Hydrogen Batteries

The Ni-H_2 battery possesses high gravimetric density, high tolerance to overcharging and reverse charging, and high power density. Furthermore, this battery does not require any maintenance and has a prolonged life cycle, which is why they are extensively used in aerospace applications [131]. At the end of the last century, Ni-H_2 batteries had successfully overtaken the Ni-Cd batteries in its use in satellites, which is evident from Figure 45. Within a short span of a decade, NiH_2 batteries proved themselves to be better candidates than NiCd batteries in satellite applications. However, they do not have wide range of application due to having a high self-discharge rate and high cost [131].

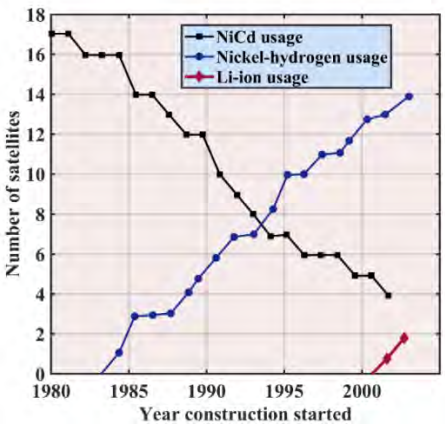

Figure 45. The precipitous rise of the usage of NiH_2 batteries and fall of the usage of NiCd batteries in satellites at the end of the 20th century [141].

The nickel-hydrogen (NiH_2) battery can be distinguished from a nickel-metal hydride battery in that it uses hydrogen in gaseous form. The hydrogen gas is stored in a pressurized cell at 1200 psi pressure. This battery has a charge/discharge efficiency of 85%. Its energy density is about 60 Wh/L. It has a specific energy of 55–75 Wh/kg. It is durable for about 20,000 cycles, which indicates its long life. Its specific power is around 220 W/kg. These rechargeable batteries are strong candidates for energy storage applications. It ise interesting to point out that the International Space Station (ISS) uses NiH_2 batteries.

Similar to the Ni-Cd and Ni-MH batteries, Ni-H_2 batteries use $Ni(OH)_2$ as the positive electrode and KOH as the electrolyte. However, the negative electrode consists of Hydrogen in gaseous form [47]. As the anode current closely resembles a fuel cell electrode, the Ni-H_2 batteries can be considered as a hybrid technology combining fuel cell and Ni-Cd batteries [48]. Here, the hydrogen is not stored or transformed but simply acts as catalytic surface. This means that hydrogen remains in gaseous form within the case, which necessitates the need for high pressure with standing case of 70 bar [47]. Therefore, the Ni-H_2 battery must be hermetically sealed. They have an equivalent circuit similar to Ni-Mh batteries. The internal construction of the Ni-H_2 battery is represented in Figure 46. The electrochemical reactions, which take place in Ni-H_2 batteries, are represented below [142].

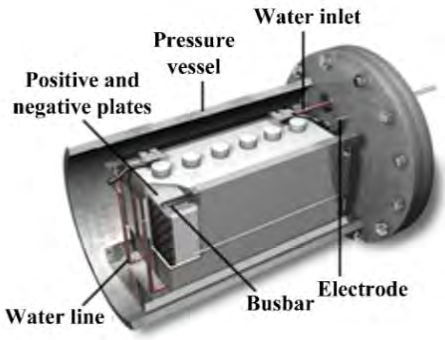

Figure 46. Internal construction of the hermetically sealed (i.e., airtight) Ni-H_2 battery [143].

Cathode: $Ni(OH)_2 + OH^- \underset{discharge}{\overset{charge}{\rightleftharpoons}} NiOOH + H_2O + e^-$

Anode: $H_2O + e^- \underset{NiMoCo,discharge}{\overset{NiMoCo,charge}{\rightleftharpoons}} \frac{1}{2}H_2 + OH^-$

Overall: $Ni(OH)_2 \underset{NiMoCo,discharge}{\overset{NiMoCo,charge}{\rightleftharpoons}} NiOOH + \frac{1}{2}H_2$

Nickel Iron Batteries

The Ni-Fe battery invented in 1908 possesses a very robust structure, which leads to high tolerance to power, temperature, and amperage [17,131]. Furthermore, it possesses a very long life cycle. Same as the case of Ni-Cd and Ni-Mh batteries, this battery consists of $Ni(OH)_2$ as positive electrode and KOH as the electrolyte. The only difference is the negative electrode, where an iron electrode is used. This eliminates the use of toxic cadmium, and as iron is not a toxic material, the Ni-Fe batteries are environmentally friendly [131]. This battery has been implemented in New York shuttle cars, subways cars, and also in London underground electromotive [18]. However, this battery technology suffers some major disadvantages such as low power density, low energy efficiency, low energy density, and excessive water consumption [17,131]. The electrochemical cell reaction of this battery is given below:

Cathode: $2NiOOH + 2H_2O + 2e^- \Rightarrow 2Ni(OH)_2 + 2OH^-; E^o = 0.49V$
Anode: $Fe + 2OH^- \Rightarrow Fe(OH)_2 + 2e^-; E^o = -0.88V$
Overall reaction: $2NiOOH + 2H_2O + Fe \Leftrightarrow 2Ni(OH)_2 + Fe(OH)_2; E^o = 1.37V$

Nickel Zinc Batteries

Just as the previously discussed nickel-based batteries, nickel-zinc (Ni-Zn) batteries use $Ni(OH)_2$ as positive electrode and alkaline KOH as the electrolyte. For the negative electrode, a paste of zinc oxide is used [17]. This battery was first invented in 1899 and the commercial production started in 1920 [17]. The cell voltage of Ni-Zn batteries is 1.65 V/cell, whereas Ni-Cd and Ni-MH can only deliver 1.20 V/cell. This high cell voltage of Ni-Zn leads to a very high energy density—almost twice the energy density of Ni-Cd and Ni-MH [17]. Ni-Zn also does not contain any heavy toxic materials and can are easily recyclable. However, as zinc is highly soluble is KOH, it reacts with and forms zinc oxide in the negative electrode, which leads to forming and growth Zn dendrites [17]. Therefore, the Ni-Zn suffers from a very short life cycle. The following reactions takes place in the Ni-Zn batteries. The comparison of different nickel-based batteries is tabulated in Table 10.

Cathode: $2NiOOH + 2H_2O + 2e^- \Rightarrow 2Ni(OH)_2 + 2OH^-; E^o = 0.49V$
Anode: $Zn + 2OH^- \Rightarrow Zn + H_2O + 2e^-; E^o = -1.25V$
Overall reaction: $Zn + 2NiOOH + 2H_2O \Leftrightarrow Zn(OH)_2 + 2Ni(OH)_2; E^o = 1.74V$

Table 10. Characteristics of nickel-based batteries [17].

Battery	Cell Voltage (V)	Specific Energy (Wh/kg)	Specific Power (W/kg)	Energy Efficiency (%)
Nickel-iron	1.2	30–60	100	60–70
Nickel cadmium	1.2	50–60	200	70–75
Nickel-zinc	1.65	80–100	170–1000	70–80
Nickel-metal hydride	1.2	60–70	170–1000	70–80
Nickel-hydrogen	1.55	55–75	220	85

3.6. Flow Batteries

A flow battery is an advanced aqueous electrolytic battery, which can be said to be a cross between conventional fuel cells and batteries [3,144]. This type of battery is different from the conventional secondary batteries in the sense that one or more electroactive species is dissolved in the electrolyte, i.e., the energy is stored in the electrolyte [3,6]. This electroactive species flows through the power core, converting the chemical energy to electricity. Therefore, the flow batteries consist of active electrolytes and do not have any self-discharge [3]. The additional electrolyte is stored in two separate external tanks, and is pumped through the reactor and causes the chemical reaction [3,6]. The electrolytes are

separated by a microscopic membrane, which permits a limited number of ions to cross through it. These ions participate in oxidation and reduction reaction inside the reactor and electricity is produced because of it [145]. The schematic diagram of the flow battery is shown in Figure 47.

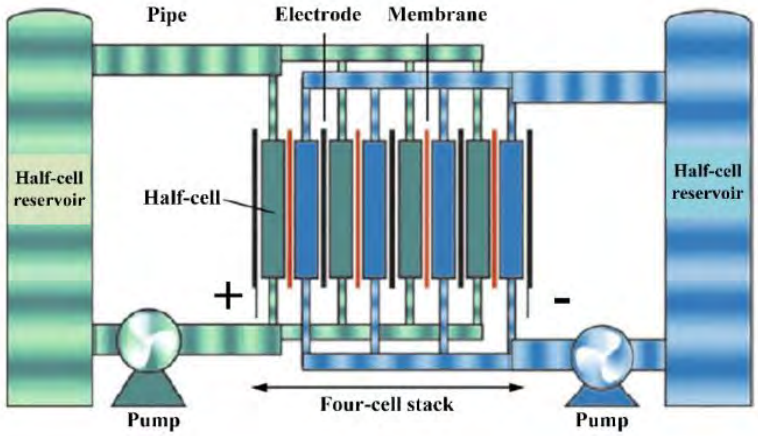

Figure 47. Schematic diagram of flow battery. The electroactive species dissolved in the electrolyte flows through the power core, converting the chemical energy to electricity [6].

In contrast to the fuel cell, the chemical reactions taking place inside the flow batteries are reversible, and thus can be recharged without replacing the electroactive material. Flow batteries are capable of releasing huge amount of energy at a high discharge rate [6]. They also possess a good life cycle and can deliver 10,000 full cycles during their lifetime [144]. The power rating of the flow batteries depends on the number stacks in the cell and also on the size of the electrode. On the other hand, the energy storage capacity depends on the volume of the reservoir and the concentration of the electrolyte. Therefore, the flow batteries have the additional feature of decoupling between the power rating and energy storage capacity, and are thus suitable for both power- and energy-related storage applications [3]. Furthermore, flow batteries are capable of operating near to the ambient temperature, have very short response time in the range of milliseconds, and can have high efficiency [146]. Based on the electroactive components of the flow batteries, they can be classified into two types: Redox flow batteries and hybrid flow batteries [26].

Redox Flow Batteries

Redox flow batteries (RFB) are the most popular flow batteries, where the electroactive materials are dissolved into liquid electrolyte [147]. By means of oxidation and reduction reaction, these batteries generate electricity, hence the name redox flow battery [148]. There are different types of redox flow batteries with different electroactive material such as Vanadium, Vanadium-polyhalide, Bromine-Polysulfide, Iron-Chromium, and Hydrogen-Bromium redox flow batteries [147]. Among them, the Vanadium and Polysulfide-Bromide redox flow batteries are most popular and are reviewed in this paper.

Vanadium Redox Flow Battery

Vanadium redox flow batteries (VRFB), patented in 1986, are the most mature technologies among the existing flow batteries [3,144]. They have low parasitic loss, life cycle above 10,000, and an efficiency of 90% at light load operation. The paramount benefits of the VRFB is that it maintains a constant voltage at all operating conditions and can be instantly recharged at any time by replacing the electrolyte [3]. These advantages make the VRFB useful for peak shaving, load levelling, integration to renewable energy systems, power quality enhancement, and UPS applications. However, the VRFB also has some major disadvantages, such as limited energy density and high cost, etc.

By employing vanadium redox couples- V^{2+}/V^{3+} in the negative and V^{4+}/V^{5+} in the positive half-cell the energy is stored in the VRFB [6]. A common electrolyte-vanadium sulphate dissolved in a sulfuric acid is used stored these ions [3]. The electrolyte from anolyte and catholyte tanks are pumped into the core and oxidation and reduction reaction occurs. During charging and discharging, H^+ ions are transferred between aforementioned vanadium redox couples. A polymer membrane is used, which allows only H^+ ions to migrate, but impedes the flow of HSO_4^- ions [3,6]. The schematic of a VRFB is represented in Figure 48. The electrochemical reaction occurring in each half cell of the VRFB are [3]:

Anode: $V^{2+} \leftrightarrow V^{3+} + e^-$
Cathode: $V^{4+} \leftrightarrow V^{5+} + e^-$
Overall: $V^{5+} + V^{2+} \leftrightarrow V^{3+} + V^{4+}$

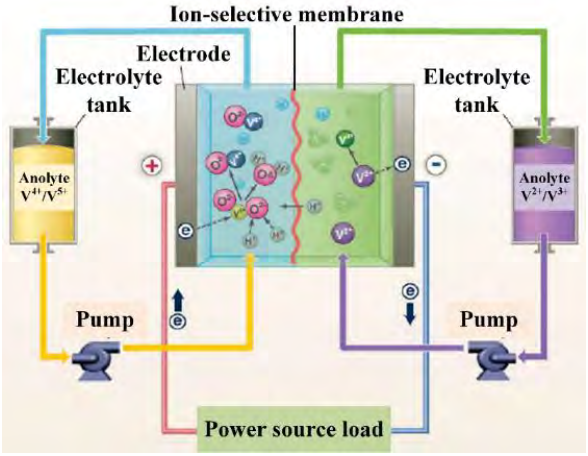

Figure 48. Schematic diagram of redox flow (vanadium) batteries. By employing vanadium redox couples V2+/V3+ in the negative V4+/V5+ in the positive half-cell the energy is stored in the vanadium redox flow batteries (VRFB) [3].

The equivalent circuit of the VRFB is represented in Figure 49, and it closely resembles Li-ion and Ni-MH batteries. $E_{cell\ (ORP)}$ is the open circuit potential, which represents the SOC and temperature of the battery. The current excitation within the cell is represented by the R_o, whereas series of parallel RC networks represents the dynamic behavior of the battery [149].

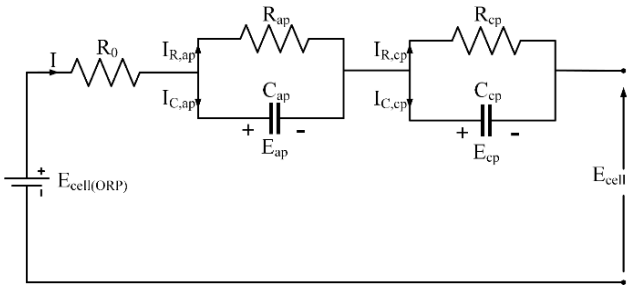

Figure 49. Equivalent electrical circuit of a unit cell, laboratory unit V-RFB system, which is very similar to Li-ion and Ni-MH batteries [149].

On the equivalent circuit of the V-RFB, applying Kirchhoff's voltage law, the terminal voltage of the cell can be expressed as [149],

$$E_{cell} = E_{cell(ORP)} - IR_O - E_{ap} - E_{cp} \quad (54)$$

Again,

$$I + I_{R,ap} + I_{C,ap} = 0 \tag{55}$$

Substituting $I_{R,ap} = \frac{E_{ap}}{R_{pc}}$ and $I_{C,ap} = C_{ap}\frac{dE_{ap}}{dt}$ into Equation (55), the ordinary differential equation (ODE) across the activation polarization RC network can be written as,

$$E_{ap} = \frac{I}{C_{ap}} - \frac{E_{ap}}{C_{ap}R_{ap}} \tag{56}$$

Since the concentration polarization of the RC network duplicates the activation polarization of the RC network,

$$E_{cp} = \frac{I}{C_{cp}} - \frac{E_{cp}}{C_{cp}R_{cp}} \tag{57}$$

Differentiating the cell potential E_{cell} with respect to time, we get,

$$\dot{E}_{cell} = \dot{E}_{cell(ORP)} - I\dot{R}_O - \dot{E}_{ap} - \dot{E}_{cp} \tag{58}$$

Substituting (56) and (57) into (58), considering only the transient response and taking the time derivative of $\dot{E}_{cell(ORP)}$ *and* $I\dot{R}_O$ negligible,

$$\dot{E}_{cell} = -\left[\frac{1}{C_{ap}} + \frac{1}{C_{cp}}\right]I + \left[\frac{1}{R_{ap}C_{ap}}\right]E_{ap} + \left[\frac{1}{R_{cp}C_{cp}}\right]E_{cp} \tag{59}$$

$$\dot{E}_{cell} = -\left[\frac{1}{C_{ap}} + \frac{1}{C_{cp}} + \frac{R_o}{R_{cp}C_{cp}}\right]I + \left[\frac{1}{R_{ap}C_{ap}} - \frac{1}{R_{cp}C_{cp}}\right]E_{ap} + \left[\frac{1}{R_{cp}C_{cp}}\right]E_{cell(ORP)} - \left[\frac{1}{R_{cp}C_{cp}}\right]E_{cell} \tag{60}$$

Polysulphide Bromide Battery

The polysulphide bromine (PSB) battery was patented by Remric in 1984 [150]. Sulfur has high theoretical capacity, is non-toxic, and inexpensive. The aqueous PSB battery consists of a Na_2S anolyte and a NaBr catholyte. Na_2S is abundant and cost-effective, and highly soluble in aqueous solvents. Redox flow batteries using 2.0 M Na_2S electrolyte provide a cell voltage of 1.36 V. Furthermore, long-chain polysulfides are highly soluble in non-aqueous electrolytes too; however, short-chain polysulfides are insoluble, which are formed at long-term cell cycling, and these precipitates can be problematic [151]. The PSB battery is a type of redox flow battery that uses a reversible reaction between two solutions of salt electrolytes: Sodium bromide (NaBr) and sodium polysulfide (Na_2S_x, where x = 2 to 5). Generally, Na_2S_2 is used as the anolyte and NaBr as the catholyte. The redox half reactions are as follows:

Reaction at anode: $2Na_2S_2 \rightarrow Na_2S_4 + 2Na^+ + 2e^-$
Reaction at cathode: $NaBr_3 + 2Na^+ + 2e^- \rightarrow 3NaBr$
Overall reaction: $3NaBr + Na_2S_4 \leftrightarrow 2Na_2S_2 + NaBr_3$

The two salt solution electrolytes in different vessels are brought together in the battery but separated by a polymer membrane, which is selectively permeable only to cations, specifically the Na^+ ions, producing a voltage difference of 1.5 V across the membrane. In order to obtain the desired voltage level, the cells are suitably connected in series or parallel. This battery has an overall efficiency of 75%, and works at room temperature [6]. Both the electrolyte species are vastly available and hence inexpensive. They are also highly soluble in aqueous solutions, which allows the production of the desired amount of charge from a small quantity of the electrolyte. Therefore, the PSB battery is very cost effective [150]. Another advantage of this battery is that it can be recharged easily, upon which the electrochemical reaction reverses and the original electrolytes can be obtained again. Moreover, the electrodes are not corroded in this system, which only increases the profitability of this system.

If electrodes made of activated Carbon or polyolefin composites are used, the bromide ions are adsorbed by the electrode. This causes the cell voltage to increase from 1.7 V to 2.1 V while charging. This, however, suffers from crossover and mixing of the electrolytes, leading to precipitation of sulfur compounds and the generation of H_2S and Br_2 [150].

Hybrid Flow Batteries

The hybrid flow batteries can be considered a combination of secondary batteries and flow batteries due to the fact that this type of electrochemical cell contains one battery electrode and one fuel cell electrode [3,148]. In this type of batteries, on electroactive material is stored inside the electrochemical cell and plated as a solid, whereas the other electroactive material is dissolved in liquid electrolyte and is stored in an external reservoir [3]. There are different types of hybrid flow batteries such as Zinc bromine, Zinc cerium batteries, etc.

Zinc Bromine Batteries

The Zinc Bromine (ZnBr) batteries developed in the early 1970s are one of the most attractive existing flow batteries, especially in the grid-scale energy storage applications [152,153]. These batteries have high energy density of 35–75 Wh/L, abundant low-cost materials, high theoretical voltage of 1.85 voltage, and a long life cycle of 10–20 years [3]. Furthermore, the batteries have large DOD capability, large charge duration of 8–10 h, inherent simple chemistry, and the chemical reversibility of the electrodes is much higher [3,153]. Owing to these attributes, the ZnBr is being currently being employed in the energy sectors of USA, Australia, and Scotland [153]. However, the ZnBr also has some major shortcomings such as, high self-discharge rate, low round trip efficiency, formation of zinc dendrite, corrosion of zinc electrode, and the toxic nature of bromine [3,146,154,155].

In this type of battery, the electrolyte used is an aqueous solution of the zinc bromide salt [147]. By means of pumps, this electrolyte is circulated on both the electrode surfaces. The electrode surfaces are separated by a microporous plastic film; thus, two different electrolytic flow steams can circulate on two different electrodes—positive and negative electrode. This microporous plastic film acts as a separator, which hampers the diffusion of bromine to zinc deposition layer, thus reducing the associated chemical reaction which leads to self-discharge [156]. The electrolyte on the negative side is a purely aqueous solution, while the electrolyte flowing through positive electrode surface contains some organic amine, which helps to hold the bromine in the solution [157]. Zinc, which has negative potential on both acidic and aqueous solution is used as the solid negative electrode [3]. Bromine is the electroactive material dissolved in an aqueous solution and used as the positive electrode. The schematic of a ZnBr battery is shown in Figure 50.

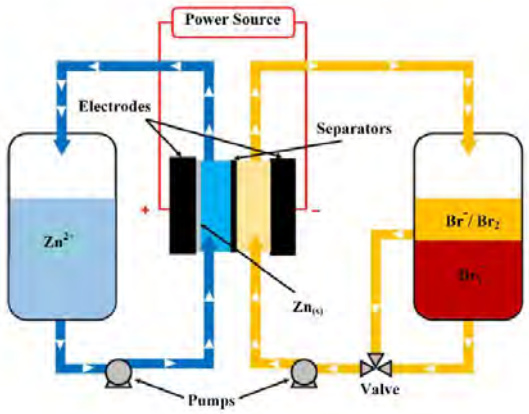

Figure 50. Simplified schematic of the Zinc-Bromine redox flow battery. Zn is used as the solid negative electrode and Br is the electroactive material dissolved in an aqueous solution and used as the positive electrode [158].

During the charge phase, metallic zinc is deposited at the negative electrode as a thin film. Concurrently, on the other side of the membrane, bromine evolves as dilute solution and reacts with the organic amine, forming a thick bromine oil, which sinks down bottom of the electrolytic tank [6]. This bromine oil is allowed to be mixed with the electrolyte during discharge. While discharging, Zn and bromine combine to form $ZnBr_2$, thus increasing the concentration of both Zn^{2+} and Br^- ions [6]. The electrochemical reactions are as follows:

$$\text{Anode: } Zn^{2+} + 2e^- \underset{discharge}{\overset{charge}{\rightleftharpoons}} Zn^0; E^o(25^oC) = 0.763V and E^o(50^oC) = 0.760V$$

$$\text{Cathode: } 2Br^- \underset{discharge}{\overset{charge}{\rightleftharpoons}} Br_2(aq) + 2e^-; E^o(25^oC) = 1.087V and E^o(50^oC) = 1.056V$$

$$\text{Overall: } \underset{dischargedstate}{ZnBr_2(aq)} \overset{charge}{\underset{discharge}{\rightleftharpoons}} Zn^0 + Br(aq); E^o_{cell}(25^oC) = 1.85V$$

An equivalent circuit modelling of ZnBr battery, comprised of inlet and outlet streams of the positive and negative electrode is represented in Figure 51. The resistances of the positive and negative electrolyte are represented by $R_m{}^+$ and $R_m{}^-$, respectively, whereas $R_c{}^+$ and $R_c{}^-$ represent the resistance of the positive and negative electrolyte in the channel.

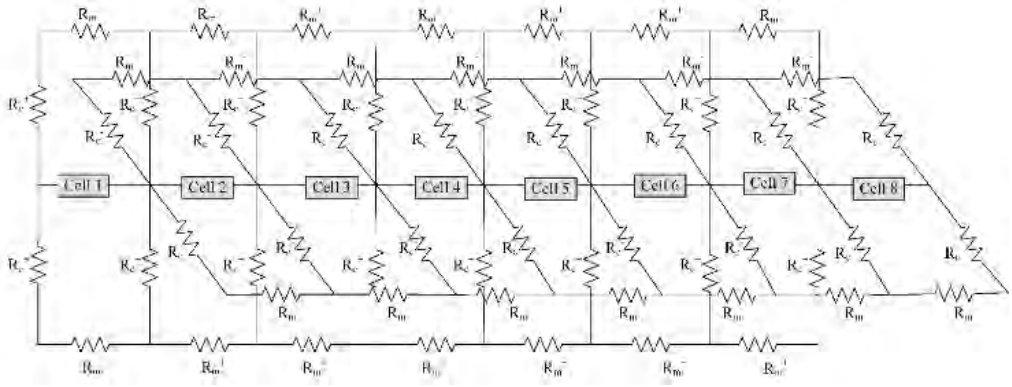

Figure 51. An equivalent circuit model of ZnBr batteries; the resistances of the positive and negative electrolyte are represented by Rm+ and Rm-, respectively. Rc+ and Rc- represent the resistance of the positive and negative electrolyte in the channel [153].

Zinc Cerium Batteries

The Zinc-Cerium (Zn-Ce) batteries is a hybrid redox flow battery, first developed by the Plurion Inc. in the beginning of 2000s [159]. It is very much similar to the Zn-Br in the sense that both batteries use Zn as electroactive material in the negative electrode. However, there are some fundamental differences, such as in Zn-Ce batteries, Ce is used in the positive electrode. In addition, methanesulfonic acid (MSA) is used as the electrolyte to avoid the precipitation of cerium hydroxide [159,160]. This battery has the highest theoretical voltage of 2.5 V, which results in higher cell capacity and power under certain electrolytic solution [160]. The positive and negative electrolyte are separated by a separator polymer cation exchange membrane [159,160]. The schematic of the Zn-Ce battery is represented in Figure 52. In this type of battery, Zn/Zn^{2+} and Ce^{4+}/Ce^{3+} redox reactions take place to produce electricity. The reactions are given below.

$$\text{Anode: } Zn^{2+} + 2e^- \underset{discharge}{\overset{charge}{\rightleftharpoons}} Zn(-0.76V\ vs.\ NHE)$$

$$\text{Cathode: } 2Ce^{3+} - 2e^- \underset{discharge}{\overset{charge}{\rightleftharpoons}} 2Ce^{4+}(between + 1.28V\ and + 1.72V\ vs.\ NHE)$$

$$\text{Overall: } Zn^{2+} + 2Ce^{3+} \underset{discharge}{\overset{charge}{\rightleftharpoons}} Zn + 2Ce^{4+}$$

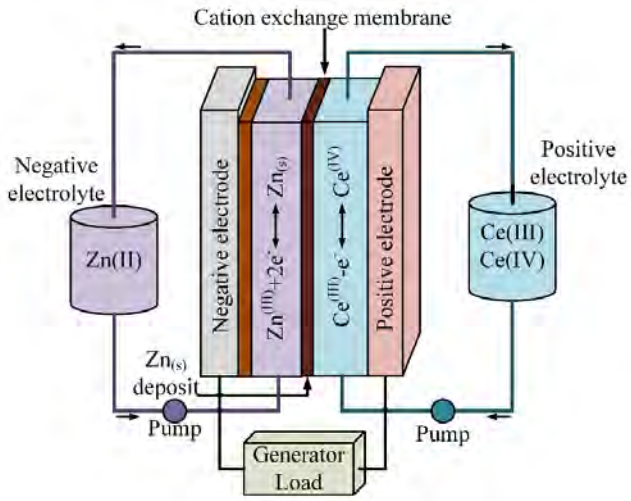

Figure 52. Schematic diagram of zinc-cerium flow battery; Zn/Zn2+ and Ce4+/Ce3+ redox reactions take place to produce electricity [160].

As previously mentioned, generally the Zn-Ce batteries use weak acid MSA as supporting electrolyte. However, operating under this type of condition results in some serious corrosion of the Zn electrode [159]. The proton exchange membrane and acidic electrolyte does not allow the integration alkaline Zn electrode-a well-developed and widely used technology. Furthermore, the use of acidic electrolyte reduces the electromotive force of Zn, which results in less output voltage. In addition, the proton exchange membrane causes Zn dendrite formation [159]. A Zn-Ce battery with an alkaline Zn electrode and mediator-ion solid state electrolyte (SSE) is proposed in [159]. In this case, alkaline liquid electrolyte is used in the negative electrode, acidic liquid electrolyte is used in the positive electrode, and they are separated by a Na^+ conductive SSE. The SSE has no influence on the chemical reactions; however, it functions as a mediator and allows charge transfer at the two electrodes [159]. The schematic of the proposed Zn-Ce battery along with corresponding theoretical potential is shown in Figure 53.

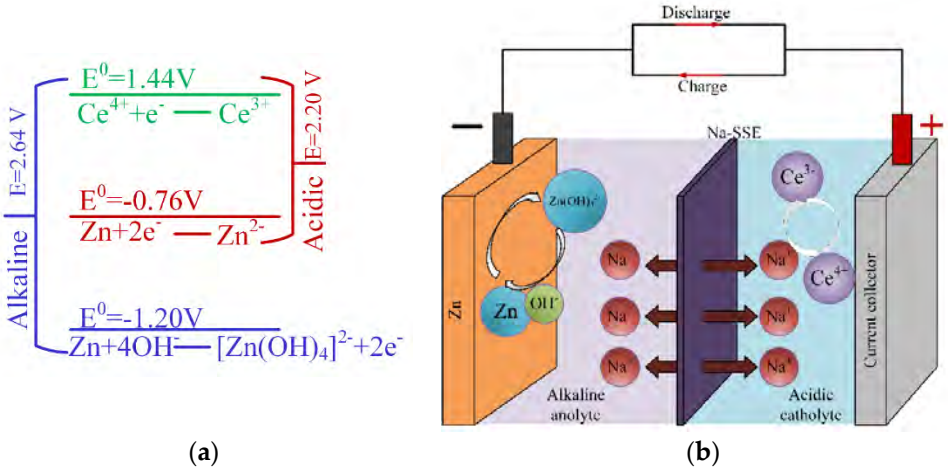

Figure 53. (**a**) Schematic illustration of the theoretical voltages of Zn-Ce batteries with an alkaline or acidic anolyte; (**b**) schematic of a Zn-Ce battery with an alkaline anolyte, an acidic catholyte, and a Na+-ion solid electrolyte (termed as Zn(NaOH) || Na-SSE || Ce4+(MSA/Na2SO4) cell) [159].

Redox Flow Batteries with Solid Electroactive Materials

The major drawback of existing commercial redox flow batteries is that their energy density is limited due to the limited solubility of the electroactive materials in the electrolyte. The energy density

can be improved by using solid electroactive material instead of materials that gets dissolved in the electrolyte. This is turn can reduce the footprint, transport, and installation cost, and can open up new applications for the flow batteries [161]. According to [161], the RFB with solid electroactive material can be categorized into four types based on the flowing condition and the role of carbon in the electrolyte, which are described below.

Flowing Carbon as Electrochemical Reaction Electrodes

In the conventional RFB, the porous carbon electrode is preferred, which increases the total surface area due to which the specific current density and total current of the battery increases. One way of conceptualizing RFB with solid carbon flowing as an electrochemical reaction electrode is that the porous electrode of the conventional RFB is broken into nano or micro sized particles of carbon and dispersing them in to the electrolyte [161]. These micro or nano sized particles do not dissolve in the electrolyte and result in less pressure drop across the electrochemical reaction as the current collector in this case would planar instead of porous carbon. This type of design is has been utilized by several battery system such as lithium polysulphide (Li-Ps), Li-air, and metal ions in aqueous solution [162–164]. The schematic of this type of battery is represented in Figure 54. These nano or micro particles of carbon transude and accumulate. Electrochemical reaction takes place in the surface of the accumulated carbon particles while they are in contact with the current collector [161].

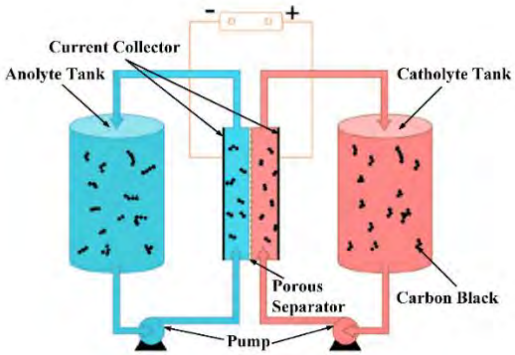

Figure 54. Schematic illustration of Type I redox flow batteries (RFB) design, which uses flowing carbon as electrochemical reaction electrodes [161].

In Li-Ps batteries, the counter electrode is solid Li metal, which means that it is also a hybrid redox flow battery. The surface of the Li metal is passivated by $LiNO_3$ to improve the coulombic efficiency [165]. Li-Ps electrolyte is used, which is pumped through the core, while a microporous separator is used to separate Li electrode and the catholyte [165–168]. In the conventional Li-Ps battery, Li_2S_8 and Li_2S_4 species are soluble; however, species like Li_2S are insoluble, resulting in reduction of the total capacity of the battery as well as energy of the cell [167]. Reported by [168], nano carbon materials are dispersed in the Li-Ps electrolyte as solid active material. The schematic of the Li-Ps semi-solid flow cell is represented in Figure 55. The flowing nano carbon material increases the energy density of the electrolyte significantly. As the charge transfer is lower even at a lower loading of carbon, the overpotential of the battery was lower. Furthermore, the estimated pumping cost was lower when compared to conventional RFB, despite the electrolyte having higher viscosity [161]. The solid nano carbon particles in the electrolyte do not take part in the redox reaction themselves as they are not electroactive materials. Nevertheless, they facilitate and improve the rate of redox reactions occurring inside of the cell.

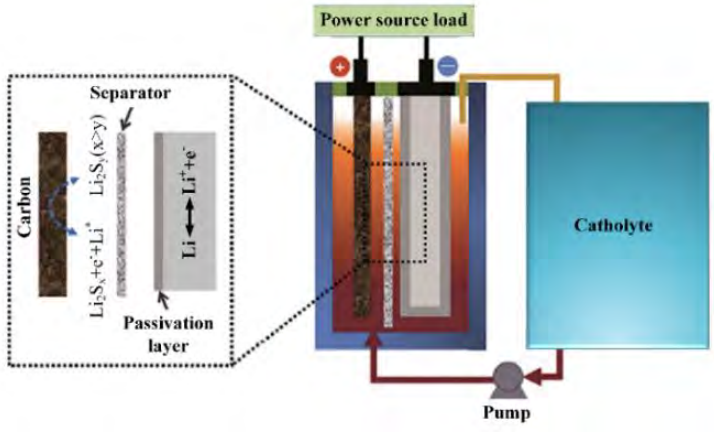

Figure 55. Schematic diagram of the Li-Ps semi solid flow cell; Li-Ps electrolyte is used, which is pumped through the core, while a microporous separator is used to separate Li electrode and the catholyte [165].

Flowing Solid Active Materials with Flowing Carbon Conducting Network

In this type of battery—previously described as semisolid flow battery—both carbon particles or other additive and electroactive material particles are dispersed in the electrolyte, where they remain in solid form and does not get dissolved [161,169]. The additive, i.e., carbon particles, need to be in the nanometer range and function as a conducting network to transfer electron between current collector and solid active particles. That means in this case, the electrochemical reaction does not take place on the surface of the carbon particles [161]. The schematic of this type of battery is represented in Figure 56.

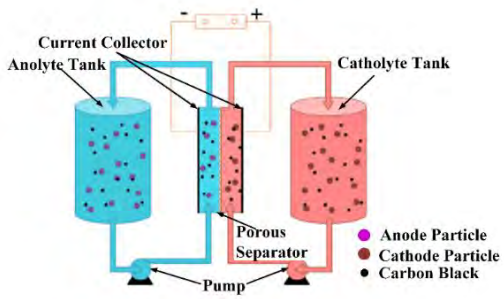

Figure 56. Schematic illustration of Type II RFB design, where the electroactive materials are solid and dispersed in the electrolyte [161].

The semisolid concept was utilized for Li-ion and Na-ion materials dispersed into both organic and liquid fluids [161]. Duduta et al. reported the semi solid Li-ion flow battery, where Li-ion active materials were circulated in slurries along with conductive additives [169]. The active material in the cathode was $LiCoO_2$, which along with Ketjen Black (KB) carbon conductive additive, was dispersed in a suspension of Li-ion organic electrolyte solution (22.4 vol%, 10.2 M) [160,161]. For the anode, $Li_4Ti_5O_{12}$ along with Ketjen Black (KB) carbon conductive additive dispersed in Li-ion organic electrolyte (10 vol %, and 2.3 M) was used.

In this type of battery system, as the solid active materials are used, the solubility issue, which results in limited capacity per volume in the conventional RFB can be overcome [161]. Furthermore, using the Li-ion materials and organic electrolytes, the voltage range of the battery can be extended beyond 4 V. Having high concentration of solid Li-ion materials, and wide potential range, these batteries have high energy density and can avoid lithium dendrite growth [151]. In addition, in this type of battery system, by utilizing the size exclusion principle, the two slurries containing solid active

material and carbon additives can be separated by means of a porous separator, which is generally less expensive, therefore resulting in low production cost of the battery. The major drawback of this type of battery is that the pumping cost is much higher due to the high viscosity of the electrolyte, which can be reduced by using suspension additives and coating the carbon particles. There is also a tradeoff between power density and coulombic efficiency of the battery [161].

Flowing Active Material Particles Colliding on Current Collectors without Carbon

Contrary to the previous type of battery discussed, where solid active material with carbon particles as additive was dispersed in the electrolyte, in this type, no carbon additive is added. This results in less viscosity of the electrolyte, and thus, the corresponding pumping requirement to maintain the high energy density is reduced [161]. Furthermore, not using carbon additive also results in reduced mass and by removing the components that do not contribute to the cell energy density lessens the volume of the electrolyte. In the absence of the percolating network, the electrochemical reaction takes place only within the particles in contact with the current collector, rather than throughout the channel, which is facilitated by the carbon particles. The chemical reaction depends on the collision of the solid electro active materials to the current collector; therefore, this type of battery requires a high flow of electrolyte [161]. The schematic diagram of the battery is represented in Figure 57.

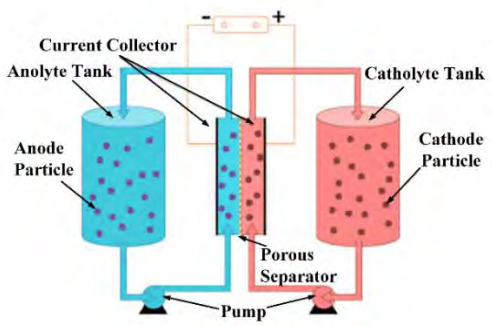

Figure 57. Schematic illustration of Type III RFB design, where flowing active material particles collide on current collectors without carbon [161].

The aforementioned carbon-free redox battery type design for both Li-ion and polymer suspension based cell have been explored by [170–174]. The main advantage of this design is its simplicity due to exclusion additive materials. Furthermore, the cheap porous separator can be used to separate the particles utilizing the size exclusion principle is another advantage of this battery system [161]. For Li-ion materials, ambipolar diffusion of Li-ion and electron occurs, thus limiting the reaction rate, which in turn results in lower power output. Therefore, materials possessing very high ionic and electronic conductivity is required for this type of battery design.

Targeted Redox Mediators as the Power Carriers with Static Solid Active Materials Providing Energy Storage

As discussed earlier, the RFB is flexible for different customized design and application due to the fact of decoupling of power output and energy storage components. However, in the previously mentioned RFBs with solid electroactive materials, the same solid materials take part in energy storage as well as delivering output power. Therefore, even though the power and storage components are decoupled, the overall performance of the cell and state of energy fluid are in fact coupled [161]. To overcome this shortcoming and improve the conductivity of Li-ion redox flow batteries without any additive, Wang et al. proposed a concept using redox shuttle [161,164]. These mediators are soluble in the electrolyte and redox reaction of L-ion proceeded through these mediators. Hence, the mediators participated in the electrochemical reaction of the cell, while the solid Li-ion active materials functioned as the energy storage materials [175]. The discharged mediators after the electrochemical gets recharged

from the redox reaction from occurring in the solid energy storage materials and consequently the solid materials get discharged [161]. The solid active materials are stored in energy tanks are pumped into the cell using pumps. Therefore, the power output and energy storage of the cell were provided by two different types of materials, which resulted in further increase in the capacity and energy density of the battery [175–177]. The schematic diagram of the battery is represented in Figure 58.

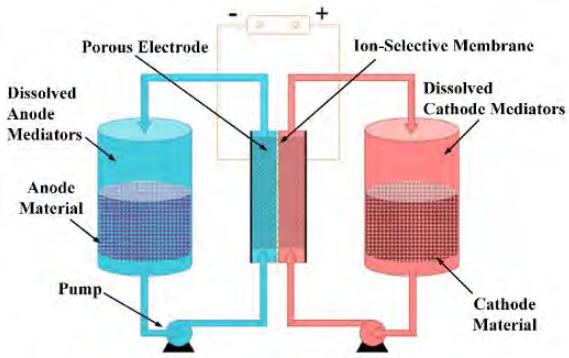

Figure 58. Schematic illustration of Type IV RFB design, which uses targeted redox mediators as the power carriers with static solid active materials providing energy storage [161].

Jia et al. reported a full cell of redox flow battery with targeted redox mediator, where $LiFeO_4$ was used as the cathode energy storage material and TiO_2 as the anode energy storage material [176–178]. For the catholyte, a pair of redox mediators—dibromo ferrocene ($FcBr_2$) and ferrocene (Fc)—was used as the oxidation and reduction agent, respectively; whereas, cobaltocene [$Co(Cp)_2$] and bis (pentamethylcyclopentadienyl) cobalt [$Co(Cp^*)_2$] were used as mediator pair for the anolyte [151]. The chemical and electrochemical reactions taking place in the solid active materials and mediator are represented in Figure 59. It is evident that redox potential of $LiFeO_4$ is above Fc but below $FcBr_2$. Fc^+, the only species involved in the electrochemical reaction, will be reduced to Fc. Thereafter, this Fc, when coming in contact with the solid $FePO_4$ particle's surface will become oxidized by it to again form Fc^+. Consequently, this process reduces the $FePO_4$ to $LiFeO_4$. The cell is considered to be fully discharged when all the $FePO_4$ is reduced to $LiFeO_4$ and all the Fc^+ ions reaches depletion [161]. The corresponding reactions take place in the anode side and the reaction in the order of (a) to (f) represents the discharge process. Reaction from (f) to (a) takes in sequence during the charging phase of the battery.

The energy density of this battery can be increased by adding more solid particles; however, this does not change the viscosity of the electrolyte. Moreover, this type of design requires less redox shuttle, which results in significant amount of volume reduction. In addition, mediators dispersed in low-viscosity liquid need to circulated, which results in less pumping energy requirement. All of these attributes to cost reduction of the battery. However, this battery also has some drawbacks. The high loading solids in order to achieve more energy density results in pressure drop arising in the particle bed. Furthermore, the cheap porous separator, which works on the principle of size exclusion principle, cannot be applicable in this type of battery. Finally, there exists a voltage difference between the solid active materials and mediators, which yields to low cycle efficiency [161].

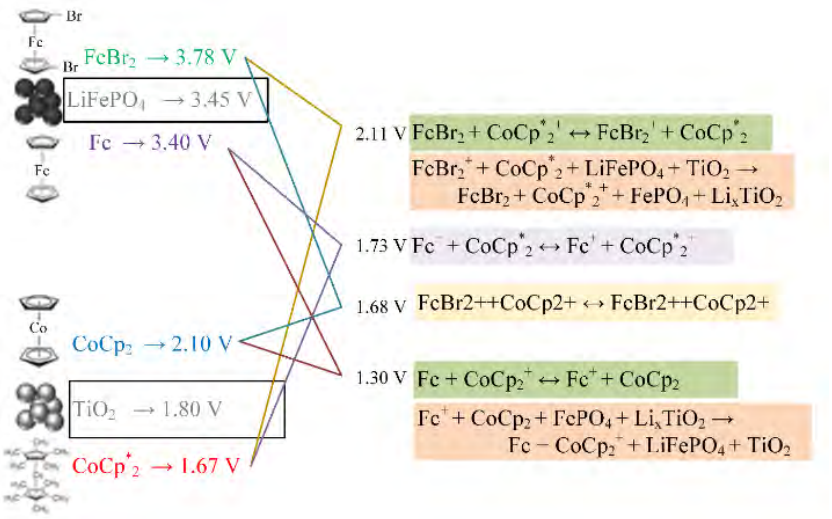

Figure 59. The chemical and electrochemical reactions in the solid active materials and mediator in the RFB, as reported by Jia et al. [161,176].

3.7. Electrochemical Capacitors

Electrochemical capacitors are similar to capacitors, but they store charge in the form of ions, rather than electrostatic energy. Faradic reactions are the principle mechanism of operation of these storage devices. There are two primary forms of electrochemical capacitors, namely pseudocapacitor and hybrid supercapacitor.

Pseudocapacitor

Contrary to the EDLC, the pseudocapacitor stores charge, i.e., their capacitance results from charge transfer between the electrolyte and pseudoelectrode [179]. This transfer occurs due to redox reaction of faradic nature, therefore the characteristics of pseudocapacitor is somewhat similar to the characteristics of batteries. This capacitance of a pseudocapacitor-pseudocapacitance is completely non-electrostatic in nature and occurs on the surface of the electrode, where faradic charge storing mechanism can be applied [180]. Metallic current collectors are conjoined with each electrode, which is merged in an electrolytic solution. The pseudocapacitors accompanied by a double layer forms a supercapacitor and the schematic diagram of it is represented in Figure 60.

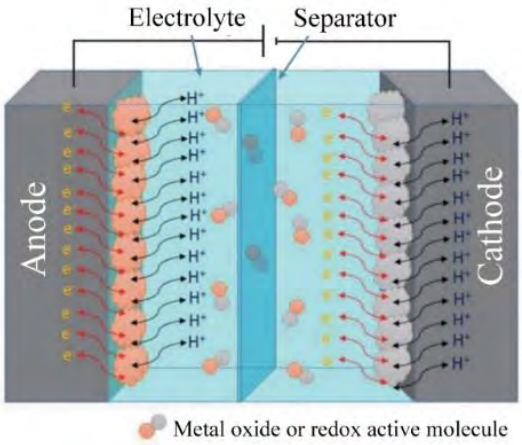

Figure 60. Schematic diagram of a pseudocapacitor, where capacitance results from charge transfer between the electrolyte and pseudoelectrode [59].

The electrode potential of the pseudocapacitors along with the charge storage due to reversible redox reaction gives a continuous logarithmic function of the sorption, hence the stored charge of the electrode is linearly dependent on the charging potential [59,181,182]. Owing to the aforementioned linear dependence, the charge storing mechanism in the pseudocapacitors is based on electron transfer rather than accumulation of ions in EDLC [183]. The specific capacitance of different pseudoactive electrode material are represented in Table 11.

Table 11. Different pseudocapacitive electrode materials with their electrolytes and specific capacitance [59].

Electrode Material	Electrolyte	Specific Capacitance F/g
RuO_2	H_2SO_4	650–735
MnO_2	K_2SO_4	261
$Ni(OH)_2$	KOH	578
$MnFeO_2$	PF_6 (Hexafluorophosphate)	126
TiN	KOH	238
V_2O_5	KCl	262
Polyaniline (PANI)	Aqueous	120–1530
	Non-Aqueous	100–670
Polypyrrole (PPy)	Aqueous	40–588
	Non-Aqueous	20–355
Polythiophene (PTh)	Non-Aqueous	1.5–6
Poly(3-methyl thiophene) (PMT)	Non-Aqueous	20–220
	Ionic liquid	15–225
Poly(3,4-ethylenedioxythiophene) (PEDOT)	Aqueous	100–250
	Non-Aqueous	121
	Ionic liquid	130
Poly(4-fluorophenyl-3-thiophene) (PFPT)	Non-Aqueous	10–48

According to [184], the pseudocapacitance of a pseudocapacitor is 10–100 times more than the capacitance of EDLC. However, as they possess poor electrical conductivity, the power density is lower along with poor cycling stability [59]. If the derivative of charge acceptance is Δq and changing potential is ΔV, then the pseudocapacitance is [59]:

$$C = \frac{d(\Delta q)}{d(\Delta V)} \tag{61}$$

Hybrid Supercapacitor

The hybrid supercapacitor concept aims to capitalize the advantages of the aforementioned EDLC and pseudocapacitors while mitigating their relative disadvantages [185]. The storage principle of the hybrid supercapacitor can be said to be the combination of the EDLC and pseudocapacitor systems [59]. Utilizing the faradaic and non-faradaic storage mechanisms, hybrid supercapacitors possess power density higher than the EDLC as well as maintaining good cycling stability and affordability, which are the main limitations of the pseudocapacitors [186]. The EDLC components of the hybrid supercapacitors contribute to having a high power density, whereas the pseudocapacitor components contribute to having a high energy density [59]. This type of system has high specific

capacitance, which leads to higher specific energy. The schematic diagram of the hybrid supercapacitor consisting of a carbon electrode and Li-insertion electrode is presented in Figure 61.

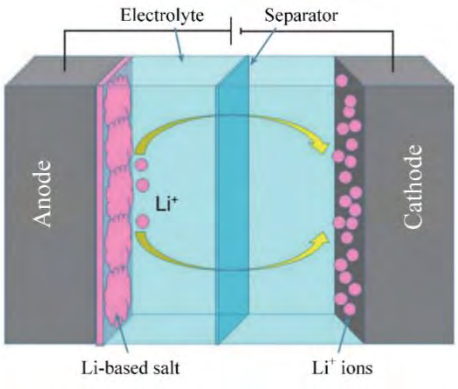

Figure 61. Schematic diagram of a hybrid supercapacitor, which combines the principles of EDLC and pseudocapacitors [59].

Based on the electrode, the hybrid supercapacitors can be categorized into three types—composite, asymmetric, and battery type. In the asymmetric hybrid supercapacitor, both ELDC electrode and pseudocapacitive electrodes are used to combine the faradaic and non-faradaic storage mechanisms [187,188]. In general, carbon-based materials are used in the negative electrode, whereas pseudoactive materials are used in the positive electrode. This design enables the asymmetric hybrid supercapacitor to have high energy density and power density than EDLC as well as better cycling stability than pseudocapacitors [188]. In the composite electrode, carbon-based materials are integrated with metal oxide or conducting polymer and both physical and chemical charge storage mechanisms occur simultaneously in a single electrode [189]. Using the carbon-based material results in having a higher surface area with the formation of double layer capacitance and it also increases the contact between the electrolyte and pseudoactive material. Due to the faradaic reactions, the pseudoactive materials are able to further increase the capacitance. The battery type hybrid supercapacitors are similar to the asymmetric hybrid supercapacitor in that sense that, they both use different types of electrodes. However, the difference is that in battery type hybrid supercapacitor, a supercapacitor electrode and a battery electrode are used. This results in having a storage system with attributes of batteries and supercapacitors. How different types of super capacitors can be merged to form a hybrid supercapacitor is represented in Figure 62. The hybrid capacitors with different electrode materials are tabulated in Table 12.

Table 12. Different hybrid supercapacitor electrode materials (MWCNT—multiwalled carbon nanotubes; CNTA—carbon nanotube arrays; PAN—polyacrylonitrile) [59].

Electrode	Electrolyte	Specific Capacitance (F/g)
Carbon/rGO	Na_2SO_4	175–430
RuO_2/MWCNT	H_2SO_4	169.4 mF/cm
MnO_2/MWCNT	Na_2SO_4	141
MnO_2/CNTA	Na_2SO_4	144
rGO/MnO_2	Na_2SO_4	60
PAN/Carbon nanofibers	KOH	134
PANI/MWCNT	H_2SO_4	360
PPY/MWCNT	H_2SO_4	200
PANI nanotubes/Titanium nanotubes	H_2SO_4	740

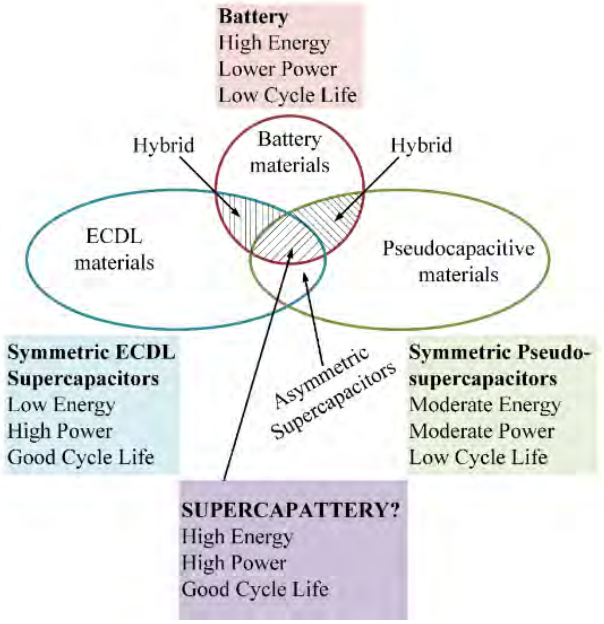

Figure 62. Merging the characteristics of EDLC, pseudocapacitive, and battery materials in battery type hybrid supercapacitors [185].

3.8. Chemical Energy Storage

Energy can be stored for a long time in the form of chemical bonds of molecules. When molecules react chemically and electron transfer takes place, energy can be produced. The reactants and products of chemical reactions are entirely different. Thus, energy can be converted from one chemical form to another. By this kind of chemical energy storage (ChES), nearly 100 GWh of energy can be stored [3]. Two main forms of ChES are thermochemical ES and electrochemical ES [37], with the latter being the most widely employed. Fuel cells are used in electrochemical energy storage, wherein continuous flow of electricity is obtained upon the availability of the chemical fuel. The following sections discuss the basics of fuel cells and their different variants.

3.8.1. Fuel Cell

A fuel cell is a cell that can convert the chemical energy of a chemical reaction directly to electrical energy and produce hydrogen and water as by-product. The concept of fuel cell was first provided by Christian Friedrich-a Swiss scientist in 1838 [190]. However, it was Sir William Grove who was the first to develop a fuel cell, which is based on the reversing the electrolysis of water in 1839 [191]. The main purpose of a fuel cell is to restore the energy used to produce hydrogen through electrolysis of water. Fuel cell is the combination of the best characteristics of engines and batteries. Under load conditions, the operation is very similar to batteries. Furthermore, it is also analogous to engines as it also can operate as long as the fuel is available [190]. The fuel cell has a long lifespan of 15 years, high charging and discharging rate, and high energy density. Therefore, the fuel cells are particularly preferred for small- and large-scale energy storage applications such as peak shaving, load levelling, intermittency reduction, and demand side management application. They are also used in distributed power generation, where they are integrated with the grid to control the voltage frequency, and hence, improve the power quality [192,193]. However, the low round trip efficiency and short life expectancy along with associated costs are the major obstacles of widespread implementation of fuel cells. Continuous research works are being conducted to overcome those aforementioned limitations of fuel cells [190].

In recent times, much emphasis has been given to hydrogen which is one of the most efficient, cleanest, and lightest fuels available. Furthermore, it can be effectively stored and reused, however,

it is not available in its pure form in nature and must be derived from primary energy sources [37]. In a fuel cell, electricity is consumed during the off-peak time for conducting electrolysis on water and producing hydrogen. During the peak time, this hydrogen along with oxygen from the atmosphere is used to generate electricity to meet with high demand [37]. The schematic diagram of the fuel cell is represented in Figure 63. Similar to batteries, it has two electrodes, which are in contact with an electrolyte layer. The electrode in which hydrogen fuel is supplied continuously is called the anode, whereas in the cathode, oxygen form air is fed continuously. In the anode, Hydrogen is decomposed into H^+ ions and electrons. The electrolyte membrane allows the H^+ to flow from anode to cathode, however does not allow the flow of electrons. These electrons travel from the anode to cathode by means of an external circuit and recombines with the H^+ and Oxygen to produce water. The cell reactions are represented below [190].

Anode: $H_2 \Rightarrow 2H^+ + 2e^-$

Cathode: $\frac{1}{2}O_2 + 2H^+ + 2e^- \Rightarrow H_2O$

Overall: $H_2 + \frac{1}{2}O_2 \Rightarrow H_2O$

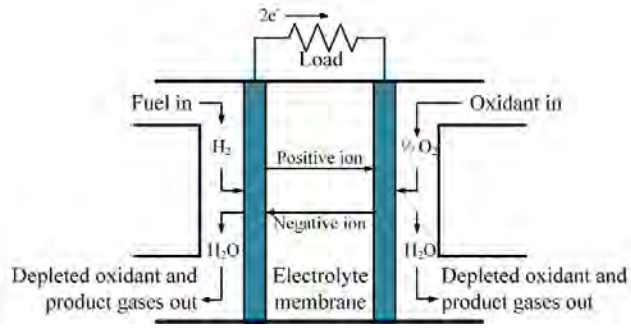

Figure 63. Fuel cell operation diagram; hydrogen and oxygen are present at the anode and cathode respectively, and water is produced as by-product [190].

Based on the electrolytes and fuel type, the fuel cells can be classified into six types, which are discussed below [190].

Proton Exchange Membrane Fuel Cell (PEMFC)

The proton exchange membrane fuel cell (PEMFC) has gained a lot of attention in recent times because it is considered as the one of the most energy-efficient and clean ESSs and is expected to have a significant role in future energy solutions [194]. In this type of fuel cell, a solid polymer Teflon-like membrane is used as the electrolyte to separate hydrogen and the oxygen. This electrolyte allows ions exchange between the two porous electrodes and is an excellent conductor of protons, hence the name. Pt and Pt-alloy nanoparticles are used as the catalyst due to the fact that Pt possesses the highest catalytic activity on both the cathode and anode side [195]. Carbons that have high specific surface areas such as porous carbon, vulcan carbon, etc., are used to support to catalyst. The schematic of PEMFC is represented in Figure 64.

The PEMFC possesses a very high power density and a very low operating temperature of around 1000 °C. These aforementioned attributes make the PEMFC system an ideal candidate for automotive vehicles, laptop, mobile phones, etc. [190]. However, it has low operating efficiency, the Pt electrode materials are very expensive, and it is not tolerant to carbon monoxide, which are major challenges in widespread commercialization of the PEMFC [190,195]. Instead of using hydrogen, ethanol or formic acid can also be used as fuel in this type of configuration; therefore, the PEMFC can be categorized into two types [190], which are discussed below.

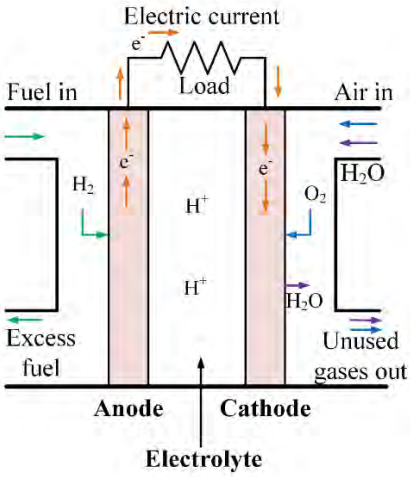

Figure 64. Schematic diagram of proton exchange membrane fuel cell (PEMFC); a solid polymer Teflon-like membrane is used as the electrolyte to separate hydrogen and the oxygen [196].

Direct Formic Acid Fuel Cell (DFAFC)

As the name suggests, direct formic acid fuel cell (DFAFC) uses formic acid as the fuel, which is fed directly into the anode electrode without any reformation [190]. The anode consists of a catalyst layer, diffusion media, and a bipolar plate, and formic acid fuel is supplied to it [197], whereas oxygen is supplied to the cathode. A perfluoro sulfonic acid membrane is used to separate the anode and cathode, which allows the flow of proton from anode to the cathode [198]. The formic acid is not permeable through the perfluoro sulfonic acid membrane due to the repulsion between the HCOO- ions and sulfuric acid group of the perfluoro sulfonic acid membrane [199,200]. This results in the DFAFC possessing a higher efficiency of concentration compared to methanol [190]. The formic acid remains in its liquid state at room temperature and is considered a strong electrolyte [199,201,202]. This results in strong oxidation and reduction reaction within the cell. Furthermore, the performance of DFAFC does not vary for a wide range of fuel concentration [203].

Theoretically, DAFC is able to produce an open circuit potential of 1.45 V, which is higher than the direct methanol fuel cell or H_2-O_2 fuel cell [199–201,204]. According to Zhu et al., the DFAFC exhibits comparatively high power density at room temperature compared to other fuel cells [205,206]. However, this technology is not without its inherent limitations. In the previous years, overvoltage problem during the loading was the major limitation of this type of storage system, where platinum was used as the catalyst. Recently, a lot of research have been conducted on this particular type of fuel cell and it was found that by using palladium catalyst, the aforementioned limitations can be overcome and the performance can be improved [190]. The corresponding anode and cathode reactions are provided below [201,207].

Reaction at cathode: $O_2 + 4H^+ + 4e^- \rightarrow 2H_2O$

Reaction at anode: $HCOOH \rightarrow CO_2 + 2e^- + 2H^+$

Overall cell reaction: $2HCOOH + O_2 \rightarrow 2CO_2 + 2H_2O$

Direct Ethanol Fuel Cell (DEFC)

This type of fuel cell also falls under the category of PEMFC due to the fact of having Nafion catalyst. In this type, instead of hydrogen or formic acid, ethanol is directly fed into the input as fuel without any reformation. This ethanol is C-2 type alcohol, which can be easily extracted from different renewable energy resources such as wheat, sugar cane, etc. by fermentation process. Theoretically, DEFC can harness more energy than the direct methanol fuel cell (DMFC) for a given weight. Furthermore, ethanol is not as toxic as methanol, which is why it is more environment friendly. In this type of fuel cell, liquid ethanol at the anode along with water is oxidized to produce CO_2,

protons, and electrons. Similar to the aforementioned PEMFC, these protons pass through the PEM to the cathode and the electrons travel through the external circuit passes from the anode to cathode, where they recombine with O_2 and the protons to produce water. The corresponding cell reactions are represented below [208].

Reaction at anode: $CH_3CH_2OH + 3H_2O \rightarrow 2CO_2 + 12H^+ + 12e^-$

Reaction at cathode: $3O_2 + 12H^+ + 12e^- \rightarrow 6H_2O$

Overall cell reaction: $CH_3CH_2OH + 3O_2 \rightarrow 2CO_2 + 3H_2O$

Alkaline Fuel Cell (AFC)

Alkaline fuel cells (AFC) also known as Bacon fuel cell after its British inventor was employed in the earlier space missions conducted by NASA [190,209]. The operating temperature of this type of fuel cell is 80 °C and it can operate at a 60–70 % efficiency [190]. The major advantage of is that it can give a quick start, which is very much essential for space program. Furthermore, the water produced by the cell reaction in this type cell is pure, which was used in drinking purpose in manned spacecraft [209]. However, this type of system is very much sensitive to CO_2, which reduces the concentration of the hydroxide ions during the chemical reactions [210,211]. In addition, the electrolyte used in this system is corrosive, which results in AFC having a shorter lifespan. Hence, AFC is much more popular in transportation and space applications rather than commercial applications [190].

The schematic diagram of the AFC is represented in Figure 65. As the name suggests, the electrolyte used in this system is alkaline fuel-aqueous solution of potassium hydroxide (KOH). The conductivity of KOH electrolytes is the highest among all available alkaline hydroxide [209]. Nevertheless, using KOH requires having a very pure hydrogen and oxygen input in the cell in order to avoid poisoning. Due to using liquid electrolyte, a Teflon-coated carbon electrode is used, which is semipermeable in nature. Platinum is used as the catalyst for the electrochemical reactions. The hydrogen is fed into the anode electrode, whereas oxygen is fed into the cathode electrode. In the anode, hydrogen reacts with the electrolyte and produces water along with two electrons. These electrons travel through the external circuit to the anode, where they recombine with oxygen and water to produce hydroxyl ions. The corresponding cell reactions are presented below [209].

Anode: $H_2 + 2OH^- \rightarrow 2H_2O + 2e^-$

Cathode: $O_2 + 2H_2O + 4e^- \rightarrow 4OH^-$

Overall: $2H_2 + O_2 \rightarrow 2H_2O + electricenergy + heat$

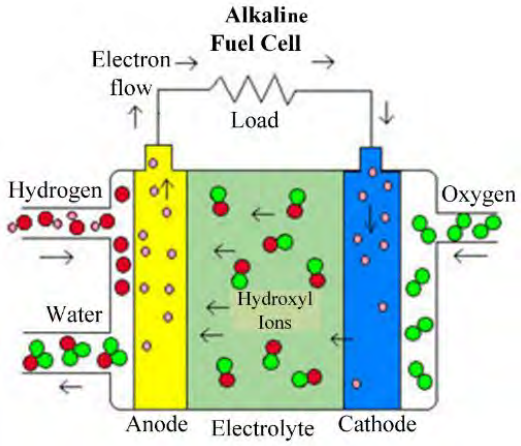

Figure 65. Operation of alkaline fuel cell; the electrolyte used in this system is alkaline fuel-aqueous solution of potassium hydroxide (KOH) [209].

Phosphoric Acid Fuel Cell (PAFC)

The phosphoric fuel cell (PAFC) comprising of phosphoric acid electrolyte was first proposed by Elmore in 1962 [209]. The schematic diagram of the PAFC is represented in Figure 66. Similar to the PEMFC, hydrogen is supplied to the anode and oxygen is supplied at the cathode electrode. The phosphoric acid electrolyte is encompassed by porous Teflon coated graphite, which blocks the leakage of liquid electrolyte, but allows the flow of gases to the reaction [209]. The operating temperature of this type cell ranges between 175–200 °C—almost twice the operating temperature of PEMFC [190]. The major advantage of PAFC is that it is very tolerant to impurities in the hydrocarbon fuels when compared to PEMFC and AFC. This is due to the fact that PAFC operates at much higher temperature as mentioned earlier. At this temperature, the reduction rate of oxygen is highest among all the different types of acids. Furthermore, operating in the aforementioned temperature range allows the toleration of 1–2% CO and few parts per million of sulfur in the reactant stream, which eliminates the need for supplying pure hydrogen in the anode. Due to the high operating temperature, cogeneration is also possible in this particular type of fuel cell [209]. The heat generated in this system is used to warm up the water as it is not sufficient enough for cogeneration of stream. However, this warming up water increases the overall efficiency of the system. The major disadvantage of PAFC is using expensive platinum electrode as the catalyst. PAFC are particularly applicable in different stationary and heating applications [190]. The electrochemical reactions are the same as for the case of PEMFC, which are represented below [209].

Anode: $H_2 \rightarrow 2H^+ + 2e^-$
Cathode: $\frac{1}{2}O_2 + H_2 \rightarrow H_2O$
Overall: $\frac{1}{2}O_2 + 2H^+ + 2e^- \rightarrow H_2O$

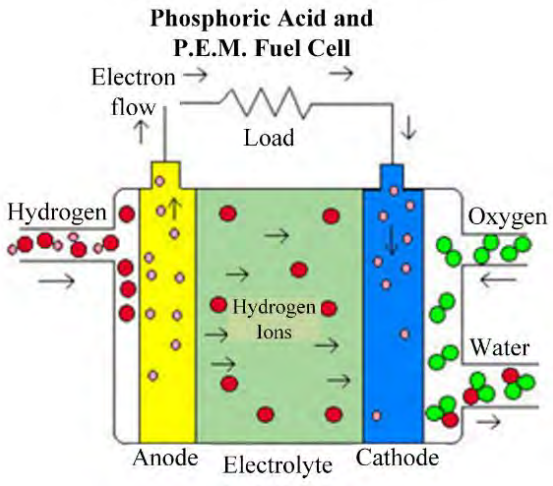

Figure 66. Schematic diagram of the phosphoric fuel cell (PAFC); phosphoric acid is used as the electrolyte in this system [209].

Direct Methanol Fuel Cell (DMFC)

The direct methanol fuel cell (DMFC) technology is one of the most advanced fuel cell technology currently existing [190]. It has similarities with both PEMFC in that sense that it uses a polymer electrolyte and a proton exchange membrane (often Nafion) to separate electrodes [6,190]. However, instead of supplying hydrogen, methanol is fed to the anode directly and the anode catalyst itself extract hydrogen from methanol, therefore eliminating the need for complex catalytic reformation [209]. Furthermore, hydrogen has to be stored in a low temperature and high pressure, whereas there is no such requirement for the storage of methanol [6]. The major disadvantage of DMFC is that the crossover of methanol from the cathode electrode to anode electrode reduces the efficiency as well as the oxidation rate of the electrochemical reaction happening inside of the cell. The operating temperature of DMFC

is 50 to 100°C, with an efficiency of nearly 40%; and with an increase in temperature, the efficiency of the cell also increases [6]. Furthermore, the toxicity of methanol is another limitation of DMFC. In the anode, the methanol is dissolved in water to form CO_2 and hydrogen is extracted from it. H^+ ions, i.e., protons, travel from the anode through the PEM to the cathode, where they recombine with oxygen to produce water. This means that water is consumed on the anode side and is produced on the cathode side. As water is needed on the anode side, pure methanol cannot be used without adding water, which in turns reduces the concentration of the methanol liquid. However, as the energy density of methanol is much higher than highly compressed hydrogen, the low concentration of methanol fuel has a very small effect on the efficiency of the cell [6]. The DMFC is particularly popular in portable electronic applications such as batteries for cameras, laptops, etc. However, their storage range is expendable from 1 W to 1 kW; therefore, they have immense potentiality in utility-scale applications [190]. The corresponding reactions [209] and the schematic of the DMFC cell is represented in Figure 67.

Anode: $CH_3OH + H_2 = CO_4 + 6H^+ + 6e^-$

Cathode: $6H^+ + 6e^- + \frac{3}{2}O_2 = 3H_2O$

Applications: EV, military, cellular phones, laptop computers.

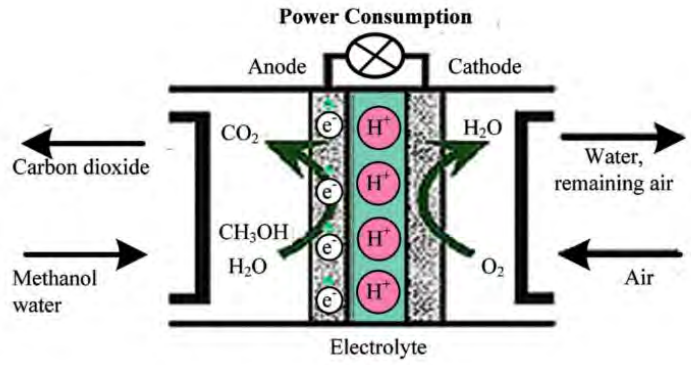

Figure 67. Schematic diagram of direct methanol fuel cells (DMFC); it uses a polymer electrolyte; instead of supplying hydrogen, methanol is fed to anode directly and the anode catalyst itself extract hydrogen from methanol [209].

Molten Carbonate Fuel Cell (MCFC)

The molten carbonate fuel cell (MCFC) was first developed by Dutch scientists in the 1950s, which was later on it was implemented by the American Military on 1960 [209]. The operating temperature of MCFC are very high, which ranges from 600–700 °C [6,190,209]. These high operating temperatures enables the MCFC to reform the hydrocarbons such as petroleum and natural gas internally and extract hydrogen gas within the structure of the cell [6]. In addition, due to these high temperatures, it is possible to cogenerate electricity by utilizing waste heat, therefore the efficiency increases. The MCFC has an efficiency of 50–60%, which eliminates the need of using expensive metal catalysts [190]. Furthermore, the high temperature also eradicates the carbon monoxide poisoning problem [209]. Due to the high efficiencies, the MCFC is best suited for utility-scale electrical energy generation and stationary applications. Currently, the MCFC has a capacity up to 2 MW; continuous research and simulations have been conducted to extend the capacity up to 50 and 100 MW [6].

The schematic representation of the MCFC is shown in Figure 68. This type of fuel cell uses CO_2 as the fuel on the cathode side, while hydrogen is extracted from hydrocarbon fuel and supplied on the anode side. The electrodes used are porous in nature with a good conductivity. Molten lithium sodium carbonate or lithium potassium carbonate salts are used as the electrolyte in MCFC. At 650 °C, these salts get molten and carbonate ions are generated, which flows from the cathode electrode to the anode electrode. In the anode, it combines with the supplied hydrogen and produces carbon dioxide,

water, and electrons. These electrons travel from the anode to cathode by an external circuit, thus producing electricity [6]. The corresponding cell reactions of the MCFC are represented below.

Anode: $H_2 + {CO_3}^{2-} \rightarrow H_2O + CO_2 + 2e^-$

Cathode: $\frac{1}{2}O_2 + CO_2 + 2e^- \rightarrow {CO_3}^{2-}$

Overall: $H_2 + \frac{1}{2}O_2 + CO_2(cathode) \rightarrow H_2O + CO_2(anode)$

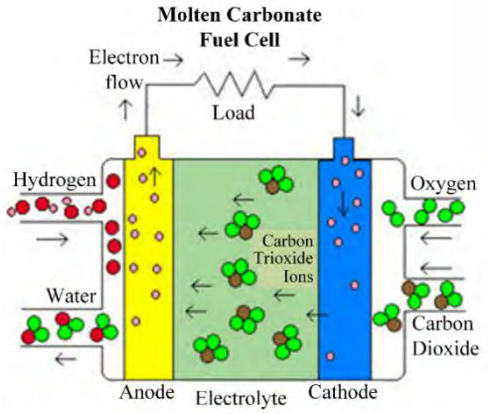

Figure 68. Operation of a molten carbonate fuel cell; uses CO2 as the fuel on the cathode side, while hydrogen is extracted from hydrocarbon fuel and supplied on the anode side. Molten lithium sodium carbonate or lithium potassium carbonate salts are used as the electrolyte [105].

Solid Oxide Fuel Cell (SOFC)

The solid oxide fuel cell (SOFC) operates at a very high temperature of nearly 1000 °C [209]. Due to the high temperature, cogeneration operation is possible, which utilizes the waste heat to generate additional electricity, hence the SOFC has a high efficiency of 50–60%. Therefore, the use of expensive catalyst is not necessary in this type of fuel system, which makes it more economic [190]. Furthermore, the high temperature means that hydrogen rich fuels can be used directly without the need of any reformer to extract hydrogen gas. In addition, the high temperature also eliminates the problem of carbon monoxide poisoning as it transforms it into carbon dioxide (CO_2). The SOFC also possesses the highest tolerance of sulfur contamination among all the existing fuel cell technologies [6]. However, the SOFC has a slow startup, which is why it cannot perform well in large fluctuations of load; this is the major disadvantage of this type of fuel cell [190]. Furthermore, controlling the intense high operating temperature is also an issue for SOFC. Nevertheless, due to the high efficiency and high-temperature operation, SOFC has high potentiality in generating heat and electricity as well as providing power in auxiliary vehicles [6].

Solid zirconium oxide stabilized with yttria oxide is used as the electrolyte, whereas hydrocarbons such as methane (CH_4) and carbon monoxide mixture is used as the fuel in this type of fuel cell. The schematic diagram of the SOFC is represented in Figure 69. The chemical reaction involving the extraction of hydrogen from carbon monoxide and methane are given by ($CO + H_2O = H_2 + CO_2$) and ($CH_4 + H_2O = 3H_2 + CO$), respectively [209]. It is worth mentioning that the aforementioned reaction concerning methane requires a very high temperature and is called steam reforming. Oxygen at the anode terminal releases two electrons to become anion, which travels from the anode to cathode and oxidizes the hydrogen gas to produce water. The two electrons also travel from the anode to cathode through an external circuit and produces electrical energy. The corresponding cell reactions are presented below [209].

Anode: $H_2 + O^{2-} \rightarrow H_2O + 2e^-$

Cathode: $\frac{1}{2}O_2 + 2e^- \rightarrow O$

Overall: $H_2 + \frac{1}{2}O_2 \rightarrow H_2O$

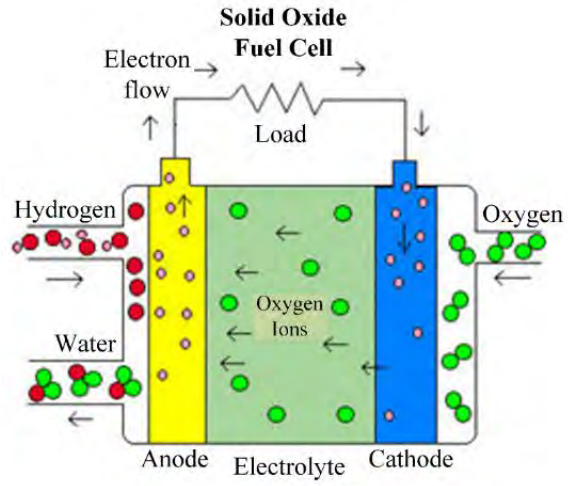

Figure 69. Operational schematic of solid oxide fuel cell; solid zirconium oxide stabilized with yttria oxide is used as the electrolyte, whereas hydrocarbons such as methane (CH4) and carbon monoxide mixture is used as the fuel in this type of fuel cell [209].

Figure 70 presents an overview of different types of fuel cell technology.

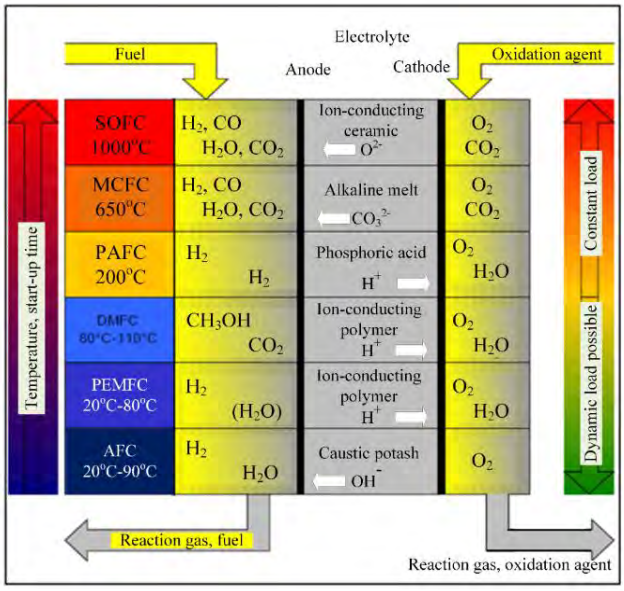

Figure 70. Different types of fuel cell technology at a glance; the abbreviations used for the different fuel cell technologies are: AFC—alkaline fuel cell, PEMFC—polymer electrolyte membrane fuel cell, DMFC—direct methanol fuel cell, PAFC—phosphor acid fuel cell, MCFC—molten carbonate fuel cell, SOFC—solid oxide fuel cell. [212].

Other Fuel Cells

Besides the aforementioned main six types, there exist two additional types of fuel, namely biologically and microorganism inspired fuel cells and regenerative fuel cells. These are explained below.

Biologically and Micro-Organism Inspired Fuel Cell

The microbial fuel cell (MFC) is similar to a bio-electrochemical system, where the metabolism of microbial and solid electron acceptor is utilized to convert the inherent chemical energy that different types of wastes possess, into electrical energy [213]. These wastes include sewage sludge, domestic wastewater, industrial waste, plant waste, food waste, landfill leachate, etc. The MFC is

more advantageous than the traditional fuel due to the fact it operates in ambient temperature and pH level. Therefore, it no additional arrangements are necessary to handle high temperatures and chemical. In addition, it is also superior to combustion of biogas in terms of efficiency [3]. However, MFC has some thermodynamic limitations along with higher internal energy, which makes them low power rating devices. In addition, the nonlinear nature of the MFC are the main reason they cannot be used in large power generation applications [214]. Nevertheless, they have high potentials in several applications such as wastewater treatment, medical applications, low-power electronic applications, hydrogen generation, etc. [213,215].

The schematic of the MFC cell is represented in Figure 71. The operating principle of MFCs are quite similar to the conventional fuel cells. At the anode, microorganisms of the biodegradable waste get oxidized and produce carbon dioxide as well as donating electrons. These electrons travel to cathode by an external circuit, where they recombine with oxygen to produce water. The carbon dioxide produced by the MFC are environmentally neutral, which means they have no effect on the global warming [216]. Depending on construction, MFCs can be categorized into two types—mediator and mediator free. In mediator-based MFC, the electrons that flow from anode to cathode are accelerated by using methyl blue or humic acid mediator, whereas electrochemical bacteria are used in the mediator-free MFCs to accelerate the flow of electron [3]. Some possible redox reactions occurring inside the MFC are presented below [206].

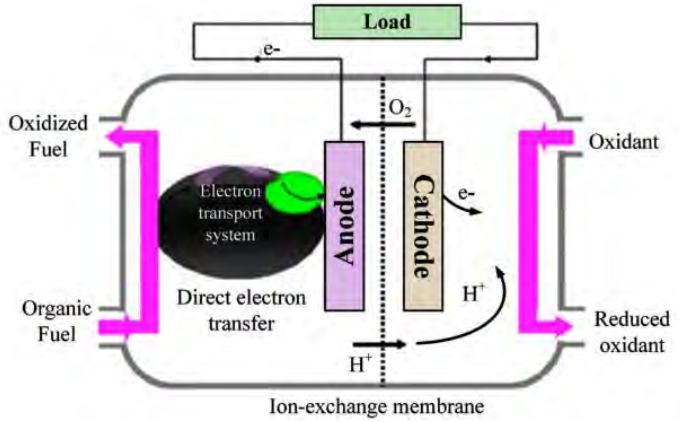

Figure 71. Electricity generation from organic wastes by microbial fuel cell (MFC); at the anode, microorganisms get oxidized and produce CO2 and donates electrons, which travel to the cathode via an external circuit, then recombine with oxygen to produce water [3].

Reactions for electron donors (oxidation reactions at anode)

I. Acetate: $CH_3COO^- + 3H_2O \rightarrow CO_2 + HCO_3^- + 8H^+ + 8e^-$
II. Glucose: $C_6H_{12}O_6 + 6H_2O \rightarrow 6CO_2 + 24H^+ + 24e^-$
III. Glycerol: $C_3H_8O_3 + 6H_2O \rightarrow 3HCO_3^- + 17H^+ + 14e^-$
IV. Domestic Wastewater: $C_{10}H_{19}O_3N + 18H_2O \rightarrow 9CO_2 + NH_4^+ + HCO_3^- + 50H^+ + 50e^-$

Reaction for electron acceptors (oxidation reactions at cathode)

Oxygen: $O_2 + 4H^+ + 4e^- \rightarrow 2H_2O$; $O_2 + 2H^+ + 2e^- \rightarrow H_2O_2$

Regenerative Fuel Cell

A regenerative fuel cell (RFC) can be thought of as the refinement of conventional PEMFC, which stores electrical energy utilizing hydrogen as the energy medium as well as possessing the additional facility of operating in the reverse mode [190,217]. It has high potentiality functioning as an energy storage device particularly in medium- and large-scale systems. The RFC has a significant advantage

over the secondary batteries as it is free of any self-discharge due to storing the active reactants separately. Another advantage of RFC is that it possesses a higher energy density than the secondary batteries. The calculated energy density of a RFC system is expected to be 400–1000 Wh/Kg, which is higher than the energy density of Li-ion battery which is 387 Wh/Kg [217].

The RFC has two distinct modes of operation—the fuel mode and the electrolysis mode. In fuel mode, the stored hydrogen fuel and oxygen are fed to the anode and cathode, respectively. Similar to the previously discussed fuel cells, hydrogen and oxygen react and generate electricity with water as a by-product. In the electrolysis mode, the RFC functions as a water/stream electrolyzer, where it uses the electric power and water to refill the storage tank with hydrogen fuel. The RFC also consists of two distinctive subunits—an energy storage subunit and a fuel/electrolyzer subunit [217]. The schematic representation along with the corresponding reaction of the RFC is shown in Figure 72.

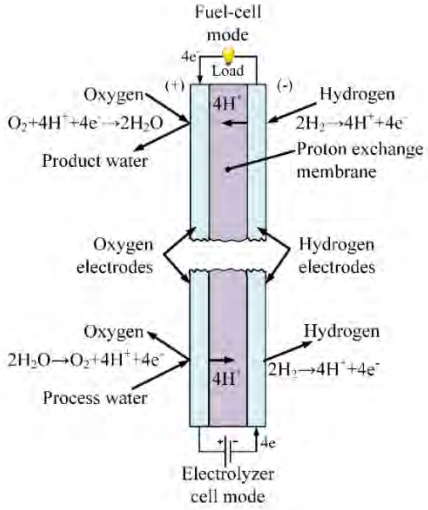

Figure 72. Example of a regenerative fuel cell; it stores electrical energy utilizing hydrogen as the energy medium as well as possesses the additional facility of operating in the reverse mode [190].

The unitized regenerative fuel cell (URFC) is an advancement of the RFC, where the fuel mode and electrochemical mode of the RFC is integrated into a single electrochemical cell [217]. The RFC can be a renewable energy storage system, where the required electricity in the electrolysis mode can be supplied by the renewable energy such as sunlight to fill up the fuel tank. The renewable energy storage using the RFC is represented in Figure 73.

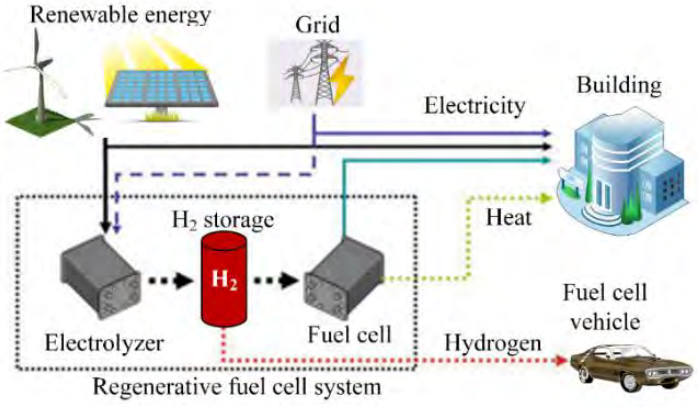

Figure 73. Renewable energy storage using a regenerative fuel cell (RFC) system for a building and vehicle [217].

3.8.2. Solar Fuels

In recent times, solar fuels have gained much attention, where the solar energy is utilized for producing clean alternative fuels [218]. Here, high temperatures are obtained by using parabolic mirrors to concentrate the diluted sunlight over a small area and extracting the radiation energy from it by suitable receivers [6,219,220]. This high temperature is utilized in endothermic chemical reactions to produce clean alternative fuels, which can easily be stored and transported [6,221]. The main operating principle of solar fuels is represented in Figure 74. The intermittent nature of the solar energy has a detrimental impact on the solar to electrical energy conversion as it compromises the stability and reliability of the grid [218]. However, for the case of solar fuel technology, the intermittent nature of the renewable energy sources has very little to no impact on the solar fuel production. The major advantage of this system is that it functions as a virtual storage system with close to 100% virtual efficiency and replaces the components, which cause more energy loses, thereby improving the overall efficiency of the system [206]. Furthermore, it has the ability to downsize the heat engine so that it can run at higher capacity. These attributes contribute to keeping the solar fuel system more economic.

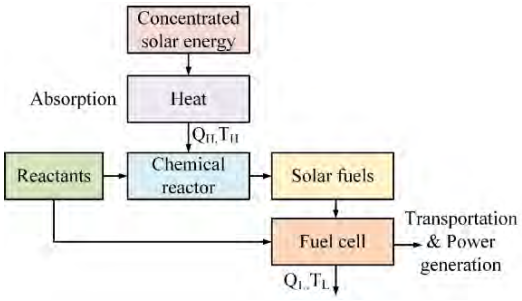

Figure 74. Manufacturing flowchart of solar fuels and subsequent use in fuel cells by using heat from concentrated solar power (CSP) [222].

Solar Hydrogen

The most elemental fuel-hydrogen has attracted the attention due to having a clean combustion, where only water is produced as by product. This hydrogen can be produced utilizing the solar energy. There exists five distinctive ways to produce solar hydrogen, which are represented in Figure 75. Hydrogen can be produced from water, other fossil fuels, or the combination of these two. Water is used in the solar thermolysis and solar thermo-chemical cycles for producing hydrogen, whereas fossil fuel is used in the solar cracking technique for hydrogen production. For solar reforming and solar gasification technique, the combination of water and fossil fuels is needed for producing hydrogen fuel. The produced solar hydrogen can be readily used as the fuel of fuel cell to convert its chemical energy to electrical energy.

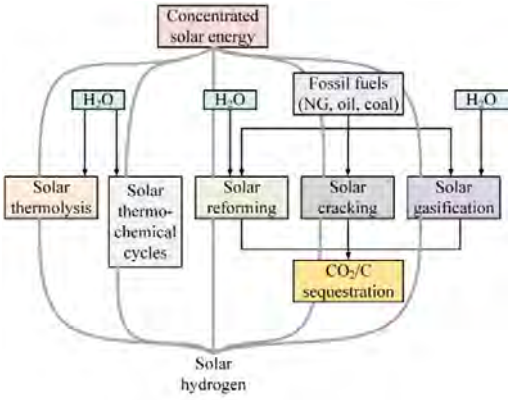

Figure 75. Five distinctive ways to produce solar hydrogen from concentrated solar power (CSP) [6].

Solar Hydrocarbon

Even though hydrogen possesses many promising attributes to be used as solar fuels, it has a low volumetric energy density. Furthermore, the storage and distributing mechanism of hydrogen is not as easy as the hydrocarbon fuels [218]. In many aspects, hydrocarbons excel all available fuel forms, which is the reason of their widespread usage. However, hydrocarbons suffer from one major disadvantage, which is the emission of CO_2 upon combustion, making them harmful for the environment. This caused the scientific community to opt for carbon-neutral hydrocarbons, which are realized as solar hydrocarbons. Solar hydrocarbons are manufactured in a solar refinery, in which the atmospheric CO_2 and H_2O are broken down using concentrated solar energy to produce hydrocarbons. This process produces harmful hydrocarbons too, but the combustion of these hydrocarbons releases the same amount of CO_2 as was originally used for manufacturing the hydrocarbon, making the net CO_2 emissions zero. Furthermore, hydrocarbons are much easier to store, transport, and can be utilized within the existing energy supply infrastructure. ETH Zurich in Switzerland has successfully produced syngas from their solar refinery. Syngas, a mixture of hydrogen and carbon monoxide, can be processed into liquid hydrocarbon fuels that can be used for purposes of transportation [223]. Other fuels, such as methane, methanol, etc., can also be produced from solar refineries [218].

Concentrated solar energy can be utilized in three main forms—as electricity, light, and heat. The electricity generated by PV cells from solar energy can be used to drive electrochemical cells to convert CO_2 and H_2O into hydrocarbons. The light energy from solar energy can be used to drive photochemical reactions to manufacture hydrocarbons. The heat energy from solar energy can be used for heating applications, thermal storage, or in thermochemical reactions [218]. Thus, solar energy can not only be directly used for generating useful energy, but also used to produce eco-friendly solar fuels in a carbon-neutral procedure. The solar fuels, usually in the form of hydrocarbons, can be used conventionally, only with the benefit of causing much less damage to the environment.

To practically implement solar refineries at large scales, it is necessary to cut down on the capture costs of CO_2 and efficiently utilize solar energy to drive the chemical reactions. Using solar hydrocarbons can buttress the penetration of RESs into the transportation sector. Rechargeable electric vehicles (EV), despite being clean forms of transportation, constitute less than 3% of all vehicles sold in the USA [218]. So, the usage of solar hydrocarbons can be promising in creating a cleaner, if not the cleanest, transportation sector.

Solar Metal

Metals are excellent conductors of heat and electricity, which makes them ideal for storing and transporting energy. They can be used to generate heat energy at high temperatures by combustion, or electrical energy using fuel cells/batteries. Both of these processes result in metal oxides, which are subject to recycling and reduction. Metals are conventionally extracted from their oxides by carbothermic processes and electrolysis, which consume a huge amount of energy and also pollute the environment. Therefore, these conventional metal extraction processes can be replaced by using concentrated heat energy from the solar energy. ZnO is dissociated by using concentrated heat energy from the sun, and this is a very popular process due to its low reaction temperature [224].

Solar Chemical Heat Pipe

It is a known fact that endothermic reactions absorb heat energy, while exothermic reactions expel heat energy. In a solar chemical reactor, the heat energy from the sun is used to carry out a reversible endothermic chemical reaction. The reaction products can be stored for as long as needed and moved to the consumer, where the reaction is reversed as an exothermic reaction and heat energy is extracted. This is basically a heat to chemical to heat energy conversion, and the derived heat energy can be used for any purpose, even for the generation of electricity. The input heat is equal to the output heat, since in a reversible reaction, the heat absorbed in the endothermic direction is equal to the heat produced in

the exothermic direction. The best thing about this system is that the original reactants are obtained as the products after the necessary heat generation, which makes this system completely renewable and almost loss-free. For usage in solar chemical heat pipes, the CO_2 reforming of methane [225] and NH_3 dissociation [226] are popular.

3.8.3. Biofuels

Biological fuels, commonly known as biofuels, are a non-polluting, locally available, accessible, sustainable, and reliable fuel obtained from renewable sources [227]. The source of biofuels are mainly plants, since they play the main role in trapping the energy from sunlight in the form of chemical energy within their bodies through the process of photosynthesis. This trapped energy can be converted into suitable forms and utilized for multidimensional energy needs. This is essentially a form of natural energy storage, where plants are the main protagonists. Biofuels provide 3% of the world's fuels for transportation. Biomass refers to the organic body of living things, particularly plants and animals, which when burnt, can produce energy. This is a renewable process because it is always possible to create more of biomass. Furthermore, it is environmentally friendly because it is a carbon-neutral process and contains low contents of sulfur and nitrogen. Biofuels are liquid or gaseous fuels that are produced from biomass by thermochemical or biological processes. Liquid fuels, such as ethanol, methanol, biodiesel, Fischer-Tropsch diesel, and gaseous fuels, such as hydrogen and methane can be produced in this way [227]. Liquid biofuels can be used as fuels in transportation, engines, or fuel cells to generate electricity. Bioalcohols, vegetable oils, biodiesels, biocrude, and bio-synthetic oils are the most widely used liquid biofuels. Biogas is the mixture of gases produced upon the anaerobic breakdown of organic matter. This gas mixture mainly consists of methane and carbon-dioxide, although it may also contain hydrogen-sulfide, moisture, and siloxanes. This gas can be effectively used for purposes of cooking, as very popular in rural places of South-East Asia. Biogas can be used for any heating applications, in gas engines, and even in power motor vehicles. The USA, Brazil, Germany, Argentina, and China are the leading countries in the world in terms of biofuel production, together producing 80.2% of the global biofuel production in 2018 [228]. Table 13 reports the amount of biofuel production and the share in global production of biofuels in 2018 of these five countries.

Table 13. The amount of biofuel production and the share in global production of biofuels in 2018 of the top five countries [228].

Country	Production (Thousand Barrels/Day)	Share in World's Total Biofuel Production in 2018 (%)
USA	1190.2	45.5
Brazil	693.2	26.5
Germany	75.8	2.9
Argentina	70.6	2.7
China	68	2.6

According to the Global Bioenergy Statistics 2019 published by the World Bioenergy Association, bioenergy is globally the largest renewable energy source. In 2017, the total primary energy supply of biomass was 55.6 EJ. Biomass accounts for 70% of the total renewable supply [229].

3.8.4. Aluminum Energy Storage

Aluminum is the third most abundant element on the earth crust, making it inexpensive, readily available, and very popular for infinite uses. This rather unique energy storage method is based on the aluminum redox cycle, i.e., $Al^{3+} \rightarrow Al \rightarrow Al^{3+}$. For charging, aluminum oxide or aluminum hydroxide is used to obtain elementary aluminium upon reduction, using electricity generated from renewables. The solid aluminum can be easily stored as long as needed, transported without hassle,

and used whenever and wherever needed, with no safety concerns since aluminum is fairly clean. For discharging, the elementary aluminum is oxidized, deriving hydrogen, heat, and the initial aluminum oxide or aluminum hydroxide. These by-products can be utilized as sources of energy. The hydrogen can be used in a fuel cell to generate electricity, whereas the heat can be used for heating applications. From as little as 1 kg of aluminum, this process can yield 0.11 kg Hydrogen and 4.2–4.3 kWh of heat energy. This process has an efficiency of about 50%, which can be ameliorated to nearly 65% upon usage of non-consumable electrodes, wetted cathodes, low temperatures, electrolysis cells, and low losses of heat. Compared to hydrogen and hydrocarbons, Aluminum ES is much safer, and has a higher energy density outperforming the former by a factor of two. The energy density of Aluminum ES is 23.5 MWh/L and the specific energy is 8.7 kWh/kg, making it a great choice for energy storage [230].

3.9. Hybrid Energy Storage System

ESS are in use for numerous applications but is so happens often that one ESS cannot suffice all the needs of a particular user. So, it becomes necessary to incorporate more than one ESS to cater to all requirements. Such a system, which uses two or more ESS combined together, is known as a hybrid ESS (HESS). ESSs can work in either of two modes—high-power mode or sprinter mode and high-energy mode or marathon mode [231]. High-power ESSs respond fast and include flywheel ES, SMES, SCES, BESS, etc., whereas high-energy ESSs respond slowly and include PHS, CAES, fuel cells, BESS, etc. Batteries such as Li-ion batteries are suitable for both high-power and high-energy applications [232]. Generally, HESSs are designed such that both modes are available for a single application. This significantly reduces the installation and maintenance costs because the same power electronic devices and grid connections are sufficient for the component ESSs. HESS may bring improved performances, increased efficiency, longer lifespan, diminished costs, and more suitable design and sizing [233]. Energy management is of vital consideration in case of HESS [234]. It determines the distribution of power among the different ESSs used in the HESS and coordinates them to fulfill one common goal. It also defines the size of the ESSs, their life cycle, efficiency, and several other characteristics. Therefore, the choice of the right energy management system algorithm is pivotal to an optimized utilization of the HESS. Based on how the different ESSs are connected, there are different topologies of HESSs, mainly classified as series or parallel; the parallel topology is mostly used. In parallel, the ESSs can be either directly connected (passive configuration), or through power converters in between (active configuration). A common bus, usually DC because of its inherent advantages over AC bus, connects the whole system. HESSs can be used in several applications, such as in hybrid electric vehicles (HEV), fuel-cell-powered electric vehicles, renewable autonomous energy supply systems employing battery/hydrogen combination, grid-tied HESS in domestic or regional use, large-scale wind and solar farms, etc. [232].

4. Comparison among the Energy Storage Systems

Many researches have been dedicated solely to the purpose of drawing an elaborate comparison among different types of ESS. ESS can be compared on the basis of a number of factors. In this paper, before going into the comparison of the different types of ESS, a glossary of the technical particulars is provided so that any novice can find it helpful to clearly interpret the comparison [235]. Tables 14–16 compare the major types of ESSs on the basis of the following technical parameters.

Table 14. Comparison of the technical parameters of different energy storage systems—I [26].

Technology	Energy Density (Wh/L)	Power Density (W/L)	Specific Energy (Wh/kg)	Specific Power (W/kg)	Rated Energy Capacity (MWh)	Power Rating (MW)
PHS	0.5–2	0.5–1.5	0.5–1.5	-	180–8000	30–5000
Large Scale CAES	2–6	0.5–2	30–60	-	580–2860	110–1000
Overground Small CAES	Higher than large scale CAES	Higher than large scale CAES	140 at 300 bar	-	0.0083–0.01	0.003–10
Flywheel	20–80	1000–5000	5–100	400–1500	0.0052–5	0.25–20
Lead Acid	50–80	10–400	25–50	75–300	0.001–40	0–40
Li-ion	200–500	1500–10,000	75–200	150–2000	0.004–10	0–100
Na-S	150–300	140–180	100–240	90–230	0.4–244.8	<34
NiCd	15–150	80–600	45–80	150–300	6.75	0–40
VRB	16–35	~<2	10–30	166	<60	0.03–50
ZnBr	30–65	~<25	30–80	100;	0.05–4	0.05–10
PSB	20–30	~<2	~15–30	-	Upto 120	0.004–15
Capacitor	0.05–10	100,000+	0.05–5; <~0.05	~100,000, >~3000–10^7	-	0–0.05
Supercapacitor	10–30	100,000+	0.05–15	500–10,000	0.0005	0–0.3
SMES	0.2–6	1000–4000; ~2500	0.5–5; 10–75	500–2000	0.0008–0.015	0.1–10
Solar fuel	500–10,000	-	800–100,000	-	-	0–20
Hydrogen Fuel Cell	500–3000	500+	800–10,000	5–800	0.312–39	<58.5
TES	80–500	-	80–250	10–30	-	0.1–300
Liquid Air Storage	4–6 times than CAES at 200 bar	-	214	-	2.5	0.3–200

Table 15. Comparison of the technical parameters of different energy storage systems—II [26].

Technology	Daily Self-Discharge (%)	Lifetime (Years)	Cycling Times (Cycles)	Discharge Efficiency (%)	Cycle Efficiency (%)	Response Time
PHS	Very small	40–60	10,000–30,000	87	70–87	Minutes
Large Scale CAES	Very small	20–40	8000–12,000	70–79	42–54; AA-CAES: 70	Minutes
Overground Small CAES	Very small	23+	30,000	75–90	-	Seconds–Minutes
Flywheel	>20% per hour	15–20	20,000	90–93	90–95	Seconds
Lead Acid	>0.3	5–15	21,000	85	63–90	Milli-seconds

Table 15. *Cont.*

Technology	Daily Self-Discharge (%)	Lifetime (Years)	Cycling Times (Cycles)	Discharge Efficiency (%)	Cycle Efficiency (%)	Response Time
Li-ion	>1	14–16	200–1800	85	75–97	Milli-seconds
Na-S	Almost zero	10–20	2500–4500	85	75–90	Milli-seconds
NiCd	>0.6	15–20	2000–3500	85	60–83	Milli-seconds
VRB	Very small	10–20	12,000	75–82	65–85	>1/4 cycle
ZnBr	Small	5–10	1500–2000	60–70	65–80	>1/4 cycle
PSB	Almost zero	10–15	-	-	60–75	20 Milliseconds
Capacitor	~50 in 15 min	1–10	5–50,000	75–90	60–70	Milliseconds
Supercapacitor	~20–30	10–30	100,000+	95–98	84–97	Milliseconds
SMES	10–15	20–30	100,000	95	95–98	Milliseconds
Solar fuel	Almost zero	-	-	-	20–50	-
Hydrogen Fuel Cell	Almost zero	~20	20,000	59	20–66	Seconds
TES	>1	20–30	-	-	30–60	Minutes
Liquid Air Storage	Small	25+	-	-	55–80	Minutes

Table 16. Comparison of the technical parameters of different energy storage systems—III [3,26].

Technology	Suitable Storage Duration	Discharge Time at Rated Power	Power Capital Cost ($/kW)	Energy Capital Cost ($/kWh)	Operating and Maintenance Cost	Maturity
PHS	Hours–months; long term	1–24 h	2000–4300	5–100	~3 $/kW/year; 0.004 $/kWh	Mature
Large Scale CAES	Hours–months; long term	1–24 h	400–1000	2–120	19–25 $/kW/year; 0.003 $/kWh	Developed
Overground Small CAES	Hours–months; long term	30 s–40 min; 3 h	517–1550	200–250	Very low	Developed
Flywheel	Seconds–minutes; short term	8 s–15 min	250–350	1000–14,000	~20 $/kW/year; 0.004 $/kWh	Commercialized
Lead Acid	Minutes–days; short to medium term	Seconds–hours	200–600	50–400	~50 $/kW/year	Mature
Li-ion	Minutes–days; short to medium term	Minutes–hours	900–4000	600–3800	-	Commercialized
Na-S	Long term	Seconds–hours	350–3000	300–500	~80 $/kW/year	Commercialized

Table 16. *Cont.*

Technology	Suitable Storage Duration	Discharge Time at Rated Power	Power Capital Cost ($/kW)	Energy Capital Cost ($/kWh)	Operating and Maintenance Cost	Maturity
NiCd	Minutes–days; short and long term	Seconds–hours	500–1500	400–2400	~20 $/kW/year	Mature
VRB	Hours–months; long term	Seconds–hours	600–1500	150–1000	~70 $/kW/year	Developing
ZnBr	Hours–months; long term	Seconds–hours	200–2500	150–1000	-	Demonstration
PSB	Hours–months; long term	Seconds–hours	700–2500	150–1000	-	Developing
Capacitor	Seconds–hours	Milliseconds–1 h	200–400	500–1000	13 $/kW/year; <0.05 $/kWh	Commercialized
Supercapacitor	Seconds–hours; short term	Milliseconds–1 h	100–450	300–2000	0.005 $/kWh; ~6 $/kW/year	Developing
SMES	Minutes–hours; short term	Milliseconds–30 min	200–489	500–72,000	18.5 $/kW/year; 0.001 $/kWh	Early commercialized
Solar fuel	Hours–months	1–24 h	-	-	-	Developing
Hydrogen Fuel Cell	Hours–months	Seconds–24 h	500–3000	2–15	0.0019–0.0153 $/kW	Developing
TES	Minutes–months	1–24 h	100–400	3–60	-	Early commercialized
Liquid Air Storage	Long term	Several hours	900–1900	260–530	-	Developing

Energy density: The amount of energy that can be stored per unit volume of the storage material is known as the energy density, and is measured in kWh/L.

Power density: The amount of energy that can be stored per unit time, i.e., the rated power output, per unit volume of the storage material is known as the power density and is measured in kW/L.

Specific energy: The amount of energy that can be stored per unit mass of the storage material is known as specific energy and is measured in kWh/kg.

Specific power: The amount of energy that can be stored per unit time, i.e., the rated power output, per unit mass of the storage material is known as the power density and is measured in kW/kg.

Power rating: The power rating or rated power output of a storage system defines the rate of storing energy in the storage medium. It is measured in kW or MW.

Energy rating: Also known as the capacity of the storage system, the energy rating defines the amount of energy that can be stored in the storage medium. This is measured in kWh or MWh.

Lifetime: The lifetime of a storage system is a measure of its reliability and can be defined as the number of years that the storage system can perform according to its rated capacity and rated power.

Life cycles: The number of complete charging and discharging cycles that a storage system can execute during its lifetime is called life cycles.

Daily self-discharge: The storage medium can discharge some energy during non-use periods. These losses are inherent and unavoidable, although can be reduced. The amount of energy that the storage system loses daily due to self-discharge is called daily self-discharge, which can be measured as a fraction of the total storage capacity.

Discharge efficiency: The ratio of energy discharged by the ESS to the amount of energy stored in it is called discharge efficiency of the ESS, expressed in percentage (%).

Cycle/round-trip efficiency: The round-trip efficiency of an ESS can be defined as the ratio of energy put in it during charging (in MWh) to energy retrieved from it during discharging (in MWh). It is also called AC/AC efficiency and expressed in percentage (%).

Response time: The response time or speed of an ESS defines how quickly the system can begin to discharge energy to a load.

Storage duration: The storage duration refers to how long the ESS can hold energy or charge without substantial self-discharge.

Discharge time at rated power: The amount of time required by the storage system to fully discharge energy at its rated power (i.e., energy per unit time) is known as its discharge time at rated power.

Power capital cost: The capital investment required for producing per unit power is known as the power capital cost and is measured in $/kW. The higher the power rating of an ESS, the lower will be its cost per unit power.

Energy capital cost: The capital investment required for producing per unit energy is known as the energy capital cost and is measured in $/kWh. The higher the energy capacity of an ESS, the lower will be its cost per unit energy.

Operating cost: The cost for operating a system is termed as operating cost. These are fixed costs and are applicable for as long as the system is in service.

Maintenance cost: All systems are subject to regular maintenance. Maintenance cost includes all costs incurred for maintenance and trivial repairs and replacements within the system.

Maturity of technology: A technology is called mature when it has passed a certain amount of time in usage that has allowed it to overcome its inherent problems and limitations. If a technology can be understood and handled by non-professionals, it can be termed mature.

Operating temperature: The temperature at which a system can operate in stable conditions is called its operating temperature.

Figure 76 demonstrates a comparative view of the power density and energy density of the most prominent ESSs. Figure 77 shows the same in terms of specific energy and specific power. Figure 78 shows the comparison of the major ESS types based on power rating, energy rating, as well as discharge time duration. Figure 79 provides a comparison of the ESSs based on some major application, power rating, and discharge time at rated power.

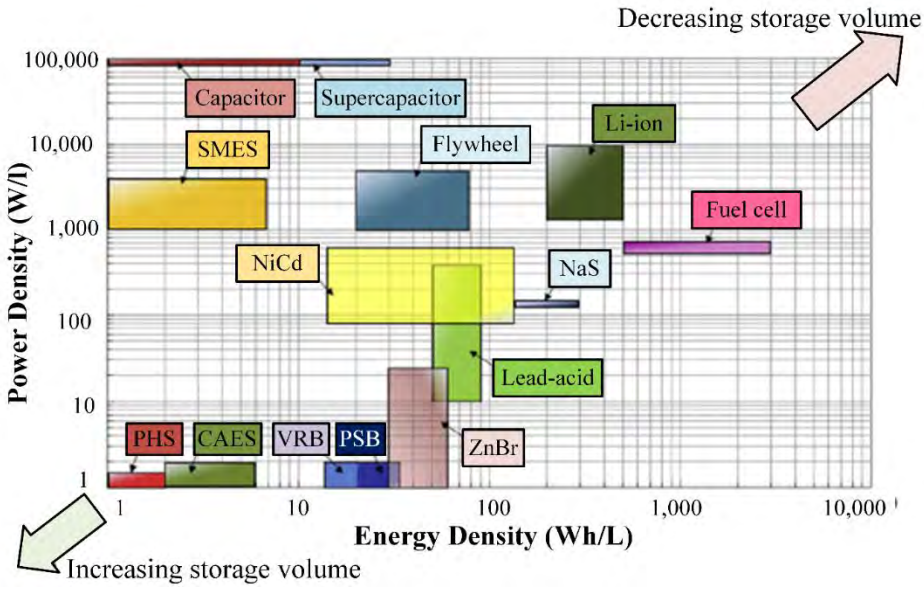

Figure 76. Comparison of power density and energy density of different types of ESSs [26].

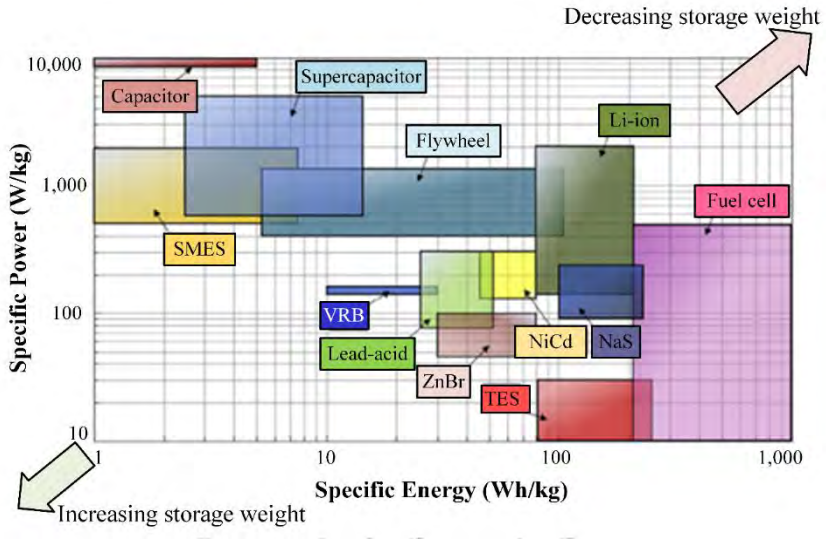

Figure 77. Comparison of specific energy and specific power of different types of ESSs [26].

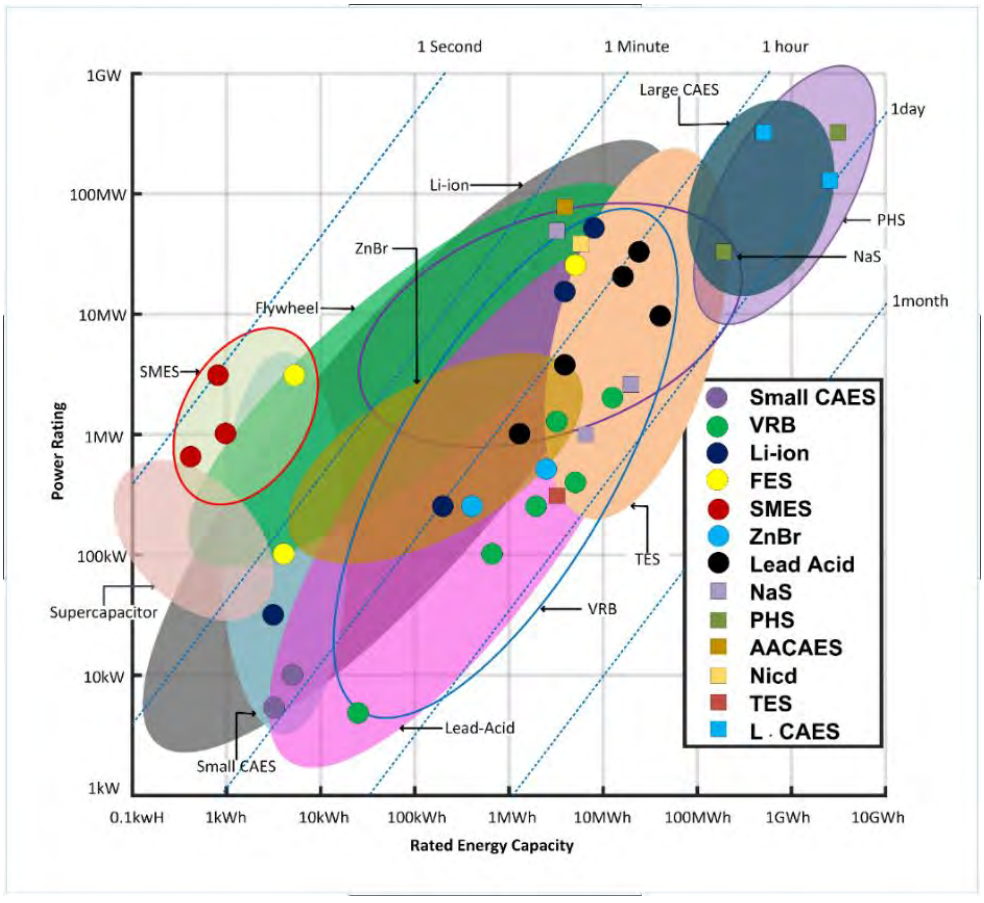

Figure 78. Comparison of power rating and rated energy capacity with discharge time duration at power rating of different types of ESSs [26].

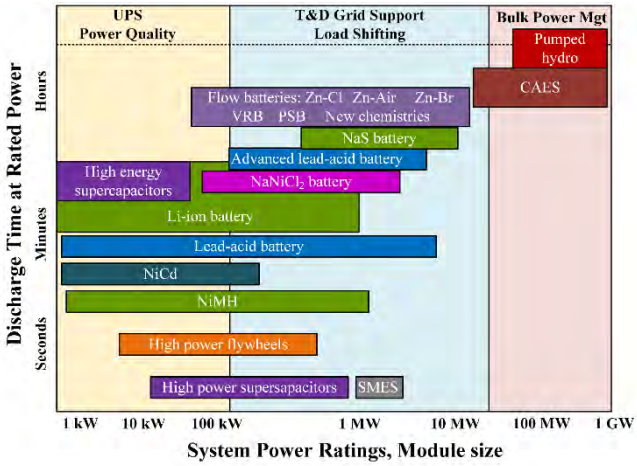

Figure 79. Globally installed energy storage capacity of different types of ESSs [19].

5. Current Scenario of Energy Storage Systems

There has been a prolific increase of the integration of intermittent renewable energy sources (RESs) such as wind and solar to the grid. The energy storage system mitigates the intermittencies introduced by these RESs and also stores the surplus energy generated by them, which can be used later. Therefore, the development and widespread deployment of energy storage for generating and storing electricity at large scale, i.e., utility scale, has attained profuse attention all around the world. The energy storage capacity in 2017 and 2018 of different countries are represented in Figure 80.

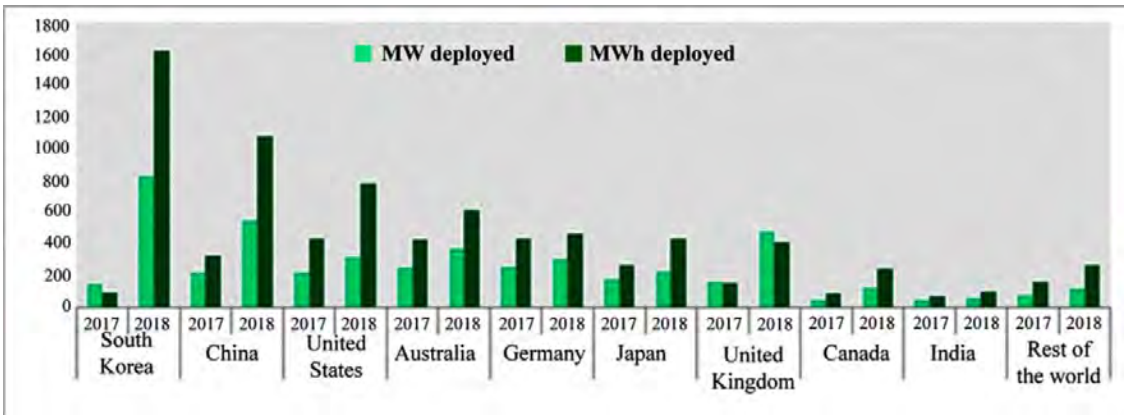

Figure 80. Global energy storage capacity in 2017 and 2018, which shows a significant rise in 2018 compared to 2017 both in terms of power and energy units [236].

In 2018 alone, the USA has deployed 311 MW or 777 MWh energy storage and this is expected to triple in 2020 [236]. In China, 300 MW or 500 MWh additional energy storage has been added in 2018, which has resulted in 40% growth of energy storage market from the previous year [236]. South Korea invested 400 million $ on energy storage in 2018, which skyrocketed its energy storage capacity to 1100 MWh [236]. The major energy storage projects in the USA and the rest of the world are represented in Table 17, which will provide a clear picture of the current scenario of ESS around the world, giving all necessary information about all the existing ESS projects in the world.

Table 17. The current scenario of energy storage projects around the world.

Regions	Project Name	Storage System Technology	Location	Rated Capacity	Services	Applications	Status	Dates	Reference
USA	UCI Microgrid: Thermal Storage	Chilled Water Thermal Storage	Irvine, California, United States	6590 kW	Ancillary service	Electric Bill Management	Operational	1993–Present	[237]
	Texas Instruments Manufacturing Plant	Chilled Water Thermal Storage	Dallas, Texas, United States	6400 kw	Ancillary services	Electric Bill Management, Electric Energy Time Shift	Operational	1989–Present	[237]
	Riverside Public Utilities 5 MW Ice Energy Project	Ice Thermal Storage	Riverside, California, United States	5000 kw	Ancillary services	Electric Energy Time Shift, Renewables Energy Time Shift, Stationary Transmission/Distribution Upgrade Deferral	Announced	2016	[237]
	Los Angeles Community College District - Calmac	Ice Thermal Storage	Los Angeles, California, United States	4620 kw	Ancillary services	Electric Bill Management, Electric Energy Time Shift, Electric Supply Reserve Capacity - Non-Spinning	Operational	2008–Present	[237]
	Raccoon Mountain Pumped Storage Plant	Open-loop Pumped Hydro Storage	Chattanooga, Tennessee, United States	1,652,000 kW	Ancillary service	Electric Energy Time Shift, Electric Supply Capacity	Operational	1978	[237]
	Ludington Pumped Storage	Open-loop Pumped Hydro Storage	Ludington, Michigan United States	1,872,000 kW	Ancillary service	Electric Energy Time Shift, Electric Supply Capacity, Electric Supply Reserve Capacity—Spinning, Load Following (Tertiary Balancing)	Operational	1973	[237]
	Castaic Pumped-Storage Plant	Open-loop Pumped Hydro Storage	Pyramid Lake, California United States	1,247,000 kW	Ancillary service	Electric Energy Time Shift, Electric Supply Reserve Capacity - Spinning	Operational	1973	[237]

Table 17. *Cont.*

Regions	Project Name	Storage System Technology	Location	Rated Capacity	Services	Applications	Status	Dates	Reference
	Green Mountain Energy Storage - NextEra	Lithium-ion Battery	Somerset County, Pennsylvania United States	10,400 kW	Ancillary service	Frequency Regulation, Renewables Energy Time Shift	Operational	2015	[237]
	STMicroelectronics UPS System - S&C Electric	Lead-acid Battery	Phoenix, Arizona United States	10,000 kW	Ancillary service	Grid-Connected Commercial (Reliability & Quality)	Operational	2000	[237]
	Kaheawa Wind Power Project II - Younicos	Advanced Lead-acid Battery	Maalaea, Hawaii United States	10,000 kW	Ancillary service	Electric Supply Reserve Capacity—Spinning, Frequency Regulation, Ramping, Renewables Capacity Firming, Renewables Energy Time Shift	Operational	2012	[237]
	Auwahi Wind Farm	Lithium-ion Battery	Kula, Hawaii United States	11,000 kW	Ancillary service	Ramping	Operational	2012	[237]
	Red Hook (Brooklyn, NY) - NY Prize Microgrid	Electro-chemical	Red Hook, Brooklyn, New York United States	10,000 kW	Ancillary service	Electric Energy Time Shift, Microgrid Capability, Renewables Energy Time Shift	Announced	2015	[237]
	Tucson Electric Power (TEP) - NextEra	Lithium Nickel Manganese Cobalt Battery	Tucson, Arizona United States	10,000 kW	Ancillary service	Demand Response, Electric Bill Management, Electric Bill Management with Renewables, Ramping, Renewables Capacity Firming, Resiliency, Transmission upgrades due to solar	Contracted	2016	[237]

Table 17. *Cont.*

Regions	Project Name	Storage System Technology	Location	Rated Capacity	Services	Applications	Status	Dates	Reference
	Kings County Energy Storage - PG&E Henrietta Substation	Zinc Air Battery	Kings County, California United States	10,000 kW	Ancillary service	Distribution upgrade due to solar Electric Energy Time Shift Ramping Renewables Capacity Firming Renewables Energy Time Shift	Contracted	2020	[237]
	McIntosh CAES plant	CAES	Alabama, USA	110 MW	Ancillary service	load management, spinning reserve, load following, and intermediate power generation	Operational	1991	[238,239]
	20 MW Flywheel Energy Storage Plant	Flywheel	Stephentown, New York, USA	20 MW	Ancillary service	Frequency regulations, and voltage regulation	Operational	2014	[238,240]
	Distributed SMES and Power Quality Industrial Voltage Regulator	Distributed SMES	Wisconsin, USA	800 kW	Ancillary service	Grid and voltage stabilization	Retired	2000–2003	[238,241]
	Metlakatla Battery Energy Storage System	VRLA battery	Alaska, USA	1 MW	Ancillary service	Voltage regulation and displacing diesel generation	Operational	1997	[238]
	Golden Valley Electric Association	NiCd battery	Fairbanks, Alaska, USA	27 MW	Ancillary service	VAR support, spinning reserve and power system stabilization	Operational	2003	[7,238]
	AEP DES system at Chemical Station,	NaS battery	N. Charleston, West Virginia, USA	1 MW	Ancillary services	Substation upgrade deferral, Optimal integration of both central and distributed energy assets.	Operational	2006	[238]

Table 17. *Cont.*

Regions	Project Name	Storage System Technology	Location	Rated Capacity	Services	Applications	Status	Dates	Reference
	Long Island Bus NaS Battery Energy Storage	NaS battery	New York, USA	1.2 MW	Ancillary services	Load shifting	Operational	2008	[238]
	Pacificorp Castle Valley	VRB flow battery	Utah, USA	250 kW	Ancillary services	Distribution line upgrade deferral and voltage support	Operational	2004	[238]
	Bath County Pumped Storage Station	Open-loop Pumped Hydro Storage	Bath County, Virginia, USA	2772 MW	Ancillary services	Load levelling and peak shaving	Operational	1985	[238]
	AES Energy Storage Laurel Mountain Battery Energy Storage	Lithium ion Battery	West Virginia, USA	32 MW	Wind energy Integration	Frequency regulation and wind energy intermittency mitigation	Operational	2011	[7,237]
	Norton	CAES	Norton, Ohio, USA	2700 MW	Ancillary service	Peak shaving and loaf shifting	Under Construction	2013	[242]
	Wallace Dam Pumped Storage	Open-loop Pumped Hydro Storage	Milledgeville, Georgia United States	208,000 kW	Ancillary service	Electric Energy Time Shift, Electric Supply Capacity	Operational	1979	[237]
Rest of the world	108 MW/648 MWh sodium-sulfur battery plant	NaS	Abu Dhabi, United Arab Emirates	108 MW	Ancillary Service	Grid stabilization, frequency regulation, voltage support, Power quality, load shifting and energy arbitrage	Operational	2019	[7,243]
	Tesla 100 MW / 129 MWh Li-ion battery storage project at Hornsdale Wind Farm	Li-ion	South Australia, Australia	100 MW	Contingency reserves and ancillary services	Frequency regulation, capacity firming	Operational	2018	[244]

Table 17. *Cont.*

Regions	Project Name	Storage System Technology	Location	Rated Capacity	Services	Applications	Status	Dates	Reference
	STEAG's 90 MW / 120 MWh battery storage project	Li-ion	Germany	90 MW	Ancillary Service	Frequency regulation	Operational	2017	[244]
	38.4 MW / 250 MWh sodium-sulphur battery by Terna	NaS	Italy	38.4 MW	Ancillary Service	Grid investment deferral, reduced RE curtailment	Operational	2015	[244]
	Audi e-gas Project	Hydrogen Storage	Werlte, Niedersachsen, Germany	6000 kW	Ancillary Service	Renewables Energy Time Shift	Operational	2013	[237]
	Energiepark Mainz	Hydrogen Storage	Mainz, Rheinland-Pfalz Germany	6000 kW	Ancillary Service	Demand Response, Load Following, (Tertiary Balancing), Ramping, Renewables Capacity Firming, Stationary Transmission/Distribution Upgrade Deferral, Transmission Congestion Relief	Operational	2015	[237]
	Hydrogenics Power-to-Gas	Hydrogen Storage	Greater Toronto Area, Ontario Canada	2000 kW	Ancillary Service	Frequency Regulation	Contracted	2019	[237]
	INGRID Hydrogen Demonstration Project	Hydrogen Storage	Troia, Apulia Region - Foggia Province Italy	1.2 KW	Ancillary Service	Renewables Capacity Firming Renewables Energy Time Shift Transportation Services	Operational	2016	[237,245]
	Huntorf	CAES	Breman, Germany	290 MW	Ancillary Service	Peak shaving, load shifting	Operational	1973	[238,242]

Table 17. *Cont.*

Regions	Project Name	Storage System Technology	Location	Rated Capacity	Services	Applications	Status	Dates	Reference
	Toronto A-CAESFacility	Advanced CAES	Lakeshore Ave Toronto, Ontario, Canada	660 kW	Ancillary service	Electric Energy Time Shift, Back-up Power	Operational	2015	[237,246]
	Angas A-CAESProject	Advanced CAES	Callington Rd. Strathalbyn, South Australia, Australia	5000 kW	Ancillary Service	Load leveling, frequency response, inertia	Under construction	2020 (will come in service)	[237,246]
	Highview's 5 MW Liquid Air Energy Storage Demonstrator	LAES	Pilsworth Power Plant, Moss Hall Road Bury, Lancashire, United Kingdom	5000 kW	Ancillary Service	Electric Supply Reserve Capacity - Non-Spinning Frequency Regulation Transmission Congestion Relief Transmission Support Voltage Support	Operational	2018	[237]
	Kannagawa Pumped Hydro Plant	Open-loop Pumped Hydro Storage	Minamiaiki, Nagano Japan	1,880,000 kW	Ancillary Service	Black Start, Frequency Regulation, Electric Supply Capacity, Electric Energy Time Shift, Electric Supply Reserve Capacity - Spinning	Operational (Partially)	2020 (Expected to be fully operational)	[237]
	Dniester Pumped Storage Power Station	Open-loop Pumped Hydro Storage	Sokyriany, Chernivtsi Oblast Ukraine	2,268,000 kW	Ancillary Service	Electric Energy Time Shift, Electric Supply Capacity, Electric Supply Reserve Capacity—Spinning, Frequency Regulation, Load Following (Tertiary Balancing)	Operational	2009	[237,238]
	Okutataragi Pumped Storage Power Station	Open-loop Pumped Hydro Storage	Kurokawa Reservoir Asago, Hyōgo Japan	1,932,000 kW	Ancillary Service	Electric Energy Time Shift, Voltage Support, Frequency Regulation	Operational	1998	[237,238]

Table 17. *Cont.*

Regions	Project Name	Storage System Technology	Location	Rated Capacity	Services	Applications	Status	Dates	Reference
	Guangzhou Pumped Storage Power Station	Open-loop Pumped Hydro Storage	Longkou East Road Guangzhou, Guangdong China	2400 MW	Ancillary Service	Electric Energy Time Shift, Electric Supply Reserve Capacity—Spinning, Frequency Regulation	Operational	2000	[237,238]
	Huizhou Pumped Storage Power Station	Open-loop Pumped Hydro Storage	Huizhou, Guangdong China	2,448,000 kW	Ancillary Service	Electric Energy Time Shift, Electric Supply Reserve Capacity—Spinning, Frequency Regulation	Operational	2011	[237]
	200 kW flywheel	Flywheel	Dogo Island, Japan	100 KW	Ancillary Service	Wind energy intermittency reduction	Operational	2003	[238]
	Sumitomo Densetsu Office Battery System	Vanadium redox flow	Osaka, Japan	3 MW	Ancillary Service	Peak shaving	Operational	2000	[7,238]
	Hyundai & Korea Zinc energy storage system	Lithium-ion	Ulsan, South Korea	150 MW	Ancillary Service	Peak shaving, intermittency reduction, Uninterrupted power supply, backup power	Operational	2018	[247,248]
	KEPCO Sin-yongin s/s	Lithium Nickel Manganese Cobalt Oxide (Hybrid ESS)	Seoul, South Korea	24 + 16 = 40 MW	Ancillary Service	Frequency regulation	Operational	2016	[249,250]

6. Applications of Energy Storage Systems

In the earlier days, the sole purpose of ESSs was to provide backup power to the system and serve as a secondary support for the utility [242]. Nevertheless, with the advancement of technology and continuous ongoing research, ESS has now become a significant part of the power and utility system [242,251]. Due to the prolific increase of integration of RESs with the grid, ESSs are now being used to reduce the intermittencies introduced by these RESs as well as to store the excess energy for avoiding energy spillage [3,6]. Furthermore, ESSs are also used in energy arbitrage applications such as load levelling, peak shaving, load following, etc. [3,26]. They are also being implemented in telecommunication, transmission, and distribution applications. Moreover, with the high penetration of electric vehicles (EV) in market, ESSs are now playing a vital role in the transportation sector [26]. Table 18 summarizes the different applications of ESS along with their required capacity, response time, and discharge duration. This table lists all probable applications of ESS besides their primary function of storing energy. Different types of ESSs are suitable for diverse applications. All of them do not perform equally well in case of a certain application. So, it needs to be analyzed beforehand whether or not a particular type of ESS is suitable for a particular application, or whether or not it outperforms its contending types. The suitability of different types of ESS for various applications are represented in Table 19. The suitability is judged as highly promising or experienced, promising, more research required, or infeasible.

Table 18. Different applications of ESS along with their required capacity, response time, and discharge duration.

Applications	Required Capacity	Required Response Time	Required Discharge Duration	Remarks	References
Power quality	~<1 MW	Milliseconds, <1/4 cycle	Milliseconds to seconds	• Steady and reliable power supply • Voltage and frequency stays within the prescribed range • Voltage wave form curve is smooth and very similar to sine wave • Compatibility between the load and generation • Requires very fast response system	[252–256]
Energy management	Large: >100 MW, medium/small: ~1–100 MW,	Minutes	hours–days	• Balancing the energy generation and energy consumption • Conserving the resources, protecting the climate, maintaining low expenditure, while meeting the requirements of the consumers energy demand • Requires moderately fast response system with long discharge duration	[257–259]
Integration with RES for mitigating intermittency	Up to ~20 MW	Up to 1 s, <1 cycle	Minutes to hours	• The inconsistencies of RESs such as wind or solar causes intermittencies, which affects the stability of the grid • ESS can mitigates these intermittencies by charging or discharging real power to the system • Requires fast response system	[259–263]

Table 18. *Cont.*

Applications	Required Capacity	Required Response Time	Required Discharge Duration	Remarks	References
Integration renewable for back-up	~100 KW–40 MW	Seconds to minute	Up to days	• RESs such as solar cannot supply rated power during rainy or cloudy condition and is unable to generate any energy during nigh time • Wind power generation depends on the velocity of the wind, which is inconsistent in nature • Integrating ESS will provide necessary back-up as well as store the excess energy generated by the RESs for later use • Requires moderately fast response system with a large discharge duration	[252,264–266]
Emergency back-up power	Up to ~1 MW	Milliseconds to minutes	Up to ~24 h	• Ensure emergency back-up power supply during power failure for important users. • Requires instant-to-medium response time and long discharge time	[264,267,268]
Telecommunications back-up	Up to a few of kW	Milliseconds	Minutes to hours	• For maintaining fluency, reliability, and continuity of communication, necessary back-up systems are required • The systems providing the back-up power must have very fast response and their discharge duration should be ranging from minutes to hours	[267,269–271]
Ramping and load following	MW level (Up to hundreds of MW)	Up to ~1 s	Minutes to a few hours	• Mitigates the fluctuation of load by charging and discharging real power to the grid • Requires fast response system with a small-to-large discharge duration	[7,264,272,273]
Time shifting	~1–100 MW and even more	Minutes	~3–12 h	• Energy is stored during off peak time when the cost is low to make use of it during peak demand hours when the cost is high • Reduces the energy consumption and the corresponding cost • Requires moderately fast response system	[252,274–276]
Peak shaving	~100 Kw–100 MW and even more	Minutes	Hour level, ~<10 h	• Storing the energy during of peak time and using it during off peak time • Peak power demand is met by stored energy during off-time periods • Minimizes the need for high power generators • Improves the power quality during the peak periods, hence, mitigates the corresponding losses • Requires moderately fast response system and long discharge time	[269,277,278]

Table 18. *Cont.*

Applications	Required Capacity	Required Response Time	Required Discharge Duration	Remarks	References
Load levelling	MW level (Up to several hundreds of MW)	Minutes	~12 h and even more	• Storing the energy during of peak time and using it during peak time • Control fluctuations which are generated during electricity demand • Helps reducing the difference between peak load and base load • Requires reduced cost with more cycling times	[279–282]
Seasonal energy storage	30–500 MW	Minutes	Up to weeks	• Storing thermal energy (heat or cold) for a large time span when it is available and • Utilizing the stored energy in the opposing season • Requires high capacity with fast discharge	[252,283]
Low voltage ridethrough	Normally less than 10 MW	~Milliseconds	Up to minutes	• Very important for devices associated with renewable generation systems • Capability of regulating the voltage, hence mitigating the voltage variation during the time, when external grid voltage dips occurs • Requires high power and fast response system	[254,264,284]
Transmission and distribution stabilizations	Up to 100 MW	~Milliseconds, <1/4 cycle	Milliseconds to seconds	• High power capacity along with instant response are desired. • Reduce congestion and control quality of power along with maintenance of standard working condition, by accommodating synchronous operation of components available in transmission line as well as distribution unit.	[252,269,285, 286]
Black-start	Up to ~40 MW	~Minutes	Seconds to hours	• Produce startup power to recover from shutdown without the help of grid-power	[67,258,287]
Voltage regulation and control	Up to a few of MW	Milliseconds	Up to ~minutes	• Improve the control of voltage dynamic behaviors. • Useful in many voltage control solutions • Requires very fast response system and the discharge duration should also be fast	[288–290]
Grid/network fluctuation suppression	Up to MW level	Milliseconds	Up to ~minutes	• Safety measure for some systems in the grid/network which are highly sensitive of fluctuations. • Requires high ramp power rates and cycling times along with fast response.	[269,291–293]
Spinning reserve	Up to MW level	Up to a few seconds	30 min to a few hours	• Assurance for compensating during decrease in load or sudden increase in generation • Response time immediate • Capability of maintaining outputs lasts up to a few hours	[294–297]

Table 18. *Cont.*

Applications	Required Capacity	Required Response Time	Required Discharge Duration	Remarks	References
Transportation applications	Up to ~50 kW	Milliseconds–seconds	Seconds to hours	• Supply power to different transportations, e.g., EVs and HEVs • Requires small dimension, light weight, high energy density, and fast response system	[298–301]
End-user electricity service reliability	Up to ~1 MW	Milliseconds, <1/4 cycle		• The ability to meet the energy requirement of the consumer at all time • Ability to withstand any kind of disturbances such as electrical short circuit • Keeping the voltage and frequency variation to a minimum • Requires very fast response system	[264,269,302]
Motor starting	Up to ~1 MW	Milliseconds–seconds	Seconds to minutes	• The inductive load of motors requires a very high starting current for short period of time during • EES having very fast response and very short discharge duration can provide this high starting current	[269]
Uninterruptible power supply	Up to ~5 MW	Normally up to seconds	~10 min to 2 h	• Reaction time instantaneous/almost instantaneous. • Protective during power surge • Handle power interruption by maintaining load power	[303–306]
Transmission upgrade deferral	~10–100+ MW	~Minutes		• Provide power as an alternative of new transmission line during the time of upgrade. • Store more power during peak periods • Moderately fast response system with high capacity required	[6,307,308]
Standing reserve	Around 1–100 MW	<10 min		• Act as a temporary generating unit to ensure balance between supply and demand of electricity • Capable of providing back-up while actual demand surpasses forecast demand or during plant breakdown • Slow response system with high capacity required	[302,309,310]

Table 19. The suitability of different energy storage systems for various applications.

Energy Storage Type	Power Quality	Energy Management	Integration with RES for Mitigating Intermittency	Integration with RES for Back-Up	Emergency Back-Up Power	Telecommunications Back-Up	Ramping and Load Following	Time Shifting	Peak Shaving	Load Levelling	Seasonal Energy Storage	Low Voltage Ride-Through	T&D Stability	Black-Start	Voltage Regulation and Control	Grid/Network Fluctuation Suppression	Spinning Reserve	Transportation Applications	End-User Electricity Service Reliability	Motor Starting	Uninterruptible Power Supply	Transmission Upgrade Deferral	Standing Reserve
PHS	X	***	X	**	X	X	X	***	***	***	**	X	X	*	X	X	X	X	X	X	X	***	**
CAES	X	***	X	**	**	X	*	***	***	***	*	X	X	***	X	X	**	X	X	X	**	**	**
LAES	X	**	X	**	**	X	X	**	***	**	**	X	X	**	X	X	*	**	X	X	*	**	**
Flywheel energy storage	***	**	***	*	***	**	*	*	**	**	X	***	***	X	**	***	**	**	**	**	***	X	X
TES	X	***	X	*	*	X	X	**	**	**	**	X	X	**	X	X	*	X	X	*	*	**	*
SCES	***	X	***	*	*	**	*	*	**	**	X	**	**	X	**	***	X	***	***	***	***	X	X
SMES	***	X	**	*	*	*	***	*	**	**	X	**	***	X	**	***	**	X	**	**	**	X	X
Lead-Acid	***	***	***	***	***	***	***	***	***	***	X	***	**	***	***	***	***	***	**	***	***	**	**
Li-Ion	***	***	***	***	***	**	***	***	***	***	X	***	***	**	**	***	***	***	***	**	***	***	**
Sodium sulfur	*	***	***	***	***	**	***	**	***	***	X	**	*	***	**	**	**	*	***	**	**	**	**
Sodium metal halide	***	*	***	***	***	**	*	*	***	**	X	**	*	**	**	***	**	**	***	*	**	X	*
Metal Air	*	*	***	**	**	*	*	*	***	**	X	**	*	*	**	**	**	**	***	*	**	X	*

Table 19. *Cont.*

Energy Storage Type	Power Quality	Energy Management	Integration with RES for Mitigating Intermittency	Integration with RES for Back-Up	Emergency Back-Up Power	Telecommunications Back-Up	Ramping and Load Following	Time Shifting	Peak Shaving	Load Levelling	Seasonal Energy Storage	Low Voltage Ride-Through	T&D Stability	Black-Start	Voltage Regulation and Control	Grid/Network Fluctuation Suppression	Spinning Reserve	Transportation Applications	End-User Electricity Service Reliability	Motor Starting	Uninterruptible Power Supply	Transmission Upgrade Deferral	Standing Reserve
Nickel Cadmium	*	***	***	***	***	**	***	***	***	***	X	**	*	***	**	**	***	**	**	**	***	***	**
Nickel–metal hydride	*	X	***	***	***	**	*	*	***	*	X	**	*	***	**	**	***	**	**	*	***	X	*
Flow batteries	**	***	**	***	***	*	***	**	**	**	X	**	**	***	***	***	**	X	**	**	**	**	**
Fuel Cell	*	**	**	**	**	**	**	**	**	**	**	*	**	**	*	*	**	***	X	**	**	**	**
Solar Fuels	*	X	*	**	X	X	*	**	**	*	**	X	X	*	*	*	X	**	*	**	*	X	**

*** Highly Promising or Experienced, ** Promising, * More research required, X Infeasible.

7. Business Models of Energy Storage Systems

Over the years, the energy storage system has served a minor role as a secondary supporting system to the utility. However, in recent times, the ESSs have become one of the most consequential components of the power system, where it serves multiple purposes such as energy arbitrage, frequency regulation, power system stability and reliability, etc. [242]. There has been a prolific increase of using renewable energy sources (RESs) such as wind, solar, etc. These RESs introduce intermittencies, which are mitigated by using ESSs, therefore, ensuring the stability of the grid. The RESs are being built on different locations and are gradually replacing the conventional power plants. The excess power generated by these RESs will cause power flow in the negative direction and so it needs to be stored to avoid the spilling of energy. Furthermore, the storage system also enables both consumers and sellers of the market to store the energy during the off-peak time, when the energy rate is low; and use or sell the stored energy during the peak time. These new storage applications are creating new business opportunities and also creating new connections between the producers and consumers [242]. To make sure that this expeditious increase of involvement of the storage system in different utility applications is sustainable, a detailed business model and profitability study on energy systems is necessary [311]. Currently, the ESSs are not able to compete with the existing power generation technologies. However, due to the technological advancement and improvement of the economic scale in the production process, the operation, maintenance, and charging, the cost is predicted to be lower, which will result in lower levelized cost of the storage (LCOS) [242]. The LCOS of 2015 versus the predicted LCOS of 2030 for different types of storage systems is represented in Figure 81. Even though the existing technologies are more than capable of meeting the demand of the current market and the corresponding cost of the ESSs will gradually decrease, their widespread profitability and implementation not only depends on technological advancements, but also on proper economic practice [251].

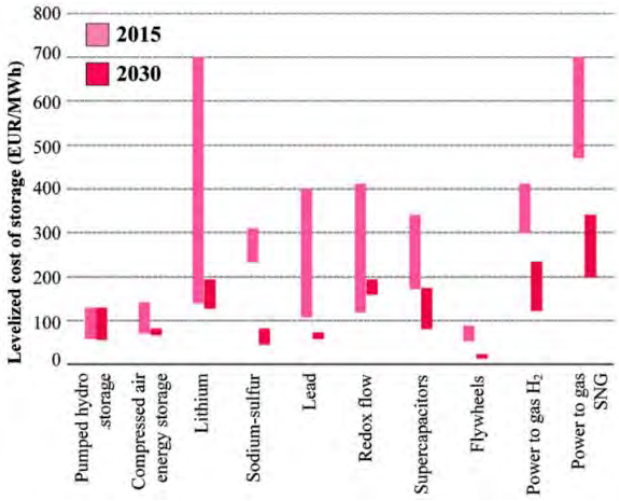

Figure 81. Levelized cost of the storage (LCOS) of 2015 versus the predicted LCOS of 2030 for different types of storage systems [source: World Energy Council, Roland Berger] [242].

This profitability relies on pursuing a specific business model for a specific type of energy storage technology. In addition, policies that support these business models are also necessary for proper flourishment of a technology in the market [50]. According to [312], a business model consists of three major components—market role of the investor, value proposition, and revenue steam. A potential investor can assume four major roles in the value chain of the energy market—transportation and distribution (T&D), trading, consumption, and production [313]. Production role consists of generation of electricity and sale, whereas trading means buying the generated electricity from the producers and selling to the consumers. Consumption is the purchase of electricity by the consumers and T&D means transportation and distribution. It is a possibility that an investor takes on multiple roles in the

aforementioned value chain. The value proposition follows two comprehensive markets—ancillary service and load shifting, which can be placated by the ESSs [314]. Business models for different energy storage applications are represented in Table 20.

Table 20. Business model framework for energy storage. Rows display market roles, columns value propositions, and colored dots revenue streams. Cells specify the business model around an application.

	Ancillary Services		**Load Shifting**	
	Stability	***Availability***	***Supply Addition***	***Demand Addition***
Trading	**Primary frequency control** ■ $ avoid cost of ramping portfolio		**Trading forecast** Meet selling forecast ■ $ avoid penalties for deviations	**Trading forecast** Meet buying forecast ■ $ avoid penalties for deviations
	Secondary frequency control ■ $ avoid cost of ramping portfolio		Trading arbitrage Sell at high prices ■ $ exploit volatility of wholesale prices	Trading arbitrage Buy at low prices ■ $ exploit volatility of wholesale prices
	Tertiary frequency control ■ $ avoid cost of ramping portfolio			
Production	**Primary frequency control** ■ $ avoid cost of ramping production	**Black start energy** ■ $ save investment in black start generator	**Schedule stabilization** ■ $ avoid cost for ramping up	**Schedule stabilization** ■ $ avoid cost for ramping down
	Secondary frequency control ■ $ avoid cost of ramping production		**Production forecast** ■ $ avoid penalties for production deficit	
	Tertiary frequency control ■ $ avoid cost of ramping production		**Generation capacity reserve** ■ $ save investment in capacity expansion	
	Voltage control ■ $ save investment in voltage regulators			
Transmission & Distribution	**Primary frequency control** ■ $ avoid cost of control services	**Black start energy** ■ $ avoid cost of black start service	**T&D peak shaving** ■ $ save investment in capacity expansion	**T&D peak shaving** ■ $ save investment in capacity expansion
	Secondary frequency control ■ $ avoid cost of control services			
	Tertiary frequency control ■ $ avoid cost of control services			
	Voltage control ■ $ save investment in voltage regulators			
Consumption	**Primary frequency control** ■ $ avoid cost of ramping consumption	**Backup energy** ■ $ save investment in black start generator	**Consumption peak shaving** ■ $ avoid demand changes	**Consumption arbitrage** ■ $ exploit volatility of consumer prices
	Secondary frequency control ■ $ avoid cost of ramping consumption		**Self-sufficiency** ■ $ exploit gap in buying and selling prices	**Self-sufficiency** ■ $ exploit gap in buying and selling prices
	Tertiary frequency control ■ $ avoid cost of ramping consumption			
	Voltage control ■ $ save investment in voltage regulators			

Here, each model has a particular role in the market, solves a specific problem in a certain way by applying the ESSs, and generates independent revenue streams [251]. From the table, it is evident that four different revenue streams can be attained for similar type of applications. The power generation is supported by both reducing the generation capacity reserves and stabilizing the generation schedules. By reducing the generation reserves, the investment in generation capacity is deferred and will be used only to meet the periodical demand peaks [315]. On the other hand, stabilizing generation schedules results in cost avoidance by reducing the high demand as well mitigating the attendant cost of ramping [251].

Each of the business models has three operational parameters that different storage technologies are expected to meet [251]. However, it is not possible to for all the storage technologies to meet all three of the operational requirements. These parameters are power capacity, discharge duration, and response time. Business models need to be matched with available storage technologies by means of an overlap of the aforementioned parameters. For this matching process, at first, the range of power capacity of the storage technology (T) must overlap with the required power capacity of the business model (BM). Therefore, the maximum power capacity of a storage technology is ${C_T}^{max}$ has to be greater or equal to the minimum power capacity of the business model ${C_{BM}}^{min}$. Again, the minimum power capacity of the storage technology ${C_T}^{min}$ must be less or equal to the maximum capacity of the business model ${C_{BM}}^{max}$ [251].

$$C_T^{max} \geq C_{BM}^{min} \text{and} C_T^{min} \leq C_{BM}^{max} \tag{62}$$

Secondly, the maximum discharge duration of the storage technology ${D_T}^{max}$ should be greater or equal to the minimum discharge duration of the business model ${D_{BM}}^{min}$ [251].

$$D_T^{max} \geq D_{BM}^{min} \tag{63}$$

Finally, the minimum response time of the storage technology ${R_T}^{min}$ must be less or equal to the maximum response time of the business model ${R_{BM}}^{max}$ [251].

$$R_T^{min} \leq R_{BM}^{max} \tag{64}$$

Using the aforementioned matching process, the technological match and profitability of the business models are represented in Table 21. When the capabilities of a storage technology overlaps with all three aforementioned operational parameters of the business model, it is indicated by green color. Yellow color is denoted when the parameter ranges overlap with only two characteristics of the business model. If the capabilities of storage technology only overlap with only one operational parameter or does not overlap at all, the match is indicated by the red color. From the table, it evident that all the business models are applicable in the current existing market using storage technologies that are now available commercially. Furthermore, most of the prescribed business models have the ability to choose between multiple storage technologies. Therefore, it can be concluded that the widespread adoption of storage technology is limited not because of the lack of functionality but due to the low profitability [251].

Table 21. Technology match and profitability of business models for energy storage. For each ESS, the first column matches the business models with storage technologies, the second column the profitability, and the third column the number of studies found that examine a match [253].

Business Models	**Market Roles**	**Mechanical**									**Thermal**						**Chemical**					
		Flywheel			*Pumped Hydro*			*CAES*			*Thermal*			*Super-capacitor*			*Batteries*			*Hydrogen*		
Ancillary Services		□	$	♯	□	$	♯	□	$	♯	□	$	♯	□	$	♯	□	$	♯	□	$	♯
Primary frequency control	All	▲	▲	1	▲	▲	2	▲	▲	4	▲	▲	1	▲	▲	1	▲	▲	6	▲	▲	1
Secondary frequency control	All	▲	▲	1	▲	▲	4	▲	▲	6	▲	▲	-	▲	▲	1	▲	▲	5	▲	▲	-
Tertiary frequency control	All	▲	▲	1	▲	▲	3	▲	▲	7	▲	▲	-	▲	▲	1	▲	▲	6	▲	▲	-
Voltage control	Prod., T&D, Cons.	▲	▲	1	▲	▲	2	▲	▲	2	▲	▲	1	▲	▲	1	▲	▲	1	▲	▲	1
Black start energy	Production, T&D	▲	▲	-	▲	▲	-	▲	▲	1	▲	▲	-	▲	▲	-	▲	▲	-	▲	▲	-
Backup energy	Consumption	▲	▲	-	▲	▲	-	▲	▲	-	▲	▲	-	▲	▲	-	▲	▲	1	▲	▲	-
Load Shifting		□	$	♯	□	$	♯	□	$	♯	□	$	♯	□	$	♯	□	$	♯	□	$	♯
Trading forecast	Trading	▲	▲	-	▲	▲	-	▲	▲	-	▲	▲	-	▲	▲	-	▲	▲	-	▲	▲	-
Trading arbitrage	Trading	▲	▲	4	▲	▲	11	▲	▲	14	▲	▲	2	▲	▲	4	▲	▲	12	▲	▲	3
Production forecast	Production	▲	▲	-	▲	▲	1	▲	▲	3	▲	▲	-	▲	▲	-	▲	▲	1	▲	▲	-
Schedule stabilization	Production	▲	▲	1	▲	▲	1	▲	▲	1	▲	▲	1	▲	▲	1	▲	▲	1	▲	▲	1
Generation capacity reserves	Production	▲	▲	1	▲	▲	5	▲	▲	2	▲	▲	1	▲	▲	1	▲	▲	2	▲	▲	1
T&D peak shaving	T&D	▲	▲	2	▲	▲	2	▲	▲	2	▲	▲	2	▲	▲	2	▲	▲	4	▲	▲	3
Consumption peak shaving	Consumption	▲	▲	2	▲	▲	2	▲	▲	2	▲	▲	1	▲	▲	2	▲	▲	9	▲	▲	1
Self-sufficiency	Consumption	▲	▲	1	▲	▲	2	▲	▲	2	▲	▲	1	▲	▲	1	▲	▲	21	▲	▲	1
Consumption arbitrage	Consumption	▲	▲	-	▲	▲	1	▲	▲	1	▲	▲	-	▲	▲	-	▲	▲	9	▲	▲	-

8. Environmental Impacts of Energy Storage Systems

Energy storage systems (ESS) are undoubtedly very green since they encourage the use of renewable sources of energy, thereby reducing the emission of greenhouse gases (GHG) and also protecting the limited reserves of fossil fuels. Environmental pollution is a huge concern not only for the scientific community, but also amongst the general conscious citizens around the globe. The energy demands of people are exponentially increasing, which resulted in the global CO_2 emissions rising by 1.7% to a record high of 33.1 Gigaton. This was the highest growth rate since 2013, and almost 70% higher than the average growth rate since 2010. About two-thirds of the emissions have arisen from the power sector alone. The extensive use of coal in the power sector exceeded 10 Gt in CO_2 emissions in Asia. The leading countries in the world with the highest energy demands, i.e., USA, India, and China, are responsible for 85% of the overall increase in emissions. On the other hand, countries like France, Germany, the UK, Mexico, and Japan have reduced their emissions.

Figure 82 shows the dreadful amounts of CO_2 emissions from combustion of coal for power generation and other uses, and from other fossil fuels from the year 1990 to 2018; it is lucid that the emissions are ever increasing. As people's standard of living is improving, with increased modern amenities and a boost in the economy, the energy demands are on a dramatic rise. Furthermore, the changing climatic conditions are responsible for increasing the energy demand for heating and cooling applications. As a result, the global CO_2 emissions are difficult to control. However, the emissions were steady between 2014 and 2016 due to deployment of low-carbon technologies and improvements in energy efficiencies. However, in 2017 and 2018, the emissions rose by about 0.5% for every 1% increase in global economy, a figure much higher than the 0.3% average rise since 2010. This acceleration was due to the fact that the energy productions could not suffice the higher energy demands, and the low-carbon technologies did not grow apace the rising energy demands. However, thankfully, renewable energy and nuclear energy have contributed in slowing the emissions by 25% compared to the rising energy demands in 2018. When the IEA examined the effect of fossil fuel usage in global temperature rise, it was revealed that the CO2 emission from coal combustion accounted for more than 0.3°C of the 1°C rise of global average temperatures, hereby ascertaining that coal is the main culprit in global warming. In 2018, the average annual concentration of atmospheric CO_2 was 407.4 ppm, which rose by 2.4 ppm since 2017. This is a huge increment from pre-industrial levels, which wavered from 180 to 280 ppm [1].

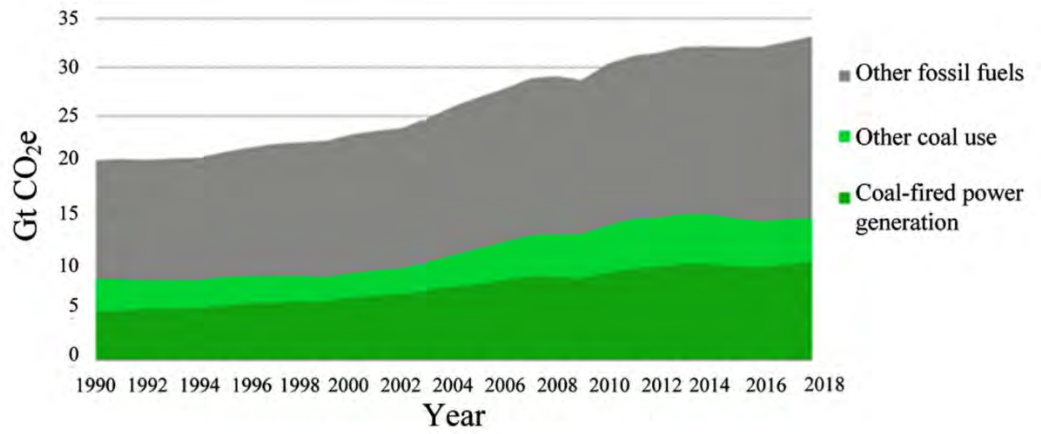

Figure 82. Global energy related carbon dioxide emissions by source, 1990–2018; the CO2 emissions are dreadfully increasing and call for immediate measures.

ES is not only a cost-effective method of utilizing renewable sources of energy at their fullest, but also benefits the environment in many ways. Since ESSs help fight the climatic vagaries and intermittencies of renewable sources, they can encourage the integration of more renewables in the

power grid. Further, ESSs can ensure that the generation system operates at optimal levels and cut down on the usage of less efficient generating units, which run only to meet peak demands. Moreover, ESSs increase the capacity of a power system, eliminating the needs for additional generating units, or transmission and distribution systems [316].

There can be some possible negative aspects of ES, but it depends on the type, materials used, and efficiency of the ESSs. For instance, some batteries, such as lithium and lead, are often harmful from an environmental perspective, and can even cause health hazards if not disposed of properly. These toxic materials need to be recycled effectively to ensure that ESSs remain a safe and reliable option for long-term applicability. Besides, the storage process involves energy conversion, which can incur loss of energy. Some energy can also be lost during the process of storage itself [316]. The carbon footprint of the ESS should be kept as low as possible. There are numerous benefits of ESS when it comes to the environmental aspect, making the adoption of ESSs an excellent choice for meeting the sustainable development goals (SDG). ESSs are capable of enhancing the overall efficiency of power grids, and therefore, they can augment the shift towards the usage of renewable sources of energy in the power system. ESS are completely free from any sort of emission that might potentially degrade the atmosphere or threaten the environment. Solar photovoltaics and ESS are a great duo, together paving way towards a GHG-free, clean, and profitable power generation system, eligible for federal investment tax credits [317].

9. Energy Storage Policies and Standards

The energy storage system (ESS), which is defined as an essential grid asset, has gained profuse attention because of its multipurpose functionality. The ESSs can reduce intermittencies caused by the integration of RESs to the grid, therefore increasing the resiliency and reliability of the grid. Furthermore, as discussed earlier, the ESS also can provide multiple services such as peak shaving, frequency regulation, black start, reactive power compensation, etc. The worldwide energy storage deployment has increased to 9 GW/17 GWh in 2018, which is almost double of that of 2017 [236]. However, this accounts for only 0.0000728 % of the total energy consumption of 2018 [1]. Therefore, to facilitate and foster the widespread deployment of energy storage, different types of federal and state regulations are required, which will ensure tax incentives and rebates for the ESS. Furthermore, policy and regulatory authorities must ensure that the ESS receives adequate compensation for different types of services they serve. In addition, the policy makers should procure laws for creating suitable markets, which will encourage the investors in investing in ESSs. The current existing policies and standards adopted by the USA and rest of the world, along with their aim and criteria regarding the ESSs, are represented in Table 22.

Table 22. Globally existing policies and standards regarding ESS.

Region	Act/Bill/Order	Date	Aim	Criteria
USA	US Federal Energy Regulatory Commission (FERC), Order 755 [235,318,319]	2011	• To ensure that flexible resources such as batteries and flywheels receive sufficient compensation from the wholesale electric markets for its provision of frequency regulation • To encourages the use of more efficient and fast-ramping energy resources	• Requires Regional Transmission Organizations (RTOs) and Independent System Operator (ISOs) to come up with a compensation structure for frequency regulation service provided by energy resources. This compensation will be based on their corresponding performance • Requires the compensation for regulation services to be split into separate payments-capacity and performance • The resources which performs frequency regulation, must hold some of its capacity in reserve in order to be able to provide frequency regulation service at any instant
	US Federal Energy Regulatory Commission (FERC), Order 784 [235,320]	2013	• To facilitate ancillary services markets in order to make it more competitive and transparent • To regulate selling rate of the ancillary services to public utility transmission providers • To report and collect all the transactions data corresponding to the use of energy storage systems in different public utility operations in order to improve the efficiency and decrease the associated errors	• The non-generation resources such as storage and demand responses must be considered as grid services by the wholesale markets • Each public utility transmission provider is obliged to submit statement to open-access transmission tariff (OATT) schedule, which contains information about the accuracy and speed of the regulation resources. Furthermore, public utility transmission provider also has to provide Area Control Error data. This information will be helpful for determining how much regulation and frequency services are needed. In addition, this data will be beneficial to review whether any customer has adopted any “alternative comparable arrangements” as required by the Schedule.

Table 22. *Cont.*

Region	Act/Bill/Order	Date	Aim	Criteria
	US Federal Energy Regulatory Commission (FERC), Order 841 [319,321]	2018	• To modify the regulations in order to eradicate the implications of integrating energy storage system to the US wholesale markets • To make certain that a resource is providing all the necessary services which it is capable of and its practical capacity and energy is in correspondence with it technical specification • To account for physical and operational characteristics of electric storage resources through bidding parameters or other means	• Requires RTOs and ISOs are to revise their tariffs and establish a participation model, which recognizes the physical and operational characteristics of energy storage resources • Sets the minimum size requirement of an energy storage systems to 100 kW • Directs Pennsylvania, Jersey, Maryland (PJM) Interconnection's and Southwest Power Pool's (SPP) to further revise and modify their tariffs and provide specification for minimum runtime and capacity requirements for different types of resources.
	California Public Utility Commission (CPUC) bill 2514 [311,322,323]	Placed on 2010 last updated on 2014	• To facilitate and promote renewable energy integration • To encourage and increase the implementation of large-scale energy storage systems	• The utilities of California State both investor-owned and publicly owned must generate 33% of their total electricity generation from RES by 2020. • Mandates California's three largest investor owned utilities: Pacific Gas and Electric (PG&E), Southern California Edison (SCE) and San Diego Gas & Electric (SDG&E) to create energy storage capacity of 1.3 GW by 2022
	New York Senate Bill S6599 [311,324]	2019	• To encourage and promote the implementation of RES and energy storage system (ESSs) in accordance with meeting the state's commitment of producing 100% clean energy by 2040 • To foster the development of renewable energy (RE) and energy storage (ES) integration by creating suitable market. • To encourage and increase the implementation of large-scale energy storage systems	• Allocates 280 million $ funding which will be invested in energy storage technologies • For the first batch of 100 MWh, the retail developers will receive $350 per KWh, however, successive projects will attain less funding • The bulk incentives will decline annually. For systems less or equal to 20 MW, the bulk incentive will be $110 per KWh. On the other hand, systems larger than 20 MW will receive $85 per KWh • Sets an energy storage target of 1800 MWh by 2025 and 3000 MWh by 2030 for the state of New York

Table 22. *Cont.*

Region	Act/Bill/Order	Date	Aim	Criteria
	Massachusetts, bill H.4857 [311,325,326]	2018	• To accelerate the Economic advancement of RES and EES and foster the economic benefits to end-users • To foster the development of renewable energy (RE) and energy storage (ES) integration by creating suitable market. • To reduce the energy consumption by making the best use of peak and off-peak periods.	• Renewable Portfolio Standards (RPS) will be increased from 1% to 2% annually, from 2020 through 2029, which will bring overall RPS to 35% by 2030 • Establishes a Clean Peak Standard (CPS) • Creates a path for the integrating of an additional offshore wind plant of capacity 1600 MW • The 'seasonal peak period' is defined for any of the four annual seasons, during which the net demand will be highest. This peak period cannot be longer than 4 h and also cannot be less than one hour. • Every retail electric supplier whose contracts executed or extended after December 31, 2018 are mandated to provide a minimum percentage of KWh sales to end-use customers from clean peak resources • Provides clarification on what information distribution companies has to supply to solar net metering customers before imposing demand charges • Allows distribution companies to consider and solicit for non-wire alternatives for the resiliency of their distribution systems • The Department of Energy Resources (DOER) is required to conduct a study on the feasibility of mobile battery storage systems • Sets an energy storage target goal of 1000 MWh by 2025

Table 22. *Cont.*

Region	Act/Bill/Order	Date	Aim	Criteria
	Oregon Public Utility Commission (PUC), law HB 2193 [319,327–329]	2015	• To adopt and modify guidelines and regulations for energy storage projects in the state which will be beneficial to utilities to design and select projects for the propose of advancement of the energy storage industry • To encourage electric companies to invest in different types of energy storage systems	• PacifiCorp and Portland General Electric Company are directed to submit proposals for qualifying energy storage project having minimum storage capacity of 5 MWh, by January 2020. • The aforementioned companies must submit system proposals by January 1, 2018 • After the submission of the proposals PUS is directed to evaluate them to determine whether it is consistent with guidelines, reasonably balances the value for ratepayers and utility operations and the costs of construction, operation, and maintenance, and whether the proposal is in accordance with the public interest • The electric companies have the leverage of recovering all the corresponding costs related to acquiring systems with required set of standards of this program, which also includes all market costs through selling the generated electricity at a convenient rate • Sets a target of integrating a minimum of 5 MWh of energy storage with the grid by 2020
	Hawaii public utilities commission, Act 155 (HRS 269-96) [330–332]	2015	• To encourage and promote the implementation of RES and energy storage system (ESSs) in accordance with meeting the state's commitment of producing 100% clean energy by 2045 • To gradually decrease fossil fuel-based electricity generation • To reduce the overall electricity consumption	• Sets a target of generating 135 MW of solar and 1378 MWh of energy storage within 2022 • Sources the equivalent of 135 MW of solar and 1378 MWh of energy storage—as well as load shifting and frequency response from distributed energy resources through aggregators by 2022 • Two 247 MW solar projects with 998 MWh of energy is approved at a very cheap rate of 8 cents per KWh • Mandates the establishing an energy efficiency portfolio standard which will be used for reducing the statewide energy consumption by 4300 GWh within 2030 • Plans to retire AES Hawaii power plant on Oahu and Maui's oil-fired Kahului Power Plant and compensate it with solar and storage projects by 2024

Table 22. *Cont.*

Region	Act/Bill/Order	Date	Aim	Criteria
	Senate and General Assembly of the State of New Jersey, Bill A3723 [333,334]		• To stabilize, promote, and expand the states renewable market • To develop a new program to support more integration of solar and stored energy to the grid	• Sets goal to increases the overall RPS to 50 percent within 2030 • The generators are required to source more of their electricity from behind-the-meter solar and it should reach 5.1 % reach within 2021 • The Solar Renewable Energy Credit (SREC) of the New Jersey state is scheduled to close 2021. • The regulators are directed to procure a new program which will support the expansion of distributed solar energy as well an "orderly transition" away from SREC • The goal of the state is to achieve 600 MW of energy storage by 2021 and 2 GW by 2030 • Conduct feasibility studies on how the additional storage energy can be deployed and how they will be beneficial to the ratepayers
	Maryland State Senate, Bill HB 650 [311,335]		• To adopt and modify guidelines and regulations for energy storage projects in the state which will be beneficial to utilities to design and select projects for the propose of advancement of the energy storage industry • To encourage the utility companies in investing in energy storage projects in the state	• The Public Service Commission (PSC) are required to set up a pilot program for the states four investor-owned utilities: Potomac Edison, Baltimore Gas and Electric, Delmarva Power and Light, and Potomac Electric Power for the advancement of energy storage projects • Requires the aforementioned four investor-owned utilities to come up with two distinct energy storage projects and submit the project proposals for PSC approval by April 15, 2020, and Sept. 15, 2020, respectively. • The projects are schedule to be operational by Feb. 28, 2022 • The bill lays out four utility ownership mode-utility-only model, utility and third-party model, a third-party ownership model, and a virtual power plant model • The aforementioned utility companies are required to solicit offers in at least two out of the four utility ownership models, mentioned above

Table 22. *Cont.*

Region	Act/Bill/Order	Date	Aim	Criteria
Rest of the World	Electricity Directive and Electricity Regulation (EU) 2019/944 [336,337]	2019	• To adopt and modify the EU policy framework for swift transition to clean energy • To enable the participation of the consumers in the energy markets • To eliminate the implications of widespread implementation energy storage system	• A wide definition of energy storage has been adopted where energy storage systems have been recognized as an asset class which is distinct from generation • Mandates organizing a flexible electricity market which can integrates and benefits all market players such as producers of energy storages, renewable energy, flexible demand, etc. • Member states and regulatory authorities are required to foster cross border access from new suppliers of electricity • Directs the member states, local energy communities, and aggregators to enable the consumers to consume, store, and sell the stored energy to the market • Mandates the member states to come up with a plan to facilitate the integration of RES and energy storage to the grid
	Germany, Renewable Energy Act (EEG) [311,338,339]	2017	• To foster the development of RES and ES integration by creating suitable market • To phase out nuclear energy for the transition to clean energy	• The stored electricity once supplied to the grid will qualify for the feed-in—premium privilege • The EEG surcharge will not be imposed on the energy storage twice, rather it will be imposed only when the store energy is supplied to the grid • Sets the target of generating 80 % of energy from the RES by 2050
	France, The Energy Transition for Green Growth Act (LTECV) [337]	2015	• To encourage and promote the implementation of RES, and energy storage system (ESSs) in accordance with target of transitioning to 100% clean energy • To gradually decrease fossil fuel-based electricity generation in order to decarbonize the energy industry	• Energy storage is referred as an essential part to achieve the policies environmental objectives • Allows individual plant to possess energy storage facility for self-consumption • In non-interconnected areas the cost associated with storage facilities, which are managed by the grid operators are offset through the public service contribution of electricity (CSPE)

10. Barriers and Potential Solutions

Even though the ESSs have multiple applications and benefits, there exists a number of barriers, which are impeding the widespread deployment of energy storage in the market. The authors of [340] categorize these barriers into five types—regulatory barriers, technological barriers, economic barriers, cross-cutting barriers, and utility and developer business model barriers. Each barrier introduces some issues, which should be dealt with for the widespread implantation of the ESS. Creating markets for the ESS, providing adequate compensation mechanism, mitigating different types of procedural delays, educating the investors about the different services ESS can provide, etc., are needed for the widespread implementation of ESS. Different types of barriers of ESS, the issues they introduce, their degree of impact, and the potential solution of overcoming these issues are represented in Table 23 [117]. Different federal and state organizations have acknowledged these aforementioned barriers and have taken initiatives in the form acts, bills, and order to overcome them. Table 24 represents the mapping of different types of policies taken by the regulatory organizations and what specific barriers they are addressing.

Table 23. Different types of barriers of ESS, the issues they introduce, their degree of impact, and the potential solution of overcoming these issues [340].

Barriers	Issues	Key Points	Degree of Impact	Potential Solution
Regulatory Barriers	Procedural issues	• Administrative delays due slow adoption and modification of the rules and slow progress • Complexity of the regulatory rules necessitates the need for a time-consuming comprehensive evaluation	Low	• Imposing additional priority to resolve and implement the pending regulations • Amending the evaluation process to reduce the corresponding delays • Dedicating additional resources to reduce the timeframes required for the evaluation process
	Functional Classification Restriction and cost allocations issues	• Energy storage systems have the ability to provide service to multiple functional classifications such as- production, transmission, and distribution • Regulatory restrictions and lack of transparency prohibits an energy storage developer or utility provider from attaining revenue for providing services under multiple classifications • This issue is only evident in ISO/RTO market regions	Severe	• Provide market access to all the resources especially the energy storage resources to provide services and attain revenue regardless of their location or type • Provide transparent and clear in regulation for accessing multiple functional classifications • Provide a clear and transparent procedure to allow bridging across generation and loading services of the energy storage system • Imposing surcharge or taxes on the energy storage system only when they are supplying energy to the grid
	Discrepancies in Rules Across Markets	• Each market has its own individual regulations, characteristics, and market design, which are mostly inconsistent with other markets • The inconsistency among different markets creates complexity in the deployment of energy storage across multiple markets • The utility providers in some markets have pay retail price on the load rather than wholesale price to charge their storage systems, which reduces the revenue and further increases the inconsistency • Before investing, the investors are required to conduct comprehensive analysis on each market structure, which is time consuming and costly	Moderate	• Simplifying and modifying the regulations with the intention to achieve better alignment with the current market requirements • Ensuring that entity of the market is complying regulatory requirements • Develop better coordination among different power system entities • Establishing increased communication requirement for ancillary services, ISOs, and non ISOS across different markets

Table 23. *Cont.*

Barriers	Issues	Key Points	Degree of Impact	Potential Solution
Economic Barriers	Revenue compensation mechanisms	• Storage systems particularly designed for ancillary service applications, market-based opportunity cost • The market price of the energy system collapses to zero when there is enough energy storage to complete the required ancillary service • Without any energy market to recover the capital cost, the energy storage device loses its economic viability	Severe	• Ensuring the storage systems providing ancillary service receive adequate compensation based on the marginal cost of generation • Performance of storage systems deployed such as speed and capacity should be taken into consideration and pay for performance scheme should be adopted • The resources deployed in ancillary service applications should receive synchronous reserve offer price plus the lost opportunity cost for the marginal unit
	Lack of market	• Lack of markets for different services provided by the energy storage systems such as- governor response, reactive power compensation, inertial response, and black start • In most regions, the energy storage resources are not considered to provide to aforementioned services • The existing compensation rate for the services mentioned above are not adequate enough	Severe	• Develop markets for governor response, reactive power compensation, inertial response, and black start services • Allow existing markets to choose the least expensive technology to meet the requirements of the aforementioned services • Additional Transparency in prices and adequate compensation mechanism for providing the services • Modification of the compensation methodology for providing reliability services in the non-ISO/RTO market regions
	Lack of Price signals	• Complication in determining the market price for various types of ancillary service • Difficulty for regulators to verify the value of a resource in utility and developer proposals • Difficulty in determining whether new resources such as energy storage can compete with the existing technologies	Moderate	• Prices of the nearby prices should be taken into consideration for estimating the values of the different types of ancillary services • Collaborate with vertically integrated utilities to evaluate the system economics • Additional Transparency in prices and adequate compensation mechanism for providing the services

Table 23. *Cont.*

Barriers	Issues	Key Points	Degree of Impact	Potential Solution
Utility and developer business model barriers	Utility and developer uncertainty issue	• Lack of knowledge about the technical capabilities, longevity, economics, services provided by the energy storage systems • Uncertainty regarding different types of pollution regulations and restrictions imposed upon the energy sector • The uncertain economic health leading to changes in demand, and prices of energy & ancillary services • Uncertainty due to continued regulatory and technological changes regarding energy storage	Moderate	• Involving third party developers to the energy storage services • Being in a long-term power purchase agreement which integrating energy storage system with renewable sources • Special incentives for reducing the risk of investing in energy storage system
Cross cutting barriers	Limited knowledge of energy storage technologies among power system stakeholders	• Lack of knowledge about the technical capabilities, longevity, services provided by the energy storage systems • Assuming that the sole purpose of energy storage is to support renewable energy integration and backup power • Lack of considering implementing energy storage systems in transmission and distribution applications • Assuming all types of energy storage systems have similar capabilities and cannot compete with the existing technologies	Low	• Educate the investors and consumer about the facilities of energy storage by arranging seminars, webinars, publication report, and conferences • Mandate the manufacturers to promote their product and identify real deployment scenarios, and presenting this work to the investors
	Modeling restrictions and the Lack of modeling Capabilities	• The integration of renewable sources and energy storage systems have increased the complexity of modelling a power system • The current existing tools utilities possesses are inadequate to model the current complex power system • The transmission coordination among the ISO/RTOs are greatly affected by the lack of modelling capabilities • The existing modeling capabilities are not enough to take into account of all different types of services that energy storage systems can provide • Regulators, developers, and utilities are not able to compare the resources fairly	Moderate	• Coordination between utilities and regulatory organizations and engineering consulting firms • The modelling tools should be continuously updated and improved • Organization developing the modelling tools should also study and evaluate the real deployment • To address the deficiencies of each entity utilities and developers should work together in improving the modelling capabilities

Table 23. *Cont.*

Barriers	Issues	Key Points	Degree of Impact	Potential Solution
Technology Barriers	High technology costs	• Even though the energy storage systems and can serve multiple purpose, and the utilities and developers have attained much experience using them, it is still not considered as a viable option due to high cost • Different alternatives to energy storage system such as wind curtailment are being preferred due its low cost • The resources life cycle cost, which is a very important factor for long—term consideration of usage of storage, is still not very clear to the developers and utilities	Severe	• Continue funding research and development (R&D) projects involving energy storage systems with the goal of reducing the cost • The major target of the research should be achieving specific performance from a specific technology at the lowest possible cost • Regulations which will support specific long-term goals of decreasing the cost of energy storage technologies

Table 24. Mapping of different types of policies taken by the regulatory organizations and what specific barriers they are addressing.

	Functional Classification & Cost Allocation	Inadequate Compensation Mechanisms	Lack of Available Market	Lack of Price Signals	Utility & Develop Risk & Uncertainty	Limited Knowledge of ES Technologies	Modeling Limitations	High Technology Costs	Discrepancies in Rules Across Markets
US Federal Energy Regulatory Commission (FERC), Order 755		✓							
US Federal Energy Regulatory Commission (FERC), Order 784	✓	✓		✓	✓				
US Federal Energy Regulatory Commission (FERC), Order 841		✓					✓		
California Public Utility Commission (CPUC) bill 2514	✓		✓		✓				

Table 24. *Cont.*

	Functional Classification & Cost Allocation	Inadequate Compensation Mechanisms	Lack of Available Market	Lack of Price Signals	Utility & Develop Risk & Uncertainty	Limited Knowledge of ES Technologies	Modeling Limitations	High Technology Costs	Discrepancies in Rules Across Markets
New York Senate Bill S6599	✓	✓	✓	✓				✓	✓
Massachusetts, bill H.4857	✓	✓		✓		✓			
Oregon Public Utility Commission (PUC), law HB 2193		✓	✓		✓	✓			
Hawaii public utilities commission, Act 155 (HRS 269-96)	✓								
Senate and General Assembly of the State of New Jersey, Bill A3723	✓	✓							✓
Maryland State Senate, Bill HB 650	✓		✓		✓		✓		
Electricity Directive and Electricity Regulation (EU) 2019/944	✓		✓						✓
Germany, Renewable Energy Act (EEG)		✓	✓		✓				
France, The Energy Transition for Green Growth Act (LTECV)	✓	✓			✓				✓

11. Future Prospects of Energy Storage

The prediction of global power capacities of different types of energy sources according to the World Energy Outlook 2019 (WEO2019) are represented in Figure 83. This prediction is based on the policies adopted by different countries and their long-term goals corresponding to the energy sector. In recent times, there has been a sudden surge in the implementation of renewable energy sources and from here it is expected to only increase. Upon continuation of the existing and already announced policies by the countries, the global capacity of the solar photo voltaic (PV) is predicted to be approximately 3142 GW and will surpass coal and gas to become the largest energy source of the world by 2040. Similarly, the share of energy generated by wind will increase from 5% (2018) to 13% (2040) and its capacity is predicted to be approximately 1856 GW. Therefore, the overall capacity of wind and solar combined will be 4998 GW. Furthermore, considering Hydro and other renewable sources, the overall share of energy generation will increase from 26% (2018) to 41% (2040) [341].

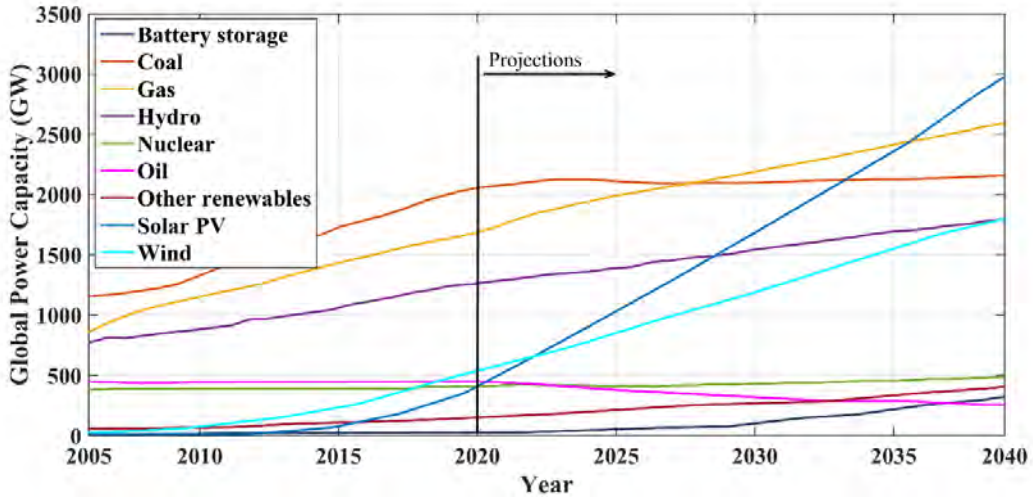

Figure 83. The prediction of global power capacity of different types of energy sources according to the World Energy Outlook 2019 (WEO2019).

As the intermittent renewable energy has become more prevalent, the large-scale implementation of energy storage system is gaining much attention. The global cumulative energy storage forecast for 2040 according to the Energy Storage Outlook 2019 by Bloomberg NEF (BNEF) is represented in Figure 83. It predicts that the worldwide capacity of energy storage will increase prolifically from 9 GW/17 GWh (2018) to 1095 GW/2850 GWh (2040) [342]. Therefore, the energy storage capacity of 2040 will be 122 times the current capacity, which will require a significant amount of investment of about $662 billion. It also predicts a 50% reduction of the cost of Li-ion batteries, on top of 85% reduction occurred in the 2010-2018 period. From Figure 84, it is evident that South Korea is currently leading the energy storage market. However, by 2040, the energy storage market will be led by the two most influential countries—USA and China. Germany, France, UK, Australia, and India will have significant contributions in the remaining markets. As discussed earlier, the predicted generation capacity of energy storage for 2040 is 1095 GW, which is only 21.9% of the predicted overall capacity of RESs (wind and solar) [338,342]. Therefore, even though there will be a boom in the energy storage market due to large investments and cost reductions, it will not be enough to compete with the renewable sources. Hence, more investments and policies in support of the energy storage market are required.

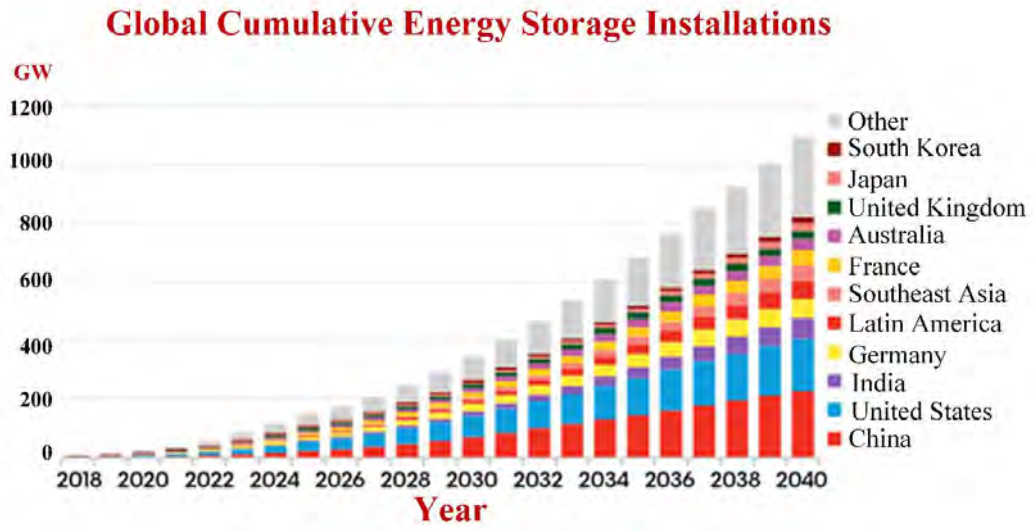

Figure 84. The global cumulative energy storage forecast for 2040 according to the Energy Storage Outlook 2019 by Bloomberg NEF (BNEF) [342].

ESSs are in the minds of the scientific community for quite a long time. It is, in fact, difficult to trace back when the idea of energy storage first came up in human minds. However, it is true that the necessity of ESSs will keep on increasing with the growth of renewable sources of energy, distributed energy resources (DERs), distributed generation (DG), microgrids, and the overall utility grid. ESSs are useful not only to tackle the intermittency of renewables, but also in numerous grid-scale applications. The most important advantage of using ESSs lies in its ability to save costs, in the form of several applications, such as demand side management, reduction of demand charges, increased PV self-consumption, time-of-use bill management, etc. As climate changes are drastically hampering the quality of life on our planet, it is imperative for humans to cut down on conventional sources of energy generation that emit greenhouse gases and threaten the environment. In such a dire situation, in the future, it will be crucial to switch to a 100% renewable-energy-dependent electricity generation system. Due to the intermittent nature of renewables, together with the ever-increasing demand for energy, there will be no way out other than adopting energy storage systems.

12. Outcome of this Study

This is a comprehensive review on energy storage systems that is aimed at encompassing everything one needs to know prior to initiating a research in this field. This paper has been designed in such a way that all necessary information about ESS are included in a single place. To summarize, the outcomes of this review are presented below:

i. A brief introduction to energy storage systems is provided, which reassures the necessity of ESSs to tackle the problem of intermittency of RESs, whose penetration into the utility grid is of vital importance in today's world due to the depletion of fossil fuels and the deteriorating condition of our planet.
ii. The chronological evolution of the several types of ESSs are described to reflect the gradual progress of this emerging technology.
iii. Energy can be stored in numerous forms. More than 45 types of storage systems are elaborately discussed here, including their detailed concept, related diagrams, equations, etc.
iv. All the different types of energy storage systems are compared on the basis of 20 technical parameters. The comparison among ESSs is a major subject of analysis before the practical deployment of an ESS.

v. At present, ESSs are flourishing in leaps and bounds, as more countries are trying to install increased capacities of ES facility. Some of the most prominent ES projects around the world have been neatly tabulated in this paper along with their specifications.
vi. The multidimensional applications of ESSs are dictated with the required specifications. Furthermore, an insight has been provided regarding the suitability of a particular type of ESS based on the particular application.
vii. The business models of ESSs are discussed in depth, because the success of an ESS not only depends on its widespread deployment, but also on proper economic practice and conducting profitability study. The business model framework is illustrated too.
viii. The environmental impacts of ESSs are narrated, with reflections on how ESSs are helping the environment, and also on their side-effects regarding disposal.
ix. The policies and existing standards regarding ESSs prevailing around the world are tabulated in this paper. These policies help to establish ESSs as a viable technology.
x. Several barriers impede the growth of ESSs. These barriers, along with their potential solutions, are tabulated. In addition, the policies undertaken by different regulatory organizations to overcome these barriers are listed.

ESSs are a promising technology, with vast possibilities to upgrade the global energy scenario. The future prospects of ESSs are discussed with relevant documents.

13. Conclusions

It is believed that this review will prove to be a valuable document in the realm of energy storage technology. With the drive towards renewable energy sources, the world is bound to be drawn more towards energy storage systems, which will require a complete understanding of all the aspects of this technology. This paper encompasses a great deal of substantial information on energy storage systems. Most of this paper has been dedicated to elaborately describing all the different types of energy storage systems. Not only that, the types have been compared based on several technical parameters, which will facilitate the choice of a particular type based on the key requirements. The paper beautifully handles the past history, present scenario, and the highly potential future of energy storage systems. In addition, the hurdles that these systems are facing and the ways to overcome those are included. A short insight has been provided into the multidimensional applications of energy storage systems, such as mitigation of intermittencies, ensuring power quality, energy management, backup power, peak shifting, load levelling, etc. On a non-technical aspect, the business models of energy storage systems are also incorporated into this paper, along with a profitability study to ensure that the energy storage systems can survive in the competitive global economy. It is true that there still remains a vast, unexplored part in energy storage technology that has not been covered in this paper. The future works in this thread will be to study and find effective ways for controlling energy storage systems and to find newer and better applications of energy storage systems.

Author Contributions: All authors have equally contributed to this paper. All authors have read and agreed to the published version of the manuscript.

Funding: This research received no external funding.

Acknowledgments: This work was supported by the Portland General Electric (PGE), USA under the Grant ELT425.

Conflicts of Interest: The authors declare no conflict of interest. The funders had no role in the design of the study; in the collection, analyses, or interpretation of data; in the writing of the manuscript, or in the decision to publish the results.

References

1. *Global Energy and CO_2 Status Report 2018*; Energy Demand; International Energy Agency (IEA): Paris, France, 2019; p. 29.
2. GLOBE-Net Global Energy Demand Rose by 2.3% in 2018, Its Fastest Pace in the Last Decade—GLOBE-Net. Available online: https://globe-net.com/global-energy-demand-rose-by-2-3-in-2018-its-fastest-pace-in-the-last-decade/ (accessed on 5 February 2020).
3. Nadeem, F.; Hussain, S.M.S.; Tiwari, P.K.; Goswami, A.K.; Ustun, T.S. Comparative Review of Energy Storage Systems, Their Roles, and Impacts on Future Power Systems. *IEEE Access* **2019**, *7*, 4555–4585. [CrossRef]
4. UN Environment and International Energy Agency. Towards a zero-emission, efficient, and resilient buildings and construction sector. *Global Status Report* **2017**, *2017*, 1–48.
5. Hossain, E.; Murtaugh, D.; Mody, J.; Faruque, H.M.R.; Haque Sunny, M.S.; Mohammad, N. A Comprehensive Review on Second-Life Batteries: Current State, Manufacturing Considerations, Applications, Impacts, Barriers & Potential Solutions, Business Strategies, and Policies. *IEEE Access* **2019**, *7*, 73215–73252.
6. Chen, H.; Cong, T.N.; Yang, W.; Tan, C.; Li, Y.; Ding, Y. Progress in electrical energy storage system: A critical review. *Prog. Nat. Sci.* **2009**, *19*, 291–312. [CrossRef]
7. Poullikkas, A. A comparative overview of large-scale battery systems for electricity storage. *Renew. Sustain. Energy Rev.* **2013**, *27*, 778–788. [CrossRef]
8. Whittingham, M.S. History, Evolution, and Future Status of Energy Storage. *Proc. IEEE* **2012**, *100*, 1518–1534. [CrossRef]
9. The History and Development of Batteries. Available online: https://phys.org/news/2015-04-history-batteries.html (accessed on 23 March 2020).
10. History of Biofuels—BioFuel Information. Available online: http://biofuel.org.uk/history-of-biofuels.html (accessed on 23 March 2020).
11. Fuel Cell History—Fuel Cell Today. Available online: http://www.fuelcelltoday.com/history (accessed on 24 March 2020).
12. Lead-Based Batteries Information—Battery University. Available online: https://batteryuniversity.com/learn/article/lead_based_batteries (accessed on 19 June 2020).
13. Hydropower, Explained. Available online: https://www.nationalgeographic.com/environment/global-warming/hydropower/ (accessed on 19 June 2020).
14. History of Flywheel Energy Storage Systems | Gerotor AG; Gerotor GmbH Akt. Energiemanagement. Available online: http://gerotor.tech/history-of-flywheel-energy-storage-systems/ (accessed on 6 February 2020).
15. A Brief History of Flow Batteries. News Energy Storage Batter. Climate Change Environment. 2017. Available online: https://www.upsbatterycenter.com/blog/flow-batteries-history/ (accessed on 24 March 2020).
16. Nickel-Based Batteries Information—Battery University. Available online: https://batteryuniversity.com/learn/article/nickel_based_batteries (accessed on 6 December 2019).
17. Omar, N.; Firouz, Y.; Abdel Monem, M.; Samba, A.; Gualous, H.; Coosemans, T.C.; Van Den Bossche, P.; Van Mierlo, J. Analysis of Nickel-Based Battery Technologies for Hybrid and Electric Vehicles. In *Reference Module in Chemistry, Molecular Sciences and Chemical Engineering*; Elsevier: Amsterdam, The Netherlands, 2014.
18. Nickel Iron Battery Information. Available online: http://www.nickel-iron-battery.com/ (accessed on 13 March 2020).
19. Sparacino, A.R.; Reed, G.F.; Kerestes, R.J.; Grainger, B.M.; Smith, Z.T. Survey of battery energy storage systems and modeling techniques. In Proceedings of the 2012 IEEE Power and Energy Society General Meeting, San Diego, CA, USA, 22–26 July 2012; pp. 1–8.
20. Hartenbach, A.; Bayer, M.; Dustmann, C.-H. The Sodium Metal Halide (ZEBRA) Battery. In *Molten Salts Chemistry*; Elsevier: Amsterdam, The Netherlands, 2013; pp. 439–450, ISBN 978-0-12-398538-5.
21. Hassenzahl, W.V. Superconducting magnetic energy storage. *Proc. IEEE* **1983**, *71*, 1089–1098. [CrossRef]
22. O'Donnell, M.; Smithrick, J. *Nickel Hydrogen Batteries—An Overview*; NASA Lewis Research Center: Cleveland, OH, USA, 1995; p. 13.
23. Supercapacitor Information—Battery University. Available online: https://batteryuniversity.com/learn/article/whats_the_role_of_the_supercapacitor (accessed on 19 June 2020).

24. Jimbo Compressed Air Energy Storage. Available online: https://www.thegreenage.co.uk/tech/compressed-air-energy-storage/ (accessed on 19 June 2020).
25. DNK. Complete Guide for Lithium Polymer(Lipo) Battery: History, Charging, Safety, Storage and Care. DNK Lithium Ion Battery Pack Manufacturer and Supplier. 2019. Available online: https://www.dnkpower.com/lithium-polymer-battery-guide/ (accessed on 24 March 2020).
26. Luo, X.; Wang, J.; Dooner, M.; Clarke, J. Overview of current development in electrical energy storage technologies and the application potential in power system operation. *Appl. Energy* **2015**, *137*, 511–536. [CrossRef]
27. Breeze, P. Power System Energy Storage Technologies. In *Power Generation Technologies*; Elsevier: Amsterdam, The Netherlands, 2019; pp. 219–249, ISBN 978-0-08-102631-1.
28. International Energy Agency. Tracking Clean Energy Progress 2017. 2017. Available online: https://www.ourenergypolicy.org/wp-content/uploads/2017/05/TrackingCleanEnergyProgress2017.pdf (accessed on 30 November 2019).
29. U.S. Department of Energy Office of Electricity Delivery and Energy Reliability. Energy Storage Program Planning Document. 2011. Available online: https://www.energy.gov/sites/prod/files/oeprod/DocumentsandMedia/OE_Energy_Storage_Program_Plan_Feburary_2011v3.pdf (accessed on 30 November 2019).
30. Antal, B.A. Pumped Storage Hydropower: A Technical Review. Boulder: Department of Civil Engineering University of Colorado Denver, 2014. Available online: https://www.ucdenver.edu/faculty-staff/dmays/3414/Documents/Antal-MS-2014.pdf (accessed on 30 November 2019).
31. Safaei, H.; Aziz, M.J. Thermodynamic Analysis of Three Compressed Air Energy Storage Systems: Conventional, Adiabatic, and Hydrogen-Fueled. *Energies* **2017**, *10*, 1020. [CrossRef]
32. Martinez, M.; Molina, M.G.; Frack, F.; Mercado, P.E. Dynamic Modeling, Simulation and Control of Hybrid Energy Storage System Based on Compressed Air and Supercapacitors. *IEEE Lat. Am. Trans.* **2013**, *11*, 466–472. [CrossRef]
33. Jannelli, E.; Minutillo, M.; Lubrano Lavadera, A.; Falcucci, G. A small-scale CAES (compressed air energy storage) system for stand-alone renewable energy power plant for a radio base station: A sizing-design methodology. *Energy* **2014**, *78*, 313–322. [CrossRef]
34. Madlener, R.; Latz, J. *Centralized and Integrated Decentralized Compressed Air Energy Storage for Enhanced Grid Integration of Wind Power*; Social Science Research Network: Rochester, NY, USA, 2010.
35. Kaldemeyer, C.; Boysen, C.; Tuschy, I. Compressed Air Energy Storage in the German Energy System—Status Quo & Perspectives. *Energy Procedia* **2016**, *99*, 298–313.
36. Wang, J.; Lu, K.; Ma, L.; Wang, J.; Dooner, M.; Miao, S.; Li, J.; Wang, D. Overview of Compressed Air Energy Storage and Technology Development. *Energies* **2017**, *10*, 991. [CrossRef]
37. Kalaiselvam, S.; Parameshwaran, R. Energy Storage. In *Thermal Energy Storage Technologies for Sustainability*; Elsevier: Amsterdam, The Netherlands, 2014; pp. 21–56, ISBN 978-0-12-417291-3.
38. Guo, H.; Xu, Y.; Chen, H.; Zhou, X. Thermodynamic characteristics of a novel supercritical compressed air energy storage system. *Energy Convers. Manag.* **2016**, *115*, 167–177. [CrossRef]
39. Vafakhah, B.; Masiala, M.; Salmon, J.; Knight, A. Emulation of flywheel energy storage systems with a PMDC machine. In Proceedings of the 2008 18th International Conference on Electrical Machines, Vilamoura, Portugal, 6–9 September 2008; pp. 1–6.
40. Liu, H.; Jiang, J. Flywheel energy storage—An upswing technology for energy sustainability. *Energy Build.* **2007**, *39*, 599–604. [CrossRef]
41. Hebner, R.; Beno, J.; Walls, A. Flywheel batteries come around again. *IEEE Spectr.* **2002**, *39*, 46–51. [CrossRef]
42. Amiryar, M.; Pullen, K. A Review of Flywheel Energy Storage System Technologies and Their Applications. *Appl. Sci.* **2017**, *7*, 286. [CrossRef]
43. Sebastián, R.; Peña Alzola, R. Flywheel energy storage systems: Review and simulation for an isolated wind power system. *Renew. Sustain. Energy Rev.* **2012**, *16*, 6803–6813. [CrossRef]
44. Emadi, A.; Nasiri, A.; Bekiarov, S.B. *Uninterruptible Power Supplies and Active Filters*, 1st ed.; Power Electronics and Applications Series; CRC Press: Boca Raton, FL, USA, 2004; ISBN 978-0-8493-3035-3.
45. Brown, D.R.; Chvala, W.D. Flywheel Energy Storage: An Alternative to Batteries for UPS Systems. *Energy Eng.* **2005**, *102*, 7–26. [CrossRef]

46. Bakay, L.; Dubois, M.; Viarouge, P.; Ruel, J. Losses in an optimized 8-pole radial AMB for Long Term Flywheel Energy Storage. In Proceedings of the 2009 International Conference on Electrical Machines and Systems, Tokyo, Japan, 15–18 November 2009; pp. 1–6.
47. Parfomak, P.W. *Energy Storage for Power Grids and Electric Transportation: A Technology Assessment*; CRS Report for Congress, Congressional Research Service: Washington, DC, USA, March 2012; p. 146.
48. Peña-Alzola, R.; Sebastián, R.; Quesada, J.; Colmenar, A. Review of flywheel based energy storage systems. In Proceedings of the 2011 International Conference on Power Engineering, Energy and Electrical Drives, Malaga, Spain, 10–11 May 2011; pp. 1–6.
49. Sarbu, I.; Sebarchievici, C. A Comprehensive Review of Thermal Energy Storage. *Sustainability* **2018**, *10*, 191. [CrossRef]
50. Supercapacitors: Past, Present, and Future. *Power Electronics*, 16 March 2018. Available online: https://www.powerelectronics.com/technologies/alternative-energy/article/21864122/supercapacitors-past-present-and-future (accessed on 5 February 2020).
51. Grama, A.; Grama, L.; Petreus, D.; Rusu, C. Supercapacitor modelling using experimental measurements. In Proceedings of the 2009 International Symposium on Signals, Circuits and Systems, Iasi, Romania, 9–10 July 2019; IEEE: Iasi, Romania, 2009; pp. 1–4.
52. Dougal, R.A.; Gao, L.; Liu, S. Ultracapacitor model with automatic order selection and capacity scaling for dynamic system simulation. *J. Power Sources* **2004**, *126*, 250–257. [CrossRef]
53. Miller, J.M.; Nebrigic, D.; Everett, M. Ultracapacitor distributed model equivalent circuit for power electronic circuit simulation. In *Ansoft Leading Insights Workshop*; PA, USA, 2006; Volume 19. Available online: https://www.google.com/url?sa=t&rct=j&q=&esrc=s&source=web&cd=&ved=2ahUKEwiG4-vO99DqAhWZPXAKHftdBqYQFjAAegQIARAB&url=https%3A%2F%2Fcourseware.zcu.cz%2FCoursewarePortlets2%2FDownloadDokumentu%3Fid%3D69439&usg=AOvVaw2s9KZwM_elP11vc1WK1vGq (accessed on 5 February 2020).
54. Kousksou, T.; Bruel, P.; Jamil, A.; El Rhafiki, T.; Zeraouli, Y. Energy storage: Applications and challenges. *Sol. Energy Mater. Sol. Cells* **2014**, *120*, 59–80. [CrossRef]
55. Zhou, Z.; Benbouzid, M.; Frédéric Charpentier, J.; Scuiller, F.; Tang, T. A Review of Energy Storage Technologies for Marine Current Energy Systems. *Renew. Sustain. Energy Rev.* **2013**, *18*, 390–400. [CrossRef]
56. Chen, W.; Ådnanses, A.K.; Hansen, J.F.; Lindtjørn, J.O.; Tang, T. Super-capacitors based hybrid converter in marine electric propulsion system. In Proceedings of the XIX International Conference on Electrical Machines—ICEM 2010, Rome, Italy, 6–8 September 2010; pp. 1–6.
57. Cultura, A.B.; Salameh, Z.M. Modeling, Evaluation and Simulation of a Supercapacitor Module for Energy Storage Application. In Proceedings of the International Conference on Computer Information Systems and Industrial Applications, Bangkok, Thailand, 28–29 June 2015; Atlantis Press: Bangkok, Thailand, 2015.
58. Guidi, G.; Undeland, T.M.; Hori, Y. An Interface Converter with Reduced Volt-Ampere Ratings for Battery-Supercapacitor Mixed Systems. *IEEJ Trans. Ind. Appl.* **2008**, *128*, 418–423. [CrossRef]
59. Muzaffar, A.; Ahamed, M.B.; Deshmukh, K.; Thirumalai, J. A review on recent advances in hybrid supercapacitors: Design, fabrication and applications. *Renew. Sustain. Energy Rev.* **2019**, *101*, 123–145. [CrossRef]
60. Philippe, B.; Pittet, S.; Rufer, A. *Series Connection of Supercapacitors, with an Active Device for Equalizing the Voltages*; PCIM2000 Power Conversion and Intelligent Motion: Nürnberg, Germany, 2000.
61. Chapman, D.L. A contribution to the theory of electrocapillarity. *Lond. Edinb. Dublin Philos. Mag. J. Sci.* **2010**, *25*, 475–481. [CrossRef]
62. Zimmermann, A.W.; Yang, Y.; Young, D.E.A. *Review of the State of the Art Superconducting Magnetic Energy Storage (SMES) in Renewable/Distributed Energy Systems*; CPE 610 Mini Project Final Report. EPSRC Centre for Doctoral Training, UK, 2017. Available online: https://energystorage-cdt.group.shef.ac.uk/outputs/cohort-3/Zimmermann+Mini+Project+Final+Report.pdf (accessed on 5 February 2020).
63. Abdullah, A.Z.; Ahmed, S.; Monira, N.J. An overview of superconducting magnetic energy storage (SMES) and its applications. In Proceedings of the International Conference on Nanotechnology and Condensed Matter Physics, International Conference on Nanotechnology and Condensed Matter Physics 2018 (ICNCMP 2018), Dhaka, Bangladesh, 11–12 January 2018.
64. Marchionini, B.G.; Yamada, Y.; Martini, L.; Ohsaki, H. High-Temperature Superconductivity: A Roadmap for Electric Power Sector Applications, 2015–2030. *IEEE Trans. Appl. Supercond.* **2017**, *27*, 0500907. [CrossRef]

65. Kumar, N. *Superconducting Magnetic Energy Storage (SMES) System*; Technical Report; p. 5. Available online: https://www.researchgate.net/profile/Nishant_Kumar28/publication/261204920_Superconducting_Magnetic_Energy_Storage_SMES_System/links/55a12e7d08aea815dffbfbf0/Superconducting-Magnetic-Energy-Storage-SMES-System.pdf (accessed on 5 February 2020).
66. Krivik, P.; Baca, P. Electrochemical Energy Storage, Energy Storage—Technologies and Applications, Ahmed Faheem Zobaa, IntechOpen. 23 January 2013. Available online: https://www.intechopen.com/books/energy-storage-technologies-and-applications/electrochemical_energy_storage (accessed on 5 February 2020). [CrossRef]
67. Divya, K.C.; Østergaard, J. Battery energy storage technology for power systems—An overview. *Electr. Power Syst. Res.* **2009**, *79*, 511–520. [CrossRef]
68. Cho, J.; Jeong, S.; Kim, Y. Commercial and research battery technologies for electrical energy storage applications. *Prog. Energy Combust. Sci.* **2015**, *48*, 84–101. [CrossRef]
69. Boi, M.; Salimbeni, A.; Damiano, A. A Thévenin circuit modelling approach for sodium metal halides batteries. In Proceedings of the IECON 2017—43rd Annual Conference of the IEEE Industrial Electronics Society, Beijing, China, 29 October–1 November 2017; IEEE: Beijing, China, 2017; pp. 7611–7616.
70. Lach, J.; Wróbel, K.; Wróbel, J.; Podsadni, P.; Czerwiński, A. Applications of carbon in lead-acid batteries: A review. *J. Solid State Electrochem.* **2019**, *23*, 693–705. [CrossRef]
71. May, G.J. Lead batteries for utility energy storage: A review. *J. Energy Storage* **2018**, *15*, 145–157. [CrossRef]
72. Study Finds Nearly 100 Percent Recycling Rate for Lead Batteries. Study Finds Nearly 100 Percent Recycling Rate for Lead Batteries. Available online: https://www.recyclingtoday.com/article/battery-council-international-lead-battery-recycling/ (accessed on 3 December 2019).
73. Lead Acid Batteries | Pulsetech Products Corporation. Available online: https://www.pulsetech.net/support/lead-acid-batteries.html/ (accessed on 3 December 2019).
74. Pratik, R.; Varun, V.; Pronay, C. Design and Analysis of Maintenance Free Lead Acid Battery System Used in UPS. 2018. Available online: https://www.researchgate.net/publication/327321203_Design_and_Analysis_of_Maintenance_Free_Lead_Acid_Battery_System_Used_in_UPS (accessed on 5 February 2020). [CrossRef]
75. Hannan, M.A.; Hoque, M.M.; Mohamed, A.; Ayob, A. Review of energy storage systems for electric vehicle applications: Issues and challenges. *Renew. Sustain. Energy Rev.* **2017**, *69*, 771–789. [CrossRef]
76. Model-based Control Approaches for Optimal Integration of a Hybrid Wind-diesel Power System in a Microgrid. In Proceedings of the 2nd International Conference on Smart Grids and Green IT Systems, 9–10 May 2013; SciTePress—Science and and Technology Publications: Aachen, Germany, 2013; pp. 12–21.
77. The Differences between AGM, GEL and FLOODED Batteries. Battery Guys. Available online: https://batteryguys.com/pages/the-differences-between-agm-gel-and-flooded-batteries (accessed on 5 December 2019).
78. Burlin, W. Lead-Acid Battery Comparison: Flooded vs Sealed & AGM vs Gel Batteries. *Wholesale Sol. Blog*, 20 December 2018. Available online: https://www.wholesalesolar.com/blog/lead-acid-battery-comparison/ (accessed on 5 December 2019).
79. Lead Acid Battery Types | Lead Acid Battery Introduction Mr Positive. Available online: https://www.mrpositive.co.nz/buying/knowledge-base/lead-acid-battery-types/ (accessed on 5 December 2019).
80. Best RV Deep Cycle Battery 2019—Best RV Battery Guide EVER. *Green Living Blog*, 20 December 2017. Available online: https://mozaw.com/best-rv-deep-cycle-battery/ (accessed on 5 December 2019).
81. The Nobel Prize in Chemistry 2019. Available online: https://www.nobelprize.org/prizes/chemistry/2019/popular-information/ (accessed on 8 July 2020).
82. Pioneers of Innovation: The Battery that Changed the World. Pioneers of Innovation: The Battery that Changed the World. *Energy Factor*, 10 October 2019. Available online: https://energyfactor.exxonmobil.com/science-technology/battery-changed-world/ (accessed on 8 July 2020).
83. Reddy, M.V.; Mauger, A.; Julien, C.M.; Paolella, A.; Zaghib, K. Brief History of Early Lithium-Battery Development. *Materials* **2020**, *13*, 1884. [CrossRef] [PubMed]
84. P. 02 J. 2020 | 16:00 GMT. The Return of the Lithium-Metal Battery—IEEE Spectrum. IEEE Spectrum: Technology, Engineering, and Science News. Available online: https://spectrum.ieee.org/energy/the-smarter-grid/the-return-of-the-lithiummetal-battery (accessed on 8 July 2020).

85. Grossman, D. Lithium Metal Could Soon Replace Lithium Ion in Batteries. *Popular Mechanics*, 29 August 2019. Available online: https://www.popularmechanics.com/cars/hybrid-electric/a28859683/lithium-metal-replace-lithium-ion-batteries/ (accessed on 8 July 2020).
86. New Electrode Design May Lead to More Powerful Batteries. MIT News. Available online: http://news.mit.edu/2020/solid-batteries-lithium-metal-electrode-0203 (accessed on 8 July 2020).
87. Li, S.; Jiang, M.; Xie, Y.; Xu, H.; Jia, J.; Li, J. Developing High-Performance Lithium Metal Anode in Liquid Electrolytes: Challenges and Progress. *Adv. Mater.* **2018**, *30*, 1706375. [CrossRef] [PubMed]
88. Hwang, J.-Y.; Park, S.-J.; Yoon, C.S.; Sun, Y.-K. Customizing a Li–metal battery that survives practical operating conditions for electric vehicle applications. *Energy Environ. Sci.* **2019**, *12*, 2174–2184. [CrossRef]
89. Tang, W.; Yin, X.; Kang, S.; Chen, Z.; Tian, B.; Teo, S.L.; Wang, X.; Chi, X.; Loh, K.P.; Lee, H.-W.; et al. Lithium Silicide Surface Enrichment: A Solution to Lithium Metal Battery. *Adv. Mater.* **2018**, *30*, 1801745. [CrossRef]
90. Yang, Q.; Li, C. Li metal batteries and solid state batteries benefiting from halogen-based strategies. *Energy Storage Mater.* **2018**, *14*, 100–117. [CrossRef]
91. Chen, L.; Fan, X.; Ji, X.; Chen, J.; Hou, S.; Wang, C. High-Energy Li Metal Battery with Lithiated Host. *Joule* **2019**, *3*, 732–744. [CrossRef]
92. Mu, D.; Jiang, J.; Zhang, C. Online Semiparametric Identification of Lithium-Ion Batteries Using the Wavelet-Based Partially Linear Battery Model. *Energies* **2013**, *6*, 2583–2604. [CrossRef]
93. Koohi-Kamali, S. Emergence of energy storage technologies as the solution for reliable operation of smart power systems—A review. *Renew. Sustain. Energy Rev.* **2013**, *25*, 135–365. [CrossRef]
94. Chung, S.-Y.; Bloking, J.T.; Chiang, Y.-M. Electronically conductive phospho-olivines as lithium storage electrodes. *Nat. Mater.* **2002**, *1*, 123–128. [CrossRef] [PubMed]
95. Okou, R.; Sebitosi, A.B.; Pillay, P. Flywheel rotor manufacture for rural energy storage in sub-Saharan Africa. *Energy* **2011**, *36*, 6138–6145. [CrossRef]
96. Barnes, F.S. *Large Energy Storage Systems Handbook*, 1st ed.; CRC Press: Boca Raton, FL, USA; ISBN 978-1-4200-8601-0.
97. Types of Lithium-Ion Batteries—Battery University. Available online: https://batteryuniversity.com/index.php/learn/article/types_of_lithium_ion (accessed on 5 December 2019).
98. Power, F. Lithium-Ion Battery Technology. Available online: https://www.fluxpower.com/lithium-ion-battery-technology (accessed on 6 July 2020).
99. Jaffe, S. The Lithium Ion Battery Market. In Proceedings of the ARPA E RANGE Conference, Cape Canaveral, FL, USA, 28–29 January 2014; p. 18.
100. Advantages & Limitations of the Lithium-Ion Battery—Battery University. Available online: https://batteryuniversity.com/learn/archive/is_lithium_ion_the_ideal_battery/ (accessed on 7 February 2020).
101. Esfahanian, M.; Mahmoodian, A.; Amiri, M.; Tehrani, M.M.; Nehzati, H.; Hejabi, M.; Manteghi, A. Large Lithium Polymer Battery Modeling for the Simulation of Hybrid Electric Vehicles Using the Equivalent Circuit Method. *IJAE* **2013**, *3*, 564–576.
102. Fattal, J.; Dib Nabil Karami, P.B. Review on different charging techniques of a lithium polymer battery. In Proceedings of the 2015 Third International Conference on Technological Advances in Electrical, Electronics and Computer Engineering (TAEECE), Beirut, Lebanon, 29 April–1 May 2015; IEEE: Beirut, Lebanon, 2015; pp. 33–38.
103. What Is Lipo Battery Pack Construction. GensTattu Blog. Available online: https://www.genstattu.com/blog/what-is-lipo-battery-pack-construction/ (accessed on 7 February 2020).
104. Yang, B.; Makarov, Y.; Desteese, J.; Viswanathan, V.; Nyeng, P.; McManus, B.; Pease, J. On the use of energy storage technologies for regulation services in electric power systems with significant penetration of wind energy. In Proceedings of the 2008 5th International Conference on the European Electricity Market, Lisboa, Portugal, 28–30 May 2008; IEEE: Lisboa, Portugal, 2008; pp. 1–6.
105. Wen, Z. Study on Energy Storage Technology of Sodium Sulfur Battery and it's Application in Power System. In Proceedings of the 2006 International Conference on Power System Technology, Chongqing, China, 22–26 October 2006; IEEE: Chongqing, China, 2006; pp. 1–4.
106. Reed, G.F.; Philip, P.A.; Barchowsky, A.; Lippert, C.J.; Sparacino, A.R. Sample survey of smart grid approaches and technology gap analysis. In Proceedings of the 2010 IEEE PES Innovative Smart Grid Technologies Conference Europe (ISGT Europe), Gothenburg, Sweden, 11–20 October 2010; IEEE: Gothenburg, Sweden, 2010; pp. 1–10.

107. NGK Insulators Sodium Sulfur Batteries for Large Scale Grid Energy Storage. Available online: http://energystoragenews.com/NGK%20Insulators%20Sodium%20Sulfur%20Batteries%20for%20Large%20Scale%20Grid%20Energy%20Storage.html (accessed on 5 December 2019).
108. Specs | NAS Energy Storage System: Sodium Sulfur Battery. Available online: https://www.ngk.co.jp/nas/specs/ (accessed on 5 December 2019).
109. Hussien, Z.F.; Cheung, L.W.; Siam, M.F.M.; Ismail, A.B. Modeling of Sodium Sulfur Battery for Power System Applications. *ELEKTRIKA* **2007**, *9*, 66–72.
110. Rijssenbeek, J.; Wiegman, H.; Hall, D.; Chuah, C.; Balasubramanian, G.; Brady, C. Sodium-metal halide batteries in diesel-battery hybrid telecom applications. In Proceedings of the 2011 IEEE 33rd International Telecommunications Energy Conference (INTELEC), Amsterdam, The Netherlands, 9–13 October 2011; IEEE: Amsterdam, The Netherlands, 2011; pp. 1–4.
111. Dustmann, C.-H. Advances in ZEBRA batteries. *J. Power Sources* **2004**, *127*, 85–92. [CrossRef]
112. O'sullivan, T.M.; Bingham, C.M.; Clark, R.E. Zebra battery technologies for all electric smart car. In *International Symposium on Power Electronics, Electrical Drives, Automation and Motion, 2006. SPEEDAM 2006*; IEEE: Taormina, Italy, 2006; p. 243.
113. David, T. *Current Status of Health and Safety Issues of Sodium/Metal Chloride (ZEBRA) Batteries*; No. NREL/TP-460-25553; National Renewable Energy Lab.: Golden, CO, USA, 1998.
114. Zhang, H.; Chow, M.Y. Comprehensive dynamic battery modeling for PHEV applications. In Proceedings of the IEEE PES General Meeting, Detroit, MI, USA, 24–29 July 2010; pp. 1–6.
115. Clark, S.; Latz, A.; Horstmann, B. A Review of Model-Based Design Tools for Metal-Air Batteries. *Batteries* **2018**, *4*, 5. [CrossRef]
116. Li, Y.; Lu, J. Metal-Air Batteries: Future Electrochemical Energy Storage of Choice? *ACS Energy Lett.* **2017**, *2*, 1370–1377. [CrossRef]
117. Li, Y.; Zhang, X.; Li, H.-B.; Yoo, H.D.; Chi, X.; An, Q.; Liu, J.; Yu, M.; Wang, W.; Yao, Y. Mixed-phase mullite electrocatalyst for pH-neutral oxygen reduction in magnesium-air batteries. *Nano Energy* **2016**, *27*, 8–16. [CrossRef]
118. Li, C.-S.; Sun, Y.; Gebert, F.; Chou, S.-L. Current Progress on Rechargeable Magnesium-Air Battery. *Adv. Energy Mater.* **2017**, *7*, 1700869. [CrossRef]
119. Chen, L.D.; Nørskov, J.K.; Luntz, A.C. Theoretical Limits to the Anode Potential in Aqueous Mg–Air Batteries. *J. Phys. Chem. C* **2015**, *119*, 19660–19667. [CrossRef]
120. Vardar, G.; Sleightholme, A.E.S.; Naruse, J.; Hiramatsu, H.; Siegel, D.J.; Monroe, C.W. Electrochemistry of Magnesium Electrolytes in Ionic Liquids for Secondary Batteries. *ACS Appl. Mater. Interfaces* **2014**, *6*, 18033–18039. [CrossRef] [PubMed]
121. Fu, G.; Chen, Y.; Cui, Z.; Li, Y.; Zhou, W.; Xin, S.; Tang, Y.; Goodenough, J.B. A novel hydrogel-derived bifunctional oxygen electrocatalyst for rechargeable air cathodes. *Nano Lett.* **2016**, *16*, 6516–6522. [CrossRef] [PubMed]
122. Mokhtar, M.; Talib, M.Z.M.; Majlan, E.H.; Tasirin, S.M.; Ramli, W.M.F.W.; Daud, W.R.W.; Sahari, J. Recent developments in materials for aluminum–air batteries: A review. *J. Ind. Eng. Chem.* **2015**, *32*, 1–20. [CrossRef]
123. Zhang, Z.; Zuo, C.; Liu, Z.; Yu, Y.; Zuo, Y.; Song, Y. All-solid-state Al–air batteries with polymer alkaline gel electrolyte. *J. Power Sources* **2014**, *251*, 470–475. [CrossRef]
124. Kim, J.; Park, H.; Lee, B.; Seong, W.M.; Lim, H.-D.; Bae, Y.; Kim, H.; Kim, W.K.; Ryu, K.H.; Kang, K. Dissolution and ionization of sodium superoxide in sodium–oxygen batteries. *Nat. Commun.* **2016**, *7*, 10670. [CrossRef]
125. Adelhelm, P.; Hartmann, P.; Bender, C.L.; Busche, M.; Eufinger, C.; Janek, J. From lithium to sodium: Cell chemistry of room temperature sodium–air and sodium–sulfur batteries. *Beilstein J. Nanotechnol.* **2015**, *6*, 1016–1055. [CrossRef]
126. Durmus, Y.E.; Aslanbas, Ö.; Kayser, S.; Tempel, H.; Hausen, F.; de Haart, L.G.J.; Granwehr, J.; Ein-Eli, Y.; Eichel, R.-A.; Kungl, H. Long run discharge, performance and efficiency of primary Silicon–air cells with alkaline electrolyte. *Electrochim. Acta* **2017**, *225*, 215–224. [CrossRef]
127. Cohn, G.; Ein-Eli, Y. Study and development of non-aqueous silicon-air battery. *J. Power Sources* **2010**, *195*, 4963–4970. [CrossRef]
128. Gilligan, G.E.; Qu, D. Zinc-air and other types of metal-air batteries. In *Advances in Batteries for Medium and Large-Scale Energy Storage*; Elsevier: Amsterdam, The Netherlands, 2015; pp. 441–461, ISBN 978-1-78242-013-2.

129. Holze, R. The Kinetics of Oxygen Reduction at Porous Teflon-Bonded Fuel Cell Electrodes. *J. Electrochem. Soc.* **1984**, *131*, 2298. [CrossRef]
130. Ma, Z.; Pei, P.; Wang, K.; Wang, X.; Xu, H.; Liu, Y.; Peng, G. Degradation characteristics of air cathode in zinc air fuel cells. *J. Power Sources* **2015**, *274*, 56–64. [CrossRef]
131. Huang, Z.; Du, G. Nickel-based batteries for medium- and large-scale energy storage. In *Advances in Batteries for Medium and Large-Scale Energy Storage*; Elsevier: Amsterdam, The Netherlands, 2015; pp. 73–90, ISBN 978-1-78242-013-2.
132. What Are Nickel Based Batteries—BatteryGuy.com Knowledge Base. Available online: https://batteryguy.com/kb/knowledge-base/what-are-nickel-based-batteries/ (accessed on 6 December 2019).
133. Dell, R.M.; Rand, D.A.J. *Understanding Batteries*; Royal Society of Chemistry: London, UK, 2001; ISBN 978-0-85404-605-8. [CrossRef]
134. Bruce, P.G. Energy storage beyond the horizon: Rechargeable lithium batteries. *Solid State Ion.* **2008**, *179*, 752–760. [CrossRef]
135. Wakihara, M. Recent developments in lithium ion batteries. *Mater. Sci. Eng. R Rep.* **2001**, *33*, 109–134. [CrossRef]
136. Connolly, D.; Lund, H.; Mathiesen, B.V.; Leahy, M. The first step towards a 100% renewable energy-system for Ireland. *Appl. Energy* **2011**, *88*, 502–507. [CrossRef]
137. Norian, K.H. Equivalent circuit components of nickel–cadmium battery at different states of charge. *J. Power Sources* **2011**, *196*, 5205–5208. [CrossRef]
138. Nickel Metal Hydride Handbook and Application Manual. Available online: www.energizer.com (accessed on 6 December 2019).
139. Tarabay, J.; Karami, N. Nickel Metal Hydride battery: Structure, chemical reaction, and circuit model. In Proceedings of the 2015 Third International Conference on Technological Advances in Electrical, Electronics and Computer Engineering (TAEECE), Beirut, Lebanon, 29 April–1 May 2015; pp. 22–26.
140. Ghossein, N.E.; Salameh, J.P.; Karami, N.; Hassan, M.E.; Najjar, M.B. Survey on electrical modeling methods applied on different battery types. In Proceedings of the 2015 Third International Conference on Technological Advances in Electrical, Electronics and Computer Engineering (TAEECE), Beirut, Lebanon, 29 April–1 May 2015; pp. 39–44.
141. Zimmerman, A. *Nickel-Hydrogen Batteries: Principles and Practice*; American Institute of Aeronautics and Astronautics, Inc.: Washington, DC, USA, 2009; ISBN 978-1-884989-20-9.
142. Chen, W.; Jin, Y.; Zhao, J.; Liu, N.; Cui, Y. Nickel-hydrogen batteries for large-scale energy storage. *Proc. Natl. Acad. Sci. USA* **2018**, *115*, 11694–11699. [CrossRef] [PubMed]
143. Molecular Expressions: Electricity and Magnetism: Nickel-hydrogen Terrestrial Battery. Available online: https://micro.magnet.fsu.edu/electromag/electricity/batteries/nickelhydrogen.html (accessed on 6 December 2019).
144. BU-210b: How does the Flow Battery Work?—Battery University. Available online: https://batteryuniversity.com/learn/article/bu_210b_flow_battery (accessed on 7 February 2020).
145. Leung, P.; Li, X.; Ponce de León, C.; Berlouis, L.; Low, C.T.J.; Walsh, F.C. Progress in redox flow batteries, remaining challenges and their applications in energy storage. *RSC Adv.* **2012**, *2*, 10125. [CrossRef]
146. Guarnieri, M.; Mattavelli, P.; Petrone, G.; Spagnuolo, G. Vanadium Redox Flow Batteries: Potentials and Challenges of an Emerging Storage Technology. *IEEE Ind. Electron. Mag.* **2016**, *10*, 20–31. [CrossRef]
147. Nguyen, T.; Savinell, R.F. Flow Batterie. *Electrochem. Soc. Interface* **2010**, *19*, 54–56. [CrossRef]
148. Devic, A.C. SusChem Battery Energy Storage. White Paper 2018. Available online: suschem.org (accessed on 7 February 2019).
149. Mohamed, M.R.; Ahmad, H.; Seman, M.N.A.; Razali, S.; Najib, M.S. Electrical circuit model of a vanadium redox flow battery using extended Kalman filter. *J. Power Sources* **2013**, *239*, 284–293. [CrossRef]
150. Weber, A.Z.; Mench, M.M.; Meyers, J.P.; Ross, P.N.; Gostick, J.T.; Liu, Q. Redox flow batteries: A review. *J. Appl. Electrochem.* **2011**, *41*, 1137–1164. [CrossRef]
151. Pan, F.; Wang, Q. Redox Species of Redox Flow Batteries: A Review. *Molecules* **2015**, *20*, 20499–20517. [CrossRef] [PubMed]
152. Wang, G.; Pou, J.; Agelidis, V.G. Reconfigurable battery energy storage system for utility-scale applications. In Proceedings of the IECON 2015—41st Annual Conference of the IEEE Industrial Electronics Society, Yokohama, Japan, 9–12 November 2015; pp. 004086–004091.

153. Koo, B.; Lee, D.; Yi, J.; Shin, C.; Kim, D.; Choi, E.; Kang, T. Modeling the Performance of a Zinc/Bromine Flow Battery. *Energies* **2019**, *12*, 1159. [CrossRef]
154. Byrne, R.; MacArtain, P. Energy performance of an operating 50 kWh zinc-bromide flow battery system. In Proceedings of the 2015 IEEE International Conference on Engineering, Technology and Innovation/ International Technology Management Conference (ICE/ITMC), Belfast, UK, 22–24 June 2015; pp. 1–6.
155. Zhang, J.; Jiang, G.; Xu, P.; Ghorbani Kashkooli, A.; Mousavi, M.; Yu, A.; Chen, Z. An all-aqueous redox flow battery with unprecedented energy density. *Energy Environ. Sci.* **2018**, *11*, 2010–2015. [CrossRef]
156. Butler, P.C.; Eidler, P.A.; Grimes, P.G.; Klassen, S.E.; Miles, R.C. Zinc/bromine batteries. In *Handbook of Batteries*; McGraw-Hill: Columbus, OH, USA, 2001; p. 37-01.
157. Solid Electrode Battery Technology | Energy Storage Assocation. Available online: https://energystorage.org/why-energy-storage/technologies/solid-electrode-batteries/ (accessed on 7 February 2020).
158. Bryans, D.; McMillan, B.G.; Spicer, M.; Wark, A.; Berlouis, L. Complexing Additives to Reduce the Immiscible Phase Formed in the Hybrid $ZnBr_2$ Flow Battery. *J. Electrochem. Soc.* **2017**, *164*, A3342–A3348. [CrossRef]
159. Yu, X.; Manthiram, A. A Zinc-Cerium Cell for Energy Storage Using a Sodium-Ion Exchange Membrane. *Adv. Sustain. Syst.* **2017**, *1*, 1700082. [CrossRef]
160. Xie, Z.; Liu, Q.; Chang, Z.; Zhang, X. The developments and challenges of cerium half-cell in zinc–cerium redox flow battery for energy storage. *Electrochim. Acta* **2013**, *90*, 695–704. [CrossRef]
161. Qi, Z.; Koenig, G.M. Review Article: Flow battery systems with solid electroactive materials. *J. Vac. Sci. Technol. B Nanotechnol. Microelectron. Mater. Process. Meas. Phenom.* **2017**, *35*, 040801. [CrossRef]
162. Petek, T.J.; Hoyt, N.C.; Savinell, R.F.; Wainright, J.S. Slurry electrodes for iron plating in an all-iron flow battery. *J. Power Sources* **2015**, *294*, 620–626. [CrossRef]
163. Mubeen, S.; Jun, Y.; Lee, J.; McFarland, E.W. Solid Suspension Flow Batteries Using Earth Abundant Materials. *ACS Appl. Mater. Interfaces* **2016**, *8*, 1759–1765. [CrossRef]
164. Ruggeri, I.; Arbizzani, C.; Soavi, F. A novel concept of Semi-solid, Li Redox Flow Air (O2) Battery: A breakthrough towards high energy and power batteries. *Electrochim. Acta* **2016**, *206*, 291–300. [CrossRef]
165. Dong, K.; Wang, S.; Yu, J. A lithium/polysulfide semi-solid rechargeable flow battery with high output performance. *RSC Adv.* **2014**, *4*, 47517–47520. [CrossRef]
166. Ding, Y.; Zhao, Y.; Yu, G. A Membrane-Free Ferrocene-Based High-Rate Semiliquid Battery. *Nano Lett.* **2015**, *15*, 4108–4113. [CrossRef] [PubMed]
167. Yang, Y.; Zheng, G.; Cui, Y. A membrane-free lithium/polysulfide semi-liquid battery for large-scale energy storage. *Energy Environ. Sci.* **2013**, *6*, 1552–1558. [CrossRef]
168. Fan, F.Y.; Woodford, W.H.; Li, Z.; Baram, N.; Smith, K.C.; Helal, A.; McKinley, G.H.; Carter, W.C.; Chiang, Y.-M. Polysulfide Flow Batteries Enabled by Percolating Nanoscale Conductor Networks. *Nano Lett.* **2014**, *14*, 2210–2218. [CrossRef]
169. Duduta, M.; Ho, B.; Wood, V.C.; Limthongkul, P.; Brunini, V.E.; Carter, W.C.; Chiang, Y.-M. Semi-Solid Lithium Rechargeable Flow Battery. *Adv. Energy Mater.* **2011**, *1*, 511–516. [CrossRef]
170. Zhao, Y.; Si, S.; Liao, C. A single flow zinc//polyaniline suspension rechargeable battery. *J. Power Sources* **2013**, *241*, 449–453. [CrossRef]
171. Zhao, Y.; Si, B.S.; Wang, Z.L.; Tang, A.P.; Caoa, H. The Electrochemical Society Electrochemical Behavior of Polyaniline Microparticle Suspension as Flowing Anode for Rechargeable Lead Dioxide Flow Ba. *Electrochem. Soc.* **2014**, *161*, 3. [CrossRef]
172. Zhao, Y.; Si, S.; Wang, L.; Liao, C.; Tang, P.; Cao, H. Electrochemical study on polypyrrole microparticle suspension as flowing anode for manganese dioxide rechargeable flow battery. *J. Power Sources* **2014**, *248*, 962–968. [CrossRef]
173. Wu, S.; Zhao, Y.; Li, D.; Xia, Y.; Si, S. An asymmetric Zn//Ag doped polyaniline microparticle suspension flow battery with high discharge capacity. *J. Power Sources* **2015**, *275*, 305–311. [CrossRef]
174. Montoto, E.C.; Nagarjuna, G.; Hui, J.; Burgess, M.; Sekerak, N.M.; Hernández-Burgos, K.; Wei, T.-S.; Kneer, M.; Grolman, J.; Cheng, K.J.; et al. Redox Active Colloids as Discrete Energy Storage Carriers. *J. Am. Chem. Soc.* **2016**, *138*, 13230–13237. [CrossRef] [PubMed]
175. Wang, Q.; Zakeeruddin, S.M.; Wang, D.; Exnar, I.; Grätzel, M. Redox Targeting of Insulating Electrode Materials: A New Approach to High-Energy-Density Batteries. *Angew. Chem. Int. Ed.* **2006**, *45*, 8197–8200. [CrossRef] [PubMed]

176. Jia, C.; Pan, F.; Zhu, Y.G.; Huang, Q.; Lu, L.; Wang, Q. High–energy density nonaqueous all redox flow lithium battery enabled with a polymeric membrane. *Sci. Adv.* **2015**, *1*, e1500886. [CrossRef]
177. Huang, Q.; Li, H.; Grätzel, M.; Wang, Q. Reversible chemical delithiation/lithiation of LiFePO4: Towards a redox flow lithium-ion battery. *Phys. Chem. Chem. Phys.* **2013**, *15*, 1793–1797. [CrossRef] [PubMed]
178. Pan, F.; Yang, J.; Huang, Q.; Wang, X.; Huang, H.; Wang, Q. Redox Targeting of Anatase TiO2 for Redox Flow Lithium-Ion Batteries. *Adv. Energy Mater.* **2014**, *4*, 1400567. [CrossRef]
179. Zhao, Y.; Zheng, M.; Cao, J.; Ke, X.; Liu, J.; Chen, Y.; Tao, J. Easy synthesis of ordered meso/macroporous carbon monolith for use as electrode in electrochemical capacitors. *Mater. Lett.* **2008**, *62*, 548–551. [CrossRef]
180. Fang, Y.; Liu, J.; Yu, D.J.; Wicksted, J.P.; Kalkan, K.; Topal, C.O.; Flanders, B.N.; Wu, J.; Li, J. Self-supported supercapacitor membranes: Polypyrrole-coated carbon nanotube networks enabled by pulsed electrodeposition. *J. Power Sources* **2010**, *195*, 674–679. [CrossRef]
181. Babeł, K.; Jurewicz, K. KOH activated lignin based nanostructured carbon exhibiting high hydrogen electrosorption. *Carbon* **2008**, *46*, 1948–1956. [CrossRef]
182. Conway, B.E.; Tilak, B.V. Interfacial processes involving electrocatalytic evolution and oxidation of H2, and the role of chemisorbed H. *Electrochim. Acta* **2002**, *47*, 3571–3594. [CrossRef]
183. Lota, G.; Fic, K.; Frackowiak, E. Carbon nanotubes and their composites in electrochemical applications. *Energy Environ. Sci.* **2011**, *4*, 1592. [CrossRef]
184. Béguin, F.; Kierzek, K.; Friebe, M.; Jankowska, A.; Machnikowski, J.; Jurewicz, K.; Frackowiak, E. Effect of various porous nanotextures on the reversible electrochemical sorption of hydrogen in activated carbons. *Electrochim. Acta* **2006**, *51*, 2161–2167. [CrossRef]
185. Alguail, A.A. Battery Type Hybrid Supercapacitor Based on Conducting Polymers. Ph. D. Thesis, Faculty of Technology and Metallurgy, University of Belgrade, Beograd, Serbia, 2018. Available online: http://uvidok.rcub.bg.ac.rs/bitstream/handle/123456789/2341/Doktorat.pdf?sequence=1 (accessed on 14 January 2020).
186. Machida, K.; Suematsu, S.; Ishimoto, S.; Tamamitsu, K. High-Voltage Asymmetric Electrochemical Capacitor Based on Polyfluorene Nanocomposite and Activated Carbon. *J. Electrochem. Soc.* **2008**, *155*, A970. [CrossRef]
187. Kötz, R.; Carlen, M. Principles and applications of electrochemical capacitors. *Electrochim. Acta* **2000**, *45*, 2483–2498. [CrossRef]
188. Halper, M.S.; Ellenbogen, J.C. *Supercapacitors: A Brief Overview*; The MITRE Corporation: McLean, VA, USA, 2006; pp. 1–34.
189. Inoue, H.; Morimoto, T.; Nohara, S. Electrochemical Characterization of a Hybrid Capacitor with Zn and Activated Carbon Electrodes. *Electrochem. Solid-State Lett.* **2007**, *10*, A261. [CrossRef]
190. Kirubakaran, A.; Jain, S.; Nema, R.K. A review on fuel cell technologies and power electronic interface. *Renew. Sustain. Energy Rev.* **2009**, *13*, 2430–2440. [CrossRef]
191. Boudghene Stambouli, A.; Traversa, E. Fuel cells, an alternative to standard sources of energy. *Renew. Sustain. Energy Rev.* **2002**, *6*, 295–304. [CrossRef]
192. Peng, F.Z. Editorial Special Issue on Distributed Power Generation. *IEEE Trans. Power Electron.* **2004**, *19*, 1157–1158. [CrossRef]
193. Meng, J. A distributed power generation communication system. In Proceedings of the CCECE 2003—Canadian Conference on Electrical and Computer Engineering. Toward a Caring and Humane Technology (Cat. No.03CH37436), Montreal, QC, Canada, 4–7 May 2003; Volume 1, pp. 483–486.
194. Park, C.-M.; Kim, J.-H.; Kim, H.; Sohn, H.-J. Li-alloy based anode materials for Li secondary batteries. *Chem. Soc. Rev.* **2010**, *39*, 3115–3141. [CrossRef] [PubMed]
195. Engineered Nanomaterials for Energy Applications. *Handbook of Nanomaterials for Industrial Applications*; Elsevier: Amsterdam, The Netherlands, 2018; pp. 751–767, ISBN 978-0-12-813351-4.
196. Akhairi, M.A.F.; Kamarudin, S.K. Catalysts in direct ethanol fuel cell (DEFC): An overview. *Int. J. Hydrogen Energy* **2016**, *41*, 4214–4228. [CrossRef]
197. Uhm, S.; Lee, J.K.; Chung, S.T.; Lee, J. Effect of anode diffusion media on direct formic acid fuel cells. *J. Ind. Eng. Chem.* **2008**, *14*, 493–498. [CrossRef]
198. Cui, J.; Jing, B.; Xu, X.; Wang, L.; Cheng, F.; Li, S.; Wen, Z.; Ji, S.; Sun, J. Performance of niobium nitride-modified AISI316L stainless steel as bipolar plates for direct formic acid fuel cells. *Int. J. Hydrogen Energy* **2017**, *42*, 11830–11837. [CrossRef]
199. Zhu, Y.; Ha, S.Y.; Masel, R.I. High power density direct formic acid fuel cells. *J. Power Sources* **2004**, *130*, 8–14. [CrossRef]

200. Hong, P.; Liao, S.; Zeng, J.; Huang, X. Design, fabrication and performance evaluation of a miniature air breathing direct formic acid fuel cell based on printed circuit board technology. *J. Power Sources* **2010**, *195*, 7332–7337. [CrossRef]
201. Rice, C.; Ha, S.; Masel, R.I.; Waszczuk, P.; Wieckowski, A.; Barnard, T. Direct formic acid fuel cells. *J. Power Sources* **2002**, *111*, 83–89. [CrossRef]
202. Ha, S.; Larsen, R.; Masel, R.I. Performance characterization of Pd/C nanocatalyst for direct formic acid fuel cells. *J. Power Sources* **2005**, *144*, 28–34. [CrossRef]
203. Aslam, N.M.; Masdar, M.S.; Kamarudin, S.K.; Daud, W.R.W. Overview on Direct Formic Acid Fuel Cells (DFAFCs) as an Energy Sources. *APCBEE Procedia* **2012**, *3*, 33–39. [CrossRef]
204. Hong, P.; Zhong, Y.; Liao, S.; Zeng, J.; Lu, X.; Chen, W. A 4-cell miniature direct formic acid fuel cell stack with independent fuel reservoir: Design and performance investigation. *J. Power Sources* **2011**, *196*, 5913–5917. [CrossRef]
205. Heidrich, E.S.; Curtis, T.P.; Dolfing, J. Determination of the Internal Chemical Energy of Wastewater. *Environ. Sci. Technol.* **2011**, *45*, 827–832. [CrossRef]
206. Oguz Koroglu, E.; Civelek Yoruklu, H.; Demir, A.; Ozkaya, B. Scale-Up and Commercialization Issues of the MFCs. In *Microbial Electrochemical Technology*; Elsevier: Amsterdam, The Netherlands, 2019; pp. 565–583, ISBN 978-0-444-64052-9.
207. Reis, A.; Mert, S.O. Performance assessment of a direct formic acid fuel cell system through exergy analysis. *Int. J. Hydrogen Energy* **2015**, *40*, 12776–12783. [CrossRef]
208. Kamarudin, M.Z.F.; Kamarudin, S.K.; Masdar, M.S.; Daud, W.R.W. Review: Direct ethanol fuel cells. *Int. J. Hydrogen Energy* **2013**, *38*, 9438–9453. [CrossRef]
209. Salameh, Z. Energy Storage. In *Renewable Energy System Design*; Elsevier: Amsterdam, The Netherlands, 2014; pp. 201–298, ISBN 978-0-12-374991-8.
210. Farooque, M.; Maru, H.C. Fuel cells-the clean and efficient power generators. *Proc. IEEE* **2001**, *89*, 1819–1829. [CrossRef]
211. *Fuel Cell Handbook*, 6th ed.; DIANE Publishing: Darby, PA, USA, 2000; ISBN 978-1-4289-1759-0.
212. Benz, J.B.; Ortiz, B.; Roth, W.; Sauer, D.U.; Steinhüser, A. Fuel cells in photovoltaic hybrid systems for stand-alone power supplies. In *2nd European PV-Hybrid and Mini-Grid Conference*; OTTI Energie Kolleg: Kassel, Germany, 2003; pp. 232–239.
213. Sun, M.; Zhai, L.-F.; Li, W.-W.; Yu, H.-Q. Harvest and utilization of chemical energy in wastes by microbial fuel cells. *Chem. Soc. Rev.* **2016**, *45*, 2847–2870. [CrossRef] [PubMed]
214. Hong, K.B.; Chang, S.; Gadd, G.M. Challenges in microbial fuel cell development and operation. *Appl. Microbiol. Biotechnol.* **2007**, *76*, 485.
215. Heidrich, E.S.; Dolfing, J.; Scott, K.; Edwards, S.R.; Jones, C.; Curtis, T.P. Production of hydrogen from domestic wastewater in a pilot-scale microbial electrolysis cell. *Appl. Microbiol. Biotechnol.* **2013**, *97*, 6979–6989. [CrossRef]
216. Khaled, F.; Ondel, O.; Allard, B. Optimal Energy Harvesting from Serially Connected Microbial Fuel Cells. *IEEE Trans. Ind. Electron.* **2015**, *62*, 3508–3515. [CrossRef]
217. Kreysa, G.; Ota, K.; Savinell, R.F. (Eds.) *Encyclopedia of Applied Electrochemistry*; Springer: New York, NY, USA, 2014; ISBN 978-1-4419-6995-8.
218. Tuller, H.L. Solar to fuels conversion technologies: A perspective. *Mater. Renew. Sustain. Energy* **2017**, *6*, 3. [CrossRef] [PubMed]
219. Steinfeld, A.; Kuhn, P.; Reller, A.; Palumbo, R.; Murray, J.; Tamaura, Y. Solar-Processed Metals as Clean Energy Carriers and Water-Splitters. *Int. J. Hydrogen Energy* **1998**, *23*, 767–774. [CrossRef]
220. Steinfeld, A. Solar hydrogen production via a two-step water-splitting thermochemical cycle based on Zn/ZnO redox reactions. *Int. J. Hydrogen Energy* **2002**, *27*, 611–619. [CrossRef]
221. Steinfeld, A. Solar thermochemical production of hydrogen—A review. *Sol. Energy* **2005**, *78*, 603–615. [CrossRef]
222. Steinfeld, A.; Palumbo, R. Solar Thermochemical Process Technology. In *Encyclopedia of Physical Science and Technology*; Elsevier: Amsterdam, The Netherlands, 2003; pp. 237–256, ISBN 978-0-12-227410-7.
223. Solar Refinery Turns Light and Air into Liquid Fuel. Available online: https://www.goodnet.org/articles/solar-refinery-turns-light-air-into-liquid-fuel (accessed on 14 February 2020).

224. Schunk, L.O.; Haeberling, P.; Wepf, S.; Wuillemin, D.; Meier, A.; Steinfeld, A. A Receiver-Reactor for the Solar Thermal Dissociation of Zinc Oxide. *J. Sol. Energy Eng.* **2008**, *130*, 021009. [CrossRef]
225. Levy, M.; Levitan, R.; Rosin, H.; Rubin, R. Solar energy storage via a closed-loop chemical heat pipe. *Sol. Energy* **1993**, *50*, 179–189. [CrossRef]
226. Luzzi, A. Endothermic Reactors for an Ammonia Based Thermo- Chemical Solar Energy Storage and Transport System. *Sol. Energy* **1996**, *56*, 361–371.
227. Demirbas, A. Biofuels sources, biofuel policy, biofuel economy and global biofuel projections. *Energy Convers. Manag.* **2008**, *49*, 2106–2116. [CrossRef]
228. Top five countries for biofuel production across the globe. *NS Energy*, 15 November 2019. Available online: https://www.nsenergybusiness.com/features/top-biofuel-production-countries/ (accessed on 14 January 2020).
229. *Global Bioenergy Statistics 2019*; World Bioenergy Association: Stockholm, Sweden, 2019; Available online: https://worldbioenergy.org/uploads/191129%20WBA%20GBS%202019_LQ.pdf (accessed on 15 November 2019).
230. Haller, M.Y.; Carbonell, D.; Dudita, M.; Zenhäusern, D.; Häberle, A. Seasonal energy storage in aluminium for 100 percent solar heat and electricity supply. *Energy Convers. Manag. X* **2020**, *5*, 100017. [CrossRef]
231. Hybrid energy storage: Are combined solutions gaining ground? *Energy Storage Forum*, 12 March 2018. Available online: https://energystorageforum.com/news/energy-storage/hybrid-energy-storage-combined-solutions-gaining-ground (accessed on 4 February 2019).
232. Bocklisch, T. Hybrid Energy Storage Systems for Renewable Energy Applications. *Energy Procedia* **2015**, *73*, 103–111. [CrossRef]
233. Serpi, A.; Porru, M.; Damiano, A. *A Novel Highly Integrated Hybrid Energy Storage System for Electric Propulsion and Smart Grid Applications, Advancements in Energy Storage Technologies, Xiangping Chen and Wenping Cao*; IntechOpen: London, UK, 2 May 2018. [CrossRef]
234. Etxeberria, A.; Vechiu, I.; Camblong, H.; Vinassa, J.M.; Camblong, H. Hybrid Energy Storage Systems for renewable Energy Sources Integration in microgrids: A review. In Proceedings of the 2010 Conference Proceedings IPEC, Singapore, 27–29 October 2010; pp. 532–537.
235. Castillo, A.; Gayme, D.F. Grid-scale energy storage applications in renewable energy integration: A survey. *Energy Convers. Manag.* **2014**, *87*, 885–894. [CrossRef]
236. Global Energy Storage Markets will Grow 13-Fold from 2018 to 2024 to Reach 158 Gigawatt-Hours and $71 Billion in Investment, Wood Mackenzie Power & Renewables Reports | Greentech Media. Available online: https://www.greentechmedia.com/articles/read/global-energy-storage-to-hit-158-gigawatt-hours-by-2024-with-u-s-and-china/ (accessed on 6 February 2020).
237. Energy Storage Exchange. Available online: https://energystorageexchange.org/projects (accessed on 14 February 2020).
238. Daud, M.Z.; Mohamed, A.; Hannan, M.A. A review of the integration of Energy Storage Systems (ESS) for utility grid support. *Przegląd Elektrotechniczny* **2012**, *88*, 185–191.
239. Michael, N.; Chiruvolu, M.; Daniel, C. Available compressed air energy storage (CAES) plant concepts. *Energy* **2010**, *4100*, 81.
240. Arseneaux, J. *20 MW Flywheel Energy Storage Plant*; Beacon Power: New York, NY, USA, 2014.
241. IEA. Technology Roadmap—Energy Storage. IEA: Paris, France, 2014. Available online: https://www.iea.org/reports/technology-roadmap-energy-storage (accessed on 5 February 2020).
242. Zhuang, X.; Huang, R.; Liang, C.; Rabczuk, T. A Coupled Thermo-Hydro-Mechanical Model of Jointed Hard Rock for Compressed Air Energy Storage. *Math. Probl. Eng.* **2014**, *2014*, 179169. [CrossRef]
243. Sodium Sulfur Battery in Abu Dhabi Is World's Largest Storage Device | CleanTechnica. Available online: https://cleantechnica.com/2019/02/03/sodium-sulfur-battery-in-abu-dhabi-is-worlds-largest-storage-device/ (accessed on 14 February 2020).
244. IRENA. Innovation landscape brief: Utility-scale batteries. International Renewable Energy Agency: Abu Dhabi, 2019. Available online: https://www.irena.org/-/media/Files/IRENA/Agency/Publication/2019/Sep/IRENA_Utility-scale-batteries_2019.pdf (accessed on 5 February 2020).
245. EA: Home. Available online: https://www.ea.tuwien.ac.at/home/ (accessed on 19 February 2020).
246. Hydrostor. Available online: https://www.hydrostor.ca/ (accessed on 14 February 2020).

247. Hyundai Building 150 MW Energy Storage Battery in South Korea. Available online: http://www.digitaljournal.com/business/hyundai-building-150-mw-energy-storage-battery-in-south-korea/article/509427 (accessed on 14 February 2020).
248. Hyundai Building the Latest "World's Largest Battery System" with 150 MW System in South Korea | CleanTechnica. Available online: https://cleantechnica.com/2018/12/04/hyundai-building-the-latest-worlds-largest-battery-system-with-150-mw-system-in-korea/ (accessed on 14 February 2020).
249. Kokam Kokam's 56 Megawatt Energy Storage Project Features World's Largest Lithium NMC Energy Storage System for Frequency Regulation. Available online: https://www.prnewswire.com/news-releases/kokams-56-megawatt-energy-storage-project-features-worlds-largest-lithium-nmc-energy-storage-system-for-frequency-regulation-300229219.html (accessed on 14 February 2020).
250. ESS (Energy Storage System)—Reference | Samsung SDI Available online:. Available online: https://www.samsungsdi.com/ess/energy-storage-system-reference.html (accessed on 14 February 2020).
251. Baumgarte, F.; Glenk, G.; Rieger, A. Business Models and Profitability of Energy Storage. *SSRN Electron. J.* **2019**. [CrossRef]
252. *Electrical Energy Storage: White Paper*; Technical Report 2011; International Electrotechnical Commission (IEC): Geneva, Switzerland, 2011.
253. Japan Looks at Recycling Vehicle Batteries for Renewable Power | OilPrice.com. Available online: https://oilprice.com/Alternative-Energy/Renewable-Energy/Japan-Looks-at-Recycling-Vehicle-Batteries-for-Renewable-Power.html (accessed on 14 March 2020).
254. Abbey, C.; Joos, G. Supercapacitor Energy Storage for Wind Energy Applications. *IEEE Trans. Ind. Appl.* **2007**, *43*, 769–776. [CrossRef]
255. Seo, H.R.; Kim, A.R.; Park, M.; Yu, I.K. Power quality enhancement of renewable energy source power network using SMES system. *Phys. C Supercond. Its Appl.* **2011**, *471*, 1409–1412. [CrossRef]
256. Shigematsu, T.; Kumamoto, T.; Deguchi, H.; Hara, T. Applications of a vanadium redox-flow battery to maintain power quality. In Proceedings of the IEEE/PES Transmission and Distribution Conference and Exhibition, Yokohama, Japan, 6–10 October 2002; Volume 2, pp. 1065–1070.
257. Katsuhiro, O.; Kawai, J.; Otsuka, S.; Wada, T.; Imano, H. Development of pump-turbine for seawater pumped storage power plant. In *Waterpower'99: Hydro's Future: Technology, Markets, and Policy*; American Society of Civil Engineers: Las Vegas, NV, USA, 1999; pp. 1–6.
258. Samir, S.; Williams, R.H. Compressed air energy storage: Theory, resources, and applications for wind power. *Princeton Environ. Inst. Report* **2008**, *8*, 81.
259. Díaz-González, F.; Sumper, A.; Gomis-Bellmunt, O.; Bianchi, F.D. Energy management of flywheel-based energy storage device for wind power smoothing. *Appl. Energy* **2013**, *110*, 207–219. [CrossRef]
260. Nakken, T.; Strand, L.R.; Frantzen, E.; Rohden, R.; Eide, P.O. The Utsira wind-hydrogen system–operational experience. In Proceedings of the European Wind Energy Conference, Athens, Greece, 27 February–2 March 2006; pp. 1–9.
261. Hamajima, T.; Amata, H.; Iwasaki, T.; Atomura, N.; Tsuda, M.; Miyagi, D.; Shintomi, T.; Makida, Y.; Takao, T.; Munakata, K.; et al. Application of SMES and Fuel Cell System Combined with Liquid Hydrogen Vehicle Station to Renewable Energy Control. *IEEE Trans. Appl. Supercond.* **2012**, *22*, 5701704-5701704. [CrossRef]
262. Barin, A.; Neves Canha, L.; Magnago, K.; da Rosa Abaide, A. Fuzzy Multi-Sets and Multi-Rules: Analysis of Hybrid Systems Concerning Renewable Sources with Conventional and Flow Batteries. In Proceedings of the 2009 15th International Conference on Intelligent System Applications to Power Systems, Curitiba, Brazil, 8–12 November 2009; pp. 1–6.
263. Yekini Suberu, M.; Wazir Mustafa, M.; Bashir, N. Energy storage systems for renewable energy power sector integration and mitigation of intermittency. *Renew. Sustain. Energy Rev.* **2014**, *35*, 499–514. [CrossRef]
264. Díaz-González, F.; Sumper, A.; Gomis-Bellmunt, O.; Villafáfila-Robles, R. A review of energy storage technologies for wind power applications. *Renew. Sustain. Energy Rev.* **2012**, *16*, 2154–2171. [CrossRef]
265. Madlener, R.; Latz, J. Economics of centralized and decentralized compressed air energy storage for enhanced grid integration of wind power. *Appl. Energy* **2013**, *101*, 299–309. [CrossRef]
266. Texas Mega-Battery Aims to Green up the Grid | New Scientist. Available online: https://www.newscientist.com/article/mg21729026-000-texas-mega-battery-aims-to-green-up-the-grid/ (accessed on 14 March 2020).

267. Ribeiro, E.; Cardoso, A.J.M.; Boccaletti, C. Fuel cell-supercapacitor system for telecommunications. In Proceedings of the 5th IET International Conference on Power Electronics, Machines and Drives (PEMD 2010), Brighton, UK, 19–21 April 2010; p. 8.
268. Kyriakopoulos, A.; O'Sullivan, D.; Hayes, J.G.; Griffiths, J.; Egan, M.G. Kinetic Energy Storage for High Reliability Power Supply Back-up. In Proceedings of the APEC 07—Twenty-Second Annual IEEE Applied Power Electronics Conference and Exposition, Brighton, UK, 19–21 April 2007; pp. 1158–1163.
269. Schoenung, S.M. *Characteristics and Technologies for Long- vs. Short-Term Energy Storage: A Study by the DOE Energy Storage Systems Program*; Sandia National Labs: Albuquerque, NM, USA; Livermore, CA, USA, 2001.
270. Horner, R.E.; Proud, N.J. The key factors in the design and construction of advanced flywheel energy storage systems and their application to improve telecommunication power back-up. In Proceedings of the Intelec'96—International Telecommunications Energy Conference, Boston, MA, USA, 6–10 October 1996; pp. 668–675.
271. Krishnan, K.J.; Kalam, A.; Zayegh, A. H2 optimisation and fuel cell as a back-up power for telecommunication sites. In Proceedings of the 2013 International Conference on Circuits, Power and Computing Technologies (ICCPCT), Nagercoil, India, 20–21 March 2013; pp. 1274–1277.
272. Li, S.; Tomsovic, K.; Hiyama, T. Load following functions using distributed energy resources. In Proceedings of the 2000 Power Engineering Society Summer Meeting (Cat. No.00CH37134), Seattle, WA, USA, 16–20 July 2000; Volume 3, pp. 1756–1761.
273. Hida, Y.; Yokoyama, R.; Shimizukawa, J.; Iba, K.; Tanaka, K.; Seki, T. Load following operation of NAS battery by setting statistic margins to avoid risks. In Proceedings of the IEEE PES General Meeting, Minneapolis, MN, USA, 25–29 July 2010; pp. 1–5.
274. Nyamdash, B.; Denny, E.; O'Malley, M. The viability of balancing wind generation with large scale energy storage. *Energy Policy* **2010**, *38*, 7200–7208. [CrossRef]
275. Rudolf, V.; Papastergiou, K.D. Financial analysis of utility scale photovoltaic plants with battery energy storage. *Energy Policy* **2013**, *63*, 139–146. [CrossRef]
276. Purvins, A.; Sumner, M. Optimal management of stationary lithium-ion battery system in electricity distribution grids. *J. Power Sources* **2013**, *242*, 742–755. [CrossRef]
277. Lobato, E.; Sigrist, L.; Rouco, L. Use of energy storage systems for peak shaving in the Spanish Canary Islands. In Proceedings of the 2013 IEEE Power Energy Society General Meeting, Vancouver, BC, Canada; 21–25 2013; pp. 1–5.
278. Oudalov, A.; Cherkaoui, R.; Beguin, A. Sizing and Optimal Operation of Battery Energy Storage System for Peak Shaving Application. In Proceedings of the 2007 IEEE Lausanne Power Tech, Lausanne, Switzerland, 1–5 July 2007; pp. 621–625.
279. Large Energy Storage Systems Handbook (The CRC Press Series in Mechanical and Aerospace Engineering)—PDF Free Download. Available online: https://epdf.pub/large-energy-storage-systems-handbook-the-crc-press-series-in-mechanical-and-aer.html (accessed on 15 March 2020).
280. Gleason, W. *Fuel Cell Technician's Guide*; Cengage Learning: Boston, MA, USA, 2012; ISBN 978-1-285-41499-7.
281. Kerestes, R.J.; Reed, G.F.; Sparacino, A.R. Economic analysis of grid level energy storage for the application of load leveling. In Proceedings of the 2012 IEEE Power and Energy Society General Meeting, San Diego, CA, USA, 22–26 July 2012; pp. 1–9.
282. Kloess, M.; Zach, K. Bulk electricity storage technologies for load-leveling operation—An economic assessment for the Austrian and German power market. *Int. J. Electr. Power Energy Syst.* **2014**, *59*, 111–122. [CrossRef]
283. Converse, A.O. Seasonal Energy Storage in a Renewable Energy System. *Proc. IEEE* **2012**, *100*, 401–409. [CrossRef]
284. Wang, W.; Ge, B.; Bi, D.; Qin, M.; Liu, W. Energy storage based LVRT and stabilizing power control for direct-drive wind power system. In Proceedings of the 2010 International Conference on Power System Technology, Hangzhou, China, 24–28 October 2010; pp. 1–6.
285. Rogers, J.D.; Schermer, R.I.; Miller, B.L.; Hauer, J.F. 30-MJ superconducting magnetic energy storage system for electric utility transmission stabilization. *Proc. IEEE* **1983**, *71*, 1099–1107. [CrossRef]
286. Irie, F.; Takeo, M.; Sato, S.; Katahira, O.; Fukui, F.; Okada, H.; Ezaki, T.; Ogawa, K.; Koba, H.; Takamatsu, M.; et al. A field experiment on power line stabilization by a SMES system. *IEEE Trans. Magn.* **1992**, *28*, 426–429. [CrossRef]

287. Zhao, H.; Wu, Q.; Hu, S.; Xu, H.; Rasmussen, C.N. Review of energy storage system for wind power integration support. *Appl. Energy* **2015**, *137*, 545–553. [CrossRef]
288. Celli, G.; Pilo, F.; Soma, G.G.; Dal Canto, D.; Pasca, E.; Quadrelli, A. Benefit assessment of energy storage for distribution network voltage regulation. In Proceedings of the CIRED 2012 Workshop: Integration of Renewables into the Distribution Grid, Lisbon, Portugal, 29–30 May 2012; pp. 1–4.
289. Wheeler, N. Voltage regulation application of a kinetic energy storage system. In Proceedings of the Second International Conference on Power Electronics, Machines and Drives (PEMD 2004), Edinburgh, UK, 31 March–2 April 2004; Volume 2, pp. 605–608.
290. Quesada, J.; Sebastián, R.; Castro, M.; Sainz, J.A. Control of inverters in a low voltage microgrid with distributed battery energy storage. Part I: Primary control. *Electr. Power Syst. Res.* **2014**, *114*, 126–135. [CrossRef]
291. Zhu, J.; Qiu, M.; Wei, B.; Zhang, H.; Lai, X.; Yuan, W. Design, dynamic simulation and construction of a hybrid HTS SMES (high-temperature superconducting magnetic energy storage systems) for Chinese power grid. *Energy* **2013**, *51*, 184–192. [CrossRef]
292. Ni, B.; Sourkounis, C. Control strategies for energy storage to smooth power fluctuations of wind parks. In Proceedings of the Melecon 2010—2010 15th IEEE Mediterranean Electrotechnical Conference, Valletta, Malta, 26–28 April 2010; pp. 973–978.
293. Voice, E. Energy Storage: Added Stability for Electrical Grids. Available online: https://www.politico.eu/article/energy-storage-added-stability-for-electrical-grids/ (accessed on 16 March 2020).
294. Kazempour, S.J.; Hosseinpour, M.; Moghaddam, M.P. Self-scheduling of a joint hydro and pumped-storage plants in energy, spinning reserve and regulation markets. In Proceedings of the 2009 IEEE Power Energy Society General Meeting, Calgary, AB, Canada, 26–30 July 2009; pp. 1–8.
295. Dursun, B.; Alboyaci, B. The contribution of wind-hydro pumped storage systems in meeting Turkey's electric energy demand. *Renew. Sustain. Energy Rev.* **2010**, *14*, 1979–1988. [CrossRef]
296. Welcome Dailyenergyreport.com—BlueHost.com. Available online: http://www.dailyenergyreport.com/business-case-3-for-advanced-energy-storagespinning-reserve/ (accessed on 16 March 2020).
297. Habibi, M.S. Model for impact of storage on spinning reserve requirements and distributed generation. In Proceedings of the 33rd Southeastern Symposium on System Theory (Cat. No.01EX460), Athens, OH, USA, 20 March 2001; pp. 161–165.
298. Torreglosa, J.P.; García, P.; Fernández, L.M.; Jurado, F. Predictive Control for the Energy Management of a Fuel-Cell–Battery–Supercapacitor Tramway. *IEEE Trans. Ind. Inform.* **2014**, *10*, 276–285. [CrossRef]
299. Thounthong, P.; Chunkag, V.; Sethakul, P.; Davat, B.; Hinaje, M. Comparative Study of Fuel-Cell Vehicle Hybridization with Battery or Supercapacitor Storage Device. *IEEE Trans. Veh. Technol.* **2009**, *58*, 3892–3904. [CrossRef]
300. Steiner, M.; Klohr, M.; Pagiela, S. Energy storage system with ultracaps on board of railway vehicles. In Proceedings of the 2007 European Conference on Power Electronics and Applications, Aalborg, Denmark, 2–5 September 2007; pp. 1–10.
301. Lukic, S.M.; Cao, J.; Bansal, R.C.; Rodriguez, F.; Emadi, A. Energy Storage Systems for Automotive Applications. *IEEE Trans. Ind. Electron.* **2008**, *55*, 2258–2267. [CrossRef]
302. *The Future Role for Energy Storage in the UK Main Report 2011*; ERP Technology Report; The Energy Research Partnership (ERP: Birmingham, UK, June 2011. Available online: https://erpuk.org/wp-content/uploads/2014/10/52990-ERP-Energy-Storage-Report-v3.pdf (accessed on 5 February 2020).
303. Hadjipaschalis, I.; Poullikkas, A.; Efthimiou, V. Overview of current and future energy storage technologies for electric power applications. *Renew. Sustain. Energy Rev.* **2009**, *13*, 1513–1522. [CrossRef]
304. Zhou, L.; Qi, Z.P. Modeling and control of a flywheel energy storage system for uninterruptible power supply. In Proceedings of the 2009 International Conference on Sustainable Power Generation and Supply, Nanjing, China, 6–7 April 2009; pp. 1–6.
305. Racine, M.S.; Parham, J.D.; Rashid, M.H. An overview of uninterruptible power supplies. In Proceedings of the 37th Annual North American Power Symposium, Ames, IA, USA, 25 October 2005; pp. 159–164.
306. Lahyani, A.; Venet, P.; Guermazi, A.; Troudi, A. Battery/Supercapacitors Combination in Uninterruptible Power Supply (UPS). *IEEE Trans. Power Electron.* **2013**, *28*, 1509–1522. [CrossRef]

307. Eyer, J.M.; Butler, P.C.; Iannucci, J.J., Jr. *Estimating Electricity Storage Power Rating and Discharge Duration for Utility Transmission and Distribution Deferral: A Study for the DOE Energy Storage Program*; No. SAND2005-7069; Sandia National Laboratories: USA, 2005. Available online: https://prod-ng.sandia.gov/techlib-noauth/access-control.cgi/2005/057069.pdf (accessed on 5 February 2020).
308. Heymans, C.; Walker, S.B.; Young, S.B.; Fowler, M. Economic analysis of second use electric vehicle batteries for residential energy storage and load-levelling. *Energy Policy* **2014**, *71*, 22–30. [CrossRef]
309. The Future Value of Storage in the UK with Generator Intermittency. 2004. Available online: https://webarchive.nationalarchives.gov.uk/20100919182205/http://www.ensg.gov.uk/assets/dgdti00040.pdf (accessed on 14 March 2020).
310. Black, M.; Strbac, G. Value of Bulk Energy Storage for Managing Wind Power Fluctuations. *IEEE Trans. Energy Convers.* **2007**, *22*, 197–205. [CrossRef]
311. Winfield, M.; Shokrzadeh, S.; Jones, A. Energy policy regime change and advanced energy storage: A comparative analysis. *Energy Policy* **2018**, *115*, 572–583. [CrossRef]
312. Massa, L.; Tucci, C.L.; Afuah, A. A Critical Assessment of Business Model Research. *Acad. Manag. Ann.* **2017**, *11*, 73–104. [CrossRef]
313. Zucker, A.; Hinchliffe, T.; Spisto, A. *Assessing Storage Value in Electricity Markets: A Literature Review*; Publications Office of the European Union, 2013. Available online: https://op.europa.eu:443/en/publication-detail/-/publication/03a334eb-5ab2-4b07-9d06-edf88cb83fc4/language-en (accessed on 5 March 2020).
314. Richter, M. Business model innovation for sustainable energy: German utilities and renewable energy. *Energy Policy* **2013**, *62*, 1226–1237. [CrossRef]
315. Akhil, A.A.; Huff, G.; Currier, A.B.; Kaun, B.C.; Rastler, D.M.; Chen, S.B.; Cotter, A.L.; Bradshaw, D.T.; Gauntlett, W.D. *DOE/EPRI 2013 Electricity Storage Handbook in Collaboration with NRECA*; Sandia National Laboratories: Albuquerque, NM, USA, 2013.
316. US EPA. Electricity Storage. Available online: https://www.epa.gov/energy/electricity-storage (accessed on 9 February 2020).
317. Five Benefits of Energy Storage: The Holy Grail of Energy. Available online: https://www.facilitiesnet.com/energyefficiency/article/Five-Benefits-of-Energy-Storage-The-Holy-Grail-of-Energy--16907 (accessed on 9 February 2020).
318. FERC Issues Order No. 755: Frequency Regulation Compensation in the Organized Wholesale Power Markets | Insights | Jones Day. Available online: https://www.jonesday.com/en/insights/2011/10/ferc-issues-order-no-755-frequency-regulation-compensation-in-the-organized-wholesale-power-markets (accessed on 15 February 2020).
319. Electricity Regulation in the USA—Lexology. Available online: https://www.lexology.com/library/detail.aspx?g=6decf3ec-4cf8-4930-8a8a-d1a69ac8ba18 (accessed on 15 February 2020).
320. FERC: Industries—Order No. 784. Available online: https://www.ferc.gov/industries/electric/gen-info/mbr/important-orders/OrderNo784.asp (accessed on 15 February 2020).
321. FERC Rules on Order No. 841 Compliance Filings | Stoel Rives—Renewable + Law—JDSupra. Available online: https://www.jdsupra.com/legalnews/ferc-rules-on-order-no-841-compliance-30198/ (accessed on 15 February 2020).
322. Ranchod, S.M. *California Enacts Landmark Energy Storage Law*; Paul Hashtings Stay Current: San Francisco, CA, USA, November 2010; Available online: https://www.paulhastings.com/docs/default-source/PDFs/1753.pdf (accessed on 5 February 2020).
323. Fact Sheet: Energy Storage (2019) | White Papers | EESI. Available online: https://www.eesi.org/papers/view/energy-storage-2019#4 (accessed on 15 February 2020).
324. New York's Energy Storage Incentive Could Spur Deployment of 1.8GWh | Greentech Media. Available online: https://www.greentechmedia.com/articles/read/new-yorks-new-energy-storage-incentive-could-spur-deployment-of-1-8-gw/ (accessed on 15 February 2020).
325. Massachusetts Passes "Minibus" Clean Energy Bill | Law and the Environment. Available online: https://www.lawandenvironment.com/2018/08/01/massachusetts-passes-minibus-clean-energy-bill/ (accessed on 15 February 2020).
326. Massachusetts H 4857—Increases State Clean Energy Requirements—Massachusetts Key Vote—The Voter's Self Defense System—Vote Smart. Available online: https://votesmart.org/bill/25271/64321#.XkgC4SgzbIV (accessed on 15 February 2020).

327. Oregon Utility Regulators Issue Guidelines, Requirements for Energy Storage | American Public Power Association. Available online: https://www.publicpower.org/periodical/article/oregon-utility-regulators-issue-guidelines-requirements-energy-storage/ (accessed on 15 February 2020).
328. Oregon Enacts Energy Storage Legislation | Stay Informed | K&L Gates. Available online: http://www.klgates.com/oregon-enacts-energy-storage-legislation-06-24-2015/ (accessed on 15 February 2020).
329. Enrolled House Bill 2193 (HB 2193-B). 78th OREGON LEGISLATIVE ASSEMBLY—2015 Regular Session. 2015. Available online: https://olis.leg.state.or.us/liz/2015R1/Downloads/MeasureDocument/HB2193 (accessed on 15 February 2020).
330. HRS. Available online: https://www.capitol.hawaii.gov/hrscurrent/Vol05_Ch0261-0319/HRS0269/HRS_0269-0096.htm (accessed on 15 February 2020).
331. Hawaii Utilities Seek More Renewables, Storage and Now Grid Services too—pv Magazine International. Available online: https://www.pv-magazine.com/2019/04/11/hawaii-utilities-seek-more-renewables-storage-and-now-grid-services-too/ (accessed on 15 February 2020).
332. Hawaiian Electric Targets Nearly 1.4 GWh Storage, 135 MW Solar Equivalent in Latest Solicitation | Utility Dive. Available online: https://www.utilitydive.com/news/hawaiian-electric-targets-nearly-14-gwh-storage-135-mw-solar-equivalent-i/552490/ (accessed on 15 February 2020).
333. New Jersey Passes wide-Ranging Energy Legislation on Solar, Batteries and Nuclear Power—pv Magazine USA. Available online: https://pv-magazine-usa.com/2018/04/13/new-jersey-passes-wide-ranging-energy-legislation-on-solar-batteries-and-nuclear-power/ (accessed on 15 February 2020).
334. New Jersey Lawmakers Pass Clean Energy Bills to Spur State's Renewable Economy | SEIA. Available online: https://www.seia.org/news/new-jersey-lawmakers-pass-clean-energy-bills-spur-states-renewable-economy (accessed on 15 February 2020).
335. Maryland Passes Energy Storage Pilot Program to Determine Future Regulatory Framework | Utility Dive. Available online: https://www.utilitydive.com/news/maryland-passes-energy-storage-pilot-program-to-determine-future-regulatory/551769/ (accessed on 15 February 2020).
336. Directive (EU) 2019/944 of the European Parliament and of the Council of 5 June 2019 on Common Rules for the Internal Market for Electricity and Amending Directive 2012/27/EU (recast) (Text with EEA Relevance). Available online: http://www.legislation.gov.uk/eudr/2019/944/introduction (accessed on 15 February 2020).
337. Regulatory Progress for Energy Storage in Europe | Global Law Firm | Norton Rose Fulbright. Available online: https://www.nortonrosefulbright.com/en/knowledge/publications/8b5285f4/regulatory-progress-for-energy-storage-in-europe (accessed on 15 February 2020).
338. Energy Storage in Germany—What You Should Know | Global Law Firm | Norton Rose Fulbright. Available online: https://www.nortonrosefulbright.com/en/knowledge/publications/1d322179/energy-storage-in-germany---what-you-should-know (accessed on 15 February 2020).
339. Renewable Energy Sources Act (EEG 2017). 2016. Available online: https://www.bmwi.de/Redaktion/DE/Downloads/E/eeg-2017-gesetz-en.pdf?__blob=publicationFile&v=8 (accessed on 5 February 2020).
340. Dhruv, B.; Currier, A.; Hernandez, J.; Ma, O.; Kirby, B. *Market and Policy Barriers to Energy Storage Deployment*; No. SAND-2013-7606; Sandia National Lab.(SNL-NM): Albuquerque, NM, USA, 2013.
341. Patel, S. IEA World Energy Outlook: Solar Capacity Surges Past Coal and Gas by 2040. *POWER Magazine*, 14 November 2019. Available online: https://www.powermag.com/iea-world-energy-outlook-solar-capacity-surges-past-coal-and-gas-by-2040/ (accessed on 12 February 2020).
342. *Bloomberg NEF*, 31 July 2019. Available online: https://about.bnef.com/blog/energy-storage-investments-boom-battery-costs-halve-next-decade/ (accessed on 12 February 2020).